UNIVERSIDAD COMPLUTENSE DE MADRID

FACULTAD DE FARMACIA

Departamento de Bioquímica y Biología Molecular II

TESIS DOCTORAL

Intracellular signaling pathways involved in L-DOPA-induced dyskinesias

Vías de señalización implicadas en disquinesias inducidas por L-DOPA

MEMORIA PARA OPTAR AL GRADO DE DOCTOR

PRESENTADA POR

Irene Ruiz de Diego

Director

Rosario Moratalla Villalba

Madrid, 2014

UNIVERSIDAD COMPLUTENSE DE MADRID
FACULTAD DE FARMACIA
Departamento de Bioquímica y Biología Molecular II

INSTITUTO CAJAL
CONSEJO SUPERIOR DE INVESTIGACIONES CIENTÍFICAS

Intracellular signaling pathways involved in L-DOPA-induced dyskinesias

TESIS DOCTORAL

Irene Ruiz de Diego

Madrid, 2014

UNIVERSIDAD COMPLUTENSE DE MADRID
FACULTAD DE FARMACIA
Departamento de Bioquímica y Biología Molecular II

INSTITUTO CAJAL
CONSEJO SUPERIOR DE INVESTIGACIONES CIENTÍFICAS

Intracellular signaling pathways involved in L-DOPA-induced dyskinesias

Memoria presentada por Irene Ruiz de Diego

para optar al título de Doctor,

elaborada a partir del trabajo realizado bajo la dirección

de la Dra. Rosario Moratalla Villalba, en el Instituto Cajal, (CSIC), Madrid.

Doña Rosario Moratalla Villalba, Profesor Titular del Instituto Cajal en el CSIC de Madrid

CERTIFICA

Que Doña Irene Ruiz de Diego ha realizado en el departamento de Neurobiología Funcional y de Sistemas, del Instituto Cajal, bajo mi dirección, el presente trabajo de investigación correspondiente a la Tesis Doctoral: “Intracellular signaling pathways envolved in L-DOPA-induced dyskinesias”.

Revisado el presente trabajo, considero que la presente memoria reúne todos los requisitos necesarios para ser sometida a juicio de la Comisión correspondiente

Y para que así conste y surta los efectos oportunos, firmo la presente en Madrid a …… de ……...de 2014.

Fdo. Rosario Moratalla Villalba

Todo hombre puede ser, si se lo propone,
escultor de su propio cerebro.

Santiago Ramón y Cajal

A mis padres

Quiero agradecer a todos los que en mayor o menor medida han hecho posible la realización de esta Tesis Doctoral. A todos los que con sus conocimientos, su apoyo, sus consejos y su ayuda me han acompañado de la mano hasta llegar aquí. Espero haber sido capaz de haceros llegar mi gratitud y mi cariño durante este tiempo; esto es gracias a vosotros.

Gracias a mi directora de Tesis, la Dra. Rosario Moratalla Villalba, por acogerme en su laboratorio y depositar en mi su confianza. Por guiarme con paciencia en este mundo y brindarme su apoyo y sus consejos; por ayudarme a crecer. Por enseñarme a ver y no sólo a mirar.

Gracias al CIBERNED y al Ministerio de Educación, Cultura y Deporte por su apoyo económico. Así mismo, gracias a todas las instituciones que han financiado este trabajo con los proyectos de investigación concedidos a la Dra. Moratalla.

Gracias al Dr. José Ramón Naranjo y a la Dr. Britt Mellström y a todo su laboratorio del CNB por ser mis colaboradores de ensueño. Nuestro DREAM se ha convertido en un sueño hecho realidad.

Gracias a mi tutora de la UCM, la Dra. Carmen de Juan Chocano, y a la Directora del Departamento, la Dra. Pilar Iniesta, por su apoyo y su entusiasmo. Por ser mis guías cuando estoy lejos de casa. Gracias a Lourdes y a Sole, por facilitarme todo el papeleo y solucionar mis mil dudas diarias.

Gracias al Dr. Yousef Tizabi, porque sin su ayuda no estoy muy segura de que nada de esto se hubiera entendido. Gracias a ti tengo una tesis decente.

Gracias a mi familia cajaliana. A mis compañeros de labo. A Noelia, por recibirme cada mañana con los brazos abiertos y dispuesta a echar un cable en lo que haga falta. Por acogerme como una mamá cuando llegué perdida. A Oskar, por ayudarme a aterrizar. A Sanja, porque me dejó todas las miguitas necesarias para que yo fuera recorriendo el camino. A Sara, por dejarme compartir con ella todo este tiempo y por hacerme cada día, hasta hoy, la vida más fácil. Ha sido un verdadero placer empezar esta aventura contigo. A Isa, por su paciencia infinita y su risa perenne. Por aguantarme todo sin haberse cambiado de sitio ni haber tirado mis cosas por la ventana. A Oscar, por *iloviarme*, por ser mi cómplice en tantas y por ayudarme siempre, siempre. Y por ser mi pubmed particular también. A Patri y a Lula. Gracias por seguir a mi lado después de mi transformación pretésica y por haber vivido todo este proceso dándome apoyo y cariño, sin dejarme caer en ningún momento. Sois un ejemplo de científicas y de personas; gracias por ser mis maestras. A Rubén, Morri, porque has sido un soplo de aire fresco. Y porque sin ti esta Tesis no sería ni su sombra, *compa*. A Emy, por no sacrificarme en estos años, aunque bien hubiera podido. Por abrirme las puertas del Cajal y ayudarme a estar como en casa. A Marco, por tu ayuda inestimable, por su organización ejemplar y por su risa contagiosa. A Bea, por ser la eficacia personificada y por hacer las cosas tan fáciles. A Ramiro, Paparra, no sólo porque fue divertido sino porque también fue provechoso. A Lorena y a Guille, porque no hay mejores manos en las que dejar el testigo. Vuestro entusiasmo y vuestra valía devuelven la fe. Si vosotros sois los científicos de mañana a mi me gustaría formar parte de esa comunidad. Y a todos aquellos que han ido pasando por el B-01 y han ido dejando su granito de arena.

Gracias a mis labos hermanos. Gracias a todo el C-15 por ser de verdad como de la familia. Y gracias a todo el B-05 por tener siempre las puertas y los brazos abiertos para mi.

Gracias de corazón a todos los que formáis esta otra casa mía. Gracias a la gente de animalario, a Mario, a Laude, a Cheli, a Emi, a Lorena. Si fuera ratoncillo querría estar en vuestras manos. Gracias a las chicas del confocal, a Carmen y a Belén. Gracias a Aurelio y a Javi, por cuidarme y mimarme como padres, las tardes muy tardes eran mejor con vosotros. A

Raúl y a José Luis, porque ganara o perdiera el Atleti o el Madrid el beso estaba garantizado. Y porque nunca me he tenido que cambiar una bombona de quirófano. Gracias a Fernando y a Jesús, porque nunca me faltó de nada y por dármelo todo con una sonrisa y un chiste siempre. Gracias Ángel, por todo, por ser mi amigo en todas. Gracias Edwin, porque por un canal puede entrar más que calcio. Gracias Marieta, por ser tan buena, por recibirme siempre con esa sonrisa y por conseguir siempre sacarme la mía. Gracias Raúl, por aguantarme tanto y cuidarme. Por disfrutar tanto con esto, por esas ganas de aprender que se contagian. Gracias Antonio, porque no sólo me enseñaste mi libro favorito. Gracias Edu, *Borro*, porque la gente debería ser más así. Gracias Miriam, porque para mi eres el mayor ejemplo de que se puede ser a la vez buen científico y buen hombre (o mujer en este caso) de mundo. Gracias Jorge, María, Víctor, Andrea, Cagla, Paloma, Natalia, Yago, Eva y Eva, Laura, Simo…. En fin, a todos los que día a día hacéis de este un sitio agradable.

Gracias a mis niñas, a Ana, Sara, Paula, Alicia, Alba, Silvia, Carmen, Almu y a mis chicos Miguel, Carlos, Adrián. Gracias.

Y gracias a mi familia y a los que sin serlo, forman ya parte de ella. Pero sobre todo gracias a mis padres. Sin vosotros, sin vuestro apoyo, vuestra ayuda infinita y vuestro entusiasmo yo no habría ni empezado a vislumbrar este camino. Esta tesis es tan vuestra como mía. Aquí está.

Index

LIST OF ABBREVIATIONS

6-OHDA	6-hydroxydopamine
A2aR	adenosine A2a receptor
AC	adenylyl cyclase
AIS	analysis image system
AMPA	alpha-amino-3-hydroxy-5-methyl-4-isoxazole propionic acid
ANOVA	analysis of variance
AP-1	activator protein 1
ATP	adenosine triphosphate
BAC	bacterial artificial cromosome
BG	basal ganglia
BSA	bovine serum albumin
cAMP	cyclic adenosine monophosphate
CaMK-II	calcium/calmodulin-dependent protein kinase type II
CBP	CREB binding protein
cDNA	complementary deoxyribonucleic acid
COMT	catechol-O-methyltransferase
CREB	cAMP-response element binding protein
CREM	cAMP responsive element modulator
D1R/drd1a	dopamine D1 receptor
D1R$^{-/-}$	dopamine D1 receptor knockout mice
D2R/drd2	dopamine D2 receptor
D2R$^{-/-}$	dopamine D2 receptor knockout mice
D2$_L$	D2R long form
D2$_S$	D2R long form
D3R	dopamine D3 receptor
D4R	dopamine D4 receptor
D5R	dopamine D5 receptor
DAB	3,3'-diaminobenzidine
daDREAM	dominant active mutant DREAM
DARPP-32	cAMP-regulated phosphoprotein of 32 kDa
DAT	dopamine transporter
DRE	downstream regulatory element
DREAM	downstream regulatory element antagonist modulator
DREAM$^{-/-}$	downstream regulatory element antagonist modulator knockout mice
EDTA	ethylenediaminetetraacetic acid
EPDA	European Parkinson's Disease Association
ERK	extracellular signal-regulated protein kinase 1 and 2
FosB	FBJ murine osteosarcoma viral oncogene homolog B
Fra-2.	Fos-related antigen-2
GABA	gamma-aminobutyric acid
Gαi/o	inhibitory type G-protein α s ubunit
Gαolf	olfactory type G-protein α subunit
GAPDH	glyceraldehyde 3-phosphate dehydrogenase
GDP	guanosine diphosphate
Gsolf	stimulatory type G-protein α subunit
GPCRs	G protein-coupled receptors
GPe	globus pallidus pars externa
GPi	globus pallidus pars interna
GTP	guanosine triphosphate
GFP	green fluorescent protein
GluR1	AMPA glutamate receptor subunit type 1
HFS	high-frequency stimulation
IRES	internal ribosome entry site sequence
KChIP3	potassium channel interacting protein 3
LB	Lewy bodies
LCD	leucine-charged residue rich domain
L-DOPA	3,4-dyhydroxyphenyl-L-alanine
LGP	lateral globos pallidus
LID	L-DOPA-induced dyskinesia
LTP	long-term potentiation
MAO	monoamine oxidase
MBF	middle forebrain bundle
MDMA	3,4metylene-dioxymethamphetamine
MSK	mitogen and stress-activated kinase 1
MSN	medium spiny neurons
mRNA	messenger RNA
MFN	medium forebrain bundle
MOR-1	μ-opioid receptor 1

PD	Parkinson's desease
P-GluR1	phospho-(Ser845)-GluR1
PKA	protein kinase A
PP-1	protein phosphatase 1
PPN	pedunculopontine nucleus
PSD-95	postsynaptic density protein 95
RNA	ribonucleic acid
rpm	revolutions per minute
RT-qPCR	real time quantitative PCR
SDS-PAGE	sodium dodecyl sulfate polyacrylamide gel electrophoresis
SEM	standard error of mean
siRNA	small interfering RNA
SN	substantia nigra
SNc	substantia nigra pars compacta
SNr	substantia nigra pars reticulata
STN	subthalamic nucleus
T-TBS	triton tris buffer solution
TH	tyrosine hydroxylase
VTA	ventral tegmental area
WT	wild type mice
w/v	weight/ volume

TABLE OF ILLUSTRATIONS

Summary

Parkinson's disease (PD) is one of the most common neurodegenerative disorders nowadays. This progressive, chronic and age-related pathology is characterized by a dramatic depletion of dopamine in the striatum due to the loss of dopaminergic neurons of the substantia nigra pars compacta. Despite extensive investigation aimed at finding new therapeutic approaches, the dopamine precursor molecule L-DOPA remains the most effective and widely used non-invasive therapy for PD. However, chronic treatment and disease progression cause the appearance of abnormal involuntary movements known as dyskinesias in the vast majority of patients. L-DOPA-induced dyskinesia interferes significantly with normal motor activity and persists unless L-DOPA dosages are reduced below therapeutic levels. Thus, controlling dyskinetic symptoms is one of the major challenges in PD therapy. Despite the progress made in recent years, the intracellular signaling mechanisms implicated in L-DOPA-induced dyskinesias are not fully established.

Previous works from our laboratory demonstrated that L-DOPA-induced dyskinesia is causally linked with hyperstimulation of dopamine D1 receptors (D1R) located on direct pathway medium spiny neurons. L-DOPA activates the cAMP-dependent signalling cascade through the olfactory type G-protein α subunit (Gαolf), which couples D1R to adenylyl cyclase. Since Gαolf levels are a limiting factor for receptor signaling, we propose that Gαolf dysregulation could be a plausible mechanism for the D1R hypersensitivity.

In the dopamine-depleted striatum, the hyperactivation of the cAMP-PKA signaling pathway (e.g., induced by L-DOPA) induces transcriptional changes resulting in increased expression of FosB, dynorphin-B, P-AcH3 and P-GluR1. The transcription of fosB, prodynorphin and as well as c-fos and Fos-related antigen-2 (fra-2) genes is repressed by DREAM (downstream regulatory element antagonist modulator). Based on these observations and on our previous data demonstrating a close association between L-DOPA-induced dyskinesia and overexpression of FosB and dynorphin-B, we propose that DREAM, located downstream of D1R-dependent cAMP/PKA activation, could play an important role in the cascade of molecular events leading to L-DOPA-induced dyskinesia.

The work presented here as my PhD Thesis is primarily focused on elucidation of the role of dopamine and dopamine receptors in striatal Gαolf expression as well as the implication of DREAM protein in L-DOPA-induced dyskinesias and in the associated molecular changes.

To achieve these aims, we used adult mice lacking D1 receptor ($D1R^{-/-}$), D2 receptor ($D2R^{-/-}$), the transcriptional factor Pitx3 ($Pitx3^{-/-}$, aphakia mice), DREAM ($DREAM^{-/-}$) and transgenic mice expressing a dominant active mutant DREAM (daDREAM) along with their

wild type littermates.

By stereotaxic procedure, mice were submitted to unilateral 6-hydroxydopamine (6-OHDA) striatal lesions to generate an established mouse model of PD. Three weeks after the lesion, animals were treated daily with 25 mg/kg of L-DOPA for three weeks. Dyskinesia was evaluated twice a week in the hemiparkinsonian mice during chronic L-DOPA, by separately analyzing the four subtypes of dyskinetic symptoms using the 0-4 severity scale previously described. During this time, the kinetic profile of L-DOPA as well as its antiparkinsonian efficacy were evaluated by the rotarod and the cylinder tests. The analysis of molecular markers of dyskinesias was carried out by immunohistochemistry, western blot, RT-qPCR and image analysis.

Immunohistochemical studies revealed the compartmentalized distribution of the Gaolf protein in adult mice striatum, with higher Gaolf expression in the striosomal compartment than in the matrix. Dopamine depletion by 6-OHDA induced a significant increase in Gaolf protein levels along with a loss of the described patchy pattern. Nevertheless, the increase in Gaolf protein was not associated with similar variations in Gaolf mRNA, which remained invariable after dopamine depletion. L-DOPA treatment restored both Gaolf protein levels and the expression pattern and induced an increase in Gαolf mRNA. These results were corroborated in the aphakia mice, our genetic mouse model of PD, affirming that the lesion procedure did not affect the results obtained in hemiparkinsonian wild type mice.

Genetic deletion of D1R increased Gαolf protein expression in the striatum of D1R null mice and induced the loss of the striosomal-matrix expression pattern. Despite these changes in protein expression, the concentration of Gαolf transcripts was not significantly different in the striatum of $D1R^{-/-}$ mutant mice compared to their wild type littermates. These results suggest that modifications in Gαolf occur at a post-transcriptional level and do not result from a change in gene expression. Contrary to that found in the wild type animals, dopamine depletion significantly decreased Gαolf expression in D1R deficient mice. L-DOPA did not re-establish Gαolf levels in mutant mice. In addition, no patchy pattern could be detected in either Parkinsonian and dyskinetic models. These results indicated that D1R is necessary for the proper expression of Gαolf protein.

In contrast, genetic deletion of D2R in D2R deficient mice did not affect Gαolf protein expression. $D2R^{-/-}$ mice showed the same levels and patter expression in all the three studied conditions, i.e., naïve, Parkinsonian and dyskinetic models. Thus, D2R does not appear to be implicated in the regulation of Gαolf following dopaminergic denervation and L-DOPA treatment.

We then examined whether changes downstream of D1R/cAMP signaling pathway could be implicated in the regulation of Gαolf expression. We found that Gαolf expression was maintained in DREAM$^{-/-}$ and in transgenic daDREAM mice despite the genetic modifications of DREAM. Thus, our results suggest that Gαolf levels are not regulated by D1R-dependent signaling downstream from cAMP stimulation.

However, our results indicate that DREAM protein regulates L-DOPA-induced dyskinesias, but does not modify basal locomotor activity and motor coordination. Overactivation of a dominant active version of DREAM in transgenic daDREAM mice dramatically reduced L-DOPA-induced dyskinesia, whereas genetic inactivation of DREAM increased dyskinetic symptoms. In strict correspondence with the behavioral observations, molecular markers of dyskinesia induced by chronic L-DOPA treatment, including FosB, dynorphin-B, P-AcH3 and P-GluR1, were decreased in daDREAM mice but increased in DREAM knockout mice.

Importantly, DREAM modifications did not affect the kinetic profile of L-DOPA, as all animals showed a similar duration of the L-DOPA response. Moreover, mutant mice showed similar motor performance skills in the cylinder and Rota-Rod tests compared to the wild type, demonstrating that the antiparkinsonian efficacy of L-DOPA was preserved in mutant animals despite DREAM modifications.

In summary, our results strongly suggest a homeostatic regulation of Gαolf expression by dopamine, with a negative correlation between their concentrations. Moreover, the data clearly show that whereas D2R does not influence Gαolf expression, D1R is necessary for an accurate regulation of both levels and pattern expression of Gαolf. These results shed light on the mechanisms underlying the pathophysiology of PD and L-DOPA-induced dyskinesias and indicate that the striosomal-matrix system plays an important role in both pathologies.

The studies on DREAM protein demonstrate the inhibitory role of DREAM in L-DOPA -induced dyskinesia. In addition, we demonstrated that this action occurs at least in part by transcriptional repression of target genes including dynorphin-B and possibly FosB, although non-transcriptional mechanisms could also be involved. Moreover, our data suggest that outside the nucleus DREAM could directly interact with the NR1 subunit and PSD-95, regulating activation of NMDAR and D1R. The findings we describe here validate DREAM as a novel therapeutic target against L-DOPA-induced dyskinesia, and we propose that specific modulators of DREAM could be useful in alleviating L-DOPA-induced dyskinesia without interfering with the antiparkinsonian effect of L-DOPA.

Resumen

La enfermedad de Parkinson es una de las enfermedades neurodegenerativas más prevalentes en la actualidad. Se caracteriza por la muerte de las neuronas dopaminérgicas de la substantia nigra pars compacta, lo que conlleva la subsecuente depleción dopaminérgica a nivel estriatal. La L-DOPA constituye desde su descubrimiento a principio de la década de los sesenta el tratamiento de elección en la enfermedad de Parkinson, ya que es la terapia no invasiva más eficaz para combatir los síntomas de esta enfermedad. A pesar de sus considerables beneficios, la administración crónica de L-DOPA junto con el avance de la enfermedad provocan la aparición de movimientos involuntarios anormales conocidos como disquinesias en la casi totalidad de los pacientes con más de 10 años de tratamiento. La disquinesia interfiere con los mecanismos fisiológicos de la actividad motora y, por tanto, constituye el desafío más importante en la terapia antiparkinsoniana. Sin embargo, se desconocen en gran medida los mecanismos moleculares involucrados en las mismas.

Trabajos previos de nuestro laboratorio demostraron que las disquinesias inducidas por L-DOPA están causalmente relacionadas con la hiperestimulación de los receptores dopaminérgicos D1 (D1R). La L-DOPA activa la vía de señalización del AMPc a través de la proteína Gαolf, la cual acopla los D1R a la enzima adenilato ciclasa. Basándonos en trabajos anteriores que demuestran que los niveles de la proteína Gαolf son uno de los factores limitantes para la señalización mediada por el D1R, nosotros proponemos que la regulación de Gαolf puede ser uno de los elementos implicados en la el mecanismo de hiperestimulación de D1R.

En el estriado carente de dopamina, la hiperestimulación de la vía de señalización de AMPc/PKA provoca cambios transcripcionales que dan lugar a la aberrante expresión de ciertos marcadores moleculares, como FosB, dinorfina-B, histona 3 fosforilada y la subunidad GluR1 del receptor AMPA. La transcripción de los genes de prodinorfina y FosB está regulada por la proteína DREAM (downstream regulatory element antagonist modulator) lo que nos permite pensar que DREAM puede jugar un papel importante en el desarrollo de las disquinesias inducidas por L-DOPA.

El trabajo desarrollado durante mi doctorado se centra en dilucidar el papel de la dopamina y de los receptores dopaminérgicos en la expresión de la proteína Gαolf así como la implicación de DREAM en las disquinesias inducidas por L-DOPA y en los cambios moleculares asociados.

Para llevar a cabo estos estudios se han utilizado ratones adultos knock-out de los receptores dopaminérgicos D1 y D2 ($D1R^{-/-}$ y $D2R^{-/-}$), del factor de transcripción Pitx3 ($Pitx3^{-/-}$

), de DREAM (DREAM$^{-/-}$) y ratones transgénicos dominantes activos de DREAM (daDREAM), que sobreexpresan una forma mutante de la proteína permanentemente activa. En todos los casos hemos contado con los respectivos animales silvestres como controles.

Mediante técnicas estereotáxicas, los animales fueron lesionados en el estriado de forma unilateral con la toxina 6-hidroxidopamina (6-OHDA) para generar nuestro modelo animal de la enfermedad de Parkinson. Tres semanas después de la lesión, los ratones fueron tratados diariamente con 25 mg/kg de L-DOPA durante tres semanas. Durante este tiempo, se llevó a cabo la evaluación de las disquinesias (dos veces por semana), analizándose de forma individual las disquinesias orofaciales, de las patas delanteras y locomotoras así como la distonia axial mediante la escala de severidad 0-4 previamente descrita. También se evaluó el efecto antiparkinsoniano de la L-DOPA mediante los tests del Rota-Rod y del cilindro así como el estudio del perfil farmacocinético de la L-DOPA, analizando el tiempo de duración de las disquinesias. Tras el sacrificio de los animales por dislocación cervical o perfusión, se llevaron a cabo los análisis moleculares. Para ello se recurrió a técnicas de inmunohistoquímica, western blot, RT-qPCR y análisis de imagen.

El estudio mediante técnicas de inmohistoquímica de la expresión de la proteína Gαolf mostró que en los animales silvestres existe un patrón de expresión definido, con una mayor concentración de Gαolf en los estriosomas que en la matriz estriatal. La depleción dopaminérgica estriatal mediada por la toxina 6-OHDA indujo en estos animales un aumento significativo en los niveles de la proteína Gαolf y una pérdida del patrón estriatal descrito. Sin embargo, este aumento en la concentración de la proteína no se correlacionó con un aumento en el ARN mensajero de Gαolf, que se mantuvo invariable. El tratamiento crónico con L-DOPA devolvió tanto los niveles como el patrón de expresión de Gαolf a los encontrados en la situación basal, mientras que por el contrario produjo un aumento en los niveles de ARNm.

Estos resultados se corroboraron en un modelo genético para la enfermedad de Parkinson, los ratones Pitx3$^{-/-}$. En estos ratones se reprodujeron los resultados encontrados en los animales hemiparkinsonianos, permitiéndonos así descartar que los cambios observados en los niveles de Gαolf y en su patrón de expresión fueran consecuencia del proceso de lesión.

La deleción genética del D1R indujo un aumento de los niveles de Gαolf en el estriado de los ratones D1R$^{-/-}$, así como la pérdida del patrón estrisoma-matriz característico. A pesar de estos cambios, los niveles de ARNm de Gαolf fueron los mismos en los animales knockout del D1R que en los animales silvestres, lo que nos indicó que los cambios en la expresión de la proteína se producen a nivel post-transcripcional. Al contrario de lo que encontramos en los

animales silvestres, la depleción dopaminérgica en los ratones $D1R^{-/-}$ provocó una disminución en la concentración de la proteína Gαolf, que no pudo ser revertida con el tratamiento con L-DOPA. Además, en ningún caso se recuperó tampoco el patrón de expresión encontrado en los animales silvestres, siendo indistinguibles los estriosomas de la matriz. Esto nos permitió afirmar que el receptor dopaminérgico D1 es necesario para la correcta expresión de la proteína Gαolf.

En contraste con estos resultados, la eliminación genética del receptor dopaminérgico D2 en los ratones $D2R^{-/-}$ no supuso cambios en la expresión de la proteína Gαolf con respecto a lo encontrado en los ratones silvestres, ni en la situación basal ni en condiciones parkinsonaina ni disquinética. Por lo tanto, el receptor dopaminérgico D2 no participa en la regulación de la expresión de la proteína Gαolf.

Una vez analizada la implicación de los receptores dopaminérgicos en la expresión de la proteína Gαolf, estudiamos el impacto de modificaciones que tuvieran lugar más abajo en la cascada de señalización de las disquinesias. Para ello recurrimos a animales que sobreexpresan la proteína DREAM (daDREAM) y a animales que carecen de ella ($DREAM^{-/-}$). En estos ratones mutantes no encontramos diferencias en la expresión de Gαolf con respecto a sus controles silvestres. Podemos por tanto afirmar que cambios por debajo del nivel de los receptores dopaminérgicos no alteran la expresión de la proteína Gαolf.

En lo que a actividad motora se refiere, los estudios conductuales realizados en condiciones basales indicaron que las modificaciones genéticas de DREAM no alteraron ni la actividad ni la coordinación motora. Por el contrario, las disquinesias inducidas por L-DOPA si fueron diferentes en los distintos genotipos estudiados. Los ratones daDREAM mostraron menor grado de disquinesias durante todo el tiempo de tratamiento. En línea con estos resultados conductuales, la sobreactivación de DREAM en estos ratones produjo una disminución significativa en los marcadores de las disquinesias inducidas por L-DOPA, en concreto en FosB, dinorfina-B, fosfo-acetil-histona H3 y en P-GluR1. Por el contrario, la inactivación genética de DREAM en los ratones $DREAM^{-/-}$ provocó un aumento en los síntomas disquinéticos así como un incremento en la expresión de los marcadores moleculares.

Cabe destacar que los animales mutantes mostraron una respuesta positiva ante el tratamiento con L-DOPA, mejorando sus capacidades motoras con respecto a las exhibidas en el estado parkinsoniano. No hubo diferencias entre genotipos indicando que las modificaciones en DREAM no alteran el efecto terapéutico de la L-DOPA.

Los resultados obtenidos sobre la proteína Gαolf nos permiten afirmar que su expresión

está regulada por los niveles de dopamina y por el receptor dopaminérgico D1R, no el D2R. Esto correlaciona con resultados obtenidos en ratones tratados con cocaína, metanfetamina y 6-OHDA. Sin embargo, es la primera vez que se reporta un cambio en el patrón de expresión de Gαolf como consecuencia de la denervación dopaminérgica. Nuestros resultados sugieren que el desequilibrio en el sistema matriz-estriosomas puede ser uno de los factores implicados en el desarrollo de las alteraciones relacionadas con el Parkinson, como se ha visto en otras alteraciones neurológicas.

Con el trabajo realizado sobre la proteína DREAM demostramos que esta proteína tiene un papel modulador en las disquinesias inducidas por L-DOPA. Esta regulación ocurre al menos en parte a nivel de represión transcripcional de los genes de FosB y dynorfina-B, aunque también participan procesos no transcripcionales como la interacción directa de DREAM con PSD-95 y con la subunidad NR1 de los receptores NMDA. Estos resultados nos permiten sugerir que moduladores específicos de DREAM podrían ser útiles para aliviar las disquinesias inducidas por L-DOPA, sin que interfieran con el efecto terapéutico de la L-DOPA.

Introduction

1. THE BASAL GANGLIA

The basal ganglia comprise a collection of subcortical structures involved in the control of motor and limbic functions including learning, memory and cognitive processes. This breadth of functions is strikingly exhibited in the range of clinical disorders related to basal ganglia alterations, such as Parkinson's disease (PD), Huntington's disease, attention-deficit hyperactivity disorder, compulsivity and obsessive-compulsive disorder and depression. The functionally connected nuclei that conform the basal ganglia belong to the forebrain, diencephalon and midbrain and include the striatum (caudate and putamen), the globus pallidus pars externa (GPe) and pars interna (GPi), the subthalamic nucleus (STN) and the substantia nigra, divided into its pars compacta (SNc) and pars reticulata (SNr). Together, all these interconnected nuclei form a highly organized and complex circuitry.

The first model of motor circuit of the basal ganglia was developed at the end of the 1980s (Penney and Young, 1986; Albin *et al.*, 1989; DeLong, 1990). According to this model, information from the cerebral cortex and thalamus is integrated in the striatum. The processed information is send to the SNr, to provide feed-back via the ventral thalamus to the cerebral cortex, forming parallel cortico-basal ganglia-thalamo-cortical loops (Lanciego *et al.*, 2012) (Figure 1).

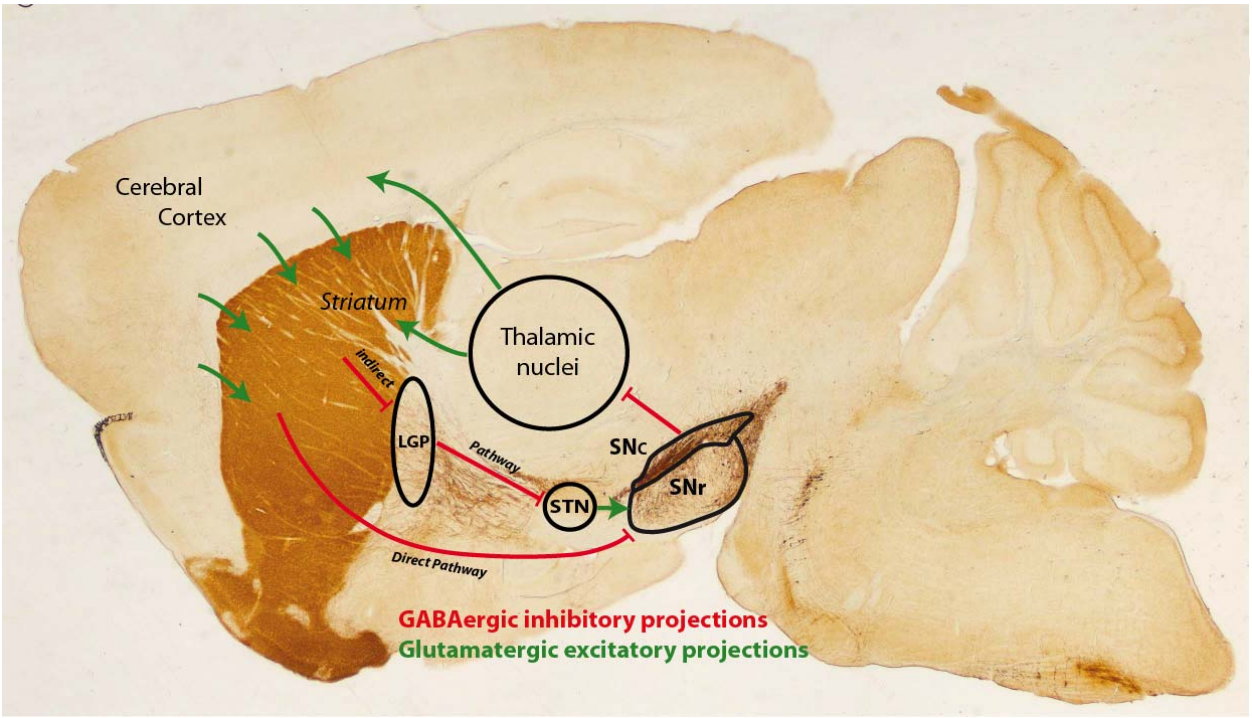

Figure 1. Schema of the cortico-basal ganglia-thalamocortical loop in the mouse brain. Sagital section of mouse brain stained with tyrosine hydroxylase antibody. Abbreviations: LGP: Lateral Globus Pallidus; SNc: Substantia nigra pars compacta; SNr: Substantia nigra pars reticulata and STN: Subthalamic Nucleus.

The striatum sends the processed information through two parallel and diametrically opposed GABAergic pathways: the *direct or striatonigral patway*, which projects to the SNr and the GPi; and the *indirect or striatopallidal patway*, which projects to the SNr and the GPi indirectly, via GPe and STN. The direct and indirect pathways exert opposing effects on movements and an imbalance in their activity is believed to lead to hypokinetic (i.e., Parkinsonism) or hyperkinetic (i.e., dyskinesia) movement disorders.

Current thinking has modified this functional model, including several loops that interact with internal reentry loops (Figure 2). The cortico-subthalamo-pallidal *hyperdirect* pathway bypasses the striatum, being the fastest route by which cortical and thalamic information can modulate the SNr/GPi activity (Nambu *et al.*, 2002; Rico *et al.*, 2010). Moreover, reciprocal connections between the GPe and the striatum (Sato *et al.*, 2000) and between the striatum and dopamine neurons in the SNc (Haber *et al.*, 2000) have been described.

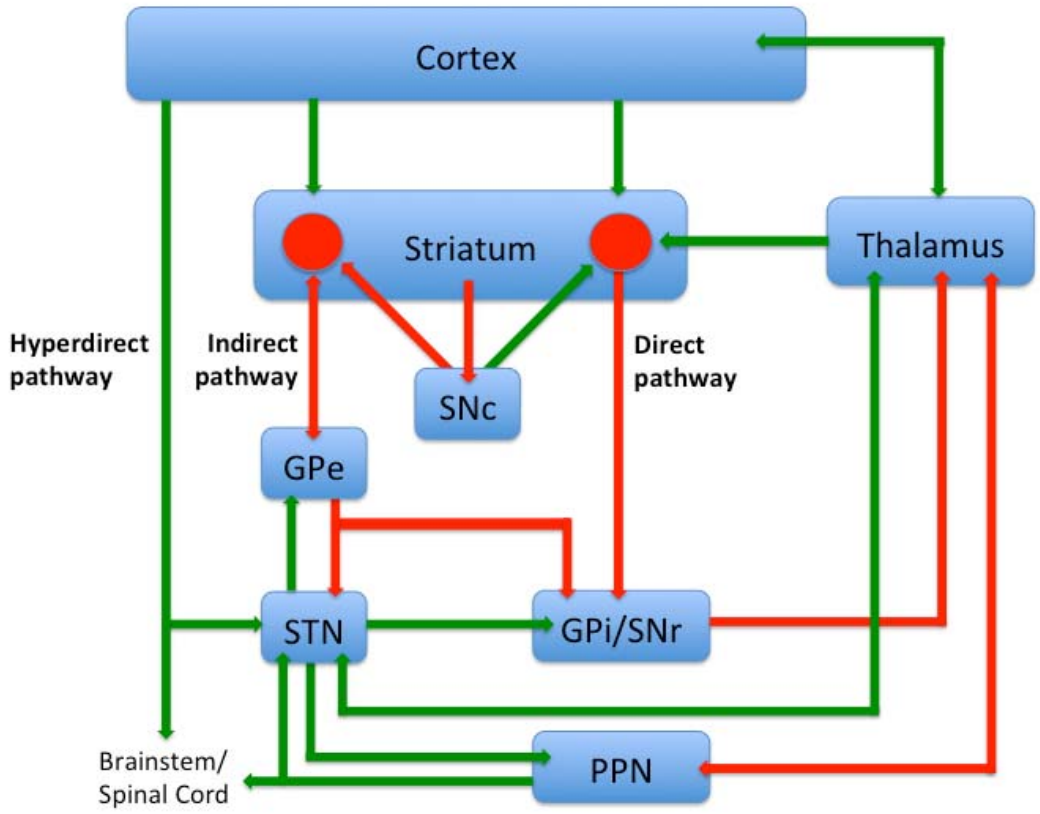

Figure 2. Simplified view of the motor circuit of the basal ganglia. Red arrows indicate inhibitory GABAergic connections; green arrows, excitatory glutamatergic connections. Abbreviations: GPe, globus pallidus pars externa; GPi, globus pallidus pars interna; PPN, pedunculopontine nucleus; SNc, substantia nigra pars compacta; SNr, substantia nigra pars reticulta; STN, subthalamic nucleus. Adapted from DeLong and Wichmann, 2007.

2. THE STRIATUM

The striatum is the primary input nucleus of the basal ganglia. The striatum is located in the forebrain and its name comes from its striped appearance, due to the myelinated axons that cross it. In higher vertebrates, the striatum is composed of the caudate nucleus and the putamen, separated by the internal capsule. In rodents, it appears as a single nucleus. Topographically, the striatum can be divided into the dorsal (caudate-putamen) and the ventral (nucleus accumbens, NAc) striatum. The dorsal part receives cortical input from neocortex, processing sensorimotor information, whereas ventral striatum receives cortical inputs from allocortical, periallocortical and proisocortical regions and processes mostly reward-related information.

2.1 Striosome and matrix organization

In addition to the topographical organization of the mammalian striatum, two different tissue compartments have been clearly identified from neurochemical and developmental points of view: the *striosomes* (or patches) and the *matrix* compartments (Graybiel, 1990). Striosomes were first recognized as compartments of low acetylcholinesterase activity (Graybiel and Ragsdale, 1978) and characterized by light or poor calbindin zones (Davis and Puhl, 2011; Watabe-Uchida *et al.*, 2012) and limited parvalbumin staining (Prensa *et al.*, 1999). In contrast, striosomal neurons are rich in μ-opiate receptors 1 (MOR1) (Breuer *et al.*, 2005; Lawhorn *et al.*, 2009; Tajima and Fukuda, 2013), dopamine D1 receptors (Kim *et al.*, 2002) and olfactory type G-protein α subunit (Gαolf) (Sako *et al.*, 2010). Taking advantage of these neurochemical characteristics, a recent study shows by immunohistochemistry a site-dependent diversity of mice striosomes along both the rostrocaudal and dorsoventral axes of the striatum based upon the distribution of staining patterns (Tajima and Fukuda, 2013). From a developmental point of view, striosomes are established earlier than the matrix components (Graybiel and Hickey, 1982; Crittenden and Graybiel, 2011) and represents approximately 15% of the total striatal volume.

The striosomes mainly receive and process limbic and reward-related information (White and Hiroi, 1998) whereas the matrix mainly received associative and sensorimotor information (Gerfen, 1984). In addition, striosomes are thought to contain the only striatal neurons that have direct projections to the dopamine-containing cells of the SNc, regulating the nigral input to the striatum. Thus, striosomes are thought to influence striatal processing by exchanging information with the surrounding matrix (Crittenden and Graybiel, 2011).

Differential activation and susceptibility of both compartments have been reported. Interestingly, matrix neurons showed a higher metabolic activity during natural behavioural

states such as rest or free moving (Brown *et al.*, 2002). In contrast, chronic cocaine or amphetamine treatments that lead to a stereotypic behaviour preferentially activate the striosomal compartment (Moratalla *et al.*, 1996a). A relative increase of striosomal activity largely due to decreased matrix activity could be linked with the development of stereotypy (Tanimura *et al.*, 2011). Moreover, striosomal dopaminergic terminals have been found to be more susceptible to the neurotoxicity induced by MDMA and methamphetamine than the surrounding matrix (Granado *et al.*, 2008a; 2010) (Figure 3). Taken together, imbalances between striosomes and matrix functions could be directly related with neurological disorders, including PD, Huntington's disease, dystonia and drug addiction (Granado *et al.*, 2008a; Crittenden and Graybiel, 2011).

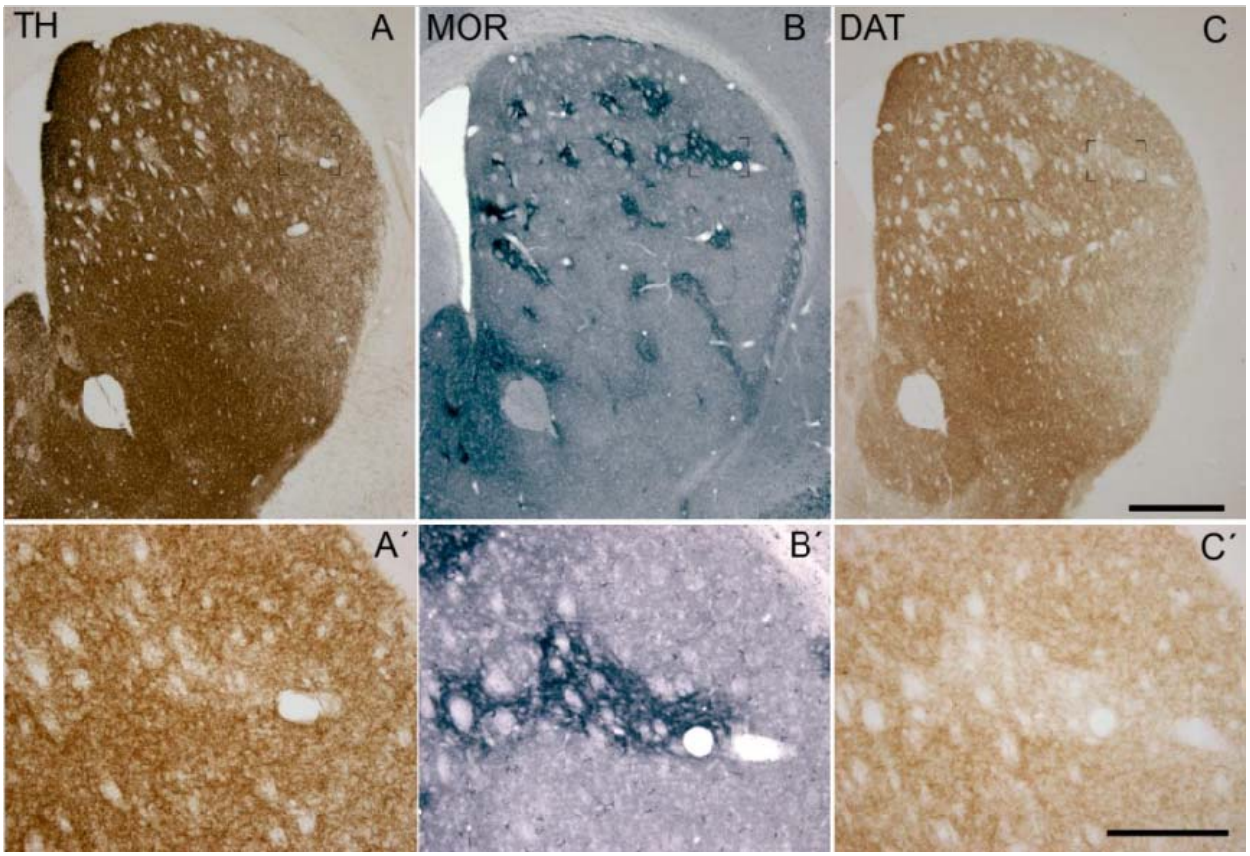

Figure 3. TH and DAT loss takes place preferentially in the striosomal compartment after methamphetamine treatment. Serially adjacent brain sections from mouse treated with methamphetamine stained for tyrosine hydroxylase (TH), μ receptor opioid 1 (MOR) and dopamine transporter (DAT). Patches of weak TH- and DAT-positive fibres correspond with striosomes identified by MOR immunostaining. From Granado *et al.*, 2010.

2.2 Neuronal components

The striatum is composed of one principal neuron cell type, the medium spiny projection neurons, accounting for 90-95% of total striatal neurons in rodents and 75-80% in primates (Kemp and Powell, 1971). The remaining striatal neurons are interneurons (DiFiglia *et al.*, 1976; Kawaguchi *et al.*, 1995).

- Projection neurons

Medium spiny projection neurons (MSN) take their name from their morphological appearance, with a medium-sized (20-25 µm) rounded or oval cell body, large axons and multiple spiny dendrites (Figure 4). All the projection neurons in the striatum are GABAergic and morphologically identical but two major subpopulations of approximately equal number may be defined on the basis of their projection targets and the expression of distinct neuropeptides and receptors (Gerfen and Surmeier, 2011):

- Direct pathway or striatonigral neurons, projecting to the substantia nigra. They express substance P, dynorphin and dopamine D1 receptor (D1R).
- Indirect pathway or striatopallidal neurons, projecting to the globus pallidus. They express enkephalin, adenosine A2a receptors (A2aR) and dopamine D2 receptor (D2R).

Activation of direct pathway D1R-neurons facilitates movements, whereas activity in the indirect pathway D2R-neurons inhibits motor function. The extended view of the anatomical organization of the striatum is that both direct and indirect neurons are intermingled throughout the striatum, displaying a uniform organization. Pioneering work with *in situ* hybridization pointed out the segregation of D1R and D2R in striatonigral and striatopallidal projection neurons, respectively (Le Moine *et al.*, 1990a, 1991). These results were challenged on the basis of single cell mRNA expression studies, which reported colocalization of both dopamine receptor subtypes in striatal neurons (Surmeier *et al.*, 1992). However, nowadays the segregation of the two populations had been solid establish with bacterial chromosome artificial (BAC) transgenic mice. These new mouse lines, in which enhanced fluo-rescent proteins are driven by D1R or D2R promoters, provide an easy way to label neurons which express high levels of D1R or D2R (Valjent *et al.*, 2009). In mice carrying BAC *drd1a*-GFP or *drd1a*-Tomato (a red fluorescent protein), striatonigral D1R-positive projection neurons are labeled, whereas striatopallidal D2R-positive projection neurons are stained in BAC *drd2*-GFP mice (Matamales *et al.*, 2009; Bertran-Gonzalez *et al.*, 2010).

- Interneurons

Striatal interneurons make up some 5-10% of the total striatal neuron population in rodents. They have short aspiny axons, which project within but never out of the striatum. Striatal interneurons may be classified depending on their cytochemical and morphological characteristics into large cholinergic cells and medium-sized GABAergic cells. Large cholinergic interneurons have a large polygonal or fusiform soma (20-50 μm) and release acetylcholine. They are the only tonically active neurons in the striatum (Aosaki *et al.*, 1994) and abundantly express dopamine D5 receptors (D5R) (Rivera *et al.*, 2002a). Medium-sized GABAergic neurons can be further divided into: 1) parvalbumin-containing, 2) calretinin-containing, and 3) somatostatin-, neuropeptide Y-, and nitric oxide synthase-containing interneurons.

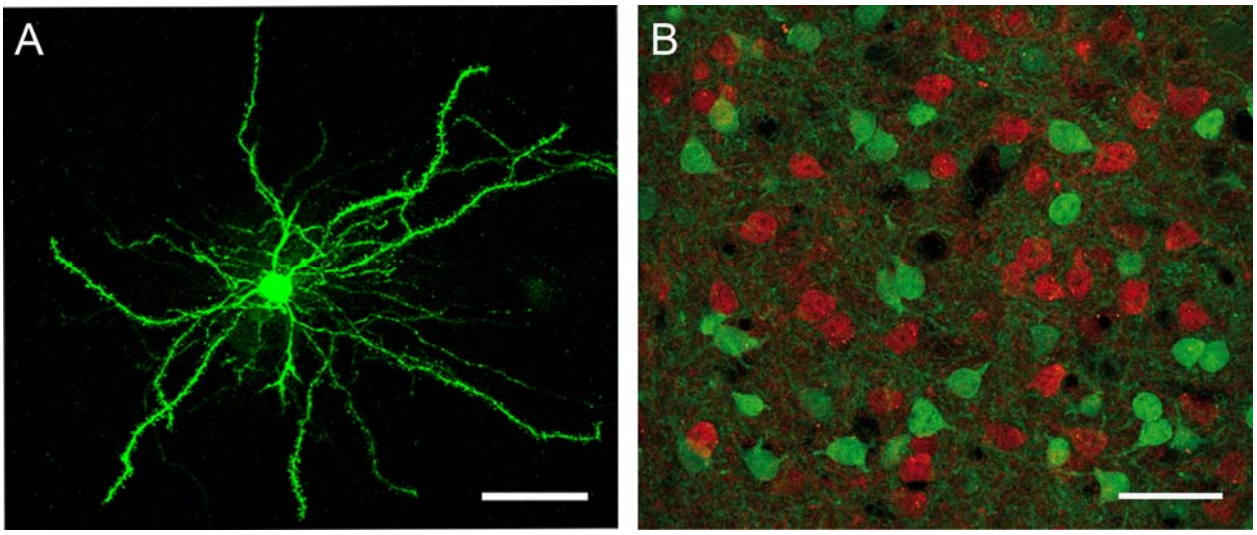

Figure 4. Medium spiny projection neurons. (A) Single MSN labeled with Lucifer Yellow. Note the high number of spines. From Suárez *et al.*, 2014. **(B)** Confocal section of D1R-Tomato/D2R-GFP BAC-transgenic mice striatum. Note the intermingled and segregated anatomical disposition of both MSN in the striatum, with no colocalization. From Ares-Santos *et al.*, 2014.

2.3 Dopamine receptors

Dopamine is a major catecholamine in the brain. Some 80% of dopamine in the brain is localized in the striatum, where their receptors are mostly expressed. Dopamine receptors belong to the superfamily of G protein-coupled receptors (GPCRs). They have seven transmembrane domains and include five different receptor subtypes. These dopamine receptor subtypes are encoded by genes with different chromosomal loci and display considerable homology in their structure.

The D1-like receptors family includes D1R and D5R, which are associated with excitatory function. Both D1R and D5R are positively coupled to adenylyl cyclase (AC), the enzyme responsible for the conversion of ATP into cAMP. D1R is mainly expressed in the striatum, NAc, cerebral cortex, olfactory tubercule, SN and amygadala, while D5R is primarily expressed in the cerebral cortex, hippocampus, striatum, lateral mammillary nucleus, and in the parafascicular nucleus of the thalamus (Rivera *et al.*, 2002a).

On the other hand, the D2-like receptors family includes D2R, D3R and D4R. They are negatively coupled to AC and generally have inhibitory function. D2R is abundant in typical dopamine rich areas such as the striatum, olfactory tubercule, NAc, SNc and VTA. It is mostly expressed in striatopallidal neurons but also found in cholinergic neurons (Le Moine *et al.*, 1990b). The D2R subtype has two splice variants coded by the same gene, the long form ($D2_L$) and the short form ($D2_S$). These two receptors have distinct functions *in vivo*; $D2_L$ acts mainly at postsynaptic sites and $D2_S$ serves presynaptic autoreceptor functions in the soma of dopaminergic neurons of the SNc (Usiello *et al.*, 2000; Anzalone *et al.*, 2012). D3R in the rat brain is restricted to a few brain regions including ventral striatum and SNc (Xu *et al.*, 1997). D4R appears to be highly expressed in the frontal cortex, amygdala, olfactory bulb, hippocampus, hypothalamus and mesencephalon (Rivera *et al.*, 2002b).

2.4 G proteins coupled to dopamine receptors

The opposing actions of D1- and D2-like receptors result from their different coupling to G protein subunits. G proteins comprise three subunits, α, β and γ, forming a heterotrimeric complex attached to the membrane. Upon binding to dopamine, GPCRs undergo conformational changes that activate their ability to catalyze the exchange of GDP with GTP. GTP binding to the α subunit causes its dissociation from the βγ complex. Both the active form of the Gα (GTP-bound) and free Gβγ interact with a range of downstream signaling molecules and modulate their activity to generate cellular responses. Depending on their role in AC activity, we can differentiate stimulatory and inhibitory Gα subunits. D1-like receptors are coupled to stimulatory Gα (Gαs/olf), activating AC; whereas D2-like receptors are coupled to inhibitory Gα subunit (Gαi/o), inhibiting AC.

Two highly homologous Gα subunits are known to activate AC: Gαs, the ubiquitous isoform, which is found in most cell types, and Gαolf (i.e., olfactory type G-protein α subunit), which has been discovered in the rat olfactory epithelium and mediates olfactory receptor signaling (Jones and Reed, 1989; Belluscio *et al.*, 1998). Gαolf is present in much higher quantities than Gαs in the striatum (Drinnan *et al.*, 1991; Hervé *et al.*, 1993). There, Gαolf

colocalizes with D1R and mediates their coupling to AC (Hervé *et al.*, 1993; Corvol *et al.*, 2001). In addition, Gαolf also colocalizes with A2aR, located in D2R-bearing neurons (Kull *et al.*, 2000; Hervé *et al.*, 2001). Thereby, Gαolf subunit protein is present in both types of MSN in the striatum, coupled to D1R in the striatonigral neurons and to A2aR in the striatopallidal ones. Interestingly, Gαolf protein expression is selectively increased in either D1R or A2aR knockout mice (Hervé *et al.*, 2001). These changes have been seen to occur in a post-transcriptional level and do not result from a change in gene expression. In line with these findings, deletion of dopamine transporter (DAT) and subsequent hyperstimulation of dopamine receptors, results in a decrease of Gαolf protein in the striatum. Taken together, these results indicate that receptor usage and dopamine tone may control Gαolf levels.

3. PARKINSON'S DISEASE

Parkinson's disease (PD) is a progressive neurodegenerative disorder with multifactorial etiology characterized by the loss of nigrostriatal dopaminergic neurons within the midbrain, particularly SNc. PD is the second most common age-related neurodegenerative disease after Alzheimer's disease, affecting more than 4 million people worldwide (de Lau and Breteler, 2006). The age of onset is usually over 60, but it is estimated that one in ten people are diagnosed before the age of 50, with slightly more men than women affected (European Parkinson's Disease Association, EPDA). PD was originally described in 1817 by the British physician James Parkinson in the classic monograph "Essay on the Shaking Palsy". PD was then known as shaking palsy or paralysis agitans; the term "Parkinson's disease" was introduced later by Jean-Martin Charcot. All the cardinal signs of PD relate to motor dysfunction and include resting tremor, bradykinesia, rigidity and postural reflex impairment.

3.1 Etiology and epidemiology

After many years of intense research, little is still known about the etiology of PD. In the last decade, perhaps the greatest single advance in the PD field has been the identification of genes that increase disease risk (Gasser, 2009). At present, 16 loci have been clearly linked to familial forms of PD (Lees *et al.*, 2009; Puschmann, 2013; Singleton *et al.*, 2013). However, these still account for less than 10-15% of all the cases of PD and most of the PD-associated genes are of unknown or poorly understood function. Thus, the cause of sporadic PD, which accounts for about 85-90% of all PD subjects, still remains uncertain. Current understanding of the etiology of sporadic PD points to multifactorial causes, combining genetic, age and environmental factors. Most cases of PD may be due to a double hit involving an interaction

between a gene mutation that induces susceptibility coupled with to a toxic environmental factor.

The strongest risk factor in PD is age. Disease incidence rises exponentially above the age of 65. Why age is such a strong risk factor is unknown, but it is widely speculated that declining mitochondrial function is a key factor (Schapira, 2008; Boumezbeur *et al.*, 2010). Others factors associated with an increased risk for PD are exposure to pesticides and metals, vascular/metabolic diseases, stress and infections as encephalitis. Factors proposed to protect against the development of PD include antioxidants, cigarette smoking, coffee, tea and wine drinking, Mediterranean diet and high physical activity.

3.2 Neuropathological features

The progressive degeneration of the dopaminergic neurons in the SNc and the appearance of intracytoplasmic inclusions called Lewy bodies (LB) represent the main neuropathological features of PD (Greenfield and Bosanquet, 1953; Braak *et al.*, 2002; 2003; Tong *et al.*, 2010). Neuronal loss in the SNc is not uniform; the neurons of the ventrolateral tier, which project to the striatum, and are involved in motor disorders, are selectively more vulnerable than the others. In contrast, dorsal neurons may be vulnerable to age-related neuronal degeneration and their loss is never as severe as that detected in PD. The medial neuronal groups, i.e. mesolimbic dopaminergic neurons in the VTA, may be affected in patients with dementia. The selective vulnerability of dopaminergic neurons in the ventral SNc has been suggested to be due to their uniquely massive, unmyelinated axonal arbor (Bolam and Pissadaki, 2012). The extreme bioenergetics demand of maintaining the massive number of synapses and the immense axonal field that these neurons give raise to makes them especially vulnerable to stressors of any sort.

Approximately 3.6% of remaining neurons in the SNc contain LB (Greffard *et al.*, 2010), which are composed of alpha-synuclein associated with other proteins such as ubiquitin. Interestingly, the proportion of LB-bearing neurons remains roughly constant. Nowadays, the precise reason why LB develops is not known and their role in neuronal degeneration remains controversial. While some authors postulate that LB represent a form of aggresome that develops in response to increased levels of misfolded proteins to segregate and facilitate the clearance of these potentially toxic proteins (Manning-Bog *et al.*, 2003; Calne and Mizuno 2004; Tanaka *et al.*, 2004), others report a toxic effect and a contribution to neurodegeneration by LB (Greffard *et al.*, 2010). Correlating with this later idea, Dr. Vila's group has recently demonstrated that intranigral or intrastriatal inoculations of PD-derived LB extracts monkeys

and mice resulted in progressive nigrostriatal neurodegeneration starting at striatal dopaminergic terminals (Recasens *et al.*, 2014).

In 2003 Heiko Braak and coworkers established a chronopathological model of PD based in the appearance of LB with a sequential and predictable fashion (Braak *et al.*, 2003). According to Braak's model, pathological process begins in the olfactory system, peripheral autonomic nervous system and dorsal motor nucleus of the vagus, extending as an oil drop to involve dopamine neurons of the SNc in the mid-stage of the disease, and affecting the cerebral hemispheres in the latter stages of the illness. While this precise sequence of degeneration may not apply to all cases, it raises the possibility that neurodegeneration might extent from affected to unaffected areas in a prion-like manner (Olanow and Brundin, 2013).

3.3 Changes in basal ganglia motor circuitry in PD

The degeneration of dopaminergic neurons in the SNc leads to a consequent striatal denervation responsible for the major symptoms of disease. This loss first affects the caudal, mainly sensorimotor, part of the striatum (Kish *et al.*, 1988; Moratalla *et al.*, 1992). Loss of striatal dopamine causes a profound imbalance between the two main striatal pathways. Dopaminergic depletion in PD reduces the activation of striatonigral neurons of the direct pathway while enhances the activation of striatopallidal projection neurons of the indirect pathway, leading to increased activity of the STN, which in turns overactivates inhibitory output neurons in the GPi/SNr. In this way, the combined reduction of GABA inhibition from the "direct" striatal output neurons and increased glutamatergic drive from the disinhibited STN leads to increased activity in the GPi/SNr output neurons, reducing their inhibitory activity and thereby impeding movement initiation and execution (Obeso *et al.*, 2013; Figure 5). This imbalance was first documented in anatomo-functional studies (Gerfen *et al.*, 1990; Gerfen, 2000) and later confirmed by electrophysiological experiments (Mallet *et al.*, 2006). More recently, Kreitzer's group has examined the behavioral effects of specifically activating by laser -illumination the direct or the indirect pathway in awake mice using an optogenetical approach (Kravitz *et al.*, 2010). They showed that bilateral excitation of indirect-pathway neurons elicited a Parkinsonian state, characterized by freezing and bradykinesia, while activation of direct-pathway neurons increased locomotion. Interestingly, in a mouse model of PD, direct pathway activation completely rescued deficits in freezing, bradykinesia, and locomotor initiation.

At the receptor level, dopamine depletion induces an increase in the number of D2R in striatopallidal neurons (Creese *et al.*, 1977; Cai *et al.*, 2002) while no significant changes and even a decrease in D1R density is found (Gerfen *et al.*, 1990; Hervé *et al.*, 1992; Hurley *et al.*,

2001). Chronic interruption of nigrostriatal dopaminergic pathway in PD increases the sensitivity of striatal D1R and D2R in response to receptor stimulation (Arnt and Hyttel, 1985). This hyper-responsiveness is attributed to elevated levels and efficiency of Gαolf after dopamine denervation (Marcotte *et al.*, 1994; Corvol *et al.*, 2004; Aubert *et al.*, 2005). Thus, the ability of dopamine to stimulate AC and PKA via activation of D1R is enhanced in PD patients and in experimental animals following dopamine depletion (Tong *et al.*, 2004; Santini *et al.*, 2008).

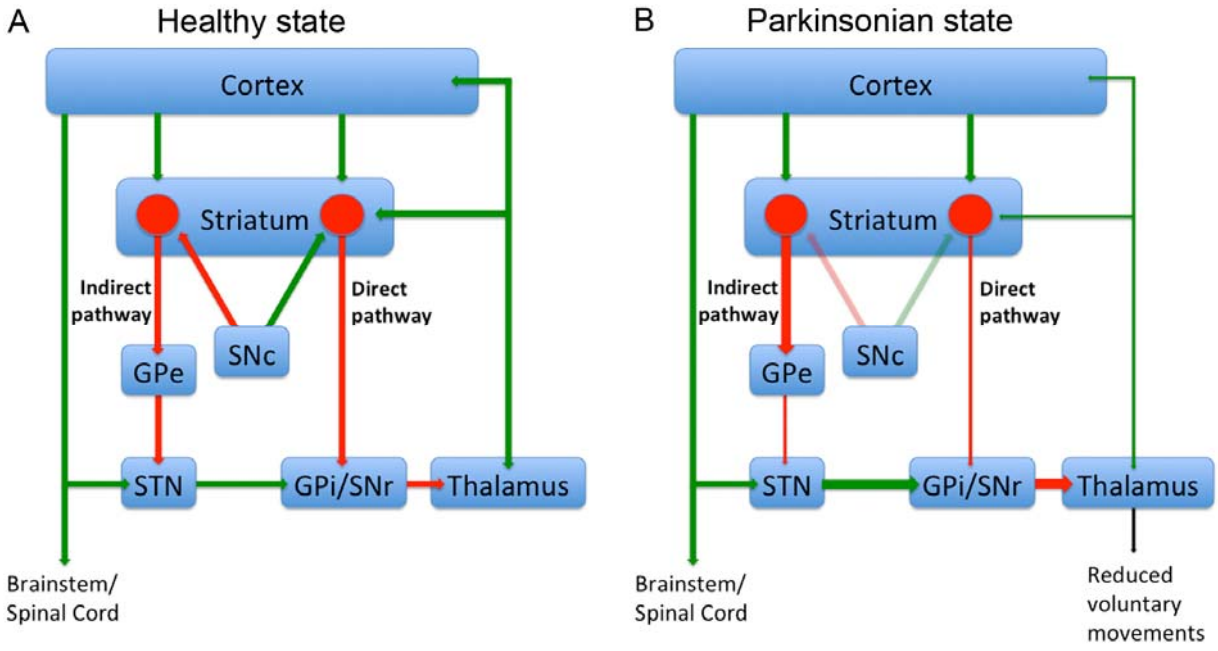

Figure 5. Simplified diagram of basal ganglia motor circuit in healthy and Parkinsonian state. (A) In healthy conditions, the balance between direct and indirect pathways inputs to the BG output structures is regulated by a normal dopamine signal. **(B)** In Parkinsonian state, the lack of dopamine stimulation in the striatum induces reduced activity of the direct pathway and increased activity of the indirect pathway, resulting in a final overactivity of the GPi/SNr and a sustained inhibition of the thalamocortical circuits. Abbreviations: GPe, globus pallidus pars externa; GPi, globus pallidus pars interna; SNc, substantia nigra pars compacta; SNr, substantia nigra pars reticulta; STN, subthalamic nucleus. Adapted from Jenner, 2008 and Lanciego, 2012.

3.4 Clinical features

PD clinical manifestations begin when dopamine concentrations in the striatum fall below 70% and more than the 50% of SNc dopaminergic neurons have been lost (Iravani *et al.*, 2012). The accepted criteria for a clinical diagnosis of PD include the presence of two of the three classical motor features (rest tremor, rigidity and bradykinesia), unilateral onset, a strong clinical response to L-DOPA and the absence of features suggestive of any other motor disorders.

- Motor features

Rest tremor is the most obvious manifestation of PD, occurring in approximately 70% of patients. The typical tremor in PD is a rest tremor, presented mainly when the patient is relaxed and when the tremulous limb is not engaged in purposeful activities. It tends to start unilaterally in the hand, subsequently involving the ipsilateral leg or the contralateral arm. On average, the tremor spreads bilaterally 6 years after the onset of the symptoms and the side initially affected continues to have more tremor than the contralateral side (Rodriguez-Oroz *et al.*, 2009).

Rigidity is characterized by unvarying increased resistance to passive limb movement, due to stiffness or inflexibility of the muscles. It is accompanied by cramps and pain. Rigidity occurs in 89-99% of patients with PD and responds better to L-DOPA treatment than the other two classical motor features of PD.

Bradykinesia, meaning slowness of movements, is the major cause of disability in PD and is eventually seen in all patients. In general, bradykinesia manifests first as a delay in the initiation of movement and is responsible for many characteristic symptoms of PD, such as micrographia, hypophonia (weak voice or whispering), masked face and drooling, decreased blink rate and slow shuffling gait.

- Non-motor features

Non-motor symptoms may include depression and anxiety, sleep disturbance, olfactory dysfunction, behavioral and cognitive impairment and autonomic dysfunction, such as urinary difficulties, constipation, sexual disturbances and cardiovascular changes (Chaudhuri and Schapira, 2009). The appearance of some of these symptoms precedes the development of the classic motor effects.

3.5 Treatment

Presently, despite extensive investigation aimed at finding new therapeutic approaches that slow or reverse the progression of the disease, PD is still incurable and progressive. However, therapeutic strategies to control motor symptoms are wide and include a high variety of pharmacologic agents as well as surgical treatments.

- L-DOPA

3,4-dyhydroxyphenyl-L-alanine (L-DOPA) remains the most effective and noninvasive therapy for alleviating motor symptoms in PD (Figure 6). As a precursor of dopamine, L-DOPA crosses the blood-brain barrier via neutral amino acid transporters. It is decarboxylated to

dopamine in the nigrostriatal pathway by dopa-decarboxylase before being stored in synaptic vesicles for subsequent release. In the peripheral system, dopamine provokes prominent adverse side effects, especially nausea and hypotension, limiting the utility of L-DOPA when it was first introduced. For that reason, L-DOPA is most commonly used in combination with a peripheral decarboxylase inhibitor, carbidopa or benserazide, which do not cross the blood-brain barrier and hence selectively block conversion of L-DOPA to dopamine outside the brain. The precise places where L-DOPA is decarboxylated in the Parkinsonian brain remains unclear, as most striatal dopamine terminals are degenerated. It has been postulated that exogenous L-DOPA can be decarboxylated and released as dopamine by serotonin terminals, striatal capillaries, noradrenergic neurons, and monoaminergic striatal interneurons (Bezard *et al.*, 2013) as well as in tyroxine hydroxylase (TH)-containing striatal neurons (Darmopil *et al.*, 2008; Espadas *et al.*, 2012). In addition, L-DOPA produces some pharmacological actions not through conversion to dopamine (Porras *et al.*, 2014) including antiparkinsonian effect (Alachkar *et al.*, 2010).

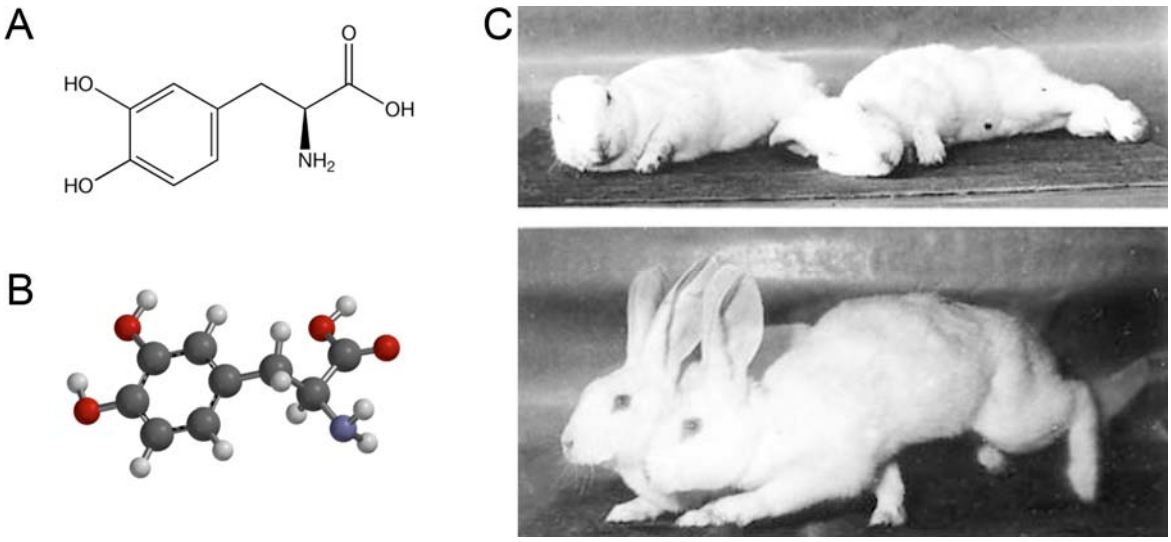

Figure 6. Reversal of dopamine depletion by L-DOPA. (A) Chemical formula and **(B)** three-dimension structure of L-DOPA. **(C)** Rabbits treated with reserpine before (top) and after (bottom) L-DOPA administration. Adapted from Carlsson, 2001. Carlsson was awarded the Nobel Prize in Physiology or Medicine in 2000 for his works on dopamine. In 1957, Carlsson and colleagues described for the first time that L-DOPA treatment restores the Parkinsonism induced by reserpine. It took another 10 years for L-DOPA to become the standard for the treatment of PD. The first large study reporting improvements in PD patients treated with L-DOPA was published in 1968 (Cotzias, 1968).

Initial treatment with L-DOPA leads to an effective and sustained control of motor symptoms of PD during a period of time often referred to as the "honeymoon period" which may last for up to 5 years. However, chronic pulsatile administration of L-DOPA and disease progression lead to a shorter, more unpredictable and inadequate response that results in motor complications in approximately 70 % of patients within 6 years of initiation of treatment. These

motor complications include a shortened duration of drug benefit termed "wearing off" and drug-induced abnormal involuntary movements known as dyskinesias (Obeso *et al.*, 2000; Pavón *et al.*, 2006; Stocchi *et al.*, 2010). The "wearing off" state in which a formerly effective dose is no longer as effective as before and PD symptoms return occurs when the plasma levels of L-DOPA decline (Figure 7). Over time, this phenomenon becomes more frequent as benefits of each dose become shorter, leading the onset of "wearing off" state before the next dose of L-DOPA. On the other hand, dyskinesias may occur at the time of maximal clinical benefit and peak concentration of L-DOPA (peak dose dyskinesias) or appear at the beginning and at the end of the dose (diphasic dyskinesias). The mechanisms by which dyskinesias develop are not yet fully understood but pulsatile stimulation of dopamine receptors and progressive striatal denervation are implicated.

These complications can be an important source of disability for some patients and in fact, they are the main cause of treatment discontinuation. Therefore, dyskinesias represent one of the main challenges to the symptomatic antiparkinsonian therapy.

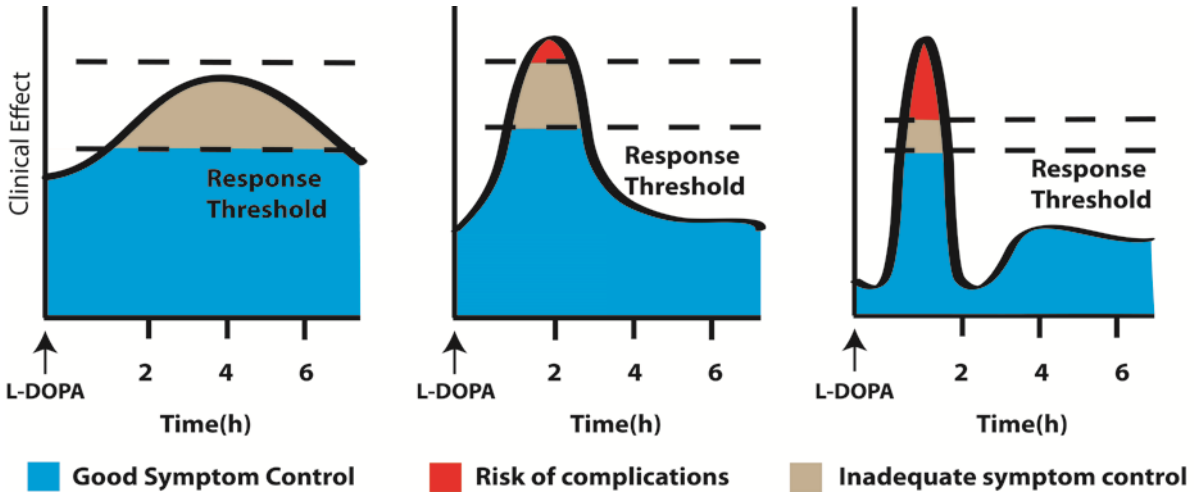

Figure 7. Changes in L-DOPA response over time. Early PD is associated with a prolonged response to L-DOPA. Chronic treatment and disease progression lead to a shorter duration of action with wearing off of motor benefit prior to the next dose. Peak dose dyskinesias begin to appear. As neurodegeneration advances and the adverse effects of L-DOPA accrue, clinical response becomes ever shorter and unpredictable, with more pronounced dyskinesias. Modified from Schapira *et al.*, 2009.

- Other treatments

Dopamine agonists are being used as monotherapy in early PD or in combination with L-DOPA in more advanced stage. They are more frequently chosen as initial therapy for PD in younger patients (<50 years of age), to help delay L-DOPA treatment. The mechanism of action of dopamine agonists involves direct stimulation of dopamine receptors. The list of dopamine agonists used today is wide and includes ergoline compounds, such as bromocriptine, pergolide,

cabergoline and lisuride, and nonergoline compounds, such as pramipexole, ropinirole, rotigotine, piribedil and apomorphine. Dopamine agonists are more likely than L-DOPA to cause cognitive side effects, such as confusion, hallucinations and impulse-control disorders.

The dopamine metabolism inhibitors are used in conjunction with L-DOPA, extending its central bioavailability and allowing a more continuous delivery of L-DOPA to the brain. This group includes the *monoamine oxidade (MAO)-B inhibitors* such as selegiline and rasagiline and the *Catechol-O-Methyltransferase (COMT)* inhibitors entacapone and tolcapone. They prevent catabolism of dopamine in the brain and the peripheral metabolism of L-DOPA, respectively.

Amantadine was first introduced as an antiviral agent for the treatment of influenza and its anti-parkinsonian effects were discovered serendipitously. Currently, it is the only antidyskinetic agent for the treatment of L-DOPA-induced dyskinesias (LID). The exact mechanism of action of amantadine is unknown, although it appears to increase dopamine release and decrease the reuptake, to inhibit the N-methyl-D-aspartate (NMDA) receptor and to have modest anticholinergic activity (Rodnitzky and Narayanan, 2014).

Anticholinergic agents act by blocking acetylcholine receptors and are the oldest treatments still in use for PD. They are useful in alleviation of restring tremor and rigidity.

Stereotaxic surgery, such as ablation and deep brain stimulation of the globus pallidus internus, the thalamus and the subthalamic nucleus is recommended as a treatment for medically refractory motor symptoms in PD and patients with LID (Guridi *et al.*, 2008). Parkinsonian motor disability tends to improve more in patients with younger age, shorter disease duration and less prominent axial symptoms.

Intrastriatal transplants of fetal mesencephalic tissue has been in the latter years one of the most attractive alternatives to treat PD. Clinical trials involving transplantation of embryonic mesencephalic dopaminergic neurons have demonstrated that grafted neurons can survive long-term (Ma *et al.*, 2010), innervate the denervated striatum (Kordower *et al.*, 1995), release dopamine (Piccini *et al.*, 1999) and become functionally integrated into host neuronal circuits (Piccini *et al.*, 2000). Unfortunately, they also produce an unknown-caused side effect called graft-induced dyskinesia, which has limited this therapeutic approach (Steece-Collier *et al.*, 2012). In addition, surviving grafted neurons in patients who died 12 to 16 years after the transplant procedure contained pathologic LB-like inclusions (Kordower *et al.*, 2008; Li *et al.*, 2008), supporting the idea that PD could be a prion-like disorder.

Genetic therapies are nowadays the new field of intense research in regenerative medicine not only for PD but for other neurodegenerative disorders.

3.6 Animal models of PD

There are many different animal models utilized in PD and basal ganglia research. None of them directly replicates all the features of human disease with respect to behavioral characteristics, brain anatomy, pathology and disease progression, but they have provided valuable insight into disease mechanisms and have led to significant advancements in the therapeutic treatment. Animal models of PD include pharmacologically-induced models (e.g., reserpine and α-methyl-para-tyrosine), neurotoxicant-induced models (e.g., MPTP and 6-OHDA), genetic models (e.g., alpha-synuclein overexpressing mice and Pitx3 knockout mice) and viral models. The 6-OHDA model and a transgenic Pitx3-deleted model have been used for the accomplishment of the specific aims of this thesis:

6-hydroxydopamine (6-OHDA) model. 6-OHDA is a specific catecholaminergic neurotoxin structurally analogous to both dopamine and noradrenaline. It has been widely used in rodents for basic research on PD since the late sixties when Ungerstedt and colleagues performed the first stereotaxic injections into the nigrostriatal pathway (Ungerstedt, 1968). Acting as a "false substrate", 6-OHDA is taken up by dopaminergic and noradrenergic transporters into monoaminergic neurons and is accumulated in the cytosol. The mechanisms of 6-OHDA toxicity are complex and involve different biochemical features including alkylation, rapid auto-oxidization that leads to the generation of reactive oxygen species and quinones, and impairment of mitochondrial energy production. Dopaminergic cell groups in the midbrain exhibit different sensitivities to 6-OHDA. Thus, those in the SNc are the most susceptible whereas tuberoinfundibular neurons are almost completely resistant. While clearly useful, the 6 -OHDA model also has some limitations. For instance, LB formation has not been reported in this model.

Since 6-OHDA cannot cross the blood-brain barrier, it must be directly delivered by stereotaxic administration into the SN, the median forebrain bundle (MFB) or the striatum. 6-OHDA lesions in the SN or the MFB induce neuronal degeneration starting within 24 hours. When 6-OHDA is injected into the striatum it is retrogradely transported to the dopaminergic cell bodies of the SN, where it produces a partial and slow degeneration of dopaminergic nigrostriatal neurones lasting 1-3 weeks. Bilateral administration of 6-OHDA produces a high degree of animal morbidity and mortality. Consequently, unilateral intracerebral injections are commonly used. Unilateral lesioning results in minimal postoperative mortality and behavioral asymmetry. In addition, a non-lesioned side may serve as a control. Approximately 90% dopamine depletion in the striatum is required before motor abnormalities are manifested, resembling what is found in clinical PD.

Genetic model: Aphakia mice. Pitx3-deficient aphakia mouse provides a faithful genetic model of neuroanatomical features and motor deficits present in PD (Hwang *et al.*, 2005; van den Munckhof *et al.*, 2006; Ding *et al.*, 2007). These mice have a spontaneous mutation in the transcription factor Pitx3, which is required for the specification and/or survival of dopaminergic precursors unique to the SN and not other dopaminergic areas (Nunes *et al.*, 2003). Lack of Pitx3 in Aphakia mice results in an abnormal development of the A9 dopamine neurons and in the selective loss of nigrostriatal dopaminergic projections (Hwang *et al.*, 2003; Nunes *et al.*, 2003; Espadas *et al.*, 2012). Therefore, this model resembles a bilateral striatal lesion and is also suitable for the study of new therapies as well as the motor complications derived from the anti-parkinsonian therapies.

4. L-DOPA-INDUCED DYSKINESIA

L-DOPA-induced dyskinesias are abnormal involuntary movements involving the limbs, trunk, or head. They can be severe enough to significantly impair the patient's life quality and can limit the dose of symptomatic therapy, complicating ongoing management of patients with advancing PD. Patients with earlier-onset PD tend to be more prone to develop LID than patients with later onset (Kumar *et al.*, 2005). LID appears to be a complex set of phenomena; this complexity perhaps explains why, despite extensive research, mechanisms underlying LID are not yet fully understood. Fortunately, a great number of animal models allow us to further investigate both abnormal motor manifestations and molecular alterations in LID. Repeated administration of L-DOPA or other dopaminomimetic compounds to MPTP-treated monkeys (Bedard *et al.*, 1986; Clarke *et al.*, 1987; Pearce *et al.*, 1995) as well as to 6-OHDA-lesioned rats (Cenci *et al.*, 1998; Perier *et al.*, 2003; Marin *et al.*, 2004) and mice (Pavón *et al.*, 2006; Darmopil *et al.*, 2009; Smith *et al.*, 2012; Suárez *et al.*, 2014) leads to development of abnormal involuntary movements within a few days of treatment resembling "peak-dose-dyskinesias" seen in patients.

4.1 Factors implicated in the generation of LID

The major factors implicated in the generation of LID seem to be the extent of nigral dopaminergic cell loss and the intermittent L-DOPA dosing.

Dopamine depletion: Progressive degeneration of nigrostriatal neurons and the consequent dopamine terminal loss and denervation of striatal neurons have been considered to be the pathophysiological basis of dyskinesias (Pavón *et al.*, 2006). Experiments with 6-OHDA -treated rats revealed that a severe depletion of dopaminergic presynaptic terminals is

necessary, while a limited dopaminergic terminal loss is insufficient to develop LID (Papa *et al.*, 1994). Moreover, recent work from Pons' group (2013) indicates that dopamine depletion by itself, instead of neuronal degeneration, is the prerequisite for the development of dyskinesias (Bezard *et al.*, 2013), supporting previous results found in partially or completely denervated striatal areas with 6-OHDA (Pavón *et al.*, 2006). This idea is further supported by the fact that patients with TH deficiency due to an autosomal recessive disorder, with intact dopamine terminals and striatal innervation, develop dyskinesias after chronic L-DOPA treatment (Pons *et al.*, 2013).

Pulsatile L-DOPA stimulation: Intermittent administration of L-DOPA along with its short plasma half-life result in peaks and troughs in plasma levels. In the early stages of PD, the administered L-DOPA can be stored and gradually released by the surviving presynaptic terminals; however, in more advanced PD, the capacity to buffer fluctuating striatal dopamine levels is lost, leading to the appearance of LID. This is supported by the fact that longer acting dopamine agonists (Nutt, 2000) or continuous infusion of L-DOPA produce less dyskinesia (Jenner, 2008).

4.2 Changes in basal ganglia motor circuitry in LID

The combination of extensive destruction of nigrostriatal dopaminergic neurons coupled with intermittent L-DOPA dosing can induce plastic changes in basal ganglia function and provide a substrate for the development of dyskinesias. It is suggested that the reversed scenario than that occurring in PD takes place following L-DOPA administration; thus, D1 and D2 receptors are overstimulated by L-DOPA, leading to overactivity of the direct output pathway and underactivity of the indirect output pathway. This situation induces a reduced activity of the STN and GPi/SNr neurons. The net effect of these imbalances would be a reduced inhibition of thalamocortical neurons and an overactivation of cortical motor areas, responsible for the appearance of abnormal motor activity that characterizes LID (Figure 8).

4.3 Dopamine D1 receptors hypersensitivity

Pharmacologic studies implicate both the D1/D5 and D2/D3 receptor families in the development of dyskinesias. However, D1-like agonists have a more powerful dyskinetogenic effect than D2-like agonists in both PD patients and animal models (Rascol *et al.*, 2001, 2006; Holloway *et al.*, 2004). Along with this, D1-like antagonists are more effective at inhibiting LID than D2-like antagonists (Taylor *et al.*, 2005; Delfino *et al.*, 2007; Westin *et al.*, 2007). Interestingly, previous studies from our laboratory with genetically engineered mice lacking the

D1R showed for the first time that D1R is causally linked with behavioral and molecular markers of LID (Darmopil *et al.*, 2009). Inactivation of D1R completely blocked LID, while D2R knockout mice developed LID as easily as control animals. In addition, it is still possible that D3R, which is abnormally expressed in the striatum after chronic L-DOPA administration, contributes to LID (Bordet *et al.*, 1997; Bezard *et al.*, 2003). However, D3R antagonists do not prevent dyskinetic movements induced by D1R agonists (Kumar *et al.*, 2009; Mela *et al.*, 2010).

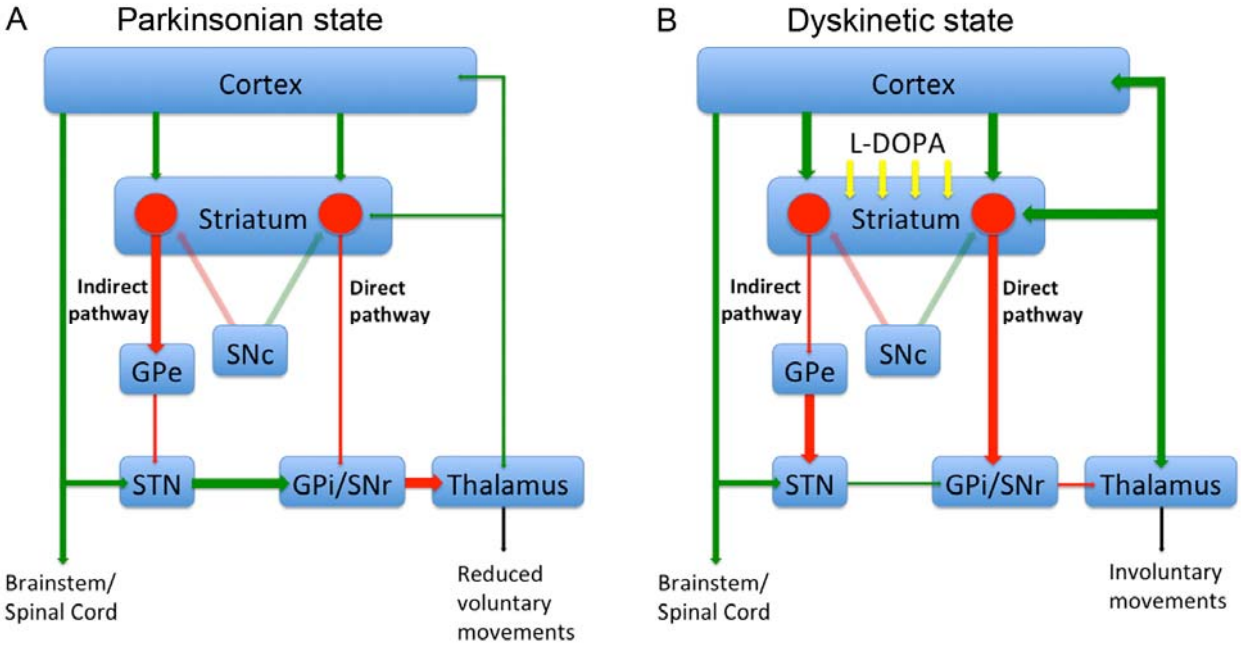

Figure 8. Simplified diagram of basal ganglia motor circuit in Parkinsonian and dyskinetic state. (A) In Parkinsonian state, the lack of dopamine stimulation in the striatum induces reduced activity of the direct pathway and increased activity of the indirect pathway, resulting in a final overactivity of the GPi/SNr and a sustained inhibition of the thalamocortical circuits. **(B)** In LID, dopamine from L-DOPA induces a hyperactivity of the direct pathway and an inhibition of indirect pathway. This results in a higher inhibition of the output structure of the BG and a reduced inhibition of the thalamocortical loop. Abbreviations: GPe, globus pallidus pars externa; GPi, globus pallidus pars interna; SNc, substantia nigra pars compacta; SNr, substantia nigra pars reticulta; STN, subthalamic nucleus. Adapted from Jenner, 2008 and Guridi *et al.*, 2012.

Enhanced synaptic transmission in LID does not appear to be related to an increase in D1R density, but is likely associated with altered redistribution and trafficking of D1R. L-DOPA-treated Parkinsonian monkeys (Guigoni *et al.*, 2007) and rats (Berthet *et al.*, 2009) showed an enhanced expression of D1R at the postsynaptic membrane and in cytoplasmic compartments. Moreover, this phenomenon is not limited to D1R, as both NMDA and AMPA receptors are also "recruited" at the membrane in dyskinetic monkeys (Hallett *et al.*, 2005; Silverdale *et al.*, 2010). These changes are associated with a massive accumulation of the synaptic scaffolding protein PSD-95 in the synaptic membrane (Nash *et al.*, 2005). Interestingly, PSD-95 has been shown to modulate LID in rats and monkeys by its direct

interaction with D1R, since PSD-95 downregulation using lentiviral vectors decreases LID (Porras *et al.*, 2012).

D1R hypersensitivity in 6-OHDA-lesioned rats and PD patients is related to increased levels and binding of Gαolf (Corvol *et al.*, 2004). However, results on Gαolf changes following L-DOPA treatment are controversial. While L-DOPA treatment has been found to reverse the increased Gαolf expression levels seen after striatal denervation in both severe and mild dyskinetic rats (Rangel-Barajas *et al.*, 2011), a more recent study from Dr. Hervé's group reports a persistent enhancement of Gαolf in dyskinetic mice as well as a correlation between LID and Gαolf levels (Alcacer *et al.*, 2012). However, heterozygous mice for the Gαolf protein do not display different dyskinetic behaviour compared to wild type animals (Alcacer *et al.*, 2012), as would have been expected.

In the dopamine-depleted striatum, L-DOPA activates a cAMP-dependent signaling cascade via PKA activation (Lebel *et al.*, 2010; Fisone and Bezard, 2011), resulting in abnormally increased phosphorylation of DARPP-32 at Thr34 in the MSN of the direct pathway (Picconi *et al.*, 2003; Santini *et al.*, 2007, 2010; Bateup *et al.*, 2010) (Figure 9). The increased activation of the cAMP/PKA/DARPP-32 pathway observed in dyskinesia induces persistent phosphorylation of the AMPA receptor subunit GluR1 at Ser845 (Santini *et al.*, 2007, 2012) via PP-1 inhibition, enhancing excitatory glutamatergic transmission in D1R-containing neurons. AMPA receptor transmission has been seen to be implicated in dyskinesia since an AMPA receptor agonist increases LID and an AMPA receptor antagonist reduces it in non-human primates (Konitsiotis *et al.*, 2000). In agreement, DARPP-32 knockout mice not only exhibit reduced LID but also show reduced phosphorylation at Ser845 in GluR1 subunit (Santini *et al.*, 2007).

Induction of the cAMP/PKA/DARPP-32 pathway by L-DOPA also induces the activation of the Ras/ERK signaling pathway in the same neurons (Pavón *et al.*, 2006; Santini *et al.*, 2007, 2012; Schuster *et al.*, 2008; Fasano *et al.*, 2010). Thus, increased phosphorylation of ERK correlates with the intensity of dyskinesias in mice (Pavón *et al.*, 2006; Santini *et al.*, 2007; Schuster *et al.*, 2008; Lindgren *et al.*, 2010).

In addition to D1R-pathway, the Ras/ERK cascade can also be activated by the NMDA receptor (Hayashi and Huganir, 2004; Ivanov *et al.*, 2006). Increasing NMDA receptor activation has been reported following L-DOPA treatment (Chase *et al.*, 2000; Hallett *et al.*, 2005; Gardoni *et al.*, 2006; Silverdale *et al.*, 2010) and the blockade of NMDA/Ras/ERK pathway by lentiviral vectors has been reported to diminish LID in monkeys (Fasano *et al.*, 2010). However, NMDA receptor antagonists do not modify ERK phosphorylation induced by

D1R agonists in the denervated striatum (Gerfen *et al.*, 2002). Thus, these data suggest that D1R plays a more important role than the NMDA receptor in the control of ERK cascade following chronic L-DOPA treatment, as we suggested (Darmopil *et al.*, 2009).

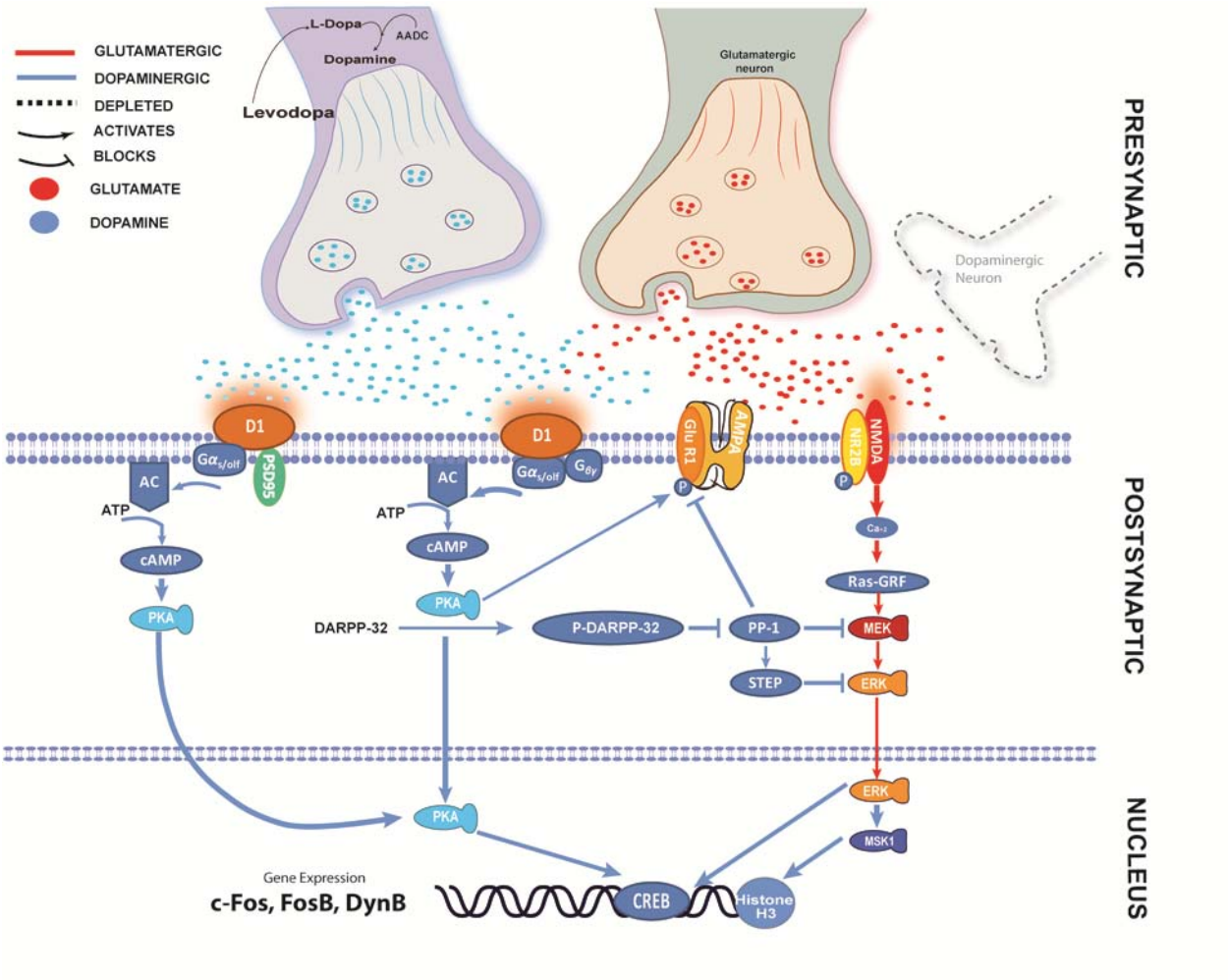

Figure 9. Schematic diagram illustrating D1R and NMDAR signaling cascades involved in L-DOPA-induced dyskinesia. In PD, depletion of dopamine results in increased responsiveness of dopamine D1 receptors. Administration of L-DOPA leads to D1R activation and stimulation of adenylyl cyclase through Gαolf protein, increasing the production of cAMP and activating PKA. PKA phosphorylates various targets, among which the GluR1 subunit of AMPA receptors and DARPP-32. PKA-mediated phosphorylation of GluR1 promotes glutamatergic transmission and is intensified by phosphor-DARPP-32 via inhibition of PP-1. In addition, increased PKA/DARPP-32 signaling as well as stimulation of NMDA receptors lead to activation of Ras/ERK signaling pathway. Phospho-ERK translocation to the nucleus results in phosphorylation/activation of CREB and histone H·. This, in turn, leads to chromatin rearrangements and transcription of immediate early genes, such as c-Fos and FosB, or neuropeptides, such as dynorphin-B. Persistent abnormal activation of theses pathways by L-DOPA appears to be involved in long-term changes responsible for dyskinesia.

ERK activation induced by L-DOPA results in the phosphorylation of the mitogen and stress-activated kinase I (MSK-1) and their targets, the transcription factor cAMP response element binding protein (CREB) and histone H3. Phosphorylation of both has been found to correlate with dyskinesia (Oh *et al.*, 2003; Darmopil *et al.*, 2009). While the signification of CREB phosphorylation remains unclear, since downregulation of CREB with an anti-sense

oligonucleotide does not affect the ability of L-DOPA to induce dyskinesia (Andersson *et al.*, 2001), phosphorylation of acetylated histone H3 has been seen to directly correlates with LID in mice (Santini *et al.*, 2007; Darmopil *et al.*, 2009; Alcacer *et al.*, 2012) and rats (Cenci and Konradi, 2010). Phosphorylation of acetylated histone H3 is involved in chromatin decondensation and regulation of nucleosomal response (Cheung *et al.*, 2000; Soloaga *et al.*, 2003; Harrison and Dexter, 2013). It is therefore likely that the capacity of L-DOPA to enhance the levels of phospho-acetylated-histone H3 in direct pathway neurons is involved in the changes in gene expression that occur specifically in this neuronal population.

These events induce transcriptional changes resulting in increased expression of several genes that are potentially involved in the development of dyskinesias. Among the various genes related to LID, the immediate early gene coding for the transcription factors FosB has received particular attention. Increased FosB expression after L-DOPA is directly linked with dyskinesia in mice (Pavón *et al.*, 2006; Darmopil *et al.*, 2009) rats (Andersson *et al.*, 1999) and macaques (Berton *et al.*, 2009). Recent studies with viral vectors show that LID appears to be dependent mostly on postsynaptic mechanisms mediated by FosB along with its alternatively spliced isoforms, collectively named ΔFosB. Recent work from Berton and collaborators has demonstrated that viral overexpression of a dominant negative ΔFosB in the striatum of dyskinetic macaques dramatically reduced already established LID (Berton *et al.*, 2009). Along with these data, viral vector-induced overexpression of ΔFosB exacerbates LID in the rat model of PD (Cao *et al.*, 2010).

Increased levels of FosB/ΔFosB induced by chronic L-DOPA treatment are involved in the concomitant up-regulation of mRNA encoding for the opioid neuropeptide dynorphin (Andersson *et al.*, 1999). Fos/Jun heterodimers activate a noncanonical AP-1 site in the prodynorphin gene (Naranjo *et al.*, 1991), inducing its transcription. Thus, it is consistently reported in the literature that L-DOPA induces dynorphin expression in PD patients (Piccini *et al.*, 1997), MPTP-treated monkeys (Tamim *et al.*, 2010) and 6-OHDA-treated mice (Darmopil *et al.*, 2009). Dynorphin, through presynaptic κ receptors on subthalamic nucleus projections, reduces glutamate release in the GPi and SNc. Enhanced opioid transmission is related with a reduction of the output inhibitory from GPi, facilitating the appearance of LID (Lavin and Garcia-Munoz, 1986; Piccini *et al.*, 1997). These results are strengthened by the fact that naloxone (an opioid receptor antagonist) has been found to alleviate L-DOPA-induced dyskinesias in PD patients (Sandyk and Snider, 1986) and MPTP-treated monkeys (Klintenberg *et al.*, 2002) and tardive dyskinesia in rodents (Stoessl *et al.*, 1993). However, the effects of opioid receptor antagonists on LID are contradictory (Samadi *et al.*, 2006) and the precise role

played by increased opioid transmission in dyskinesia remains unclear.

In addition, D1R-mediated activation of adenylyl cyclase/PKA triggers calcium entry through voltage-dependent calcium channels (Surmeier *et al.*, 1995) and treatment with the L-type calcium channel antagonist isradipine diminishes dyskinesias (Schuster *et al.*, 2009), further supporting the idea that calcium entry into direct pathway striatal neurons after D1R stimulation contributes to LID.

Altogether, L-DOPA-induced hyperactivation of D1R signaling pathway is directly implicated in LID generation. Inhibition of this pathway at different levels is therefore considered an attractive target to treat LID in PD patients. However, interventions in this signaling cascade may also deregulate a wide range of neuronal functions. Based on these accounts, it seems logical to propose that interventions downstream from this pathway would have a clear advantage in finding a suitable target for LID.

5. DREAM protein

The downstream regulatory element antagonist modulator (DREAM) is a calcium binding protein which belongs to the Neuronal Calcium Sensor (NCS) protein family (Burgoyne and Weiss, 2001). It was first cloned by Dr. Naranjo's group in the search for nuclear proteins that regulate the transcription of human prodynorphin gene (Carrión *et al.*, 1999). DREAM is also known as calsenilin, as it binds presenilin and may promote amyloidogenesis (Buxbaum *et al.*, 1998; Lilliehook *et al.*, 2003) and KChIP3, one of the four members of the voltage gated Potassium Channel Interacting Protein subfamily of NCS (An *et al.*, 2000), which interact with Kv4 potassium channels to regulate their membrane expression and gating.

The mouse DREAM cDNA shares an overall identity of 85% with its human counterpart and, at the amino acid level, mouse and human proteins are 91% identical (Spreafico *et al.*, 2001). The full length DREAM protein consists of 256 amino acids with a predicted molecular mass of around 32 kDa. It contains four EF-hands of which three (II, III and IV) bind calcium while the first one is a non-canonical and not functional EF-hand. DREAM protein can also interact with other proteins through two leucine-charged residue rich domains (LCD) located in positions 47 and 155. Binding of DREAM to calcium or to proteins regulates its physiological functions.

DREAM is expressed in all embryonic stages and in adult mice in the central and peripheral nervous system and in other tissues such as heart, thymus, gonads and thyroid. RT-PCR and *in situ* hybridization experiments (Spreafico *et al.*, 2001; Xiong *et al.*, 2004) showed a

diffuse expression in almost all brain regions.

DREAM plays different roles depending on its subcellular localization. In the nucleus, DREAM acts as a mediator of calcium- and cAMP-dependent transcriptional responses (Ledo *et al.*, 2000a) and regulates activity-dependent gene expression through direct interaction with regulatory sites in the DNA (Carrión *et al.*, 1999). The initial downstream regulatory element (DRE) sequence was first found in the promoter region of the human prodynorphin gene (Carrión *et al.*, 1998). It was defined as the element responsible for its basal and induced expression and was localized within the first exon in the 5' untranslated region of the gene, only functional when located downstream from the TATA box (i.e., initiation transcription site). In basal conditions, DREAM binds as a tetramer to the DRE site in the promoter of target genes, repressing their transcription. The protein is also capable of binding to the DRE sequence as a monomer or as a dimer, but with lower affinity.

DREAM-mediated repression of target genes can be reversed upon cellular stimulation by two different mechanisms. Following an increase in intracellular calcium, DREAM detaches from DNA allowing transcription (Carrión *et al.*, 1999) (Figure 10A). Previous works have demonstrated that mutation of two key amino acids within any of the three functional EF-hands results in mutated forms of DREAM insensitive to calcium that stay bound to DRE sites, blocking the transcription process (Savignac *et al.*, 2005).

In addition to calcium and independently of it, transcriptional repression can be reversed by the direct interaction between DREAM and the nucleoproteins α and ε CREM, the cAMP responsive element modulators (Ledo *et al.*, 2000b) (Figure 10B). The phosphorylation of α and ε CREM by PKA strengthens the interaction between both proteins but is not required for the detachment of DREAM from the DRE sites. Site-directed mutagenesis of one residue in any of the LCD of DREAM blocks the interaction with CREM and produces DREAM mutants insensitive to PKA-dependant derepression (Ledo *et al.*, 2000b).

Besides the direct repression of transcription by binding to DRE sites in the DNA, DREAM can also regulate CRE-mediated transcription (Ledo *et al.*, 2002). In absence of calcium, DREAM binds to CREB, avoiding the CREB-CBP interaction and blocking CRE-mediated transcription. Upon calcium stimulation, DREAM detaches from CREB, allowing transcription. Thus, DREAM represents a point of cross talk between cAMP and calcium signaling pathways in the nucleus.

The non-transcriptional effects of DREAM have been shown to regulate cell function and synaptic activity, mostly through a variety of specific protein-protein interactions outside the nucleus (Rivas *et al.*, 2011). The list of target proteins includes cationic channels (An *et al.*,

2000), membrane receptors such as the NR1a C terminus subunit of the NMDA receptor (Rivas *et al.*, 2009; Zhang *et al.*, 2010) and membrane docking proteins such as PSD-95 (Wu *et al.*, 2010), thus inhibiting NMDA receptor activity and its surface expression.

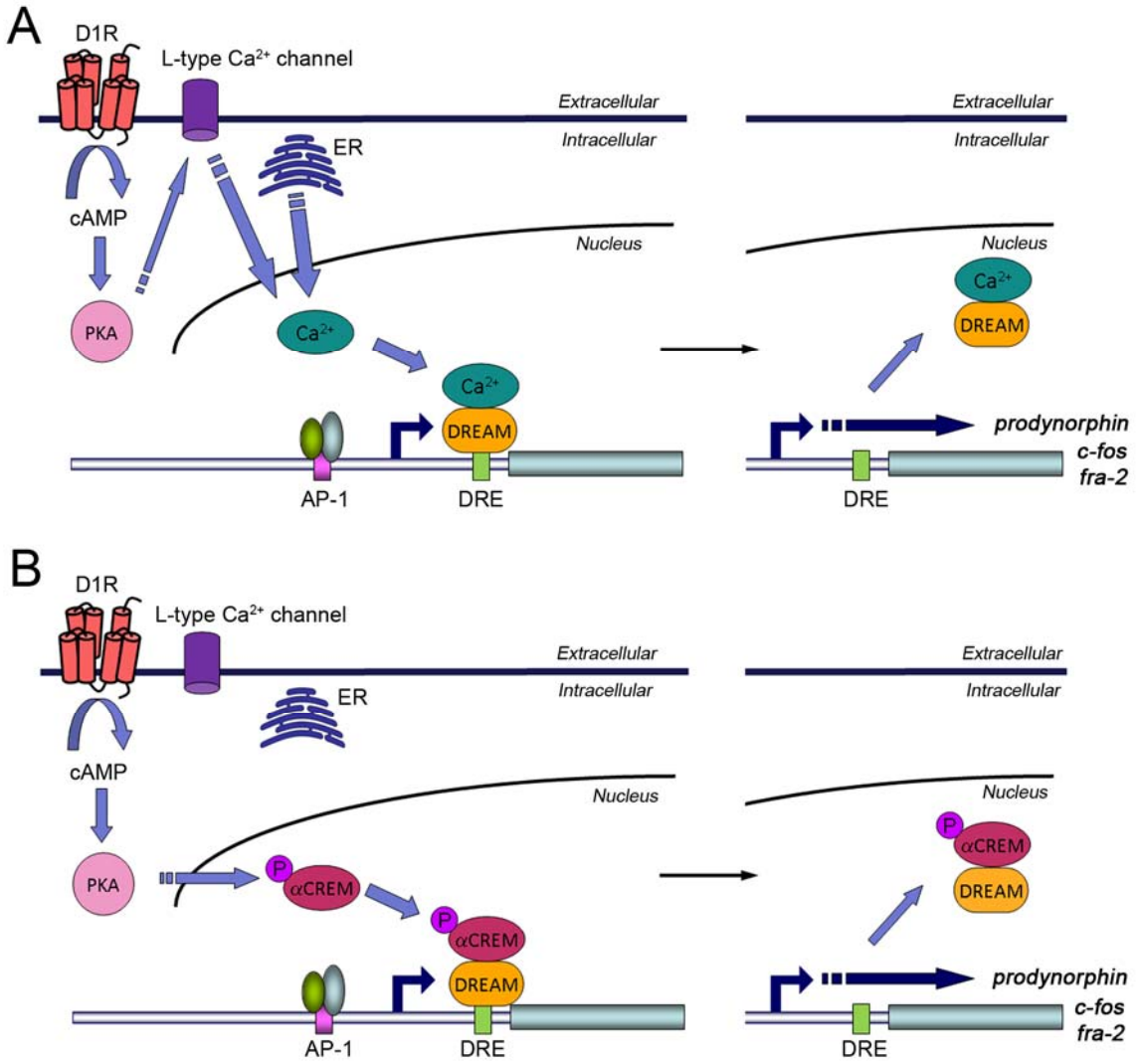

Figure 10. Repression of target genes by DREAM can be reversed by calcium and CREM. In the nucleus, DREAM represses gene expression through direct interaction with DRE sites in the DNA. **(A)** Following an increase in intracellular calcium, DREAM binds to calcium and detaches from DNA, allowing transcription of target genes. **(B)** In addition to calcium and independently of it, transcriptional repression by DREAM can be reversed by the direct interaction between DREAM and the nucleoproteins α and ε CREM.

Based on these observations and on the previous data demonstrating a close association between LID and overexpression of FosB and dynorphin-B (Pavón *et al.*, 2006; Darmopil *et al.*, 2009), we propose that DREAM, located downstream of D1R-dependent cAMP/PKA activation, plays an important role in the cascade of molecular events leading to LID. If this is so, DREAM could provide a site for intervention to improve the efficacy of L-DOPA treatment while preventing the upregulation of target genes associated with dyskinesia.

Hypotheses & Objectives

HYPOTHESES

1. Dopamine differentially regulates striatal Gαolf expression through D1 and D2 receptor signaling.

2. DREAM protein activation diminishes L-DOPA-induced dyskinesias, decreasing D1R-dependent signaling, by transcriptional and non transcriptional mechanisms.

GENERAL OBJECTIVES

1. To elucidate the role of dopamine-dependent signaling in striatal Gαolf expression.

2. To determine the role of DREAM protein in L-DOPA-induced dyskinesias and in the associated molecular changes in hemiparkinsonian mice.

SPECIFIC OBJECTIVES

1.1 To establish the role of dopamine in striatal Gαolf expression using 6-OHDA-lesioned mice or aphakia mice.

1.2 To investigate the role of dopamine receptors in striatal Gαolf expression using D1R and D2R knockout mice.

2.1 To analyze the impact of DREAM genetic modulation on L-DOPA-induced dyskinesias.

2.2 To examine whether DREAM activation diminishes L-DOPA-induced dyskinesias by decreasing cAMP-dependent transcription of FosB and dynorphin-B in striatal neurons.

Materials & Methods

1. ANIMALS

During the development of this thesis, adult mice of 3-6 months of age and 25-30 g weight at the beginning of the experiments were used (Cajal Institute, CSIC, Madrid, Spain). Experiments for the study of Gαolf protein expression were performed in mice lacking D1 receptor ($D1R^{-/-}$) (Moratalla *et al.*, 1996b; Centonze *et al.*, 2003; Granado *et al.*, 2008b; Espadas *et al.*, 2012), D2 receptor ($D2R^{-/-}$) (Kelly *et al.*, 1997; Darmopil *et al.*, 2009; Granado *et al.*, 2011; Murer and Moratalla, 2011; Espadas *et al.*, 2012) and in Pitx3-deficient aphakia mice ($Pitx3^{-/-}$) described previously by Smidt and colleagues (2004).

The study of the DREAM protein was carried out in transgenic mice expressing a dominant active mutant DREAM (daDREAM) (Gomez-Villafuertes *et al.*, 2005; Savignac *et al.*, 2005) or in $DREAM^{-/-}$ deficient mice (Cheng *et al.*, 2002; Cebolla *et al.*, 2008) provided by Dr. Jose Ramón Naranjo from Centro Nacional de Biotecnología (CNB, CSIC, Madrid). In the daDREAM transgenic mice, expression of the transgene, a bi-cistronic construct including the daDREAM mutant, an IRES sequence and the lacZ reporter, was driven by the calcium/ calmodulin-dependen protein kinase type II (CaMK-II) alpha promoter (Mayford *et al.*, 1996). The transgenic line (JN26) used in this study has a telencepahlic-specific expression with high levels of transgene expression in the striatum. Bacterial artificial chromosome (BAC)-transgenic D1R-tomato mice (Suárez *et al.*, 2014) were used to study DREAM striatal localization.

Genetically modified animals and wild-type controls were maintained in a C57-BL/6 background and derived from mating the corresponding heterozygous mice. Genotyping was performed by PCR analysis.

Mice were housed in standard Plexiglas cages with maximally 6 animals/cage with *ad libitum* access to food and water. The environmental conditions were strictly controlled, with a 12 hours light/dark cycle, temperature of 22°C±2 and 44%±2 humidity.

Experimental protocols were designed in order to minimize the number of mice used in these studies as well as their discomfort. All animal procedures followed guidelines from European Union Council Directive (86/609/European Economic Community) and experimental protocols were approved by the CSIC Ethics Committee.

2. DOPAMINE DENERVATING LESIONS

Insomuch as 6-OHDA produces selective degeneration of catecholamine neurons, mice received an intraperitoneal injection of 20 mg/kg of the noradrenaline reuptake inhibitor

desipramine hydrochloride (Sigma-Aldrich, St. Louis, Missouri, USA) thirty minutes before lesion (Breese and Traylor, 1971) in order to protect the noradrenergic neurons from 6-OHDA neurotoxicity and to achieve specific dopaminergic lesions.

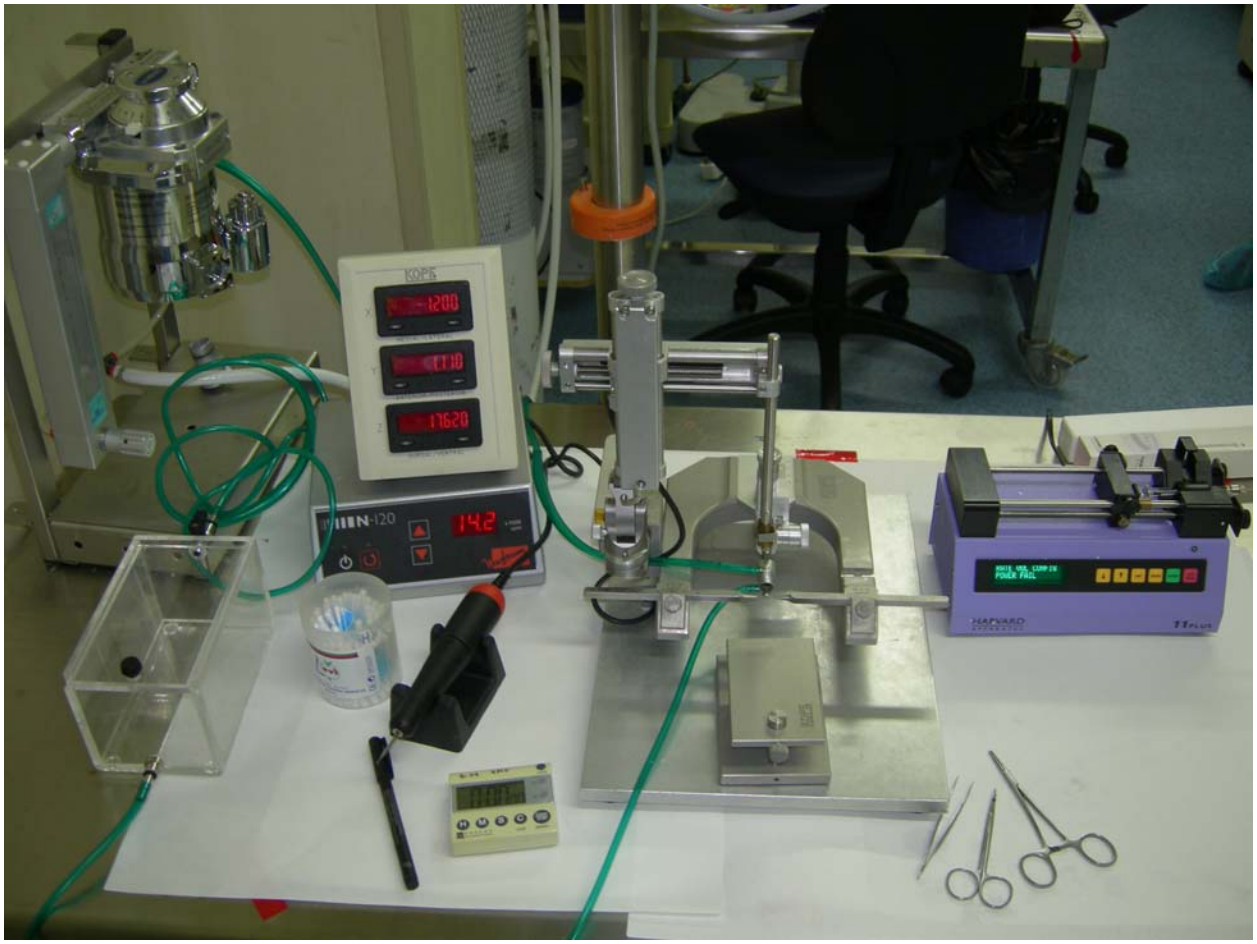

Figure 11. Stereotaxic instrument to 6-OHDA lesion procedure. Mice were mounted on a stereotaxic frame equipped with a mouse adaptor and maintained under isofluorane anesthesia. A hole was drill on the skull and 6-OHDA was injected using a Hamilton syringe connected to a pump.

Animals were anesthetized with 2% v/v isoflurane at a flow rate of 0.4-0.6 l/min oxygen, placed in a stereotaxic frame equipped with a mouse-adaptor (Kopf Instruments, Tujunga, CA, USA) and kept anesthetized using 1-1.5% v/v isoflurane (Figure 11). Antibiotic cream or vaseline were used to protect the eyes from drying during surgery. Using a 10 µl Hamilton syringe (Hamilton, Bonaduz, Switzerland), animals received unilateral stereotaxic injections (2 x 2 µl) of 6-OHDA-HBr (5 µg/µl, 20 mM, containing 0.02 % ascorbic acid; Sigma -Aldrich) at the following coordinates (mm from bregma and dural surface; cf. Paxinos and Franklin 2004): AP = +0.65, L = -2 and V = -4 and -3.5, targeting the left dorsolateral striatum. For each deposit, toxin was infused at 0.5 µl/min flow rate and the needle was left in place for 10 minutes before being slowly removed, in order to favor 6-OHDA diffusion and to avoid

reflux along the track. After the injection, the skin was sutured and the animals, once removed from the stereotaxic instrument, were placed in a clean cage on a heating pad until complete recovery from anesthesia. During the days following surgery, mice received subcutaneous injections of saline solution to prevent dehydration, as well as supplementary food and hand-feeding when necessary.

3. L-DOPA TREATMENT

All drugs used in these studies were dissolved in saline solution (0.9% w/v NaCl) and intraperitoneally (i.p.) administrated in a final volume of 10 ml/kg body weight.

Mice were left to recover 3 weeks after the lesion and then were submitted to L-DOPA methyl ester (Sigma-Aldrich) treatment during the following 3 weeks. Animals received a daily intraperitoneal injection of 25 mg/kg of L-DOPA 20 minutes after benserazide hydrochloride (10 mg/kg body weight, Sigma-Aldrich), a peripheral blocker of the DOPA decarboxylase. This protocol of administration has been previously seen to induce a gradual development of dyskinetic-like movements described in 6-OHDA lesioned rats (Winkler *et al.*, 2002) and mice (Lundblad *et al.*, 2004; Pavón *et al.*, 2006).

4. BEHAVIORAL ANALYSIS

4.1 Locomotor activity

We carried out spontaneous locomotor activity tests in basal conditions (i.e. before 6-OHDA lesion) to rule out any motor impairment in our DREAM mutant mice that could interfere with L-DOPA behavioral studies. To achieve this goal, we analyzed horizontal and vertical activity as well as total distance traveled during 60 minutes using a multicage activity monitoring system (AccuScan Instruments, Inc.; Versamax Software) with a set of 8 individual cages measuring 20 x 20 x 28 cm. Horizontal movements were detected by 2 arrays of 16 infrared beams spaced 2.5 cm, whereas a third array positioned 4 cm above the floor detected vertical movements. The software allowed a distinction to be made between repetitive interruptions of the same photobeam and interruptions of adjacent photobeams. Thus, horizontal and vertical activities were measured as the total number of beam interruptions that occurred in the horizontal and the vertical sensor respectively during the sample period while the total distance indicates the distance traveled in centimeters and is used as an index of ambulatory activity.

Mice were habituated to the cages in 1 hour sessions for 2 days to avoid exploratory

behavior due to the novel environment. The third day, animals were recorded for 1 hour during the light phase of the light-dark cycle.

4.2 Motor coordination

To further study motor function in our mutant mice, animals were submitted to the rotarod test (Ugo Basile, Varese, Italia). The rotarod is a beam that can rotate at a fixed or an accelerated speed. Mice are placed on the beam and their latency to fall off the rod provides a measurement of their motor coordination. To test our animals we used an accelerating version of the test, with increasing speed from 4 to 40 rpm over a 5 minutes period.

Before the test, animals were habituated to the rotarod for 30 seconds in the immobile rod followed for 1 minute in a low fixed speed. If the mouse fell from the rotarod during the training session, it was placed back. Then the performance of the mice was tested in 6 consecutive trials 20 minutes apart (Figure 12A).

This test was also used to measure the antiparkinsonian effect of the L-DOPA. To achieve this goal, mice were tested before 6-OHDA (naïve), 3 weeks after lesion (parkinsonian) and during L-DOPA treatment (dyskinetic) on day 9, 24 hours after the last L-DOPA injection in order to avoid exhaustion and the peak dyskinesia, which could interfere with the performance of the test. It is noteworthy that the parkinsonian condition should be measured when the animals are completely recovered from the surgical intervention and when the plastic changes caused by dopamine cell degeneration have stabilized.

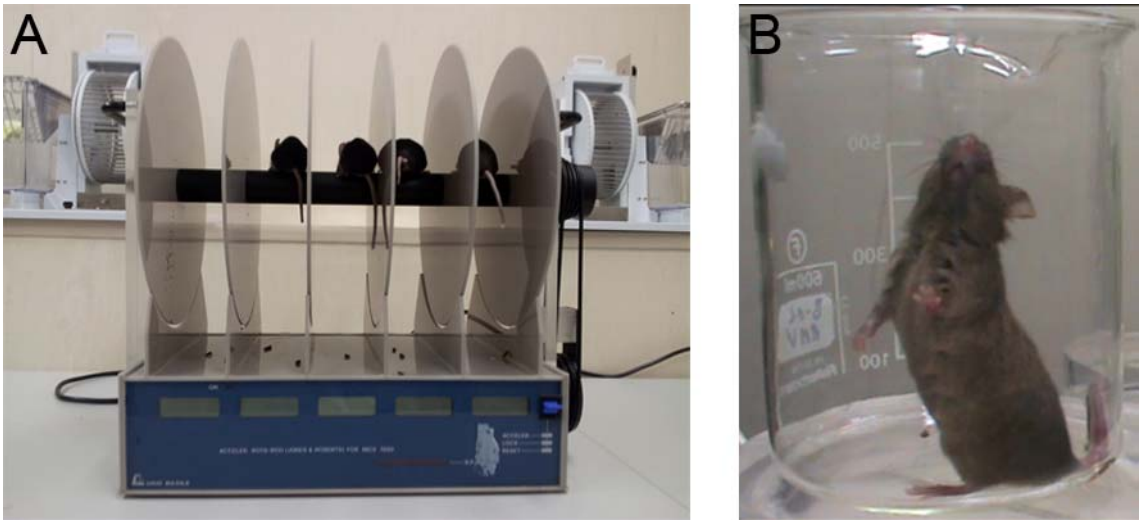

Figure 12. Rotarod and cylinder tests. (A) The rotarod test is used to evaluate motor coordination. Mice are placed in the rotating rod and their latency to fall off the rod provides a measurement of their motor coordination. **(B)** The cylinder test is frequently used to evaluate forelimb akinesia and asymmetry in unilateral rodent models of PD. Mice are placed in a glass cylinder and the number of wall contacts performed independently with the left and the right forepaw are counted per session.

4.3 Cylinder test

The cylinder test is frequently used to evaluate forelimb akinesia and asymmetry in unilateral rodent models of PD (Francardo *et al.*, 2011; Espadas *et al.*, 2012). This test takes advantage of the exploratory response that is typical for rodents. A rodent placed in a novel environment will explore the enclosing walls by standing on its hindlimbs and using its forelimbs to support the body against a nearby wall. A measure of limb use asymmetry is obtaining by counting the number of supporting wall contacts that the rodent executes independently with each paw. A unilateral 6-OHDA lesion will cause a notable reduction in the spontaneous use of the contralateral paw, which will be restored by an effective L-DOPA therapy.

For the evaluations, mice were placed individually inside a 10 cm diameter glass cylinder, which was located in front of a mirror, in order to be able to view the mice from all the angles, and videotaped for 3 minutes (Figure 12B). No habituation of the animals to the testing cylinder was allowed before videorecording them. The number of wall contacts performed independently with the left and the right forepaw were counted per session. Only wall contacts where the animal supported body-weight on the paw with extended digits were counted whereas simultaneous ipsilateral and contralateral forelimb touches were excluded from the count. Forelimb asymmetry was expressed as percentage of contra-lateral touches ± SEM over the total number of wall contacts.

Cylinder test was performed before the 6-OHDA lesion (naïve), 3 weeks after lesion (parkinsonian) and on day 17 of the chronic L-DOPA treatment (dyskinetic), 140 minutes after L-DOPA injection to avoid dyskinetic symptoms.

5. L-DOPA-INDUCED DYSKINESIA

L-DOPA-induced dyskinesias were evaluated twice a week for 3 weeks, 40 minutes after L-DOPA administration using a 0-4 severity scale as previously described (Pavón *et al.*, 2006). Mice were placed individually into a 10 cm diameter glass cylinder and videotaped for 4 minutes. The time course of L-DOPA response for each genotype was evaluated on day 20 of chronic treatment, for 1 minute every 20 minutes during 160 minutes post-L-DOPA injection.

As in the rat (Cenci *et al.*, 1998; Winkler *et al.*, 2002) and in the mice model (Lundblad *et al.*, 2004; Pavón *et al.*, 2006), we have separately evaluated four subtypes of dyskinetic symptoms according to their topographical distribution (Figure 13):

- *Locomotive dyskinesia*: Circular asymmetric locomotion, towards the contralateral side to the lesion.
- *Axial dystonia*: Deviation or torsion of the head, neck and trunk towards the contralateral side, leading to a loss of the orthostatic equilibrium, with a choreiform twisting character.
- *Limb dyskinesia*: Jerky movements of the forelimb contralateral to the lesion with choreic or ballistic nature.
- *Orofacial dyskinesia*: Jaw movements more pronounced toward the contralateral side, sometimes including tongue protusion. They are usually complicated by self-mutilative biting of the fur and the skin on the forelimb contralateral to the lesion.

To assess dyskinesia's severity we have used the scale developed previously in rat (Winkler *et al.*, 2002) and adapted to mouse model (Pavón *et al.*, 2006).

Severity rating scale

0: Absent, no dyskinesia.

1: Occasional dyskinetic symptoms, present during less than half of the observation time.

2: Frequent dyskinetic symptoms, present during more than half of the observation time.

3: Continuous dyskinetic symptoms during all the observation time but suppressible by external stimuli, i.e., sudden, noisy opening of the cage or a slow blow to the glass cylinder.

4: Continuous dyskinetic symptoms during all the observation time not suppressible by external stimuli.

Upon uncertainly between two consecutive grades of the scale, the corresponding half score was given.

6. IMMUNOHISTOCHEMISTRY

Following behavioral analysis, mice were sacrificed 3 weeks after 6-OHDA lesion or 1 hour after last L-DOPA administration, by an overdose of pentobarbital (Laboratorios Normon, Madrid, Spain). They were injected intracardially with 0.5 ml of 1 % heparin (Rovi, Madrid, Spain) and perfused with 10 ml of saline solution, followed by 60 ml of 4 % paraformaldehyde in phosphate buffer pH 7.4. The brains were post-fixed for 24 hours and were then transferred to a 0.1 M phosphate buffer solution (PBS) containing 0.02 % sodium azide for storage at 4ªC. Brains were further immersed in 3 % agarose and they were cut in 30-µm-thick coronal sections using a vibratome (Leica, Wetzlar, Germany). They were stored at 4ºC in 0.1 M PBS containing 0.02 % sodium azide, ortavanadate 1mM and NaF 5mM, to avoid phosphoproteins degradation.

6.1 Single antigen DAB immunostaining

Immunostaining was carried out in free-floating sections using a standard avidin-biotin immunocytochemical protocol (Rivera *et al.*, 2002b; Grande *et al.*, 2004). Endogenous peroxidase activity was quenched by incubation for 10 min in 0.1 M PBS containing 0.2% Triton X-100 (PBS-TX) with 3 % hydrogen peroxide. Non-specific binding sites were blocked for 60-90 min with 5-10 % of goat serum in PBS-TX followed by incubation at 4ºC with the indicated primary antibodies (see Table I). After incubation with the primary antibody, the sections were washed and incubated with the goat anti-rabbit biotinylated secondary antibody

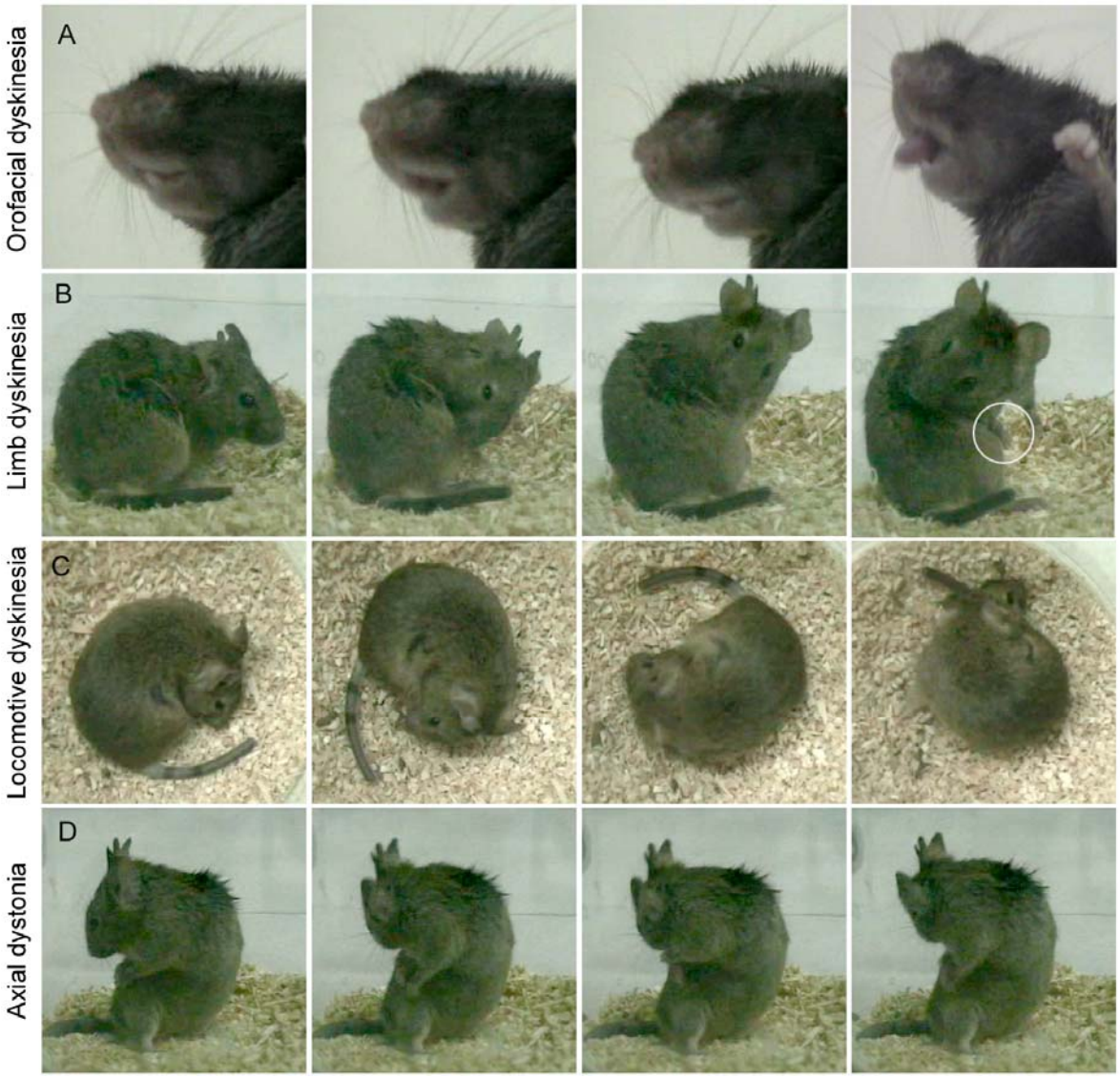

Figure 13. Dyskinetic symptoms induced by chronic L-DOPA treatment in hemiparkinsonian mice. Time-lapse video photographs illustrating representative dyskinetic symptoms 30 minutes after 25 mg/kg L-DOPA administration. **(A)** Orofacial dyskinesia, expressed as tongue protrusion and vacuous chewing movements. **(B)** Limb dyskinesia, seen as jerks on the side contralateral to the lesion. **(C)** Locomotive dyskinesia, manifested as a tendency to turn toward the side contralateral to the lesion. **(D)** Axial dystonia of the trunk toward the contralateral side. Adapted from Pavón *et al.*, 2006.

(1:500, Vector Labs, Burlingame, CA, USA) for 1-2 h at room temperature. After washing, the sections were incubated with streptavidin (Zymed, San Francisco, CA, USA) for 1 h and antibody staining was developed using only DAB (Sigma-Aldrich) for TH, calbindin, Gαolf, DREAM and P-AcH3 or DAB with addition of nickel to intensify the reaction in case of MOR-1, FosB and dynorphin-B immunohistochemistry. After developing the reaction, stained sections were mounted, dried, dehydrated and cover slipped with Permount mounting medium (Fisher Chemicals, Fair Lawn, NJ, USA) and examined using a light microscope (Leica, Heidelberg, Germany).

Primary antibody		Dilution	Incubation	Brand
Rabbit anti-calbindin	Polyclonal	1:1500	1 ON, 4ºC	Millipore
Rabbit anti-DREAM	Polyclonal	1:250	1 ON, 4ºC	Santa Cruz Int
Rabbit anti-DynB	Polyclonal	1:500	3 ON, 4ºC	Dr. Watson Lab
Rabbit anti-FosB	Polyclonal	1:7500	3 ON, 4ºC	Santa Cruz Int
Rabbit anti-Gαolf	Polyclonal	1:4000	1 ON, 4ºC	Dr. Hervé Lab
Goat anti-mCherry	Polyclonal	1:500	1 ON, 4ºC	Acris Antibodies
Rabbit anti-MOR-1	Polyclonal	1:10000	3 ON, 4ºC	Millipore
Rabbit anti-P-AcH3	Polyclonal	1:1500	2 ON, 4ºC	Millipore
Rabbit anti-TH	Polyclonal	1:1000	1 ON, 4ºC	Millipore

Table I. Primary antibodies used for the immunohistochemical studies. ON: Over-night.

6.2 Fluorescent labelling immunostaining

To identify DREAM striatal localization in direct and indirect projection neurons, we used a rabbit DREAM antiserum (1:250, Santa Cruz Biotechnology, Santa Cruz, CA, USA) and a goat mCherry antiserum (1:500, Acris Antibodies, San Diego, CA, USA) which labeled the tomato protein expressed by the direct pathway neurons in our (BAC)-transgenic D1R-tomato mice. The aim of immunolabing the tomato protein is to extend the half-life of the red fluorescence when examined by laser confocal microscopy, as the fluorescence of the native fluorophore is rapidly extinguished under laser excitation.

Free-floating sections were incubated for 1 hour with 10% of donkey serum in PBS-TX followed by an overnight incubation at 4ºC with DREAM antibody diluted in 0.1 M PBS-TX

with 2 % donkey serum. After incubation with the primary antibody, the sections were washed and incubated with the donkey anti-rabbit Alexa 488-conjugated antibody (1:500, Molecular Probes, Invitrogen, Eugene, OR, USA) for 4 hours at room temperature. In order to protect DREAM immunostaining, sections were incubated with 4 % paraformaldehyde in phosphate buffer pH 7.4 for 10 minutes at room temperature before being blocked again with 10% of donkey serum and incubated overnight with mCherry antiserum. Donkey anti-goat Alexa 594-conjugated antibody (1:500, Molecular Probes) was used to detect mCherry. Finally, sections were incubated with Hoechst (1 µg/ml, Sigma-Aldrich) for 10 minutes at room temperature to stain the nuclei.

Sections were mounted in fluorescent mounting medium (DABCO, Fluka, Buchs, Switzerland), coverslipped, kept in the dark at 4 °C until they were examined by laser confocal microscopy (Leica). The specific immunofluorescence of the Alexa 488 or Alexa 568/594 fluorophores was visualized by excitation at 488 nm or 568 nm, respectively.

7. QUANTITATIVE REAL-TIME PCR

Animals were killed by decapitation 1 hour after last L-DOPA administration. Tissue samples from striatum and substantia nigra were stored at -80ºC immediately after obtaining. RNA was extracted and purified with the QuickGene RNA tissue kit S II (RT-S2) and the QG-Mini80 system device (Fujifilm). RNA quality was determined using a NanoDrop. Reverse transcription was performed with 50 ng/µl of RNA using iScript Reverse Transcription Supermix for RT-qPCR kit (BioRad). Quantitative real-time PCR was performed with 25 ng of cDNA and 1 µl of Taqman probes (Applied Biosystems, CA, USA) to detect TH, FosB, PDyn, DREAM, Gαolf and GAPDH and 18S as reference genes, using a 7000 Fast Real-Time PCR system device and TaqMan universal PCR Master Mix (Applied Biosystems). Expression of target genes was normalized using the GAPDH or 18S expression and calculated using the comparative cycle threshold method, $2^{-\Delta\Delta Ct}$, where $\Delta\Delta C_t = (C_{t,\text{target gene}} - C_{t,\text{reference gene}})_{\text{treated}} - (C_{t,\text{target gene}} - C_{t,\text{reference gene}})_{\text{untreated}}$ (Livak *et al.*, 2001).

8. WESTERN BLOTTING

Animals were sacrificed by decapitation 30 min after the last L-DOPA injection. Striatal tissue was dissected, homogenized on ice in 150 µl of lysis buffer [Hepes pH 7.4, 50 mM; NA Pirophsphate 10 mM; Triton 1%; Glycerol 10%; EDTA 2 mM; Ortovanadate 2 mM; NaF 100 mM; protease inhibitor cocktail (Roche Applied Science)]. The homogenates were cleared by

centrifugation for 30 min at 4ºC and 10,000 g. Supernatants were placed into new tubes and the final protein concentration was quantified by the Bradford method (BioRad, Madrid, Spain).

Western blot analyses were carried out with 20 µg of protein, separated on SDS/7.5% PAGE by constant amperage and 100V electrophoresis. Proteins transfer was done onto 0.45 µm polyvinylidene fluoride membranes (Pall Corporation, Pensacola, Florida, USA) with a semy-dry transfer system (Trans-Blot Turbo, Bio-Rad) at 100V and 2.5 A for 30 minutes. After rinsing membranes briefly in water and T-TBS (Tris 20 mM pH 7.4; NaCl 137 mM; Ortovanadate 1 mM; NaF 5 mM; Tween 1%), they were blocked with 5% non-fat dry milk (TH and β-actin detection) or with 10% BSA (P-GluR1 immunoblot) in T-TBS for 1-2 hours and incubated overnight at 4ºC with the indicated antibodies. Immunodetection was performed with primary monoclonal antisera against phospho-Ser845-GluR1 (1:7500; Millipore) and β-actin (1:50000; Sigma-Aldrich) as loading control. Antibody against TH (1:4000; Millipore) was used to prove the 6-OHDA lesion. Blots were incubated for 1-2 hours at room temperature with a peroxidase-conjugated secondary antibody (Vector Labs, Burlingame, CA, USA), developed by enhanced chemiluminiscence (ECL-plus, GE Healthcare, UK) and quantified by densitometric scanning of films (Quantity One, BioRad).

9. QUANTIFICATIONS

9.1 Striatal lesions

Measurement of the extent of the dopaminergic lesion was performed using Neurolucida software (Microbrightfield Bioscience, Williston, Vermont, USA). The borders of the areas of striatum with complete loss of TH-immunoreactive fibers were outlined from a live image with a 4x objective using 7-9 serial rostrocaudal sections per animal. Area of interest was calculated by determining the coordinates of each point around the contour and summing the contained area by the software.

9.2 Nuclear density

Quantification of FosB and P-AcH3 immunoreactivity was carried by nucleus count (Darmopil *et al.*, 2009), with the aid of an image analysis system (AIS, Imaging Research Inc., Linton, England). For both lesioned and unlesioned striatal sides, number of immunolabelled nuclei was determined in 4-6 animals per group using 5 serial rostrocaudal sections per animal and 3 counting frames (dorsal, dorsolateral and lateral) per section (0.091 mm^2 each frame). Images were digitized with Leica microscope under 40x lens. Before counting, images were

thresholded at a standardized gray-scale level, empirically determined by 2 different observers to allow detection of stained nuclei from low to high intensity, with suppression of very lightly stained nuclei. The data are presented as number of stained nuclei per mm^2 (mean ± standard error) in the lesioned and unlesioned striatum.

9.3 Proportional stained area

Quantification of dynorphin-B and Gαolf expression was carried out using an image analysis system (AIS, Imaging Research, Linton, UK) as in Granado *et al.*, 2008c and Ares-Santos *et al.*, 2012. Images were digitized using a light microscope (Leica, Heidelberg, Germany) under 4x lens. The proportional Gαolf-stained area was determined in 4–6 animals per group using 5-7 serial rostrocaudal sections per animal. Images were thresholded at a standardized gray-scale level and the area of staining in the striatum was quantified. Data are presented as the proportional area (total positive area/scan area).

10. STATISTICAL ANALYSIS

Basal locomotor activity and dyskinetic behavioral data were analyzed using two-way ANOVA with repeated measures using genotype and time/trial as variables, followed by planned comparisons (a priori analysis, Newman-Keuls post hoc test). Rotarod and cylinder tests significances were estimated by two-way ANOVA with genotype and trial/treatment as variables, followed by Newman-Keuls post hoc test. Quantifications of immunolabeling were analyzed by two-way ANOVA with genotype and lesion as between-subject variables, followed by Student-Newman-Keuls post hoc test. The extent of the dopaminergic lesion and the mRNA expression were analyzed by one-way ANOVA.

Data are expressed as mean ± standard error of mean (SEM). Differences were considered statistically significant at $p<0.05$.

Results

1. GαOLF EXPRESSION

In rodents, the olfactory type G-protein α subunit (Gαolf protein) couples striatal dopamine D1 receptors and adenosine A2a receptors to adenylyl cyclase, mediating the cAMP production. Alterations in the cAMP-signaling pathway have been reported to directly lead to L-DOPA-induced dyskinesias (Pavón *et al.*, 2006; Darmopil *et al.*, 2009; Lebel *et al.*, 2010; Fisone and Bezard, 2011; Alcacer *et al.*, 2012; Santini *et al.*, 2012). However, despite the progress made in the last decades, changes in Gαolf expression following striatal dopamine depletion and L-DOPA treatment are not yet fully established. The experimental results presented here aim to shed light to the Gαolf regulation by dopamine, as the key protein of cAMP-dependent signaling after D1R activation.

1.1. Pattern of Gαolf expression in basal conditions

We carried out immunohistochemical studies of serial adjacent rostrocaudal sections of adult mice, in naïve conditions, in order to test the specificity of our antibody and to confirm the Gaolf expression pattern described before (Sako *et al.*, 2010).

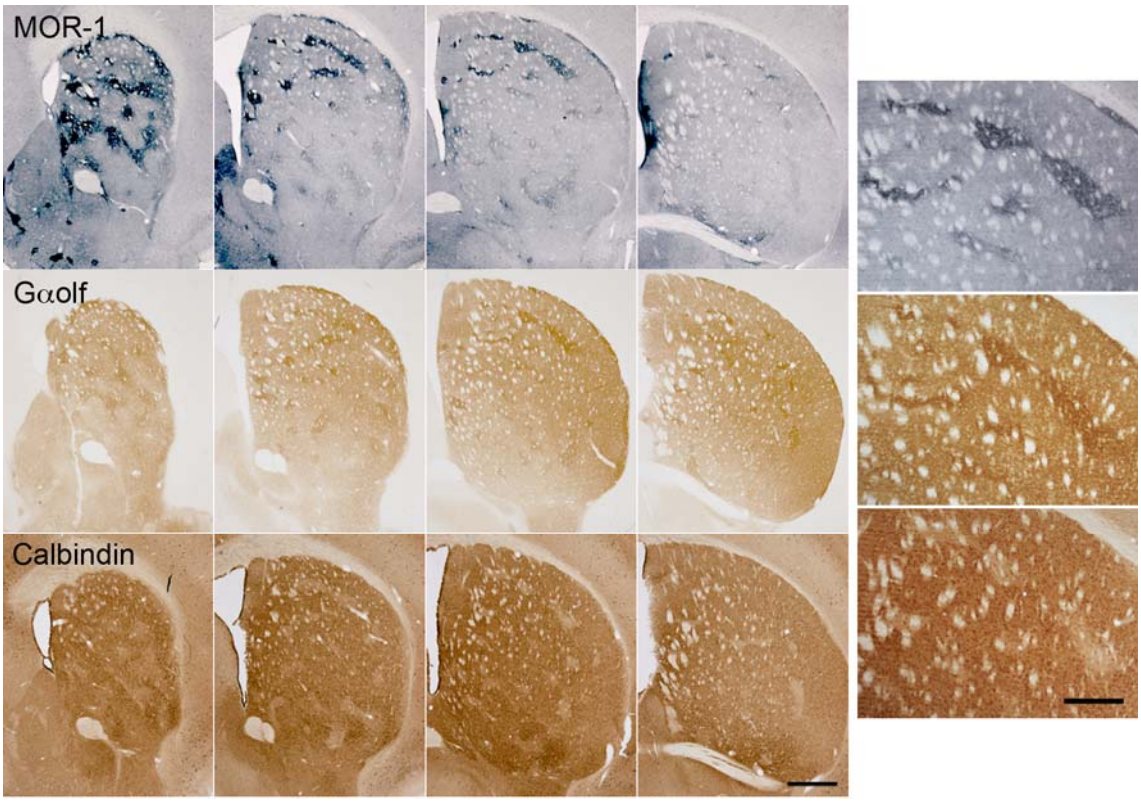

Figure 14. Striatal localization of Gαolf in adult mice. Representative photomicrographs of serial adjacent rostrocaudal brain sections from adult mice immunostained for MOR-1, Gαolf and calbindin. Right panels show an example of striosomes. Notice the higher expression of Gαolf in the striosomes compared to the matrix area. Bars indicate 500 µm and 250 µm.

As expected, Gαolf protein showed a patchy distribution all along the rostrocaudal axis (Figure 14). To confirm that the patches of higher Gαolf expression corresponded with the location of striosomes, adjacent brain sections were immunostained for MOR-1 (μ opioid receptor-1), a marker for striosomes (Breuer *et al.*, 2005; Lawhorn *et al.*, 2009; Tajima and Fukuda, 2013), and for the calcium-binding protein calbindin D_{28K}, a marker for the large matrix compartment surrounding the striosomes (Davis and Puhl, 2011; Watabe-Uchida *et al.*, 2012). This strategy permitted direct comparisons of the Gαolf-positive patches with the striosomes labeled with MOR-1 and with the matrix labeled with calbindin. The zones of heightened Gαolf signal corresponded with the MOR-1-enriched areas and with the calbindin-poor areas, evidencing the compartmentalized distribution of the Gαolf protein in the adult mice striatum.

1.2. Regulation of Gαolf expression by dopamine: Parkinsonian and dyskinetic mice

To examine the role of dopamine in Gαolf expression, we used a mouse model of nigrostriatal dopaminergic denervation with a robust reduction of dopamine levels in the striatum, resembling the loss of dopamine found in the putamen of patients with PD. Wild type mice were submitted to unilateral 6-OHDA striatal lesions to obtain the hemiparkinsonian model. Three weeks after the lesion, when the plastic changes caused by dopaminergic cell degeneration were stabilized, striatal Gαolf expression was investigated by immunohistochemistry. Striatal Gαolf levels in wild type animals were higher in Parkinsonian than in naïve condition (Figure 15A), in agreement with previous results (Hervé *et al.*, 1993; Marcotte *et al.*, 1994; Corvol *et al.*, 2004) obtained by western blot experiments in rodents. Quantification analysis carried out by optical density showed a 15 % increase in the lesioned striatum compared to the unlesioned one (Figure 15B). Interestingly, the striosomal pattern described for the naïve wild type animals was not evident in the dopamine-depleted striatum ipsilateral to 6-OHDA injections. Both the increase in Gαolf expression and the loss of pattern suggest that dopamine depletion induces an increase of Gαolf expression levels in the matrix compartment reaching those of the striosomes.

Because the increase in Gαolf levels could be induced by the lack of dopamine stimulation, we studied the effect of exogenous dopamine replacement on Gαolf expression. To achieve this goal, we treated hemiparkinsonian wild type mice chronically with 25 mg/kg of L-DOPA. We have demonstrated that this protocol of administration besides inducing severe L-DOPA-induced dyskinesia in wild type animals (Pavón *et al.*, 2006; Darmopil *et al.*, 2009; Suárez *et al.*, 2014), temporarily increases striatal dopamine levels (Espadas *et al.*, 2012).

Treatment with 25 mg/kg of L-DOPA for 3 weeks in Parkinsonian mice reversed the

increase in Gαolf expression, which returned to naïve/control levels (Figure 15A,B). Moreover, image analysis of microscopic photographs indicates that this down-regulation of Gαolf may take part mainly in the matrix, as some Gαolf striosomes can be observed in the ipsilateral striatum of dyskinetic mice.

However, these changes in protein levels were not associated with similar variations in Gαolf mRNA. RT-qPCR experiments showed that dopamine depletion did not modify Gαolf mRNA regardless of the increase in the protein levels found in the hemiparkinsonian mice. Intriguingly, L-DOPA treatment induced a 50% increase of Gαolf mRNA levels, in sharp contrast to its effect in the protein concentrations (Figure 15C).

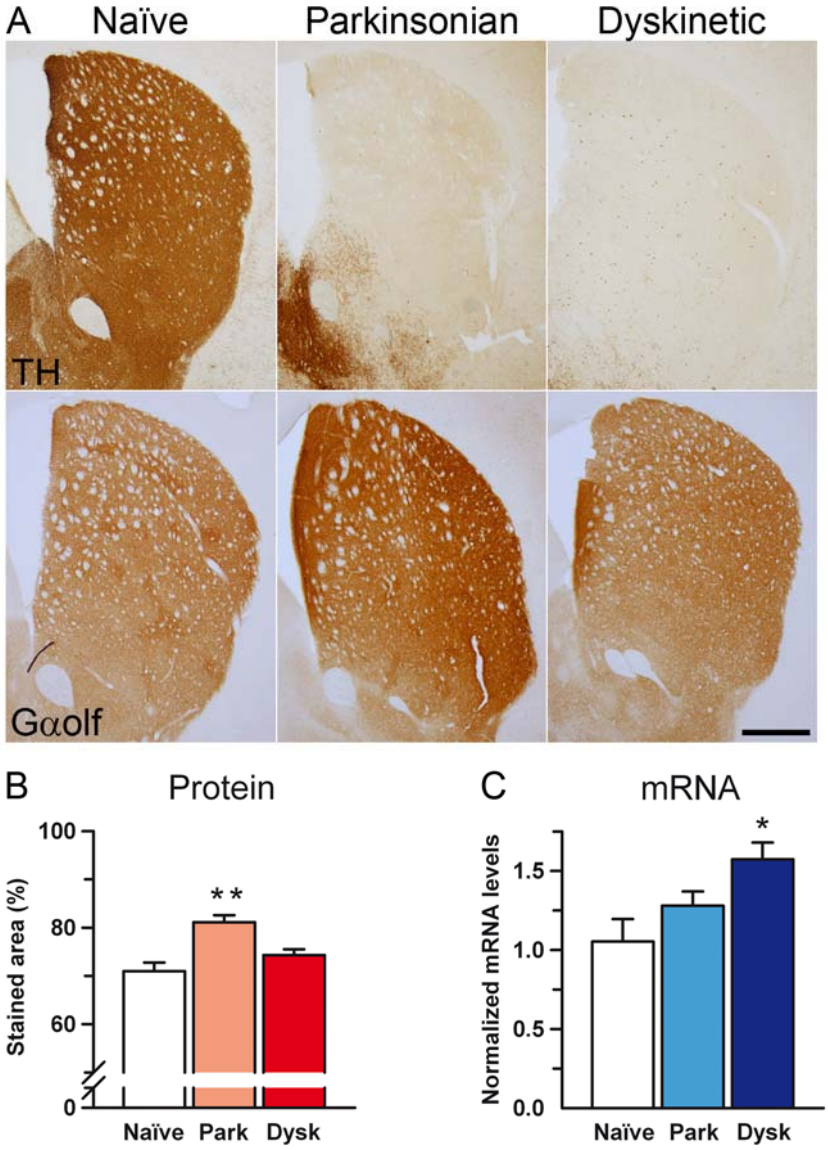

Figure 15. Gαolf expression in the striatum of Parkinsonian and dykinetic mice. **(A)** Representative photomicrographs of striatal rostrocaudal sections from adult mice in naïve, Parkinsonian and dyskinetic condition, immunostained for TH and Gαolf. Histograms show quantifications of **(B)** Gαolf protein measured as the proportional stained area of Gαolf-immunoreactivity and **(C)** Gαolf mRNA expressed as normalized mRNA levels to GAPDH. Data (mean ± SEM) were analyzed by one-way ANOVA followed by Newman-Keuls test. *p<0.05, **p<0.001 vs saline. Bar = 500 µm. n=5-7.

1.3. Genetic inactivation of Pitx3 increases Gαolf expression and induces the loss of striosomal pattern, while L-DOPA treatment restores both

In order to control for the effect of chemical lesions in our dopamine depletion experiments, we analyzed Gαolf expression in the striatum of Pitx3-deficient aphakia mice, a genetic model of PD. The lack of the transcription factor Pitx3 expressed in dopaminergic neurons in the midbrain results in an abnormal development of the dopaminergic system and in a selective loss of TH and dopamine in the striatum (Hwang *et al.*, 2003). Therefore, aphakia mice provide a genetic model of the dopamine depletion in the striatum present in PD (Hwang *et al.*, 2005; Ding *et al.*, 2007).

Immunohistochemical studies revealed that aphakia mice showed an enhanced striatal Gαolf expression compared to that found in the wild type naïve animals but very similar to the Gαolf levels observed in wild type hemiparkinsonian mice (Figure 16A). Moreover, aphakia mice also showed a uniform patter of Gαolf expression, in which the striosomes were indistinguishable from the matrix compartment. Remarkably, chronic L-DOPA treatment restored Gαolf protein expression in aphakia mice, reaching similar levels to those found in L-DOPA-treated wild type animals. L-DOPA administration also re-established the normal patched pattern, with a higher expression of Gαolf in the striosomes than in the matrix in both Parkinsonian models, 6-OHDA-lesioned and aphakia mice.

Densitometric measurements of immunostained striata revealed a 35% of decrease in Gαolf protein expression in L-DOPA-treated aphakia mice compared to the saline-treated animals (Figure 16B). On the contrary, L-DOPA treatment induces a 20% of increase in striatal Gαolf mRNA (Figure 16C). The increase in Gαolf mRNA levels correlated well with that seen in the 6-OHDA-lesioned wild type mice.

1.4. Genetic inactivation of D1R, but not D2R, increases Gαolf expression and induces the loss of its patchy pattern

We next wanted to establish the role of the dopamine D1 and D2 receptor subtypes in Gαolf expression since Gαolf is coupled to D1 receptors. We used genetically engineered adult mice lacking either the dopamine D1 receptor ($D1R^{-/-}$) (Moratalla *et al.*, 1996b; Centonze *et al.*, 2003; Granado *et al.*, 2008b; Espadas *et al.*, 2012) or the dopamine D2 receptor ($D2R^{-/-}$) (Kelly *et al.*, 1997; Darmopil *et al.*, 2009; Granado *et al.*, 2011; Murer and Moratalla, 2011; Espadas *et al.*, 2012).

Analysis of serial rostrocaudal sections immunostained for Gαolf indicated that striatal Gαolf levels were much higher in D1R null mice than in their wild type littermates, whereas

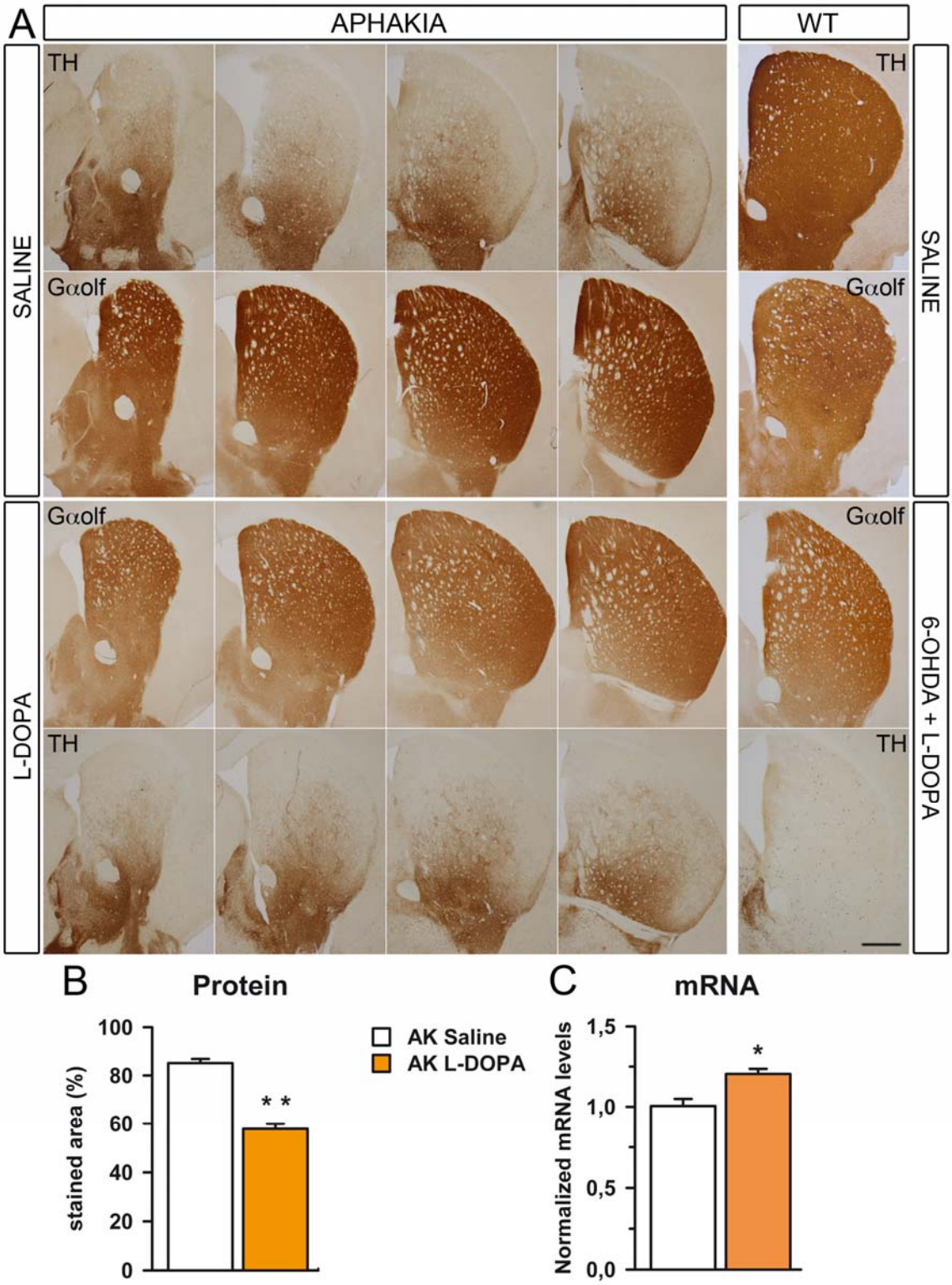

Figure 16. L-DOPA decreases Gαolf expression in the striatum of aphakia mice. **(A)** Photomicrographs of serial striatal rostrocaudal sections from adult aphakia mice treated chronically with saline or L-DOPA compared to wild type naïve or 6-OHDA-lesioned mice treated with saline or L-DOPA, immunostained for TH and Gαolf. Histograms show quantifications of striatal **(B)** Gαolf protein measured as the proportional stained area of Gαolf-immunoreactivity in the striatum and **(C)** Gαolf mRNA expressed as normalized mRNA levels to GAPDH. Data (mean ± SEM) were analyzed by one-way ANOVA followed by Newman-Keuls test. **p*<0.01, ***p*<0.001 vs saline. Bar = 500 µm. n=5.

deletion of D2R did not alter Gαolf expression (Figure 17A). In addition, genetic deletion of D1R induced a loss of the Gαolf expression pattern, increasing Gαolf expression in the striatal matrix and making striosomes indistinguishable from the surrounding matrix. On the other hand, the patched pattern described previously for the wild type animals was preserved in D2R-deficient mice, which showed Gαolf-enriched striosomes. Densitometric measurements of negative images showed a 25% increase in Gαolf expression in $D1R^{-/-}$ mice compared to their wild type littermates (Figure 17B). Significant differences in $D1R^{-/-}$ mice were found by one-way ANOVA following by Newman-Keuls test [$F_{3,8}$ = 10.45; p<0.01] compared to wild type mice.

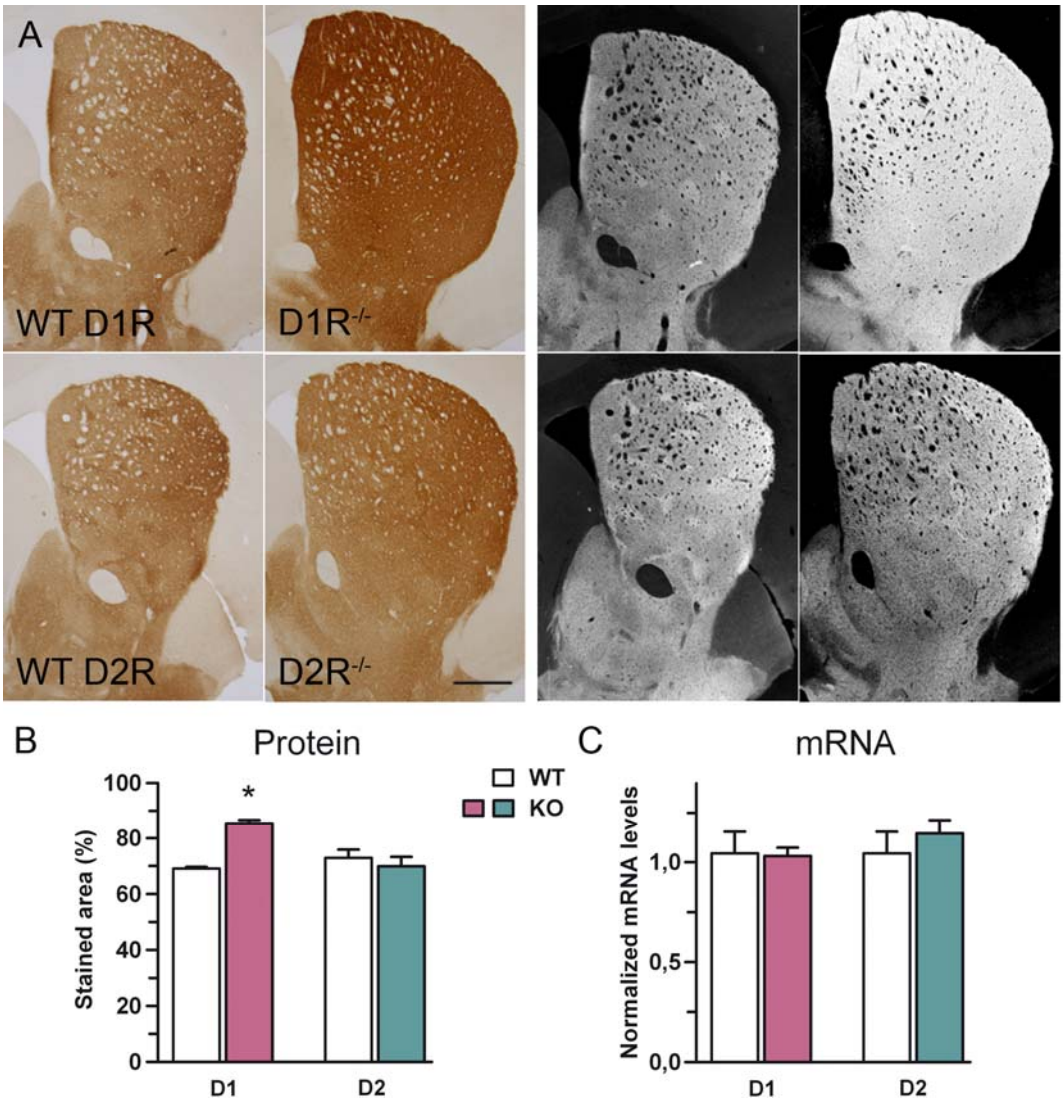

Figure 17. Inactivation of D1R but not of D2R increases Gαolf expression and induces the loss of patched pattern. (A) Representative photomicrographs of striatal coronal sections from adult mice immunostained for Gαolf and their negative prints. Notice the higher expression of Gαolf and the loss of patched pattern in the striatum of the $D1R^{-/-}$ mice. Bar = 500 mm. Histograms show **(B)** Gαolf protein levels measured as the proportional stained area of Gαolf-immunoreactivity in the striatum and **(C)** Gαolf mRNA levels in the striatum analyzed by RT -qPCR and normalized to GAPDH. Data expressed as mean ± SEM were analyzed by one-way ANOVA followed by Newman-Keuls test. *p<0.01 vs WT D1R. n=3-5.

We then examined Gαolf mRNA levels by RT-qPCR to determine whether the increase in Gαolf protein observed in the striatum of mutant D1R$^{-/-}$ mice resulted from an increase in the transcription of the Gαolf gene and/or a post-transcriptional mechanism. The concentration of Gαolf transcripts was not significantly different in the striatum of either D1R$^{-/-}$ mice or D2R$^{-/-}$ mice compared to their littermates wild type animals (Figure 17C; [$F_{3,15}$ = 0.05; p=0.98]). These results indicate that the increase in Gαolf protein observed in the striatum of D1R$^{-/-}$ mice is not the consequence of alterations in Gαolf mRNA levels.

Thus, D1R seems to regulate Gαolf expression not only in a quantitative way but also its pattern of expression, while modifications of D2R do not affect such effects. Moreover, these modifications take place in a post-transcriptional level and do not result from a change in gene expression

1.5. Dopamine depletion with 6-OHDA decreases Gαolf expression in D1R $^{-/-}$ mice

To further elucidate the role of dopamine in Gαolf expression, we subjected D1R$^{-/-}$ mice to 6-OHDA unilateral striatal lesion. Striatal dopamine depletion decreases the elevated Gαolf levels found in D1R$^{-/-}$ mice, contrary to what we found in the wild type animals. In addition, as observed in the naïve D1R$^{-/-}$ animals, no patched pattern was detected in ipsi- and contralateral striatum (Figure 18A).

Interestingly, L-DOPA treatment in D1R$^{-/-}$ mice was unable to modify striatal Gαolf levels as happened in the wild type hemiparkinsonian animals. Immuno quantification experiments by image analysis showed that Gαolf levels measured in the denervated striatum of D1R$^{-/-}$ mice were 15% lower than in naïve D1R$^{-/-}$ mice but not different from those measured in the dyskinetic condition, meaning that L-DOPA did not affect Gαolf expression in D1R$^{-/-}$ mice (Figure 18B). Moreover, no striosome could be observed in the ipsi- and contralateral striatum of D1R null mice in any of the conditions. Significant differences were found by two-way ANOVA followed by Newman-Keuls test for genotype [$F_{1,13}$ = 26.83; p<0.001], treatment [$F_{2,13}$ = 4.78; p<0.05] and genotype x treatment [$F_{2,13}$ = 43.09; p<0.001]. These differences between genotypes cannot be attributed to different striatal dopaminergic denervation, as no differences in TH immunostaining were detected (Figure 18C).

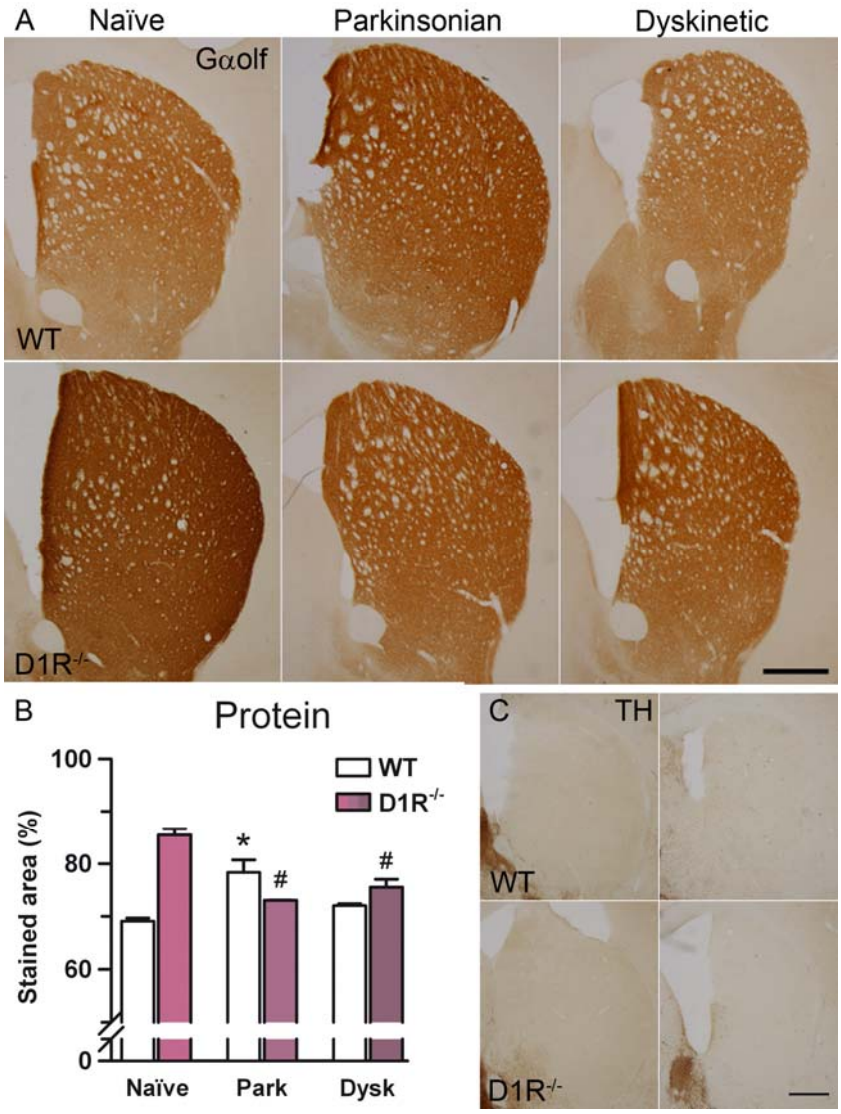

Figure 18. Dopamine depletion with 6-OHDA decreases Gαolf expression in D1R$^{-/-}$ mice. (A) Representative photomicrographs of striatal sections from WT and D1R$^{-/-}$ mice immunostained for Gαolf. **(B)** Histogram shows the proportional stained area of Gαolf-immunoreactivity in the striatum. **(C)** TH immunostaining was performed to confirm the efficacy of 6-OHDA lesion. Data (mean ± SEM) were analyzed by two-way ANOVA followed by Newman-Keuls test. *p<0.001 vs WT naïve, #p<0.001 vs D1R$^{-/-}$ naïve. Bar = 500 mm. n=3-4.

1.6. Genetic inactivation of D2R does not modify Gαolf changes in Parkinsonian and dyskinetic mice

We then explored the implication of D2R in Gαolf expression changes induced by dopamine using D2R deficient mice. We found that striatal dopaminergic denervation by 6-OHDA induced an up-regulation in Gαolf levels in D2R$^{-/-}$ mice similar to that found in their wild type littermates (Figure 19A). In addition, D2R null mice also showed the same pattern changes in Gαolf expression as the wild type animals, with no apparent Gαolf-enriched striosomes in the depleted striatum likely due to an increase in Gαolf protein in the matrix area. Quantification

experiments revealed a 20% increase in Gαolf levels after dopamine depletion relative to the basal situation (Figure 19B). Significant differences were found by two-way ANOVA followed by Newman-Keuls test for treatment [$F_{2,14} = 14.06$; $p<0.001$] but not for genotype [$F_{1,14} = 1.46$; $p=0.25$].

Chronic L-DOPA treatment of D2R deficient mice reduced Gαolf levels compared to those found in the Parkinsonian lesioned striatum. This reduction was similar to that observed in the wild type mice. Moreover, D2R$^{-/-}$ mice also showed a recovery in the patched pattern expression of Gαolf, with Gαolf-enriched striosomes, similar to that observed in wild type animals. In summary, D2R does not appear to be implicated in the regulation of Gαolf following dopaminergic denervation and L-DOPA treatment.

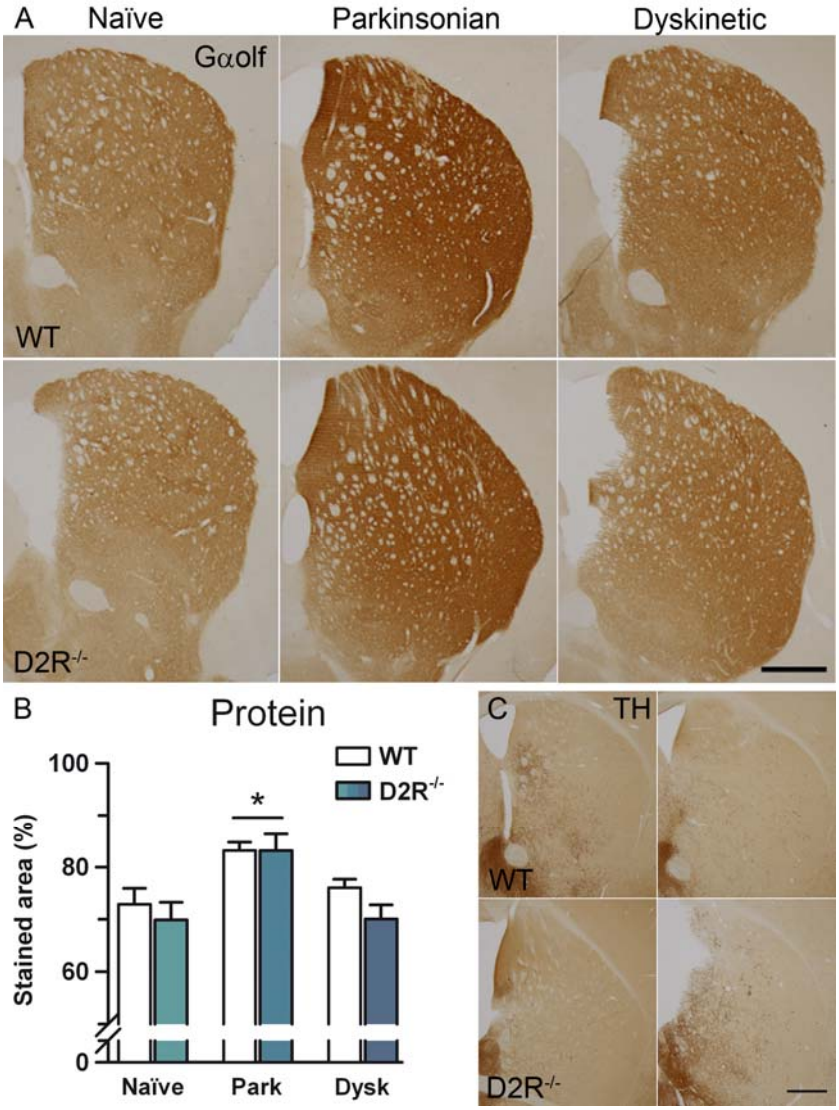

Figure 19. Genetic deletion of D2R does not alter changes in Gαolf expression after dopamine depletion and L-DOPA treatment. (A) Representative photomicrographs of striatal sections from WT and D2R$^{-/-}$ mice immunostained for Gαolf. **(B)** Histogram shows the proportional stained area of Gαolf-immunoreactivity in the striatum. **(C)** TH immunostaining was performed to confirm the efficacy of 6-OHDA lesion. Data (mean ± SEM) were analyzed by two-way ANOVA followed by Newman-Keuls test. *$p<0.001$ vs naïve condition. Bar = 500 mm. n=3-4.

1.7. Genetic modifications in DREAM do not alter Gαolf expression changes induced by 6-OHDA and L-DOPA treatment

Once we had studied Gαolf regulation by dopamine upstream G-proteins, we then wonder if changes downstream could also influence Gαolf expression. We investigated the impact of DREAM, located downstream PKA and calcium, on striatal Gαolf levels. DREAM, a calcium-binding protein, binds to DRE sites in the DNA and represses transcription of target genes, such as c-fos, Fos-related antigen-2 (fra-2) and prodynorphin, among others. This repression is released by calcium and PKA activation following dopamine stimulation of D1R. To achieve this goal, we used DREAM$^{-/-}$ mice (Cheng *et al.*, 2002; Cebolla *et al.*, 2008) and transgenic mice expressing a dominant active mutant DREAM (daDREAM) (Gomez-Villafuertes *et al.*, 2005; Savignac *et al.*, 2005).

As expected, daDREAM and DREAM$^{-/-}$ mice showed the same Gαolf protein levels and the same patchy pattern of Gαolf-enriched striosomes as their wild type littermates (Figure 20A). These results indicate that genetic modifications in DREAM protein do not modify basal Gαolf expression.

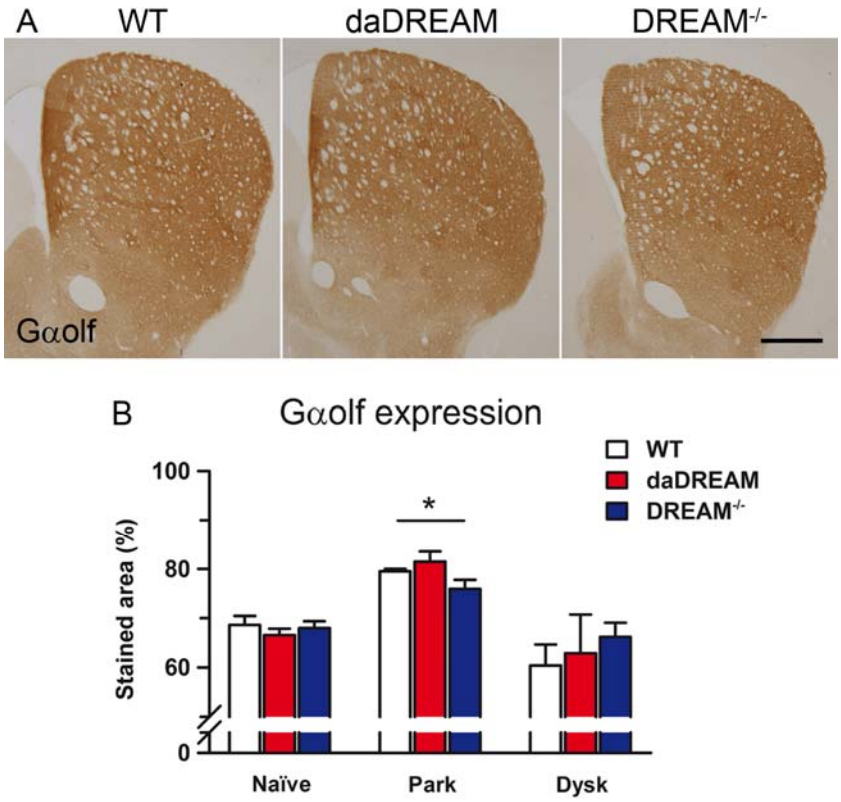

Figure 20. **DREAM does not modify Gαolf expression changes induced by dopamine depletion. (A)** Representative photomicrographs of striatal sections from adult wild type, daDREAM and DREAM$^{-/-}$ mice immunostained for Gαolf. **(B)** Histogram shows the proportional stained area of Gαolf-immunoreactivity staining in the striatum from the three genotypes in naïve, Parkinsonian (Park) and dyskinetic (Dysk) conditions. Notice that modifications in DREAM protein do not alter either the levels or the pattern of Gαolf expression. Data expressed as mean ± SEM were analyzed by two-way ANOVA followed by Newman-Keuls test. *p<0.05 vs naïve condition. Bar indicates 500 µm. n=3-7.

Furthermore, dopamine depletion following 6-OHDA lesion induced a significant increase in Gαolf expression ($F_{2,35}$ = 14.74; p<0.001) of about 20% in all hemiparkinsonian mice compared to the levels seen in the naïve situation (Figure 20B). The uniform pattern of expression found after denervation in the wild type animals was also evident in DREAM mutant mice, with no distinguishable striosomes from the surrounding matrix. L-DOPA treatment restored Gαolf protein levels as well as the patched pattern of expression in all three genotypes. These results indicate that changes in DREAM protein do not affect Gαolf expression changes induced by dopamine depletion or L-DOPA administration.

2. ROLE OF DREAM PROTEIN IN L-DOPA-INDUCED DYSKINESIA

In the second part of my Thesis, we have studied the role of DREAM in L-DOPA-induced dyskinesia. We target DREAM protein because is a downstream element in the cAMP-dependent pathway and, for this reason, it could exercise a finer regulation of the target genes implicated in dyskinesia. To establish the role of the DREAM protein in the development of L-DOPA-induced dyskinesia and in the associated molecular changes, we used genetically DREAM deficient mice (DREAM$^{-/-}$) and the transgenic dominant active mutant DREAM mice (daDREAM).

We have previously demonstrated that L-DOPA-induced dyskinesia is causally linked with hyperstimulation of D1Rs located on direct pathway medium spiny neurons of the severely denervated striatum (Pavón *et al.*, 2006; Murer and Moratalla, 2011). In the dopamine-depleted striatum, L-DOPA activates a cAMP-dependent signaling cascade via PKA activation (Lebel *et al.*, 2010; Fisone and Bezard, 2011), inducing transcriptional changes that result in increased expression of FosB, P-AcH3 and dynorphin-B (Darmopil *et al.*, 2009). The magnitude of these molecular changes correlates with the intensity of dyskinesia.

DREAM is a calcium-binding protein that mediates calcium- and cAMP-dependent transcriptional responses (Ledo *et al.*, 2000a; Cebolla *et al.*, 2008). As seen before, in basal conditions DREAM binds to DRE, located downstream from the transcription initiation site, repressing the transcription of target genes including prodynorphin, c-fos and Fos-related antigen-2 (fra-2) (Carrión *et al.*, 1999; Link *et al.*, 2004). DREAM-mediated repression is reversed by calcium and by its PKA-dependent interaction with phospho-CREM, the cAMP responsive element modulator (Carrión *et al.*, 1999; Ledo *et al.*, 2000b, 2002; Osawa *et al.*, 2001).

Based on these observations and on our previous data demonstrating a close association between L-DOPA-induced dyskinesia and overexpression of FosB and dynorphin-B, we studied the role of DREAM in L-DOPA-induced dyskinesia.

2.1. Wild type and mutant DREAM expression

The first point to clarify about DREAM protein was its localization in the adult mouse brain. Immunohistochemical studies from brain sections revealed marked expression in striatum, cortex, SN and hippocampus (Figure 21). DREAM is more abundant in the pyramidal layers from CA1 to CA3 areas in the hippocampus and in the granular layer of the dentate gyrus. In the striatum, DREAM is expressed in the neuropil and in the soma of large and medium sized striatal neurons, with a higher expression in the matrix compartment. Moreover, DREAM protein is abundantly expressed in the dopaminergic neurons and processes of the SNc and SNr.

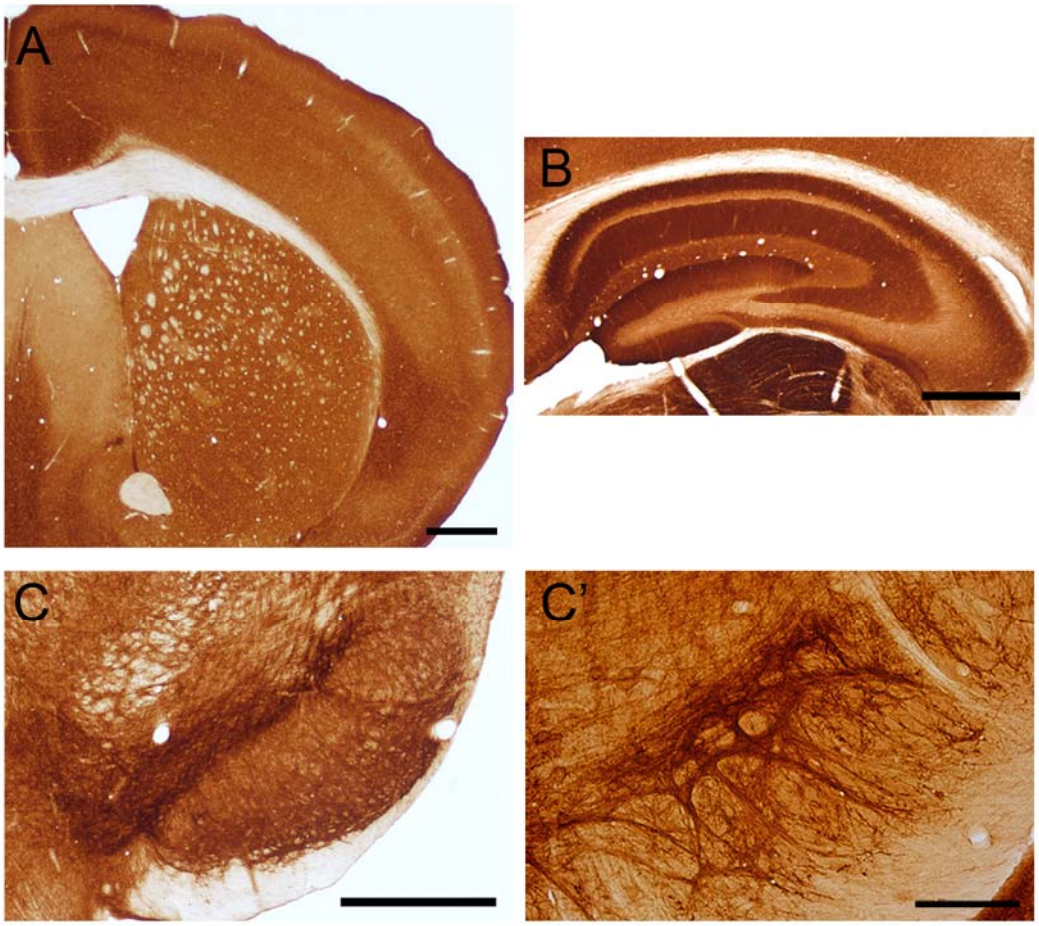

Figure 21. Distribution of DREAM protein in the adult mouse brain. Photomicrographs of brain sections from adult wild type mice immunostained for DREAM and illustrating DREAM expression in **(A)** the striatum, **(B)** the hippocampus and **(C,C')** the substantia nigra. Scale bars indicate 500 mm **(A,B,C)** and 100 mm **(C')**.

DREAM is also found in the cerebral cortex, in all layers except the molecular one.

In the daDREAM transgenic mice, expression of the transgene, a bi-cistronic construct including the daDREAM double mutant, an IRES sequence and the lacZ reporter, was driven by the CaMK-II alpha promoter (Figure 22A). The CaMK-II alpha promoter was chosen to guarantee a telencepahlic-specific expression of the transgene (Mayford *et al.*, 1996). The lacZ reporter allowed us to confirm the specific expression of the daDREAM transgene by a b-galactosidase staining. It showed high levels of transgene expression in the striatum as well as in the cortex and the hippocampus (Figure 22B,C). The daDREAM transgenic protein results in a mutant protein with the functional EF-hands and the leucine-charged reside-rich domains insensitive to calcium and to CREB/CREM proteins, respectively. Thus, mutant daDREAM remains bound to the DNA, inhibiting transcription.

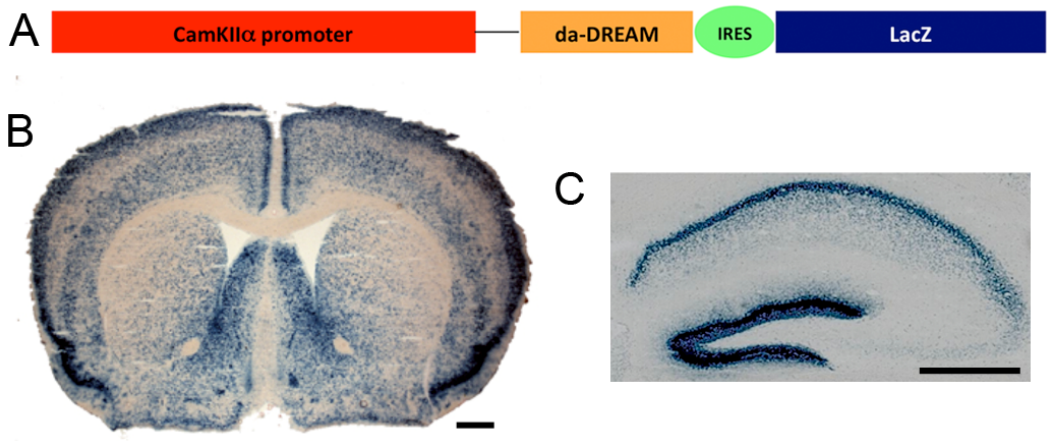

Figure 22. Construct and expression of daDREAM transgene. **(A)** Schematic representation of the construct used for preparation of transgenic mice. **(B)** Coronal section of daDREAM transgenic mouse forebrain showing the distribution of b-galactosidase staining. **(C)** Sagital section of hippocampus from daDREAM transgenic mouse brain showing the distribution of b-galactosidase staining. Scale bars = 500 mm.

2.2. Basal locomotor activity and motor coordination are normal in DREAM mutant mice

From a morphological point of view, mutant mice were indistinguishable from their wild type littermates. No differences in weight, fertility and longevity were evident between the three genotypes of mice, i.e., daDREAM, DREAM$^{-/-}$ and wild type. In addition to these direct observations, we carried out behavioral tests prior to the 6-OHDA lesion to rule out any motor impairment in the mutant animals that could interfere with later L-DOPA behavioral studies. To achieve this goal, we submitted the mice to spontaneous locomotor activity and coordination tests.

We used an automated multicage activity monitoring system to measure basal locomotor activity. Mice were first habituated to the system for two days to avoid exploratory behavior due to the novel environment. The third day we found that in the absence of any external challenge, daDREAM, DREAM$^{-/-}$ and wild type mice showed similar horizontal and vertical activity, as indicated by the number of beam breaks measured for one hour (Figure 23A,B). Ambulatory activity measured as total distance traveled was also similar among the three genotypes (Figure 23C). Over time, as the mice habituated to the environment, the number of beam breaks and the distance traveled diminished, with a similar profile in all three genotypes.

To further strengthen these results, we analyzed the basal motor coordination of mutant mice. Animals were submitted to an accelerated version of the rotarod test, in six trials 20 minutes apart. No statistically significant differences between genotypes were found regarding mo-

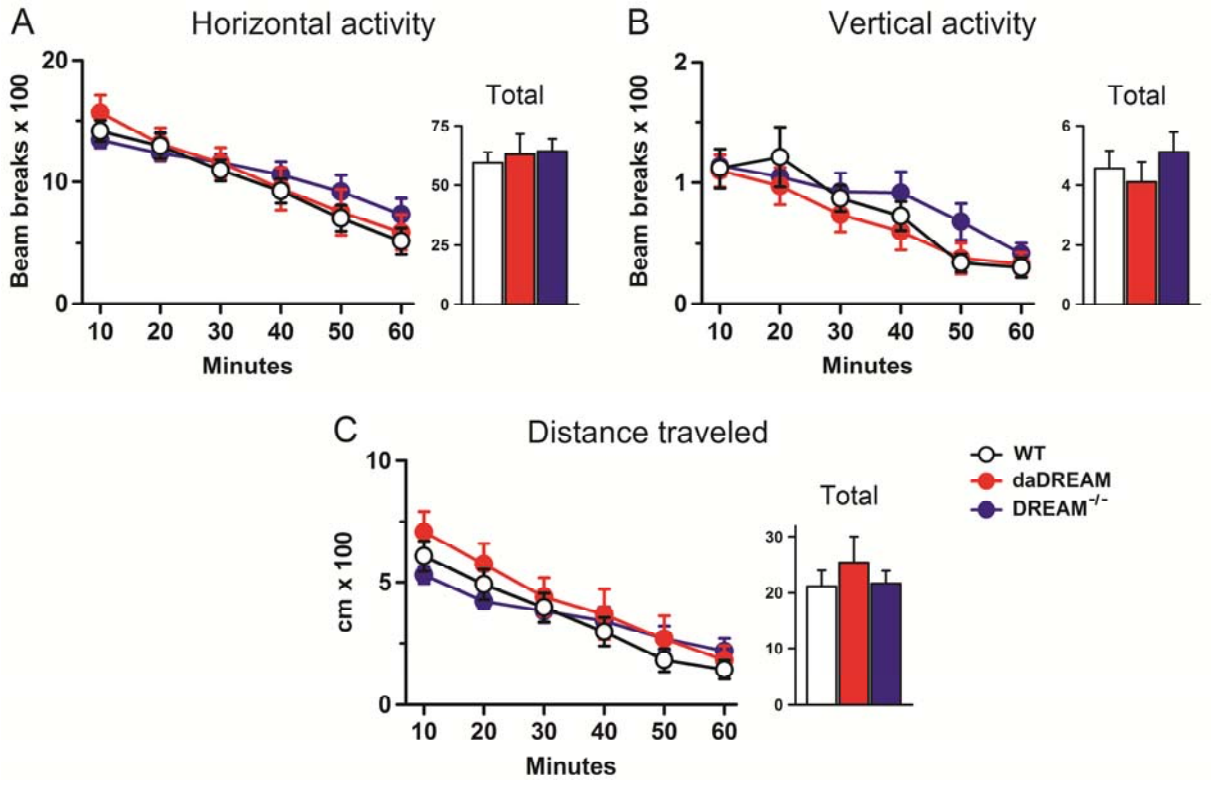

Figure 23. Genetic modification of DREAM protein levels does not alter basal locomotor activity. (A) Horizontal and **(B)** vertical locomotor activity (beam breaks) and **(C)** total distance traveled (cm) during 60 min were measured in a multicage activity monitoring system. Transgenic (daDREAM) and knockout (DREAM$^{-/-}$) mice behaved similarly to wild type mice and showed similar performance in motor coordination.

tor coordination (Figure 24). All animals achieved a significant increase ($F_{2,64}$ = 22.38; p<0.001) in the latency to fall from the rotating rod at the sixth and last trial compared to the first trial, showing a similar capacity of motor learning in the rotarod.

Taken together, these results indicate that modifications in DREAM protein expression do not modify spontaneous locomotor activity or motor coordination.

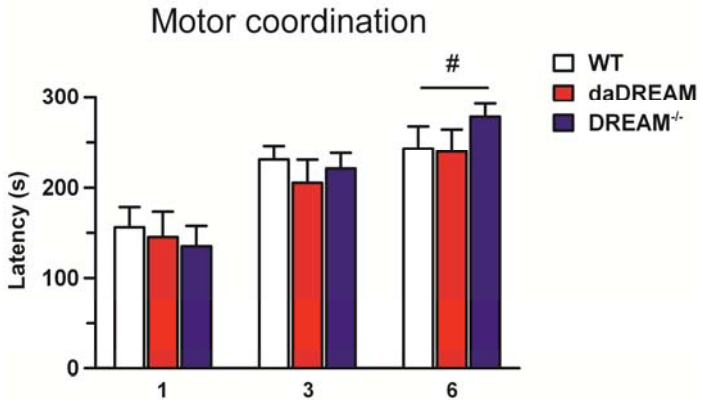

Figure 24. Modifications in DREAM do not alter basal coordination in mutant mice. Latency (s) to fall in the rotarod test at constant acceleration. daDREAM and DREAM$^{-/-}$ mice behave similarly to WT mice and show similar improvement in motor coordination following the initial performance. Data expressed as mean ± SEM were analyzed by two-way ANOVA with repeated measures followed by Newman-Keuls test. #p<0.01 vs. trial 1. n=10 -12.

2.3. DREAM modulates L-DOPA-induced dyskinesia

To examine the role of DREAM in the development of dyskinesia, animals were unilaterally lesioned with 6-OHDA and treated for three weeks with 25 mg/kg of L-DOPA to generate our mouse model of dyskinesia. We assessed axial dystonia and forelimb, orofacial and locomotive dyskinesia in daDREAM, DREAM$^{-/-}$ and the corresponding wild type littermates 40 minutes after L-DOPA administration. L-DOPA was given daily and assessments were done twice a week, as described (see *Material and Methods*).

In wild type mice, all four types of dyskinetic symptoms were already apparent at the beginning of the treatment and progressively increased to reach a plateau in the second week of administration (Figure 25), similar to that found earlier (Pavón *et al.*, 2006; Darmopil *et al.*, 2009). Interestingly, daDREAM mice showed a significant reduction in dyskinetic movements,

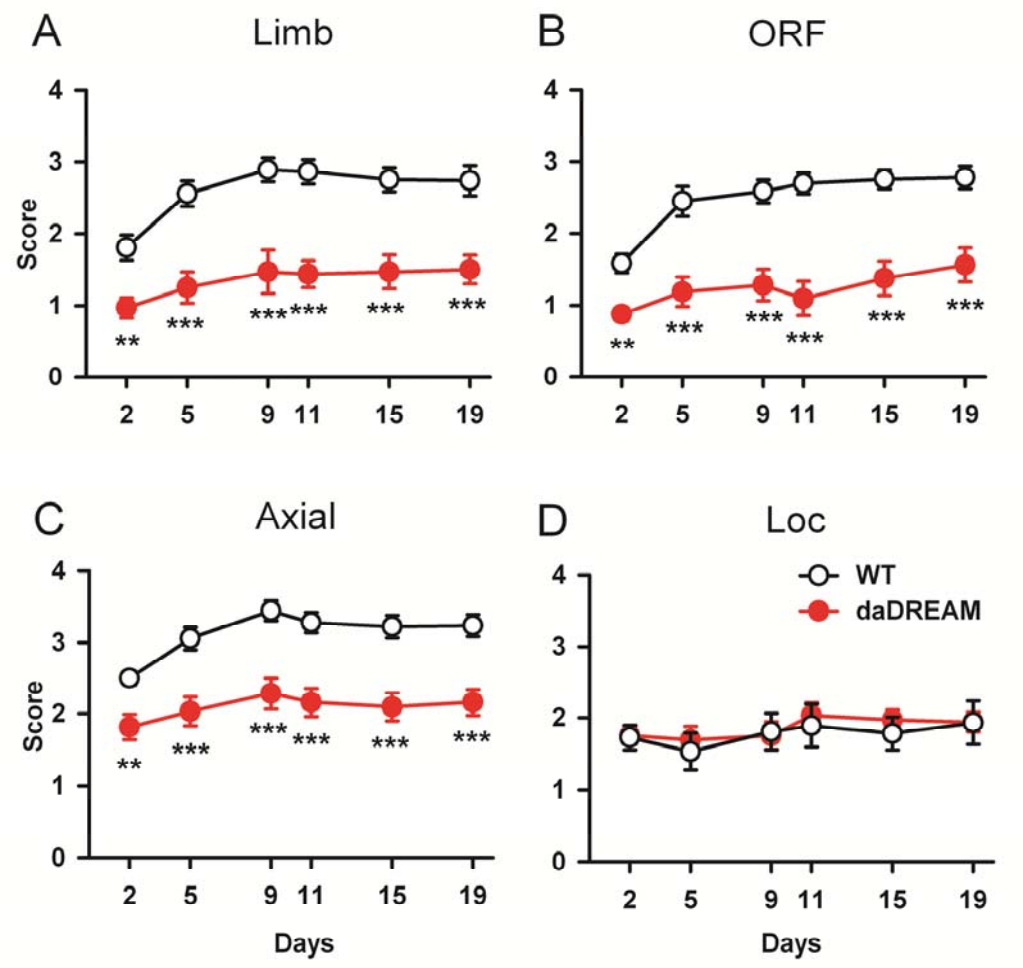

Figure 25. DREAM overexpression in daDREAM mice decreases L-DOPA-induced dyskinesia in hemiparkinsonian mice. Time course of appearance of dyskinetic symptoms is shown: limb dyskinesia (Limb), orofacial dyskinesia (ORF), axial dystonia (Axial) and locomotive dyskinesia (Loc). Movements were evaluated 40 min after L-DOPA (25 mg/kg) administration at the indicated days. daDREAM mice show a lower dyskinetic score for limb and orofacial dyskinesia and for axial dystonia compared to wild type mice. No significant differences were found for locomotive dyskinesia. Data expressed as mean ± SEM were analyzed by two-way ANOVA with repeated measures followed by Newman-Keuls test. * $p<0.01$, ** $p<0.001$ vs WT. n=15.

in particular for limb (p<0.001) and orofacial (p<0.001) symptoms as well as for axial dystonia (p<0.001) compared to their wild type littermates. These changes were apparent from the first day of L-DOPA administration and lasted over the entire 3-week treatment.

In sharp contrast, a significant enhancement in limb (p<0.05) and orofacial (p<0.01) dyskinesia as well as axial dystonia (p<0.05) was observed in DREAM$^{-/-}$ mice compared to their wild type littermates (Figure 26). While the wild type animals reached dyskinetic severity grade 2-3 (indicating alternation between dyskinetic movements and short time of normal activity, similar to that found by Francardo et coworkers (2011) in striatal lesioned mice), DREAM$^{-/-}$ mice exhibited continuous dyskinetic behaviors, reaching the highest severity grade (3–4) on the rodent dyskinetic scale. Notably, no statistically significant difference in locomotive dyskinesia was observed among genotypes, indicating that DREAM modifications do not compromise the motor stimulant effect of L-DOPA.

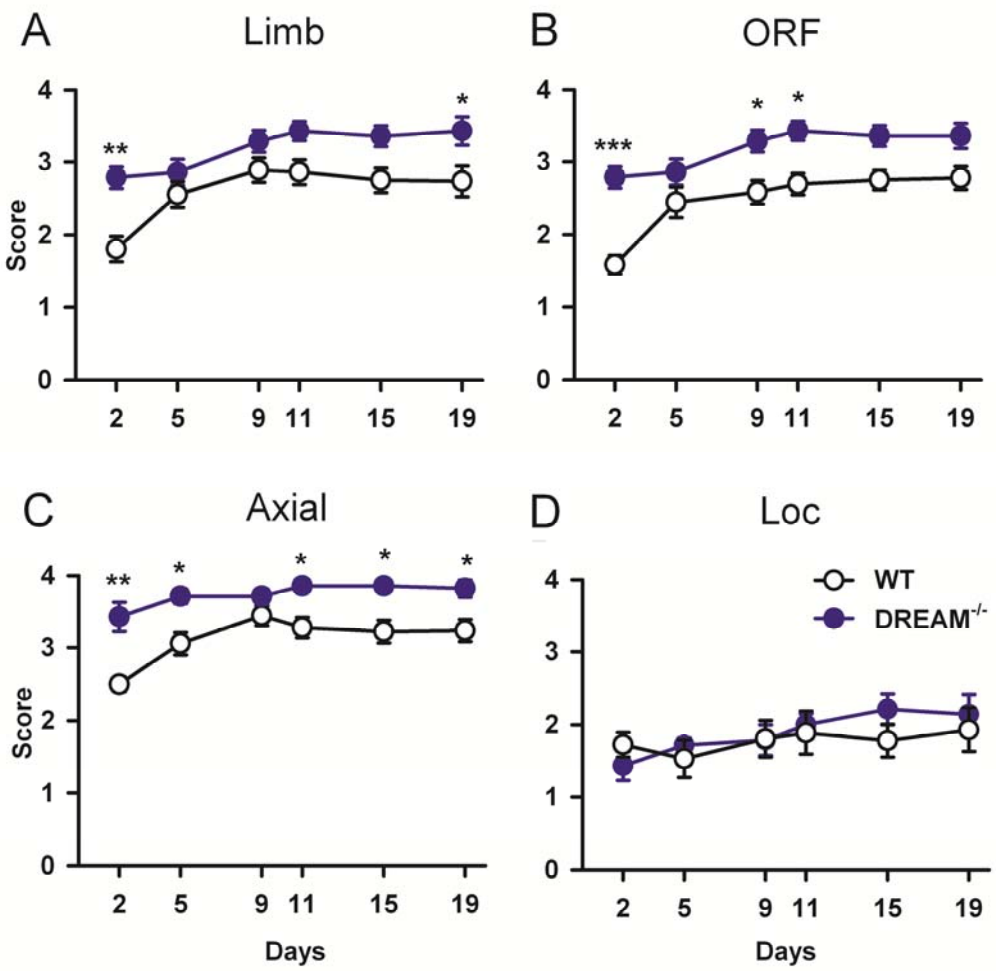

Figure 26. Genetic inactivation of DREAM potentiates L-DOPA-induced dyskinesia in hemiparkinsonian mice. Graphs show the time course of appearance of dyskinetic symptoms evaluated 40 min after 25 mg/kg L-DOPA administration at the indicated days: limb dyskinesia (Limb), orofacial dyskinesia (ORF), axial dystonia (Axial) and locomotive dyskinesia (Loc). Inactivation of DREAM in DREAM$^{-/-}$ mice significantly increased limb and orofacial dyskinesia and axial dystonia compared to wild type mice. Data expressed as mean ± SEM were analyzed by two-way ANOVA with repeated measures followed by Newman-Keuls test. * p<0.05, ** p<0.01, *** p<0.001 vs WT. n=8-12.

We then calculated the global dyskinetic score of daDREAM and DREAM$^{-/-}$ mice. Although dyskinesia was observed in both daDREAM and wild type mice, the total score achieved by daDREAM mice was significantly lower (p<0.001) compared to wild type mice for all time points evaluated (Figure 27). On the other hand, the total dyskinetic score was higher in DREAM$^{-/-}$ animals compared to that reached by their wild type littermates (p<0.05), although this difference was smaller to that observed between the daDREAM and the wild type mice. Significant differences were found for genotype [$F_{2,190}$ = 34.01, p<0.001], time [$F_{5,190}$ = 19.34; p<0.001] and genotype x time [$F_{10,190}$ = 2.12, p<0.05] by two-way ANOVA with repeated measures followed by Newman-Keuls test.

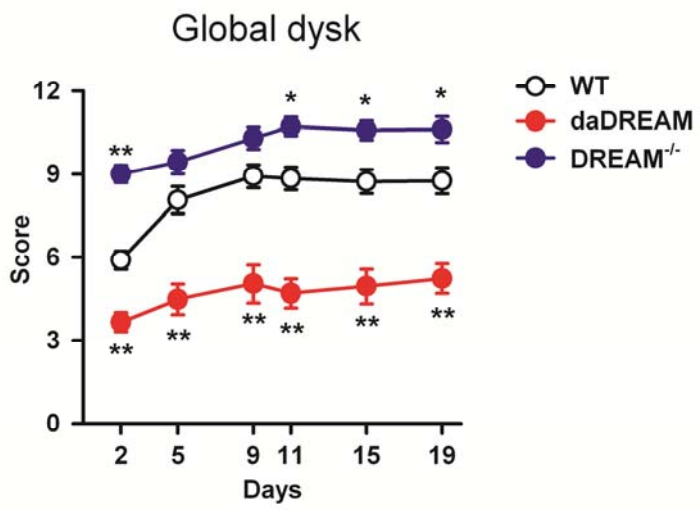

Figure 27 DREAM content modulates the global dyskinetic score. Time course of global dyskinetic score (Global dysk) in daDREAM and in DREAM$^{-/-}$ mice compared to their wild type littermates, evaluated 40 min after L-DOPA (25 mg/kg) administration at the indicated days. DREAM overexpression decreased LID score for the entire treatment period, while inactivation of DREAM increased LID score. Global LID scores expressed as mean ± SEM were analyzed by two-way ANOVA with repeated measures followed by Newman-Keuls test. *p<0.05, **p<0.001 vs WT. n=8-15.

To look for differences in the kinetic profile of L-DOPA responses among genotypes, which could interfere with the development of L-DOPA-induced dyskinesia, we determined the duration of the dyskinetic response and the peak severity of the symptoms. To achieve this goal, we evaluated the time course of L-DOPA response in daDREAM and DREAM$^{-/-}$ mice on day 20 of L-DOPA administration (Figure 28). Dyskinetic symptoms were scored for 1 minute every 20 minutes during the 160 minutes following L-DOPA administration. Dyskinesia was evident at 20 minute, peaked between 40 and 60 minutes, and declined significantly at 100 minute after L-DOPA before disappearing at 140 minutes for both genotypes. Although the time course of L-DOPA response was similar in both groups of mice, daDREAM mice exhibited significantly lower dyskinesia compared to wild type animals across the entire duration of the L-DOPA response. Finally, there were no statistically significant differences between DREAM$^{-/-}$

and wild type mice in the duration of the L-DOPA response. As in daDREAM mice, the response was evident 20 minutes after L-DOPA and disappeared after 140 minutes. However, a difference was again observed in the intensity of the dyskinetic symptoms, which were stronger in DREAM$^{-/-}$ mice until 120 minutes, when the dyskinetic scores were similar for the duration of the effect. Significant differences were found for genotype [$F_{2,196}$ = 13.51, p<0.001], time [$F_{7,196}$ = 99.56; p<0.001] and genotype x time [$F_{14,196}$ = 5.44, p<0.001] by two-way ANOVA with repeated measures followed by Newman-Keuls test. These temporal course results showed that changes in DREAM do not alter the kinetic profile of L-DOPA as demonstrated by the duration of the L-DOPA response, which was similar in the three genotypes of mice.

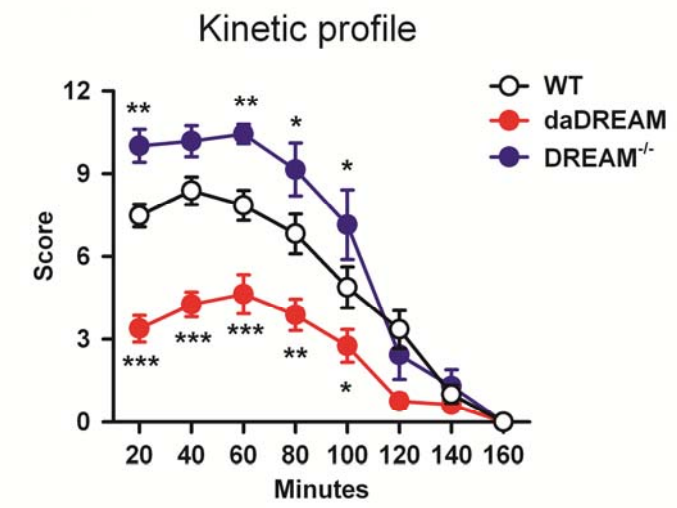

Figure 28. DREAM content does not alter the kinetic profile of L-DOPA. Kinetic profile of dyskinetic symptoms was evaluated one every 20 min during 160 min on day 20 of L-DOPA treatment. DREAM overexpression reduced LID score during the entire half-life of L-DOPA, while genetic inactivation of DREAM increased dyskinesia. Global LID scores expressed as mean ± SEM were analyzed by two-way ANOVA with repeated measures followed by Newman-Keuls test. *p<0.05, **p<0.01, ***p<0.001 vs WT. n=8-15.

2.4. Antiparkinsonian effect of L-DOPA is maintained in DREAM mutant mice

To rule out that the different dyskinetic score induced by L-DOPA in DREAM mutant mice was not due to an altered motor response to L-DOPA in these mice, we carried out the cylinder and rotarod tests to measure the antiparkinsonian effect of L-DOPA (Francardo *et al.*, 2011; Espadas *et al.*, 2012). The cylinder test is used to evaluate the forelimb akinesia and asymmetry in unilateral rodent models of PD, by counting the contralateral and ipsilateral forelimb touches that the mouse performs against the surrounding glass wall.

In the naïve situation, i.e., in the absence of any external challenge, mice used both forelimbs similarly (Figure 29A). However, 3 weeks after 6-OHDA lesions, when the animals are

completely recovered from the surgical intervention, hemiparkinsonian mice showed a significant asymmetry in forelimb use ($F_{2,61}$ = 48.228; p<0.001). Importantly, no significant differences were observed among the three genotypes, indicating that the changes in DREAM expression do not affect motor impairment induced by the lesion. Moreover, the genetic manipulation of DREAM did not affect forelimb recovery after L-DOPA injection, measured 140 minutes post-treatment to avoid the motor interferences due to dyskinesias. Thus, daDREAM, DREAM$^{-/-}$ and wild type mice showed a significant recovery (p<0.001) of contralateral paw use and showed a positive response to L-DOPA, independent of the dyskinetic score.

To further strengthen these results, we tested the mice on the rotarod to evaluate the effects of L-DOPA on motor coordination. Parkinsonian mice significantly decreased the time on the rotating rod with similar latency to fall in all three genotypes compared to latency before lesion, making evident the akinetic state of the mice (Figure 29B). Chronic L-DOPA treatment significantly improved motor performance and recovery of the initial latency in all three genotypes, indicating a similar therapeutic L-DOPA response ($F_{2,83}$ = 27.70; p<0.001).

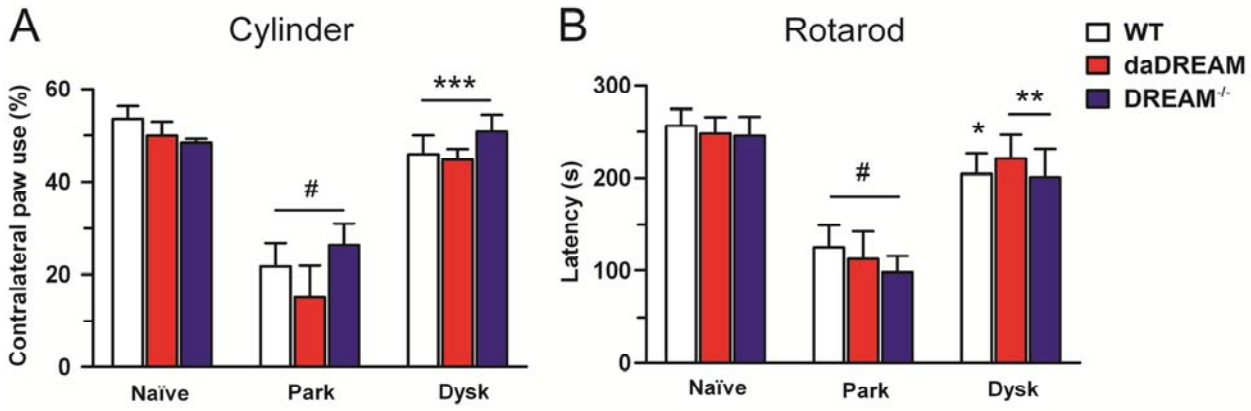

Figure 29. Genetic manipulation of DREAM does not modify the therapeutic effect of L-DOPA. **(A)** Forelimb use asymmetry was assessed with the cylinder test and **(B)** motor coordination with the rotarod before (naïve), 3 weeks after 6-OHDA lesion (parkinsonian, Park) and during chronic L-DOPA (dyskinetic, Dysk) on day 17, 140 min post-L-DOPA **(A)**, or on day 9, 24 hours after the administration of L-DOPA **(B)**. Data from the cylinder test are expressed as % of wall contacts performed with the contralateral limb and in sec for the rotarod. Mean ± SEM were analyzed by two-way ANOVA followed by Newman-Keuls test. #p<0.001 vs. naïve; *p<0.05, **p<0.01, ***p<0.001 vs. Park group. No statistically significant differences among genotypes were found in any of the three conditions tested, i.e., naïve, Parkinsonian and dyskinetic. n=6-9

The performance of the mice in the rotarod after L-DOPA was measured 24 hours after administration to avoid exhaustion due to dyskinetic symptoms. The rotarod is a demanding test regarding motor condition, and the fatigue could interfere with the performance of the test. Moreover, recent results from our laboratory showed that L-DOPA acts for at least 4 days after

a chronic L-DOPA treatment (Espadas *et al.*, 2012), thus measuring efficacy of L-DOPA 24 hours post-administration seems reasonable and convenient.

These results from the rotarod correlated with the previous data from the cylinder test and confirm that modifications in DREAM content do not alter the antiparkinsonian efficacy of the L-DOPA, since all animals recover motor capacities after treatment.

As a matter of fact, the phenomenology of L-DOPA-induced dyskinesias in the rodent model, in terms of severity and amplitude, is conditioned by the degree of dopaminergic denervation within the striatum (Winkler *et al.*, 2002, Darmopil *et al.*, 2009; Francardo *et al.*, 2011). Thus, to exclude that the extent of the dopaminergic lesion in the three genotypes was different and possibly influencing the results, we assessed the percentage of striatal volume with a complete loss of TH-immunoreactive fibers for each group of animals (Figure 30). We found no significant differences between groups (44.2 ± 2% for daDREAM, 48.7 ± 2% for DREAM$^{-/-}$ and 46.2 ± 2% for the WT mice), indicating that the volume of dopamine-depleted striatum was similar among all groups studied and that the different dyskinetic behavior exhibited by mutant mice could not be attributable to different lesion degree.

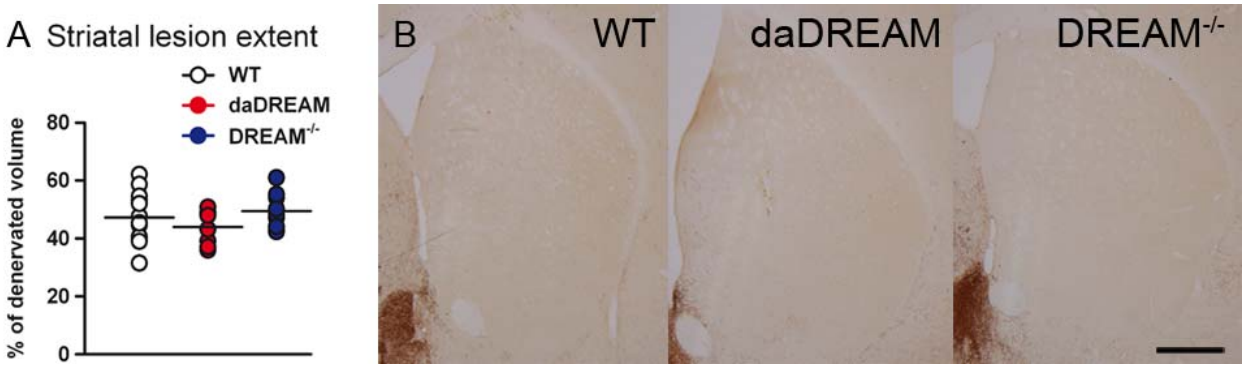

Figure 30. Striatal lesion extent in the three studied groups. (A) Scatter diagram of the extent of striatal lesions assessed by percentage of striatal volume completely denervated. No statistically significant differences were found among genotypes by one-way ANOVA analysis. **(B)** Coronal sections through the lesioned striatum of mice from the three studied genotypes immunostained for TH. Scale bar = 500 mm.

2.5. DREAM is expressed in direct and indirect striatal projection neurons

The positive distributed DREAM immunostaining in the striatum indicated to us that at least, striatal projection neurons were able to express the protein, although it was unknown whether DREAM is differentially expressed in direct versus indirect pathway neurons. We approached this question by using naïve BAC-transgenic D1R-tomato mice to differentiate direct from indirect pathway neurons. Striatal coronal sections from BAC-transgenic D1R-tomato mice were immunostained for DREAM. Confocal imaging analysis showed moderate DREAM signal in both, D1R-positive (red fluorescence) and D1R-negative (no fluorescence) medium

spiny neurons (Figure 31), suggesting that DREAM is expressed in both direct and indirect pathway neurons. This immunolabeling was preferentially nuclear, but was also evident in the cytoplasm and in the neuropil.

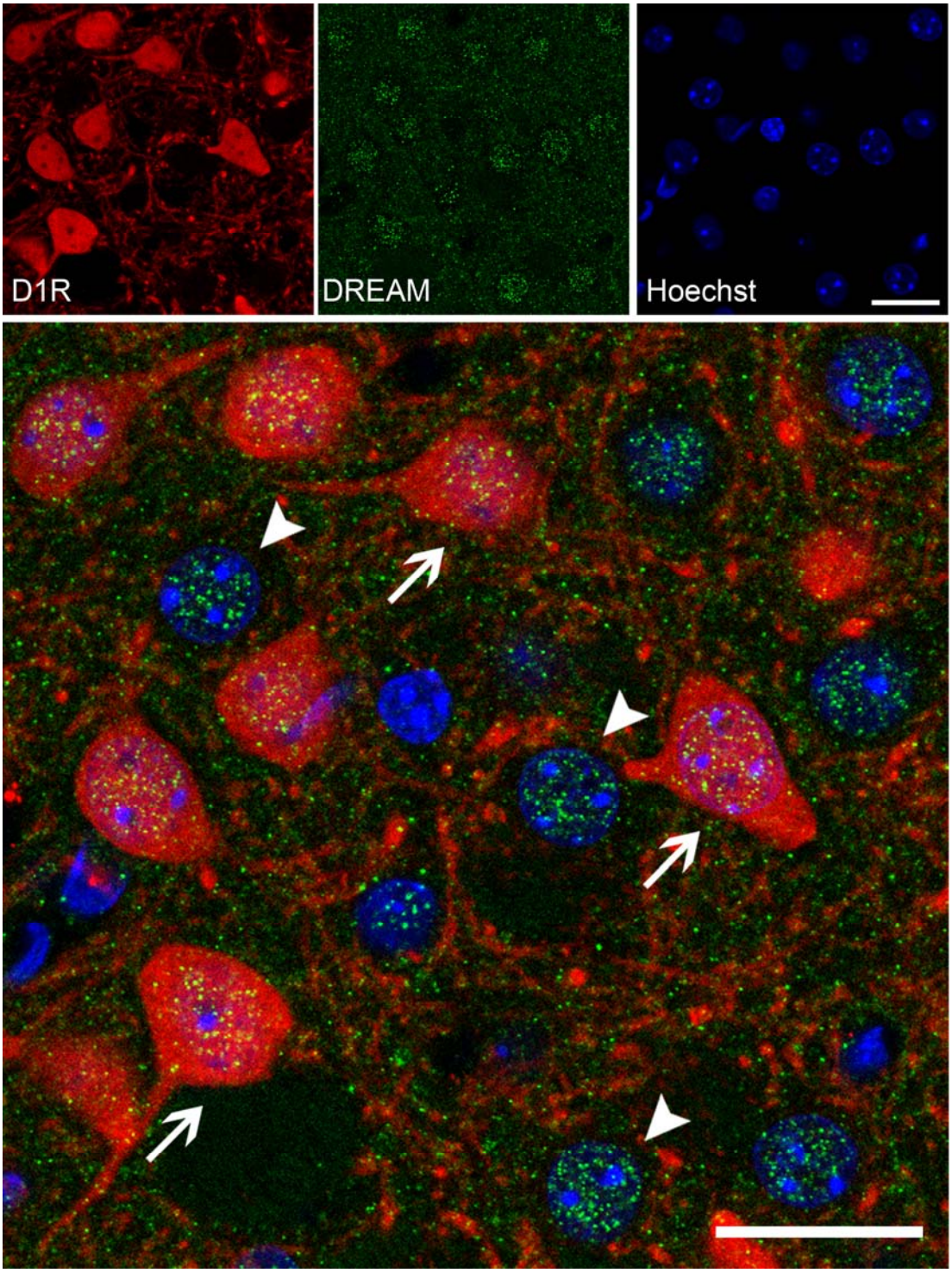

Figure 31. DREAM is expressed by both D1R-positive and D1R-negative medium spiny neurons. Representative high-resolution striatal confocal images of naïve BAC-transgenic D1R-tomato mice illustrating DREAM (green) expression in D1R-positive (red) and in D1R-negative medium spiny neurons. Hoechst (blue) stain identifies the nuclei. Arrows indicate examples of dual DREAM- and D1R-positive neurons while arrowheads point to DREAM-positive/D1R-negative neurons. Scale bar = 25 µm.

We therefore investigated the effect of 6-OHDA lesion and L-DOPA treatment in DREAM expression. To do so, we performed RT-qPCR experiments, which demonstrated that L-DOPA administration to sham or lesioned animals did not modify DREAM mRNA expression in the striatum or in the substantia nigra of wild type mice (Figure 32A). TH mRNA in the substantia nigra was also measured in the same animals by RT-qPCR to confirm the efficacy of 6-OHDA lesion (Figure 32B, [$F_{2,17} = 10.54$, $p<0.001$]).

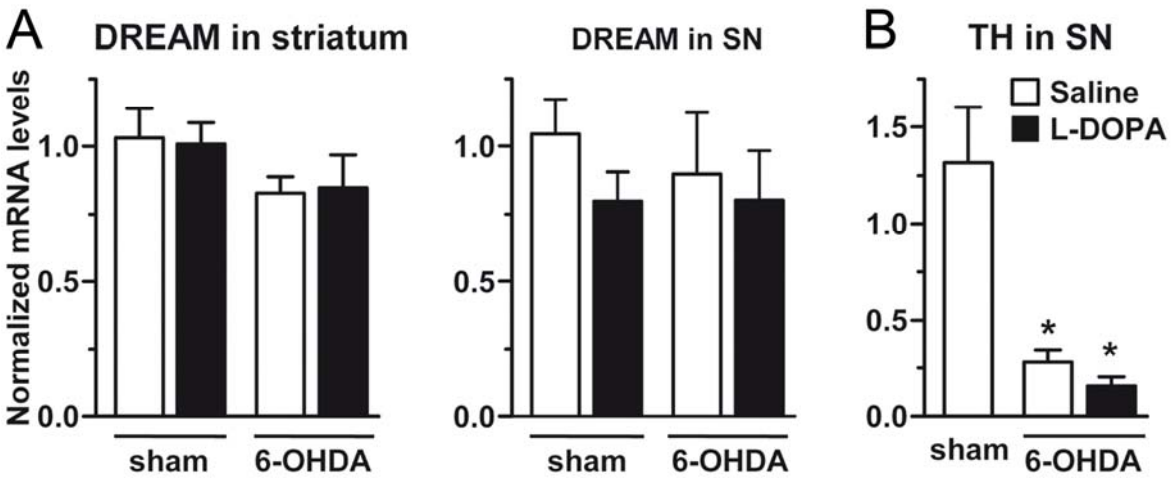

Figure 32. DREAM mRNA levels are not modified by dopamine depletion or L-DOPA treatment. Histograms show DREAM **(A)** and TH **(B)** mRNAs levels analyzed by RT-qPCR and normalized to 18S mRNA in wild type mice. **(B)** The TH mRNA levels in substantia nigra (SN) were quantified to confirm the efficacy of 6-OHDA lesion. Data (mean ± SEM) are expressed as normalized values and analyzed by one-way ANOVA followed by Newman-Keuls test. *$p<0.01$ vs. WT naïve animals. n=5-7.

2.6. DREAM regulates key molecular determinants of LID

Several studies have correlated the increased levels of FosB, dynorhin-B and P-AcH3 in the dorsolateral lesioned striatum with the appearance of L-DOPA-induced dyskinesia (Andersson *et al.*, 1999; Pavón *et al.*, 2006; Darmopil *et al.*, 2009). We evaluated the effect of the genetic modification of DREAM on the striatal levels of these markers after chronic L-DOPA administration in hemiparkinsonian mice. To carry out the molecular studies, animals were sacrificed 1 hour after the last L-DOPA injection, in the peak moment, on day 20 of chronic treatment, when molecular changes due to L-DOPA are fully established. Coronal striatal sections were immunostained for FosB, dynorhin-B and P-AcH3. The number of stained nuclei (for FosB and P-AcH3) as well as the proportional stained area (for dynorphin-B) were measured in 5 serial rostrocaudal sections per animal and 3 counting frames with the aid of an image analysis system.

As expected, L-DOPA treatment induced marked expression of FosB in the dorsolateral part of the lesioned striatum, sparing the unlesioned side in wild type animals. Notably, the number of FosB-positive neurons was threefold lower in the lesioned striatum of daDREAM transgenic mice and just slightly increased in DREAM$^{-/-}$ mice compared to wild type mice (Figure 33, [$F_{2,47}$ = 31.14; p<0.001]). These results are in agreement with the dyskinetic scores found for daDREAM and DREAM$^{-/-}$ mice.

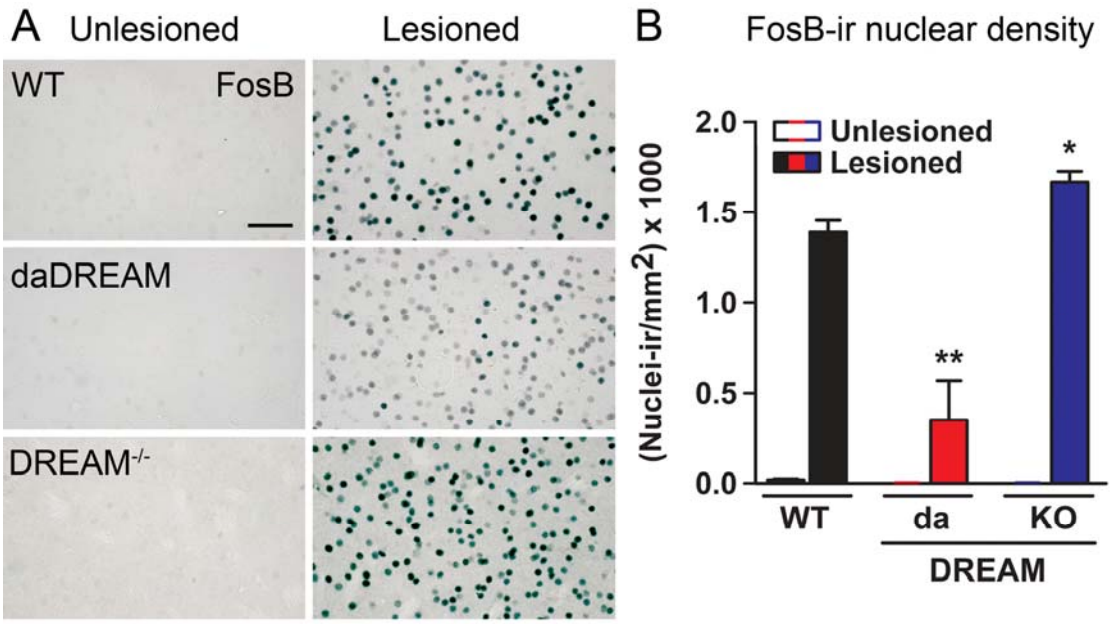

Figure 33. DREAM overexpression reduces, while its inactivation potentiates FosB protein expression induced by L-DOPA. (A) High power photomicrographs of unlesioned and lesioned striatum of WT, daDREAM and DREAM$^{-/-}$ mice sacrificed 1 hour after the last L-DOPA injection, immunostained for FosB. Scale bar = 50 µm. **(B)** Histograms represent the quantification of FosB-immunoreactive positive nuclei in the unlesioned and lesioned striatum of hemiparkinsonian WT, daDREAM and DREAM$^{-/-}$ mice. Note the higher expression in DREAM$^{-/-}$ compared to WT and the decreased expression in daDREAM mice. Data (mean ± SEM) representing positive nuclei were analyzed by two-way ANOVA followed by Newman-Keuls test. *p<0.01, **p<0.001 vs lesioned WT.

Furthermore, scanning of the dynorphin-B-positive area, including cytoplasm and neuropil, revealed a 39% reduction and a 65% increase relative to the total area scanned in daDREAM and DREAM$^{-/-}$ mice, respectively (Figure 34, [$F_{2,24}$ = 12.13; p<0.001]).

Finally, phosphorylation on Ser10-acetyl-Lys14 histone 3 was significantly modified in the striatum ipsilateral to the lesion with a 2.5-fold decrease in the number of P-AcH3-positive nuclei in daDREAM mice and a 1.5-fold increase in DREAM$^{-/-}$ mice compared to wild type mice (Figure 35, [$F_{2,41}$ = 21.67; p<0.001]).

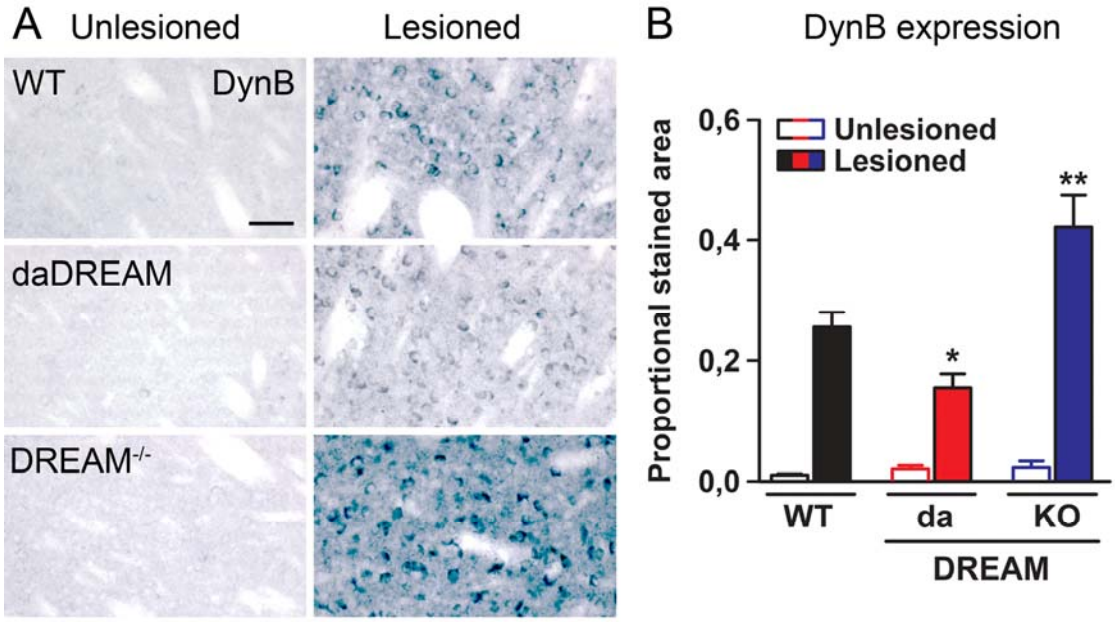

Figure 34. DREAM overexpression reduces, while its inactivation potentiates dynorphin-B protein expression induced by L-DOPA. (A) Representative photomicrographs of unlesioned and lesioned striatum of WT, daDREAM and DREAM$^{-/-}$ mice sacrificed 1 hour after the last L-DOPA injection, immunostained for dynorphin-B (DynB). Scale bar = 50 µm. **(B)** Histograms represent the quantification of the proportional dynorphin-B immunoreactive area in the unlesioned and lesioned striatum of hemiparkinsonian WT, daDREAM and DREAM$^{-/-}$ mice. Data (mean ± SEM) representing proportional stained area were analyzed by two-way ANOVA followed by Newman-Keuls test. **p*<0.01, ***p*<0.001 vs lesioned WT.

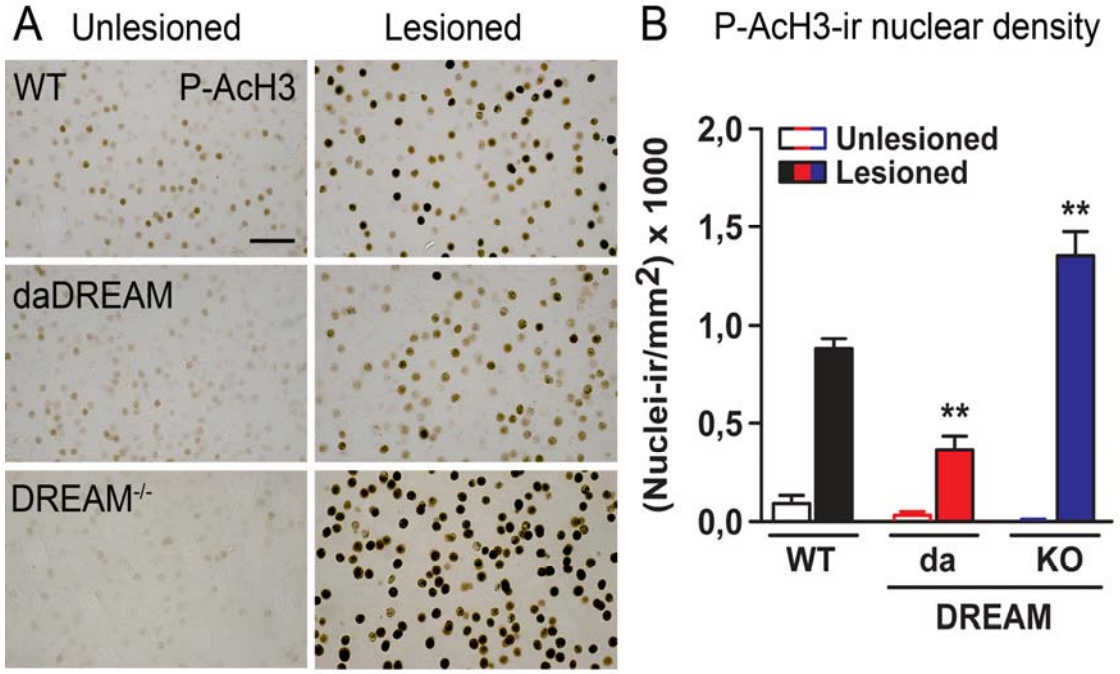

Figure 35. DREAM regulates P-AcH3 expression induced by L-DOPA. (A) High power photomicrographs of unlesioned and lesioned striatum of L-DOPA-treated WT, daDREAM and DREAM$^{-/-}$ mice, immunostained for P-AcH3. Scale bar = 50 µm. **(B)** Histograms represent the quantification of P-AcH3 -immunoreactive positive nuclei in the unlesioned and lesioned. DREAM overexpression reduces, while its inactivation potentiates P-AcH3 expression induced by L-DOPA. Data (mean ± SEM) representing positive nuclei were analyzed by two-way ANOVA followed by Newman-Keuls test. **p*<0.01, ***p*<0.001 vs lesioned WT.

The unlesioned striatum served as the negative control for these experiments: no statistically significant differences were found in any of these molecular markers in the unlesioned striatum of daDREAM, DREAM$^{-/-}$ and wild type mice. Furthermore, as an additional control for the specificity of these changes, we verified that the expression of L-DOPA-induced molecular determinants was strictly restricted to the completely denervated striatal area (Figure 36), as we have shown before (Darmopil *et al.*, 2009; Murer and Moratalla, 2011; Suárez *et al.*, 2014). These results indicate that genetic manipulation of DREAM does not modify the expression pattern of the molecular markers of dyskinesia in mice. These findings correlate well with

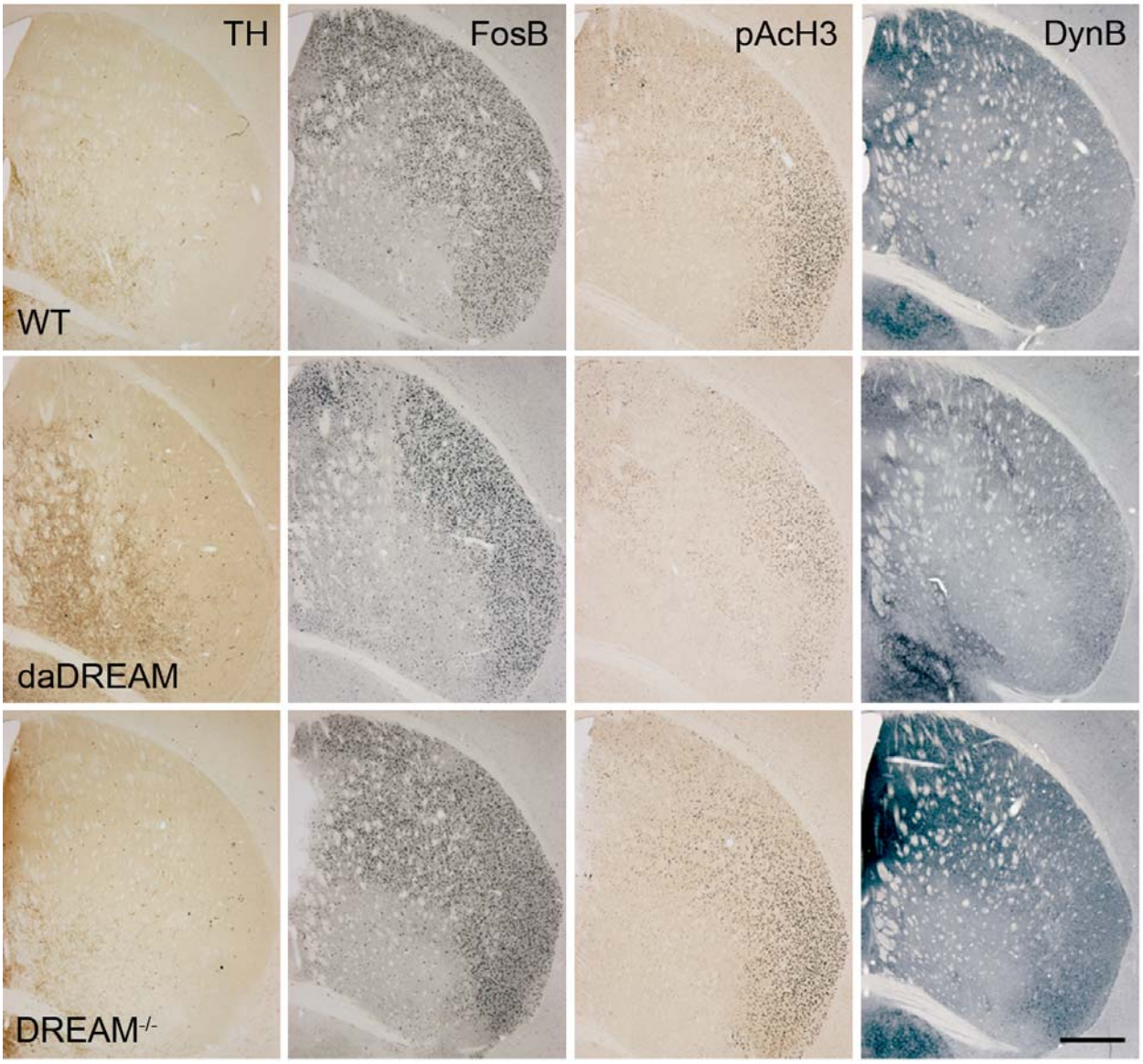

Figure 36. Genetic manipulation of DREAM does not alter the expression pattern of key molecular determinants induced by chronic L-DOPA in the lesioned striatum. Photomicrographs of adjacent striatal sections from WT, daDREAM and DREAM$^{-/-}$ mice sacrificed 1 hour after the last L-DOPA injection and immunostained for TH, FosB, P-AcH3 and dynorphin-B (DynB). Chronic L-DOPA administration induces marked FosB, P-AcH3 and dynorphin-B expression in the completely denervated striatal areas. Note that genetic manipulation of DREAM does not modify the expression pattern of molecular markers of dyskinesia. Scale bar = 500 μm.

our behavioral results and implicate DREAM in the regulation of FosB, dynorphin-B and P -AcH3 levels.

In line with the results from the immunohistochemistry experiments showed before, mRNA levels were analyzed to determine whether the observed changes in FosB and dynorphin -B expression were a consequence of modifications in a translational level or were due to changes in the expression of the genes under investigation. To answer this question, we carried out RT-qPCR experiments with control, unlesioned and lesioned striata. As expected from our previous results, L-DOPA dramatically increased FosB mRNA in the denervated striatum of wild type, daDREAM and DREAM$^{-/-}$ animals. Remarkably, in daDREAM mice this increase was significantly reduced compared to wild type mice (Figure 37A). Significant differences were found for genotype [$F_{2,40} = 3.29$, $p<0.05$], treatment [$F_{2,40} = 96.74$; $p<0.001$] and genotype x time [$F_{4,40} = 4.52$, $p<0.01$] by two-way ANOVA with repeated measures followed by Newman-Keuls test. Correlating with these findings, although L-DOPA treatment increased dynorphin-B mRNA levels in the striatum of DREAM$^{-/-}$ and wild type lesioned mice, this increase was not evident in the daDREAM mice (Figure 37B). No differences were found in sham and in unlesioned striatum between genotypes.

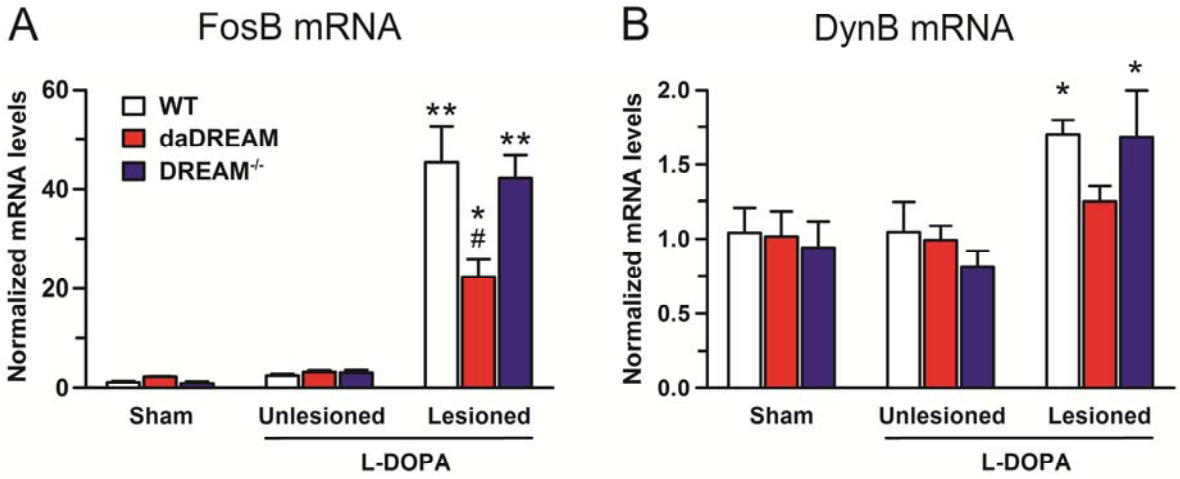

Figure 37. DREAM regulates L-DOPA induced FosB and DynB mRNAs expression in the denervated striatum. Histograms show FosB **(A)** and dynorphin-B (DynB) **(B)** mRNAs analyzed by RT-qPCR and normalized to GAPDH mRNA as reference gene. Note that L-DOPA induces both FosB and dynorphin-B transcripts up-regulation in the lesioned striatum of DREAM$^{-/-}$ and WT mice. Whereas, overexpression of DREAM diminishes FosB and blocks DynB mRNA up-regulation induced by L-DOPA. Data are expressed as normalized values (mean ± SEM) and analyzed by two-way ANOVA followed by Newman-Keuls test. *$p<0.01$, **$p<0.001$ vs. WT sham-operated animals; #$p<0.001$ vs. WT lesioned + L-DOPA. n=4-7.

2.7. LID-associated phosphorylation of GluR1 is attenuated in daDREAM mice

It has been well documented in the literature that chronic L-DOPA administration produces a PKA-dependent hyperphosphorylation at serine 845 of the GluR1 subunit of the glutamate AMPA receptor in the striatum of 6-OHDA lesioned mice (Santini *et al.*, 2007) and MPTP-lesioned monkeys (Santini *et al.*, 2010). Therefore, we examined whether the genetic modification of DREAM protein modifies the phosphorylation state of GluR1 induced by L-DOPA. Analysis of striatal extracts by western blot showed that L-DOPA treatment provokes an increase in P-GluR1 levels in wild type lesioned mice, as expected. This increase was evident also in the DREAM$^{-/-}$ mice; however, DREAM overexpression in daDREAM mice inhibited the hyperphosphorylation of GluR1 induced by L-DOPA (Figure 38A). Significant differences for genotype [$F_{2,55} = 3.23$, $p<0.05$] and for treatment [$F_{2,55} = 12.77$, $p<0.001$] were found by two-way ANOVA followed by Newman-Keuls test. In parallel, measurement of levels of TH protein confirmed a similar efficacy of the 6-OHDA lesion in all samples (Figure 38B).

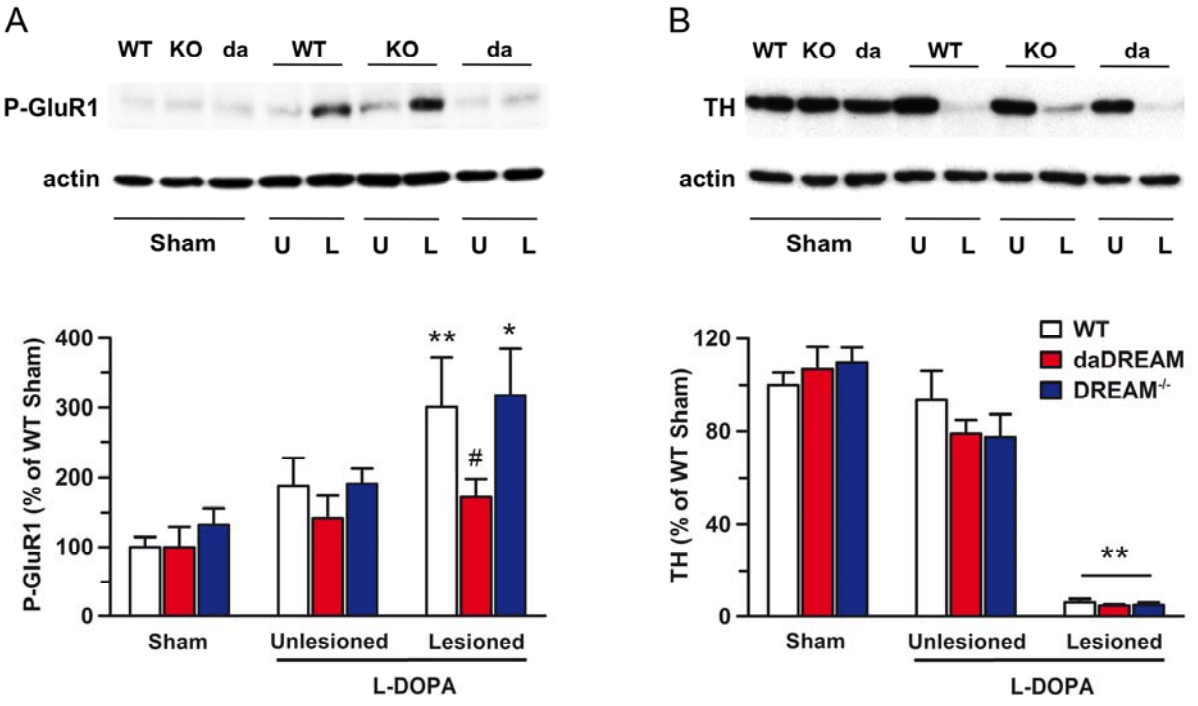

Figure 38. DREAM overexpression inhibits L-DOPA-induced phosphorylation of GluR1 at Ser845. Upper panels show representative autoradiograms of P-GluR1 **(A)** and TH **(B)** western blots of extracts from sham-operated, unlesioned (U) and lesioned (L) striatum of WT, daDREAM and DREAM$^{-/-}$ mice chronically treated with 25 mg/kg L-DOPA. Lower panels show the quantification of western blots in triplicates. **(A)** Chronic L-DOPA increases GluR1-phosphorylation at Ser845 in DREAM$^{-/-}$ and WT mice, whereas DREAM overexpression blocks it. **(B)** TH levels were quantified to confirm the efficacy of 6-OHDA lesion and no statistically significant differences were found among genotypes. Relative intensities versus loading control actin (normalized to WT Sham) were analyzed by two-way ANOVA followed by Newman-Keuls test. #$p<0.05$ vs WT lesioned + L-DOPA, *$p<0.01$, **$p<0.001$ vs WT sham-operated mice. n=4-5.

Discussion

The results presented in this Thesis pertain to Parkinson's disease (PD) which is one of the most common neurodegenerative disorders. The central neuropathology of PD is the degeneration of dopaminergic neurons in the substantia nigra, leading to dramatic striatal dopamine depletion, but the etiology and mechanisms of this disease are not fully understood. Despite extensive investigation aimed at finding new therapeutic approaches, the dopamine precursor molecule L-DOPA remains the most effective and widely used non-invasive therapy for PD. However, chronic treatment and disease progression cause the appearance of abnormal involuntary movements known as dyskinesia in the vast majority of patients. L-DOPA-induced dyskinesia interferes significantly with normal motor activity and persists unless L-DOPA dosages are reduced below therapeutic levels. Thus, controlling dyskinetic symptoms is one of the major challenges in PD therapy. Despite the progress made in recent years, the intracellular signaling mechanisms implicated in L-DOPA-induced dyskinesia are not fully established.

The results presented here shed some light on these mechanisms by specifically investigated the roles of two important proteins. In the first part of this discussion, I will be presenting the results and the interpretation regarding Gαolf protein (the olfactory type G-protein α subunit which couples D1R to adenylyl cyclase). In the second part, I will be presenting the results about DREAM (downstream regulatory element antagonist modulator) protein and its possible therapeutic implications in L-DOPA-induced dyskinesia.

1. ROLE OF DOPAMINE AND DOPAMINE RECEPTORS IN GαOLF EXPRESSION

The findings we described in this thesis demonstrate that striatal Gαolf expression is regulated by dopamine and by dopamine D1 receptor. The striosomal-matrix pattern that characterizes striatal Gαolf expression is loss in the dopamine depleted striatum and slightly normalized after chronic L-DOPA treatment in mice. These changes in the expression pattern are accompanied by modifications in Gαolf levels, showing an increase in the protein concentrations following striatal denervation and a reestablishment after L-DOPA administration. Importantly, this regulation is not evident in D1R null mice, which show not only a higher expression of Gαolf but also a complete loss of the striosomal-matrix pattern in the naïve situation. Moreover, dopaminergic denervation induces a decrease of Gαolf in the 6-OHDA-lesioned striatum of hemiparkinsonian $D1R^{-/-}$ mice and L-DOPA treatment does not restore either levels or pattern of Gαolf expression in these animals. On the contrary, dopamine D2 receptors are not involved in these changes as D2R null mice show the same expression pattern as their wild type littermates. In the same line, modifications in the calcium binding protein DREAM, located downstream from D1R/PKA pathway, do not alter the expression profile of the Gαolf protein.

1.1 Gαolf is expressed in the striatum with a striosomal-matrix pattern

In this work, we first examined the localization pattern of Gαolf in the striosomal-matrix system of naïve adult mice. Gαolf protein was preferentially expressed in the striosomal compartment of the striatum, as previously shown by Sako and coworkers (2010). Gαolf protein couples D1R to adenylyl cylclase (Zhuang *et al.*, 2000; Corvol *et al.*, 2001) but, surprisingly, Gαolf and D1R are not equally distributed in the striatum. While Gαolf is more concentrated in the striosomes, D1R is homogeneously expressed in all the striatum, without apparent compartmentalization from P10 onwards (Kim *et al.*, 2002). This divergence in the expression pattern could be due to the presence of "spare" D1R not coupled to adenylyl cyclase in the striatum (Hess *et al.*, 1987; Hervé *et al.*, 1989). According to Hess and coworkers (1987), this population corresponds approximately to 40 % of the total population of D1R. The higher density of these "spare" D1Rs in the matrix than in the striosomal compartments could be related to their different developmental origin, which indicates that striosomes may form an ontogenetic unit (Graybiel and Hickey, 1982) with different characteristics than matrix elements.

1.2 Dopamine depletion increases striatal Gαolf expression level

Following dopamine depletion by 6-OHDA administration, wild type animals showed a significant increase in Gαolf protein expression in the striatum, in line with previous works (Hervé *et al.*, 1993; Marcotte *et al.*, 1994; Penit-Soria *et al.*, 1997; Corvol *et al.*, 2004; Rangel-Barajas *et al.*, 2011; Alcacer *et al.*, 2012). The ability of dopamine to stimulate adenylyl cyclase and PKA via activation of D1R is enhanced in PD patients and in experimental animals after dopamine depletion (Tong *et al.*, 2004; Santini *et al.*, 2008). This hyper-responsiveness of D1R in the denervated striatum could be attributed to the increased levels of Gαolf. Furthermore, studies using electron microscopy also support this hypothesis. Thus, Gαolf up-regulation takes place in the plasma membrane of projection neurons, where it is functionally associated with D1R (Corvol *et al.*, 2004).

In line with the increase of Gαolf found in 6-OHDA-lesioned mice, previous works have reported changes in Gαolf expression following variations in dopamine levels. Treatment with a neurotoxic methamphetamine regimen decreases the dopaminergic tone and increases Gαolf expression in the striatum of wild type mice (Boikess *et al.*, 2010). On the other hand, deletion of the dopamine transporter in DAT knockout mice induces an increase in the extracellular concentration of dopamine along with a decrease in Gαolf protein expression (Hervé *et al.*, 2001). Taken together all these results, we suggest that dopamine regulates Gαolf expression and that a negative correlation exists between the striatal dopaminergic tone and the striatal Gαolf levels.

In the striatum, Gαolf protein not only couples adenylyl cyclase to D1R, but also to adenosine A2a receptors (A2aR) in D2R-bearing projection neurons (Corvol *et al.*, 2001). The increase in Gαolf levels could also be due to a reduction in the stimulation of A2aR since Gαolf expression is regulated by receptor usage (Corvol *et al.*, 2001). Previous findings from Dr. Morrelli's group support this idea since extracellular adenosine levels, measured by in vivo microdialysis, were significantly lower (-35%) in the dopamine depleted striatum fifteen days after 6-OHDA infusion (Pinna *et al.*, 2002). The decrease in adenosine transmission and the subsequent diminution of A2aR stimulation following nigrostriatal dopamine neuron degeneration should induce the accumulation of Gαolf protein. The increase in Gαolf would render A2aR hypersensible to adenosine stimulation therefore inducing the hyperactivity of the indirect pathway characteristic of PD. Correlating with this, an increase in adenylyl cyclase in response to A2a agonist has been seen in dopamine depleted striatum suggesting a hypersensitivity of A2aR (Premont *et al.*, 1979).

1.3 Dopamine depletion induces the loss of striatal Gαolf expression pattern

In addition, we provide evidence for the first time that the increase in Gαolf protein following dopamine depletion is accompanied by a loss in the compartmentalization pattern of expression, suggesting that the increase in Gαolf protein takes place mainly in the matrix compartment. It is not known whether there is differential vulnerability of dopamine in striosome and matrix compartments in PD. However, in a primate model of Parkinsonism generated by exposure to low-dose of MPTP, the dopamine-containing input to striosomes was found to be relatively spared in the caudal striatum, whereas dopaminergic inputs to the matrix were severely diminished (Moratalla *et al.*, 1992). The predominant loss of dopaminergic activity in the matrix compartment at caudal (sensorimotor) striatum might result in paucity of movement, thereby resulting in hypokinetic Parkinsonian symptoms. Moreover, the decrease of the dopaminergic tone in the matrix compartment in the Parkinsonian situation could be the cause of increased Gαolf expression in this area, as dopamine can regulate Gαolf expression.

1.4 L-DOPA restores striatal Gαolf expression levels

In agreement with the regulatory role of dopamine on Gαolf levels, 3-week treatment with L-DOPA reversed Gαolf up-regulation in the striatum of hemiparkinsonian mice. These results are consistent with previous data from dyskinetic rats (Corvol *et al.*, 2004; Rangel-Barajas *et al.*, 2011). However, it should be noted that persistent increase in Gαolf levels was recently reported in dyskinetic L-DOPA-treated mice (Alcacer *et al.*, 2012), in contrast to our

results. This discrepancy could result from the different measurement methodology. While Dr. Alcacer's group compares Gαolf protein levels between the lesioned and the non-lesioned striatum, we always compare protein measures to the naïve situation. Previous works have reported an increase in TH levels (Schlachetzki *et al.*, 2014) as well as in dopamine (Espadas *et al.*, 2012; Del-Bel *et al.*, 2013) in the non-lesioned hemisphere of the 6-OHDA model of PD. These data, along with the fact that L-DOPA is administered systemically, allow us to suggest that Gαolf expression could be also modified in the non-lesioned striatum compared to a naïve situation. Thus, comparisons between lesioned and naïve striatum seems to be a more accurate measure of L-DOPA impact on striatal Gαolf protein expression.

The reduction in the Gαolf protein levels following chronic L-DOPA treatment could be due to the reported increase in the G protein coupling efficiency at the levels of D1R in dyskinetic monkeys (Aubert *et al.*, 2005). So, the hyper-responsiveness of the D1R/PKA pathway induced by L-DOPA may not be mediated solely by an increase in D1R levels (Gerfen *et al.*, 1990; Hervé *et al.*, 1992; Hurley *et al.*, 2001) or an increase in the Golf protein expression, but their coupling.

In addition to this mechanism, and in line with the idea that receptor usage can control Gαolf expression, an abnormal increase in A2a signaling has been reported in the striatum of 6-OHDA-lesioned rats, MPTP-treated primates as well as in PD patients chronically treated with L-DOPA (Pinna *et al.*, 2002; Calon *et al.*, 2004; Tomiyama *et al.*, 2004). The prevailing tone of the A2aR following long-term L-DOPA administration could contribute to the aberrant decrease in Gαolf protein levels that is found in the dopamine depleted striatum.

1.5 L-DOPA restores striatal Gαolf expression pattern

Interestingly, our data show that L-DOPA treatment not only restores Gαolf protein concentration in the denervated striatum but also its striosomal-matrix characteristic expression pattern, diminishing Gαolf levels in the matrix compartment. These findings correlate with the expression pattern of two regulators of ERK signaling pathway (Crittenden *et al.*, 2009), which is directly involved in L-DOPA-induced dyskinesia (Pavón *et al.*, 2006; Darmopil *et al.*, 2009). Crittenden and coworkers reported that CalDAG-GEFII gene, an ERK activator, is strongly up-regulated in a rat model of L-DOPA-induced dyskinesia, and has a striking striosome-enriched pattern. By contrast, the matrix-enriched gene CalDAG-GEFI is down-regulated in this model. Taken together, these data suggest that striosomal neurons are over-activated relative to the matrix neurons in L-DOPA-induced dyskinesia. Interestingly, an imbalance in the activity of the two compartments favouring striosomes over matrix has been suggested to take place in dopa-

mine-dependent stereotypies (Moratalla *et al.*, 1996c; Canales and Graybiel, 2000; Saka *et al.*, 2004). Viewed in this context, our findings raise the possibility that the preferential striosomal expression of Gαolf could also participate in the development of L-DOPA-induced dyskinesia.

1.6 Regulation of Gαolf by dopamine takes place in a post-transcriptional level

Intriguingly, changes in Gαolf protein are not linked to parallel modifications in Gαolf mRNA. Despite the increase of Gαolf protein in hemiparkinsonian mice, our RT-qPCR experiments showed that the concentration of Gαolf transcripts did not vary significantly in the 6-OHDA-lesioned striatum, in agreement with previous findings by Northern blot (Hervé *et al.*, 1993). Dr. Hervé raises the possibility that lack of stimulation in dopamine depleted striatum could lower the Gαolf degradation rate and lead to accumulation of the protein (Hervé *et al.*, 2001), without a concomitant increase in the Gαolf mRNA. In line with this idea, L-DOPA induces opposite changes in Gαolf protein and mRNA. We described by the first time that while L-DOPA reduces Gαolf protein, transcripts are increased in dyskinetic mice. This finding is supported by several studies on Gαs (the stimulatory Gα ubiquitous isoform) that is a protein very close to Gαolf. In cell culture, long-lasting stimulation of Gαs induced a down-regulation of this protein (Adie and Milligan, 1994) by releasing Gαs from membranes along with an enhanced degradation rate (Levis and Bourne, 1992; Yajima *et al.*, 1998). We propose that in the dyskinetic scenario, L-DOPA stimulation of Gαolf also induces a down-regulation of the Gαolf protein probably due to an enhanced degradation and a concomitant enhanced transcription process. However, further studies are needed to confirm this hypothesis.

1.7 Modifications in striatal Gαolf expression are not due to chemical lesions but to dopamine stimulation

Pitx3 is a homeodomain transcription factor expressed in dopaminergic neurons in the brain and is essential for the normal development of the midbrain dopaminergic system (Jacobs *et al.*, 2007, 2009). Inactivation of Pitx3 in aphakia mice induces selective loss of dopaminergic neurons in the SNc and, as a consequence, major dopamine depletion in the striatum, providing a genetic model of PD (Hwang *et al.*, 2003; Ding *et al.*, 2007, 2011). Importantly, the results obtained in 6-OHDA lesioned wild type mice were corroborated in aphakia mice. Thus, in this genetic model of PD we found an increase in striatal Gαolf levels compared to those found in the wild type mice and very similar to those measured in 6-OHDA-lesioned mice. In the same line, L-DOPA treatment also restored Gαolf protein expression in aphakia mice. These data allow us to suggest that the results obtained are not due to the lesion procedure but to the dopamine deficit found in both 6-OHDA lesioned and aphakia mice.

1.8 Dopamine D1 receptor regulates Gαolf expression in the striatum

Importantly, genetic inactivation of D1R results not only in an increase of Gαolf expression, as seen by Dr. Hervé's group (2001) by Western blot, but also in a loss of the compartmentalized distribution of Gαolf protein as shown by our immunohistochemical results. This loss of pattern is in line with previous results obtained by Xu and colleagues (1994), who showed a loss in the characteristic striosomal dynorphin immunostaining in D1R null mice. The loss of Gαolf pattern in D1R deficient mice could be due to the differentially strong developmental expression of the D1R in the striosomes. Besides, we suggest that there might be developmental effects to compensate for the loss of D1R in these mice.

On the other hand, our RT-qPCR results showed no difference in Gαolf mRNA between D1R null mice and wild type, indicating that changes in Gαolf occur at a post-transcriptional level and do not result from a change in gene expression. This hypothesis is supported by the homogenous patter of Gαolf mRNA expression throughout striatal development in rats (Sakagami *et al.*, 1995), which contrasts with the striosomal-matrix patched pattern described in this work. Taken together, our results suggest that D1R regulates both protein level and expression pattern of Gαolf in basal conditions.

Contrary to that found in wild type animals, deletion of D1R in D1R knockout mice decreases Gαolf expression in the dopamine depleted striatum. These results are in agreement with previous findings in cocaine-treated mice (Zhang *et al.*, 2002), where cocaine binds to the dopamine transporter to block dopamine reuptake. Thus, dopamine stimulation is constant in this situation. Zhang's group (2002) reported an increase in the Gαolf protein levels in this scenario. The opposite happens in the denervated striatum of $D1R^{-/-}$ mice, where there is no dopamine stimulation. D1R null mice showed a decrease in Gαolf protein expression after 6-OHDA lesion. Significantly, chronic L-DOPA treatment did not modify Gαolf expression in D1R knockout mice. The lack of effect of L-DOPA on Gαolf expression in these mice correlated with previous findings from our laboratory, where it was shown that D1R is causally and necessary linked with L-DOPA-induced dyskinesia (Darmopil *et al.*, 2009). In that work it was demonstrated that D1R is required not only for the development of the L-DOPA-induced dyskinetic symptoms but also for the induction of the associated molecular changes, including FosB and dynorphin-B expression. Thus, stimulation by L-DOPA does not produce changes in elements downstream from D1R in D1R knockout mice, supporting our results with Gαolf protein expression.

1.9 Dopamine D2 receptor is not implicated in the regulation of striatal Gαolf

In relation to D2R, our data demonstrate that D2R is not implicated in the regulation of Gαolf expression. Genetic deletion of D2R in D2R null mice does not alter either levels or pattern expression of Gαolf in any of the studied situations, i.e., naïve, Parkinsonian and dyskinetic. This is in agreement with previous studies suggesting that striatonigral activity is not increased in D2R deficient mice (Baik *et al.*, 1995; Kelly *et al.*, 1998) and that Gαolf mRNA levels are not modified in these animals (Zahniser *et al.*, 2000). Interestingly, this latter work from Dr. Fredholm's group reported a reduction in A2a function in mice lacking D2R. Regarding their in situ hybridization experiments, which show same concentrations of Gαolf transcripts in both $D2R^{-/-}$ and wild type mice, they suggest that the decreased A2a activity could be due to a functional uncoupling of A2aR and Gαolf, and not to a lower expression of Gαolf. Our results corroborate this hypothesis since we found similar amounts of protein and equal expression pattern of Gαolf in both genotypes of mice.

1.10 Genetic modifications of DREAM protein, located downstream from D1R activation, do not affect Gαolf expression.

Finally, our results suggest that Gαolf levels are not regulated by D1R-dependent signaling downstream from cAMP stimulation. We found that genetic modification of DREAM protein, located downstream from the cAMP-regulated elements, do not induce any changes in the level or in the expression patter of Gαolf. This correlates with previous findings in mice lacking DARPP-32, which is also located downstream from the cAMP-regulated protein phosphorylation pathway (Hervé *et al.*, 2001, unpublished observations).

In summary, this study allows a better understanding of the mechanisms implicated in the regulation of striatal Gαolf expression. Our results strongly suggest a homeostatic regulation of Gαolf expression by dopamine, with a negative correlation between their concentrations. Moreover, our data clearly show that whereas D2R does not influence Gαolf expression, D1R is necessary for an accurate regulation of both levels and pattern expression of Gαolf. These results shed light on the mechanisms underlying the pathophysiology of PD and L-DOPA-induced dyskinesia and indicate that the striosomal-matrix system plays an important role in both pathologies.

2. ROLE OF DREAM PROTEIN IN L-DOPA-INDUCED DYSKINESIA AND IN THE ASSOCATED MOLECULAR CHANGES

In this study we have provided evidence that the DREAM protein plays a modulatory role in the establishment and development of L-DOPA-induced dyskinesia in mice and in the underlying molecular changes within the denervated striatum. **Overexpression of a dominant active version of DREAM in transgenic mice dramatically reduced L-DOPA-induced dyskinesia, whereas genetic inactivation of DREAM increased dyskinetic symptoms** (i.e. orofacial and limb dyskinesia and axial dystonia). In strict correspondence with the behavioral observations, molecular markers of dyskinesia induced by chronic L-DOPA treatment, including FosB, dynorphin-B, P-AcH3 and P-GluR1, were decreased in daDREAM mice but increased in DREAM knockout mice. Importantly, modifications in DREAM protein did not alter the kinetic profile or the antiparkinsonian efficacy of L-DOPA, suggesting that modulation of DREAM function could serve as an intervention target in therapies designed to alleviate L-DOPA-induced dyskinesia without interfering with the beneficial effects of L-DOPA treatment.

2.1 DREAM regulates L-DOPA-induced dyskinesia without alter either basal locomotor activity or antiparkinsonian efficacy of L-DOPA

In our behavioral analysis, we first tested spontaneous locomotor activity and motor coordination to rule out any motor impairment in mutant mice, which could interfere with the dyskinetic experiments. Performance in the open field and in the rotarod showed that mutant mice were indistinguishable from their wild type littermates, in agreement with previous observations in naïve DREAM$^{-/-}$ (Cheng *et al.*, 2002; Alexander *et al.*, 2009) and daDREAM (Dierssen *et al.*, 2012) adult mutant mice. These results suggest that the differences observed in L-DOPA-induced dyskinesia among genotypes are not due to any motor impairment, but rather to the modifications related to DREAM levels.

The main finding of this study is that, in our mouse model of L-DOPA-induced dyskinesia, dyskinetic symptoms generated by repeated administration of L-DOPA are increased in DREAM-deficient mice, whereas overactivation of DREAM in daDREAM animals diminishes dyskinesias. Importantly, dyskinetic differences among genotypes after L-DOPA treatment are not due to alterations of the kinetic profile of L-DOPA by DREAM, as all animals showed a similar duration of the L-DOPA response. Interestingly, mutant mice displayed similar motor performance skills in the cylinder and rotarod tests after L-DOPA administration, demonstrating that the antiparkinsonian effect of L-DOPA is preserved in mutant animals despite DREAM modifications.

2.2 DREAM represses FosB and dynorphin-B expression in direct pathway neurons

DREAM is a multi-functional calcium binding protein (Naranjo and Mellström, 2012) that acts as a transcriptional repressor to regulate activity-dependent gene expression through direct interaction with regulatory sites in the DNA (Carrión *et al.*, 1999). Our inmunnohistochemical studies revealed high levels of DREAM protein in the striatum, the cortex, the hippocampus and the substantia nigra of mouse brain, in line with previous immunohistochemical and in situ hybridization works (Spreafico *et al.*, 2001; Xiong *et al.*, 2004; Duncan *et al.*, 2009). In particular, immunohistochemical studies performed by the Weickert's group (2009) indicate that DREAM is expressed in the neuropil and in the soma of large and medium sized striatal neurons. Our data show now that DREAM is also present in the nucleus of striatal projection neurons, including D1R-positive neurons. In these neurons, increased expression of FosB and dynorphin-B after L-DOPA treatment correlates with dyskinesia in: PD patients (Piccini *et al.*, 1997; Tekumalla *et al.*, 2001), MPTP-treated monkeys (Berton *et al.*, 2009; Tamim *et al.*, 2010), and in 6-OHDA-treated rats (Andersson *et al.*, 1999) and mice (Pavón *et al.*, 2006; Darmopil *et al.*, 2009; Suárez *et al.*, 2014). Thus, transcriptional repression of FosB and prodynorphin genes in daDREAM mice could be directly related to the observed reduction in L-DOPA-induced dyskinesia development.

Correlating with the behavioral response to L-DOPA, our immunohistochemistry results show that overexpression of daDREAM diminishes FosB and dynorphin-B protein expression induced by L-DOPA in denervated striatal neurons, while genetic inactivation of DREAM induces the opposite effect. The small increase of FosB and dynorphin-B protein expression observed in the striatum of DREAM-deficient mice after L-DOPA is in agreement with similar increases observed previously in the spinal cord of DREAM$^{-/-}$ mice (Cheng *et al.*, 2002).

However, the RT-qPCR experiments showed that this modulation exerted by DREAM is more evident in daDREAM mice, in which we found a 50% decrease in FosB mRNA and a blockade of dynorphin mRNA increase after L-DOPA treatment. In the DREAM$^{-/-}$ mice we did not see any increase, either in FosB or in dynorphin mRNA levels compared to wild type mice as would have been expected, despite the small but significant increase observed in both proteins after L-DOPA treatment compared to wild type mice. This discrepancy between mRNA and protein levels could be due to the methodology. While the immnuhistochemistry allows us to selectively analyze the complete denervated striatal areas, where the molecular changes takes place (Pavón *et al.*, 2006; Darmopil *et al.*, 2009; Suárez *et al.*, 2014), in the RT-qPCR experiments the entire dorsal striatum is analyzed. Thus, small changes in FosB or/and dynorphin expression may go unnoticed.

DREAM represses the transcription of the immediate early genes Fos-related antigen-2 (fra-2) and c-fos as well as prodynorphin by binding to DRE sites located in the 5'-untranslated sequence downstream from the TATA box (Carrión *et al.*, 1999; Link *et al.*, 2004). Although not previously studied, taken together our data indicate that DREAM may also repress FosB transcription, consistent with the presence of two DRE sites in this gene (Lazo *et al.*, 1992).

In addition to DREAM regulation, dynorphin-B expression is also regulated by D1R activation (Moratalla *et al.*, 1996b) and by binding of Fos/Jun heterodimers to an AP-1 site in the prodynorphin gene (Naranjo *et al.*, 1991). Moreover, overexpression of FosB after L-DOPA treatment induces a concomitant increase of dynorphin-B expression in the 6-OHDA lesioned striatum (Andersson *et al.*, 1999). Therefore, our data support the notion that DREAM exerts a double synergistic effect: directly, blocking prodynorphin transcription by anchoring to its DRE site, and indirectly, diminishing FosB expression, resulting in dynorphin-B down-regulation via AP-1. This double synergistic effect of DREAM could explain our RT-qPCR results, which show that overexpression of DREAM in daDREAM mice completely inhibits L-DOPA-induced up-regulation of dynorphin mRNA, whereas this inhibition is only partial for FosB.

2.3 DREAM decreases L-DOPA-induced dyskinesia also by non-transcriptional mechanisms: role of NMDAR-DREAM interaction

The non-transcriptional effects of DREAM have been shown to regulate cell function and synaptic activity, mostly through a variety of specific protein-protein interactions (Rivas *et al.*, 2011). The list of target proteins include cationic channels (An *et al.*, 2000), membrane receptors (Rivas *et al.*, 2009; Zhang *et al.*, 2010) and membrane docking proteins (Wu *et al.*, 2010). A wide variety of mechanisms underlie synaptic changes associated with L-DOPA-induced dyskinesia, including abnormal dendritic spine increases in denervated D2R-containing striatal neurons (Suárez *et al.*, 2014) concomitant with abnormal increases in corticostriatal synapses (Zhang *et al.*, 2013). These synaptic changes may trigger the impaired synaptic plasticity and the persistent LTP found in the striatum of dyskinetic animals (Picconi *et al.*, 2003). The increase in dyskinesias that we observe in DREAM$^{-/-}$ mice is also in line with these results, since inactivation of DREAM has been shown to strongly potentiate LTP in free-moving mice (Fontán-Lozano *et al.*, 2009) and in hippocampal slices (Lilliehook *et al.*, 2003) after HFS. However, several additional mechanisms could be related to DREAM-mediated changes in L-DOPA-induced dyskinesias based on its presence in the cell body as discussed below.

In addition to D1R stimulation, NMDAR activation plays an important role in dyskinesia, as treatment with NMDAR antagonists such as MK-801 or amantadine completely abol-

ishes L-DOPA-induced dyskinesia (Papa *et al.*, 1995; Blanchet *et al.*, 2003). Interestingly, DREAM has been shown to diminish NMDAR activation (Wu *et al.*, 2010; Zhang *et al.*, 2010). DREAM knockdown with siRNAs significantly enhanced NMDAR-mediated currents in cultured neurons, while overexpression of DREAM reduced NMDAR activation and its presence in the plasma membrane, indicating that DREAM modulates NMDAR function. Taken together, these data correlate well with our dyskinetic behavioral results. Inactivation of DREAM, which potentiates NMDAR-mediated currents, potentiates dyskinesia, while DREAM overexpression, which inhibits NMDAR function, decreases dyskinesia. Thus, it is possible that the inhibitory role of DREAM in L-DOPA-induced dyskinesia reported here could be partially related to the negative regulation exerted by DREAM on NMDAR. DREAM may directly interact with the NR1 subunit preventing full activation of NMDAR complex as shown in cultured hippocampal neurons (Zhang *et al.*, 2010). In addition, the documented capacity of DREAM to bind PSD-95 (Wu *et al.*, 2010) impairing the recruitment of PSD-95 by D1 receptors (Porras *et al.*, 2012) could contribute to the observed reduction of L-DOPA-induced dyskinesia. Disruption of the NMDAR-PSD-95 complex increases L-DOPA-induced dyskinesia (Gardoni *et al.*, 2006), probably by making PSD-95 available for interaction with D1R in the synaptic membrane. Thus, displacement of the normal PSD-95 interactome from D1R due to increased DREAM levels could also contribute to the decrease in dyskinesia in daDREAM mice.

2.4 Activation of DREAM decreases histone H3 phosphorylation

Acetylated histone H3 is associated with active chromatin and gene transcription (Harrison *et al.*, 2013), and this effect is synergistically potentiated by histone H3 phosphorylation (Cheung *et al.*, 2000). Since phosphoacetylation of histone H3 correlates with the intensity of dyskinesia (Santini *et al.*, 2007, 2009; Darmopil *et al.*, 2009; Alcacer *et al.*, 2012), the presence of increased phosphoacetylated histone H3 in DREAM-deficient animals is consistent with increased dynorphin-B and FosB expression and with increased L-DOPA-induced dyskinesia. On the contrary, in the presence of the daDREAM repressor, we observed decreased P-AcH3, dynorphin-B, FosB and decreased L-DOPA-induced dyskinesia, as expected. In line with these observations, DREAM has been shown to inhibit transcription by blocking the CREB-CBP histone acetylase complex (Ledo *et al.*, 2002). On the other hand, histone H3 phosphorylation depends on the stimulation of the D1R-pathway (Darmopil *et al.*, 2009). Although it is possible that this occurs through the D1R/cAMP/PKA/DARPP-32 signaling pathway, it could also be mediated by the reported NMDAR-DREAM interaction through the NR1 receptor subunit (Zhang *et al.*, 2010).

2.5 Activation of DREAM diminishes phosphorylation of AMPA receptors

Although a direct DREAM and AMPA receptor interaction has not been described, it is possible that an indirect interaction occurs, since overexpression of DREAM significantly blocked L-DOPA-induced phosphorylation of the PKA substrate AMPA receptor subunit GluR1 at Ser845. GluR1-phosphorylation after L-DOPA treatment is in line with recent work from our laboratory (Suárez *et al.*, 2014) showing dendritic spine re-growth in denervated striatal areas. Indeed, spine regrowth leads to a recruitment of AMPA receptors to the postsynaptic site (Malinow *et al.*, 2000; Malenka, 2003; Shepherd and Huganir, 2007) in an activity -dependent manner. Thus, under L-DOPA activation, there is AMPA receptors recruitment whereas no such recruitment is evident in basal conditions. This is also in line with our Western blot experiments, which revealed similar levels of GluR1-phosphorylation in basal conditions in all mutant mice, consistent with work of Wu and colleagues (2010).

2.6 Calcium in L-DOPA-induced dyskinesia: DREAM regulation of voltage-dependent calcium channels

Finally, DREAM overexpression could control L-DOPA-induced dyskinesia development through the regulation of voltage-dependent calcium channels. It has been shown that blockade of L-type calcium channels using the antagonist isradipine decreases dyskinetic symptoms (Schuster *et al.*, 2009), while DREAM overexpression reduces the expression of the Cav1.2 gene, encoding the L-type calcium channel (Naranjo and Mellström, 2012) and decreases calcium permeability by direct protein-protein interaction with the L- and the T-type channel complexes (Thomsen *et al.*, 2009; Anderson *et al.*, 2010; Rivas *et al.*, 2011).

2.7 Alternative mechanisms of DREAM regulation

We found a decrease in both dyskinetic symptoms and L-DOPA-induced molecular markers in the daDREAM mice but this decrease was not a complete blockade. This lack of complete blockade may be due to other alternative mechanisms that modulate DREAM biological activity. Thus, in addition to αCREM and/or calcium interaction, other mechanisms can regulate DREAM function. These may include differential splicing (Spreafico *et al.*, 2001), cleavage of N-terminal (Choi *et al.*, 2003), palmitoylation (Takimoto *et al.*, 2002) and phosphorylation by downstream kinases of the PI3 kinase pathway (Sanz *et al.*, 2001).

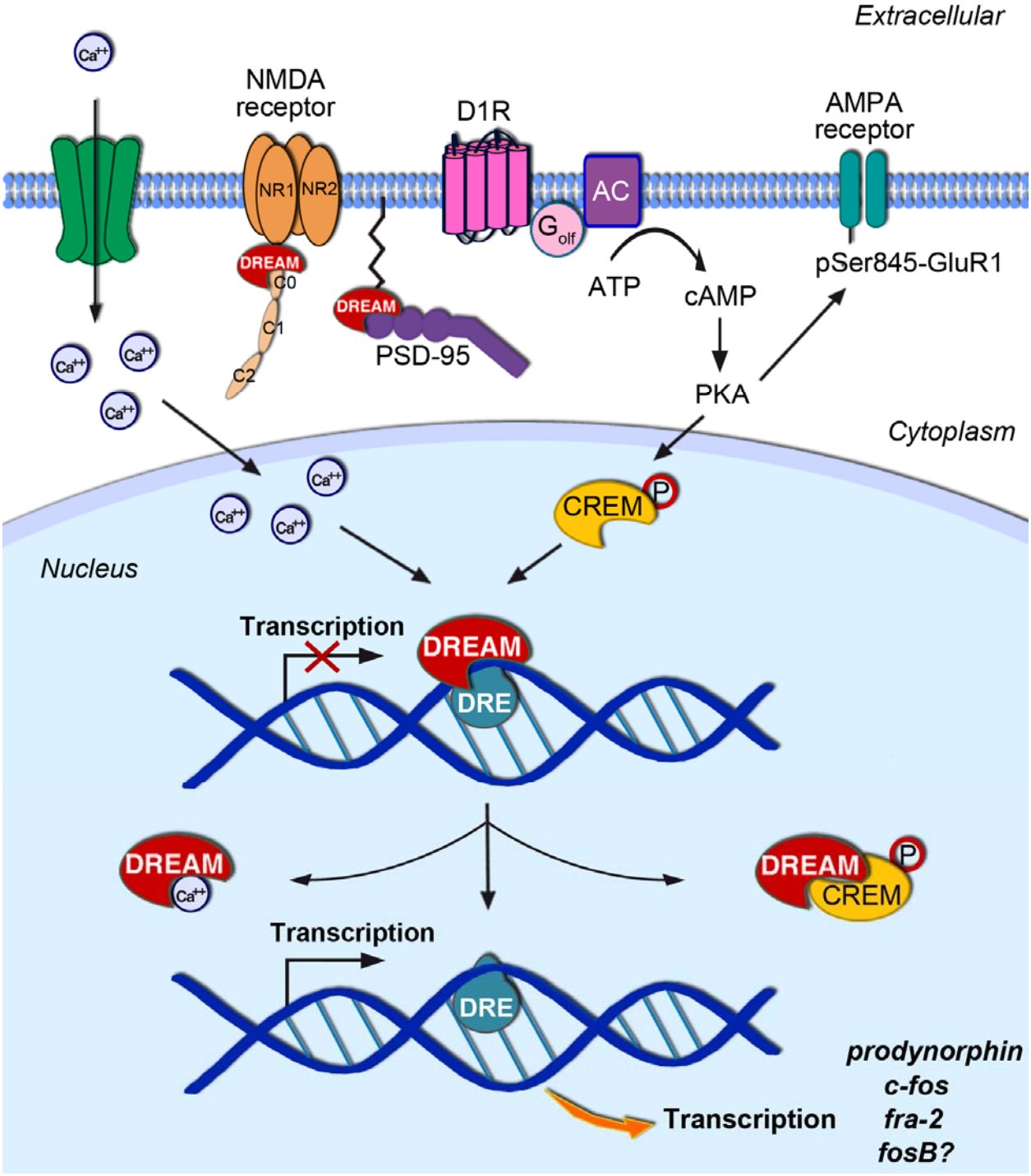

Figure 39. Schematic diagram illustrating the regulatory role of DREAM in the transcriptional and non-transcriptional mechanisms involved in LID. In the nucleus, the DREAM protein regulates dynorphin-B and possibly FosB expression (and subsequent LID) by anchoring to DRE sites located downstream from the transcription initiation site of the DNA. This repression is released under conditions of Ca^{2+} and PKA-dependent interaction with phospho-CREM. In addition, outside the nucleus, DREAM could directly interact with NR1 subunit, inhibiting activation of NMDA receptors, and with PSD-95, impairing its recruitment by D1R and decreasing the cAMP/PKA signaling pathway.

In summary, this study demonstrates the inhibitory role of DREAM in L-DOPA-induced dyskinesia as evidenced by reduction of dyskinetic symptoms in daDREAM mice and a potentiation of symptoms in DREAM$^{-/-}$ mice. In addition, we demonstrate that this action occurs at least in part by transcriptional repression of target genes, although non-transcriptional mechanisms could also be involved. Thus, DREAM regulates dynorphin-B and possibly FosB expression, repressing their transcription by anchoring to DRE sites in the DNA, and reducing L-DOPA-induced dyskinesia. In addition, outside the nucleus DREAM could directly interact with the NR1 subunit and PSD-95, regulating activation of NMDAR and D1R (Figure 39). The findings we describe here validate DREAM as a novel therapeutic target against L-DOPA-induced dyskinesia, and we propose that specific modulators of DREAM could be useful in alleviating L-DOPA-induced dyskinesia without interfering with the antiparkinsonian effect of L-DOPA. However, other transcriptional and non-transcriptional targets of DREAM, as yet uncharacterized, could also be important, directly or indirectly, in the regulation of L-DOPA-induced dyskinesia. Future genome-wide analysis during L-DOPA-induced dyskinesia in daDREAM and DREAM$^{-/-}$ mice might expand our understanding of the role of DREAM in L-DOPA-induced dyskinesia.

Conclusions

The results obtained in the aforementioned studies lead us to the following conclusions:

1. In the striatum, Gαolf is primarily expressed in the striosomal compartment. Dopamine depletion by 6-OHDA lesion or genetic manipulation increases Gαolf protein and changes its expression pattern.

2. L-DOPA treatment restores both Gαolf protein levels and Gαolf expression pattern in the striatum of either 6-OHDA-lesioned or genetically manipulated mice.

3. Dopamine D1 receptor, but not D2 receptor, regulates Gαolf expression in the striatum.

4. Genetic modifications of DREAM, a downstream signaling element of D1R activation, do not affect Gαolf expression.

5. Genetic modifications of DREAM do not alter basal locomotor activity or motor coordination.

6. Overactivation of DREAM decreases L-DOPA-induced dyskinesia, while inactivation DREAM increases dyskinetic symptoms.

7. The therapeutic efficacy of L-DOPA is maintained despite genetic modifications of DREAM.

8. DREAM is expressed in both D1R-positive and D1R–negative projection neurons in the striatum.

9. DREAM levels in the striatum or substantia nigra are not affected by either 6-OHDA or L -DOPA treatment.

10. Overactivation of DREAM decreases the key molecular determinants of L-DOPA-induced dyskinesias including FosB, dynorphin-B, P-AcH3 and P-GluR1, whereas DREAM inactivation increases them.

In summary our data suggest that DREAM activators may be useful in alleviating L-DOPA-induced dyskinesias without interfering with its therapeutic motor effects.

Bibliography

Adie, E. J. & Milligan, G. (1994). Agonist regulation of cellular Gs alpha-subunit levels in neuroblastoma x glioma hybrid NG108-15 cells transfected to express different levels of the human beta 2 adrenoceptor. *Biochem J* 300 (Pt 3), 709-15.

Alachkar, A., Brotchie, J. M. & Jones, O. T. (2010). Locomotor response to L-DOPA in reserpine-treated rats following central inhibition of aromatic L-amino acid decarboxylase: further evidence for non-dopaminergic actions of L-DOPA and its metabolites. *Neurosci Res* 68, 44-50.

Albin, R. L., Young, A. B. & Penney, J. B. (1989). The functional anatomy of basal ganglia disorders. *Trends Neurosci* 12, 366-75.

Alcacer, C., Santini, E., Valjent, E., Gaven, F., Girault, J. A. & Herve, D. (2012). Galpha(olf) mutation allows parsing the role of cAMP-dependent and extracellular signal-regulated kinase-dependent signaling in L-3,4-dihydroxyphenylalanine-induced dyskinesia. *J Neurosci* 32, 5900-10.

Alexander, J. C., McDermott, C. M., Tunur, T., Rands, V., Stelly, C., Karhson, *et al*. (2009). The role of calsenilin/DREAM/KChIP3 in contextual fear conditioning. *Learn Mem* 16, 167-77.

An, W. F., Bowlby, M. R., Betty, M., Cao, J., Ling, H. P., Mendoza, G., *et al*. (2000). Modulation of A-type potassium channels by a family of calcium sensors. *Nature* 403, 553-6.

Anderson, D., Mehaffey, W.H., Iftinca, M., Rehak, R., Engbers, J.D., Hameed, S., *et al*. (2010). Regulation of neuronal activity by Cav3-Kv4 channel signaling complexes. *Nat Neurosci* 13, 333-7.

Andersson, M., Hilbertson, A. & Cenci, M. A. (1999). Striatal fosB expression is causally linked with l-DOPA-induced abnormal involuntary movements and the associated upregulation of striatal prodynorphin mRNA in a rat model of Parkinson's disease. *Neurobiol Dis* 6, 461-74.

Andersson, M., Konradi, C. & Cenci, M. A. (2001). cAMP response element-binding protein is required for dopamine-dependent gene expression in the intact but not the dopamine-denervated striatum. *J Neurosci.* 21, 9930-43.

Anzalone, A., Lizardi-Ortiz, J. E., Ramos, M., De Mei, C., Hopf, F. W., Iaccarino, C., *et al*. (2012). Dual control of dopamine synthesis and release by presynaptic and postsynaptic dopamine D2 receptors. *J Neurosci.* 32, 9023-34.

Aosaki, T., Tsubokawa, H., Ishida, A., Watanabe, K., Graybiel, A. M. & Kimura, M. (1994). Responses of tonically active neurons in the primate's striatum undergo systematic changes during behavioral sensorimotor conditioning. *J Neurosci.* 14, 3969-84.

Ares-Santos, S., Granado, N., Espadas, I., Martinez-Murillo, R. & Moratalla, R. (2014). Methamphetamine causes degeneration of dopamine cell bodies and terminals of the nigrostriatal pathway evidenced by silver staining. *Neuropsychopharmacology* 39, 1066-80.

Ares-Santos, S., Granado, N., Oliva, I., O'Shea, E., Martin, E. D., Colado, M. I., *et al*. (2012). Dopamine D(1) receptor deletion strongly reduces neurotoxic effects of methamphetamine. *Neurobiol Dis.* 45, 810-20.

Arnt, J. & Hyttel, J. (1985). Differential involvement of dopamine D-1 and D-2 receptors in the circling behaviour induced by apomorphine, SK & F 38393, pergolide and LY 171555 in 6-hydroxydopamine-lesioned rats. *Psychopharmacology (Berl)* 85, 346-52.

Aubert, I., Guigoni, C., Hakansson, K., Li, Q., Dovero, S., Barthe, N., *et al*. (2005). Increased D1 dopamine receptor signaling in levodopa-induced dyskinesia. *Ann Neurol* 57, 17-26.

Baik, J. H., Picetti, R., Saiardi, A., Thiriet, G., Dierich, A., Depaulis, A., *et al*. (1995). Parkinsonian-like locomotor impairment in mice lacking dopamine D2 receptors. *Nature* 377, 424-8.

Bateup, H. S., Santini, E., Shen, W., Birnbaum, S., Valjent, E., Surmeier, D. J., *et al*. (2010). Distinct subclasses of medium spiny neurons differentially regulate striatal motor behaviors. *Proc Natl Acad Sci U S A* 107, 14845-50.

Bedard, P. J., Di Paolo, T., Falardeau, P. & Boucher, R. (1986). Chronic treatment with L-DOPA, but not bromocriptine induces dyskinesia in MPTP-parkinsonian monkeys. Correlation with [3H] spiperone binding. *Brain Res* 379, 294-9.

Belluscio, L., Gold, G. H., Nemes, A. & Axel, R. (1998). Mice deficient in G(olf) are anosmic. *Neuron* 20, 69-81.

Berthet, A., Porras, G., Doudnikoff, E., Stark, H., Cador, M., Bezard, E. & Bloch, B. (2009). Pharmacological analysis demonstrates dramatic alteration of D1 dopamine receptor neuronal distribution in the rat analog of L-DOPA-induced dyskinesia. *J Neurosci* 29, 4829-35.

Berton, O., Guigoni, C., Li, Q., Bioulac, B. H., Aubert, I., Gross, C. E., *et al*. (2009). Striatal overexpression of DeltaJunD resets L-DOPA-induced dyskinesia in a primate model of Parkinson disease. *Biol Psychiatry* 66, 554-61.

Bertran-Gonzalez, J., Herve, D., Girault, J. A. & Valjent, E. (2010). What is the Degree of Segregation between Striatonigral and Striatopallidal Projections? *Front Neuroanat*.4

Bezard, E., Ferry, S., Mach, U., Stark, H., Leriche, L., Boraud, T., *et al*. (2003) Attenuation of levodopa-induced dyskinesia by normalizing dopamine D3 receptor function. *Nat Med*. 9, 762-7.

Bezard, E., Olanow, C. W. & Obeso, J. A. (2013). Levodopa-induced dyskinesias in the absence of nigrostriatal degeneration. *Mov Disord* 28, 1023-4.

Blanchet, P. J., Metman, L. V. & Chase, T. N. (2003). Renaissance of amantadine in the treatment of Parkinson's disease. *Adv Neurol* 91, 251-7.

Boikess, S. R., O'Dell, S. J. & Marshall, J. F. (2010). Neurotoxic methamphetamine regimens produce long-lasting changes in striatal G-proteins. *Synapse* 64, 839-44.

Bolam, J. P. & Pissadaki, E. K. (2012). Living on the edge with too many mouths to feed: why dopamine neurons die. *Mov Disord* 27, 1478-83.

Bordet, R., Ridray, S., Carboni, S., Diaz, J., Sokoloff, P. & Schwartz, J. C. (1997). Induction of dopamine D3 receptor expression as a mechanism of behavioral sensitization to levodopa. *Proc Natl Acad Sci U S A.* 94, 3363-7.

Boumezbeur, F., Mason, G. F., de Graaf, R. A., Behar, K. L., Cline, G. W., Shulman, G. I., *et al*. (2010). Altered brain mitochondrial metabolism in healthy aging as assessed by in vivo magnetic resonance spectroscopy. *J Cereb Blood Flow Metab.* 30, 211-21.

Braak, H., Del Tredici, K., Bratzke, H., Hamm-Clement, J., Sandmann-Keil, D. & Rub, U. (2002). Staging of the intracerebral inclusion body pathology associated with idiopathic Parkinson's disease (preclinical and clinical stages). *J Neurol* 249 Suppl 3, III/1-5.

Braak, H., Del Tredici, K., Rub, U., de Vos, R. A., Jansen Steur, E. N. & Braak, E. (2003). Staging of brain pathology related to sporadic Parkinson's disease. *Neurobiol Aging* 24, 197-211.

Breese, G. R. & Traylor, T. D. (1971). Depletion of brain noradrenaline and dopamine by 6-hydroxydopamine. *Br J Pharmacol* 42, 88-99.

Breuer, O., Lawhorn, C., Miller, T., Smith, D. M. & Brown, L. L. (2005). Functional architecture of the mammalian striatum: mouse vascular and striosome organization and their anatomic relationships. *Neurosci Lett* 385, 198-203.

Brown, L. L., Feldman, S. M., Smith, D. M., Cavanaugh, J. R., Ackermann, R. F. & Graybiel, A. M. (2002). Differential metabolic activity in the striosome and matrix compartments of the rat striatum during natural behaviors. *J Neurosci* 22, 305-14.

Burgoyne, R. D. & Weiss, J. L. (2001). The neuronal calcium sensor family of Ca2+-binding proteins. *Biochem J* 353, 1-12.

Buxbaum, J. D., Choi, E. K., Luo, Y., Lilliehook, C., Crowley, A. C., Merriam, D. E. *et al*. (1998). Calsenilin: a calcium-binding protein that interacts with the presenilins and regulates the levels of a presenilin fragment. *Nat Med* 4, 1177-81.

Cai, G., Wang, H. Y. & Friedman, E. (2002). Increased dopamine receptor signaling and dopamine receptor-G protein coupling in denervated striatum. *J Pharmacol Exp Ther* 302, 1105-12.

Calne, D. B. & Mizuno, Y. (2004). The neuromythology of Parkinson's Disease. *Parkinsonism Relat Disord* 10, 319-22.

Calon, F., Dridi, M., Hornykiewicz, O., Bedard, P. J., Rajput, A. H. & Di Paolo, T. (2004). Increased adenosine A2A receptors in the brain of Parkinson's disease patients with dyskinesias. *Brain* 127, 1075-84.

Canales, J. J. & Graybiel, A. M. (2000). A measure of striatal function predicts motor stereotypy. *Nat Neurosci* 3, 377-83.

Cao, X., Yasuda, T., Uthayathas, S., Watts, R. L., Mouradian, M. M., Mochizuki, H. *et al*. (2010). Striatal overexpression of DeltaFosB reproduces chronic levodopa-induced involuntary movements. *J Neurosci.* 30, 7335-43.

Carlson, A. (2001). A paradigm shift in brain research. *Science*. 294, 1021-4.

Carrion, A. M., Link, W. A., Ledo, F., Mellstrom, B. & Naranjo, J. R. (1999). DREAM is a Ca2+-regulated transcriptional repressor. *Nature* 398, 80-4.

Carrion, A. M., Mellstrom, B. & Naranjo, J. R. (1998). Protein kinase A-dependent derepression of the human prodynorphin gene via differential binding to an intragenic silencer element. *Mol Cell Biol.* 18, 6921-9.

Cebolla, B., Fernandez-Perez, A., Perea, G., Araque, A. & Vallejo, M. (2008). DREAM mediates cAMP -dependent, Ca2+-induced stimulation of GFAP gene expression and regulates cortical astrogliogenesis. *J Neurosci.* 28, 6703-13.

Cenci, M. A. & Konradi, C. (2010). Maladaptive striatal plasticity in L-DOPA-induced dyskinesia. *Prog Brain Res* 183, 209-33.

Cenci, M. A., Lee, C. S. & Bjorklund, A. (1998). L-DOPA-induced dyskinesia in the rat is associated with striatal overexpression of prodynorphin- and glutamic acid decarboxylase mRNA. *Eur J Neurosci.* 10, 2694-706.

Centonze, D., Grande, C., Saulle, E., Martin, A. B., Gubellini, P., Pavon, N., *et al*. (2003). Distinct roles of D1 and D5 dopamine receptors in motor activity and striatal synaptic plasticity. *J Neurosci.* 23, 8506-12.

Chase, T. N., Oh, J. D. & Konitsiotis, S. (2000). Antiparkinsonian and antidyskinetic activity of drugs targeting central glutamatergic mechanisms. *J Neurol* 247 Suppl 2, II36-42.

Chaudhuri, K. R. & Schapira, A. H. (2009). Non-motor symptoms of Parkinson's disease: dopaminergic pathophysiology and treatment. *Lancet Neurol* 8, 464-74.

Cheng, H. Y., Pitcher, G. M., Laviolette, S. R., Whishaw, I. Q., Tong, K. I., Kockeritz, L. K., *et al*. (2002). DREAM is a critical transcriptional repressor for pain modulation. *Cell* 108, 31-43.

Cheung, P., Tanner, K. G., Cheung, W. L., Sassone-Corsi, P., Denu, J. M. & Allis, C. D. (2000). Synergistic coupling of histone H3 phosphorylation and acetylation in response to epidermal growth factor stimulation. *Mol Cell* 5, 905-15.

Choi, E. K., Miller, J. S., Zaidi, N. F., Salih, E., Buxbaum, J. D. & Wasco, W. (2003). Phosphorylation of calsenilin at Ser63 regulates its cleavage by caspase-3. *Mol Cell Neurosci* 23, 495-506.

Clarke, C. E., Sambrook, M. A., Mitchell, I. J. & Crossman, A. R. (1987). Levodopa-induced dyskinesia and response fluctuations in primates rendered parkinsonian with 1-methyl-4-phenyl-1,2,3,6-tetrahydropyridine (MPTP). *J Neurol Sci* 78, 273-80.

Corvol, J. C., Muriel, M. P., Valjent, E., Feger, J., Hanoun, N., Girault, J. A., *et al*. (2004). Persistent increase in olfactory type G-protein alpha subunit levels may underlie D1 receptor functional hypersensitivity in Parkinson disease. *J Neurosci* 24, 7007-14.

Corvol, J. C., Studler, J. M., Schonn, J. S., Girault, J. A. & Herve, D. (2001). Galpha(olf) is necessary for coupling D1 and A2a receptors to adenylyl cyclase in the striatum. *J Neurochem* 76, 1585-8.

Cotzias, G. C. (1968). L-Dopa for Parkinsonism. *N Engl J Med.* 278-630.

Creese, I., Burt, D. R. & Snyder, S. H. (1977). Dopamine receptor binding enhancement accompanies lesion-induced behavioral supersensitivity. *Science* 197, 596-8.

Crittenden, J. R., Cantuti-Castelvetri, I., Saka, E., Keller-McGandy, C. E., Hernandez, L. F., Kett, L. R., *et al*. (2009). Dysregulation of CalDAG-GEFI and CalDAG-GEFII predicts the severity of motor side-effects induced by anti-parkinsonian therapy. *Proc Natl Acad Sci U S A* 106, 2892-6.

Crittenden, J. R. & Graybiel, A. M. (2011). Basal Ganglia disorders associated with imbalances in the striatal striosome and matrix compartments. *Front Neuroanat.* 5-59.

Darmopil, S., Martin, A. B., De Diego, I. R., Ares, S. & Moratalla, R. (2009). Genetic inactivation of dopamine D1 but not D2 receptors inhibits L-DOPA-induced dyskinesia and histone activation. *Biol Psychiatry.* 66, 603-13.

Darmopil, S., Muneton-Gomez, V. C., de Ceballos, M. L., Bernson, M. & Moratalla, R. (2008). Tyrosine hydroxylase cells appearing in the mouse striatum after dopamine denervation are likely to be projection neurones regulated by L-DOPA. *Eur J Neurosci.* 27, 580-92.

Davis, M. I. & Puhl, H. L., 3rd. (2011). Nr4a1-eGFP is a marker of striosome-matrix architecture, development and activity in the extended striatum. *PLoS One* 6, e16619.

De Lau, L. M. & Breteler, M. LM. (2006). Epidemiology of Parkinson's disease. *Lancet Neurol.* 5, 525-35.

Del-Bel, E., Padovan-Neto, F. E., Szawka, R. E., da-Silva, C. A., Raisman-Vozari, R., Anselmo-Franci, J., *et al*. (2014). Counteraction by nitric oxide synthase inhibitor of neurochemical alterations of dopaminergic system in 6-OHDA-lesioned rats under L-DOPA treatment. *Neurotox Res.* 25, 33-44.

Delfino, M., Kalisch, R., Czisch, M., Larramendy, C., Ricatti, J., Taravini, I. R., *et al*. (2007). Mapping the effects of three dopamine agonists with different dyskinetogenic potential and receptor selectivity using pharmacological functional magnetic resonance imaging. *Neuropsychopharmacology* 32, 1911-21.

DeLong, M. R. (1990). Primate models of movement disorders of basal ganglia origin. *Trends Neurosci* 13, 281-5.

DeLong, M. R. & Wichmann, T. (2007). Circuits and circuit disorders of the basal ganglia. *Arch Neurol.* 64, 20-4.

Dierssen, M., Fedrizzi, L., Gomez-Villafuertes, R., de Lagran, M. M., Gutierrez-Adan, A., Sahun, I., *et al*. (2012). Reduced Mid1 Expression and Delayed Neuromotor Development in daDREAM Transgenic Mice. *Front Mol Neurosci.* 5-58.

DiFiglia, M., Pasik, P. & Pasik, T. (1976). A Golgi study of neuronal types in the neostriatum of monkeys. *Brain Res* 114, 245-56.

Ding, Y., Restrepo, J., Won, L., Hwang, D. Y., Kim, K. S. & Kang, U. J. (2007). Chronic 3,4-dihydroxyphenylalanine treatment induces dyskinesia in aphakia mice, a novel genetic model of Parkinson's disease. *Neurobiol Dis* 27, 11-23.

Ding, Y., Won, L., Britt, J. P., Lim, S. A., McGehee, D. S. & Kang, U. J. (2011). Enhanced striatal cholinergic neuronal activity mediates L-DOPA-induced dyskinesia in parkinsonian mice. *Proc Natl Acad Sci U S A* 108, 840-5.

Drinnan, S. L., Hope, B. T., Snutch, T. P. & Vincent, S. R. (1991). G(olf) in the basal ganglia. *Mol Cell Neurosci.* 2, 66-70.

Duncan, C. E., Schofield, P. R. & Weickert, C. S. (2009). K(v) channel interacting protein 3 expression and regulation by haloperidol in midbrain dopaminergic neurons. *Brain Res.* 1304, 1-13.

Espadas, I., Darmopil, S., Vergano-Vera, E., Ortiz, O., Oliva, I., Vicario-Abejon, C., *et al*. (2012). L-DOPA-induced increase in TH-immunoreactive striatal neurons in parkinsonian mice: insights into regulation and function. *Neurobiol Dis*. 48, 271-81.

Fasano, S., Bezard, E., D'Antoni, A., Francardo, V., Indrigo, M., Qin, L., *et al*. (2010). Inhibition of Ras-guanine nucleotide-releasing factor 1 (Ras-GRF1) signaling in the striatum reverts motor symptoms associated with L-dopa-induced dyskinesia. *Proc Natl Acad Sci U S A. 107, 21824-9.*

Fisone, G. & Bezard, E. (2011). Molecular mechanisms of l-DOPA-induced dyskinesia. *Int Rev Neurobiol.* 98, 95-122.

Fontan-Lozano, A., Romero-Granados, R., del-Pozo-Martin, Y., Suarez-Pereira, I., Delgado-Garcia, J. M., Penninger, J. M., *et al*. (2009). Lack of DREAM protein enhances learning and memory and slows brain aging. *Curr Biol.* 19, 54-60.

Francardo, V., Recchia, A., Popovic, N., Andersson, D., Nissbrandt, H. & Cenci, M. A. (2011). Impact of the lesion procedure on the profiles of motor impairment and molecular responsiveness to L-DOPA in the 6-hydroxydopamine mouse model of Parkinson's disease. *Neurobiol Dis* 42, 327-40.

Gardoni, F., Picconi, B., Ghiglieri, V., Polli, F., Bagetta, V., Bernardi, G., *et al*. (2006). A critical interaction between NR2B and MAGUK in L-DOPA induced dyskinesia. *J Neurosci.* 26, 2914-22

Gasser, T. (2009). Molecular pathogenesis of Parkinson disease: insights from genetic studies. *Expert Rev Mol Med* 11, e22.

Gerfen, C. R. (1984). The neostriatal mosaic: compartmentalization of corticostriatal input and striatonigral output systems. *Nature* 311, 461-4.

Gerfen, C. R. (2000). Molecular effects of dopamine on striatal-projection pathways. *Trends Neurosci* 23, S64-70.

Gerfen, C. R., Engber, T. M., Mahan, L. C., Susel, Z., Chase, T. N., Monsma, F. J., Jr. *et al*. (1990). D1 and D2 dopamine receptor-regulated gene expression of striatonigral and striatopallidal neurons. *Science* 250, 1429-32.

Gerfen, C. R., Miyachi, S., Paletzki, R. & Brown, P. (2002). D1 dopamine receptor supersensitivity in the dopamine-depleted striatum results from a switch in the regulation of ERK1/2/MAP kinase. *J Neurosci* 22, 5042-54.

Gerfen, C. R. & Surmeier, D. J. (2011). Modulation of striatal projection systems by dopamine. *Annu Rev Neurosci.* 34, 441-66.

Gomez-Villafuertes, R., Torres, B., Barrio, J., Savignac, M., Gabellini, N., Rizzato, F., *et al.* (2005). Downstream regulatory element antagonist modulator regulates Ca2+ homeostasis and viability in cerebellar neurons. *J Neurosci.* 25, 10822-30.

Granado, N., Ares-Santos, S., Oliva, I., O'Shea, E., Martin, E. D., Colado, M. I., *et al*. (2011). Dopamine D2-receptor knockout mice are protected against dopaminergic neurotoxicity induced by methamphetamine or MDMA. *Neurobiol Dis*. 42, 391-403.

Granado, N., Ares-Santos, S., O'Shea, E., Vicario-Abejon, C., Colado, M. I. & Moratalla, R. (2010). Selective vulnerability in striosomes and in the nigrostriatal dopaminergic pathway after methamphetamine administration: early loss of TH in striosomes after methamphetamine. *Neurotox Res.* 18, 48-58.

Granado, N., Escobedo, I., O'Shea, E., Colado, I. & Moratalla, R. (2008a). Early loss of dopaminergic terminals in striosomes after MDMA administration to mice. *Synapse*. 62, 80-4.

Granado, N., Ortiz, O., Suarez, L. M., Martin, E. D., Cena, V., Solis, J. M., *et al.* (2008b). D1 but not D5 dopamine receptors are critical for LTP, spatial learning, and LTP-Induced arc and zif268 expression in the hippocampus. *Cereb Cortex*. 18, 1-12.

Granado, N., O'Shea, E., Bove, J., Vila, M., Colado, M. I. & Moratalla, R. (2008c). Persistent MDMA-induced dopaminergic neurotoxicity in the striatum and substantia nigra of mice. *J Neurochem* 107, 1102-12.

Grande, C., Zhu, H., Martin, A. B., Lee, M., Ortiz, O., Hiroi, N., *et al.* (2004). Chronic treatment with atypical neuroleptics induces striosomal FosB/DeltaFosB expression in rats. *Biol Psychiatry.* 55, 457-63.

Graybiel, A. M. (1990). Neurotransmitters and neuromodulators in the basal ganglia. *Trends Neurosci* 13, 244-54.

Graybiel, A. M. & Hickey, T. L. (1982). Chemospecificity of ontogenetic units in the striatum: demonstration by combining [3H]thymidine neuronography and histochemical staining. *Proc Natl Acad Sci U S A* 79, 198-202.

Graybiel, A. M. & Ragsdale, C. W., Jr. (1978). Histochemically distinct compartments in the striatum of human, monkeys, and cat demonstrated by acetylthiocholinesterase staining. *Proc Natl Acad Sci U S A* 75, 5723-6.

Greenfield, J. G. & Bosanquet, F. D. (1953). The brain-stem lesions in Parkinsonism. *J Neurol Neurosurg Psychiatry* 16, 213-26.

Greffard, S., Verny, M., Bonnet, A. M., Seilhean, D., Hauw, J. J. & Duyckaerts, C. (2010). A stable proportion of Lewy body bearing neurons in the substantia nigra suggests a model in which the Lewy body causes neuronal death. *Neurobiol Aging* 31, 99-103.

Guigoni, C., Doudnikoff, E., Li, Q., Bloch, B. & Bezard, E. (2007). Altered D(1) dopamine receptor trafficking in parkinsonian and dyskinetic non-human primates. *Neurobiol Dis.* 26, 452-63.

Guridi, J., Gonzalez-Redondo, R. & Obeso, J. A. (2012). Clinical features, pathophysiology, and treatment of levodopa-induced dyskinesias in Parkinson's disease. *Parkinsons Dis.* 2012, 943159.

Guridi, J., Obeso, J. A., Rodriguez-Oroz, M. C., Lozano, A. A. & Manrique, M. (2008). L-dopa-induced dyskinesia and stereotactic surgery for Parkinson's disease. *Neurosurgery* 62, 311-23; discussion 323-5.

Haber, S. N., Fudge, J. L. & McFarland, N. R. (2000). Striatonigrostriatal pathways in primates form an ascending spiral from the shell to the dorsolateral striatum. *J Neurosci* 20, 2369-82.

Hallett, P. J., Dunah, A. W., Ravenscroft, P., Zhou, S., Bezard, E., Crossman, A. R., *et al*. (2005). Alterations of striatal NMDA receptor subunits associated with the development of dyskinesia in the MPTP-lesioned primate model of Parkinson's disease. *Neuropharmacology* 48, 503-16.

Harrison, I. F. & Dexter, D. T. (2013). Epigenetic targeting of histone deacetylase: therapeutic potential in Parkinson's disease? *Pharmacol Ther* 140, 34-52.

Hayashi, T. & Huganir, R. L. (2004). Tyrosine phosphorylation and regulation of the AMPA receptor by SRC family tyrosine kinases. *J Neurosci* 24, 6152-60.

Herve, D., Le Moine, C., Corvol, J. C., Belluscio, L., Ledent, C., Fienberg, A. A., *et al*. (2001). Galpha (olf) levels are regulated by receptor usage and control dopamine and adenosine action in the striatum. *J Neurosci* 21, 4390-9.

Herve, D., Levi-Strauss, M., Marey-Semper, I., Verney, C., Tassin, J. P., Glowinski, J. *et al*. (1993). G (olf) and Gs in rat basal ganglia: possible involvement of G(olf) in the coupling of dopamine D1 receptor with adenylyl cyclase. *J Neurosci.* 13, 2237-48.

Herve, D., Trovero, F., Blanc, G., Glowinski, J. & Tassin, J. P. (1992). Autoradiographic identification of D1 dopamine receptors labelled with [3H]dopamine: distribution, regulation and relationship to coupling. *Neuroscience* 46, 687-700.

Herve, D., Trovero, F., Blanc, G., Thierry, A. M., Glowinski, J. & Tassin, J. P. (1989). Nondopaminergic prefrontocortical efferent fibers modulate D1 receptor denervation supersensitivity in specific regions of the rat striatum. *J Neurosci.* 9, 3699-708.

Hess, E. J., Battaglia, G., Norman, A. B. & Creese, I. (1987). Differential modification of striatal D1 dopamine receptors and effector moieties by N-ethoxycarbonyl-2-ethoxy-1,2-dihydroquinoline in vivo and in vitro. *Mol Pharmacol* 31, 50-7.

Holloway, R. G., Shoulson, I., Fahn, S., Kieburtz, K., Lang, A., Marek, K., *et al*. (2004). Pramipexole vs levodopa as initial treatment for Parkinson disease: a 4-year randomized controlled trial. *Arch Neurol.* 61, 1044-53.

Hurley, M. J., Mash, D. C. & Jenner, P. (2001). Dopamine D(1) receptor expression in human basal ganglia and changes in Parkinson's disease. *Brain Res Mol Brain Res* 87, 271-9.

Hwang, D. Y., Ardayfio, P., Kang, U. J., Semina, E. V. & Kim, K. S. (2003). Selective loss of dopaminergic neurons in the substantia nigra of Pitx3-deficient aphakia mice. *Brain Res Mol Brain Res* 114, 123-31.

Hwang, D. Y., Fleming, S. M., Ardayfio, P., Moran-Gates, T., Kim, H., Tarazi, F. I., *et al.* (2005). 3,4-dihydroxyphenylalanine reverses the motor deficits in Pitx3-deficient aphakia mice: behavioral characterization of a novel genetic model of Parkinson's disease. *J Neurosci.* 25, 2132-7.

Iravani, M. M., McCreary, A. C. & Jenner, P. (2012). Striatal plasticity in Parkinson's disease and L-dopa induced dyskinesia. *Parkinsonism Relat Disord* 18 Suppl 1, S123-5.

Ivanov, A., Pellegrino, C., Rama, S., Dumalska, I., Salyha, Y., Ben-Ari, Y., *et al.* (2006). Opposing role of synaptic and extrasynaptic NMDA receptors in regulation of the extracellular signal-regulated kinases (ERK) activity in cultured rat hippocampal neurons. *J Physiol.* 572, 789-98.

Jacobs, F. M., Smits, S. M., Noorlander, C. W., von Oerthel, L., van der Linden, A. J., Burbach, J. P. *et al*. (2007). Retinoic acid counteracts developmental defects in the substantia nigra caused by Pitx3 deficiency. *Development*. 134, 2673-84.

Jacobs, F. M., van Erp, S., van der Linden, A. J., von Oerthel, L., Burbach, J. P. & Smidt, M. P. (2009). Pitx3 potentiates Nurr1 in dopamine neuron terminal differentiation through release of SMRT-mediated repression. *Development* 136, 531-40.

Jenner, P. (2008). Molecular mechanisms of L-DOPA-induced dyskinesia. *Nat Rev Neurosci* 9, 665-77.

Jones, D. T. & Reed, R. R. (1989). Golf: an olfactory neuron specific-G protein involved in odorant signal transduction. *Science* 244, 790-5.

Kawaguchi, Y., Wilson, C. J., Augood, S. J. & Emson, P. C. (1995). Striatal interneurones: chemical, physiological and morphological characterization. *Trends Neurosci* 18, 527-35.

Kelly, M. A., Rubinstein, M., Asa, S. L., Zhang, G., Saez, C., Bunzow, J. R., *et al*. (1997). Pituitary lactotroph hyperplasia and chronic hyperprolactinemia in dopamine D2 receptor-deficient mice. *Neuron* 19, 103-13.

Kelly, M. A., Rubinstein, M., Phillips, T. J., Lessov, C. N., Burkhart-Kasch, S., Zhang, G., *et al*. (1998). Locomotor activity in D2 dopamine receptor-deficient mice is determined by gene dosage, genetic background, and developmental adaptations. *J Neurosci* 18, 3470-9.

Kemp, J. M. & Powell, T. P. (1971). The structure of the caudate nucleus of the cat: light and electron microscopy. *Philos Trans R Soc Lond B Biol Sci* 262, 383-401.

Kim, D. S., Froelick, G. J. & Palmiter, R. D. (2002). Dopamine-dependent desensitization of dopaminergic signaling in the developing mouse striatum. *J Neurosci* 22, 9841-9.

Kish, S. J., Shannak, K. & Hornykiewicz, O. (1988). Uneven pattern of dopamine loss in the striatum of patients with idiopathic Parkinson's disease. Pathophysiologic and clinical implications. *N Engl J Med* 318, 876-80.

Klintenberg, R., Svenningsson, P., Gunne, L. & Andren, P. E. (2002). Naloxone reduces levodopa-induced dyskinesias and apomorphine-induced rotations in primate models of parkinsonism. *J Neural Transm* 109, 1295-307.

Konitsiotis, S., Blanchet, P. J., Verhagen, L., Lamers, E. & Chase, T. N. (2000). AMPA receptor blockade improves levodopa-induced dyskinesia in MPTP monkeys. *Neurology* 54, 1589-95.

Kordower, J. H., Chu, Y., Hauser, R. A., Freeman, T. B. & Olanow, C. W. (2008). Lewy body-like pathology in long-term embryonic nigral transplants in Parkinson's disease. *Nat Med* 14, 504-6.

Kordower, J. H., Freeman, T. B., Snow, B. J., Vingerhoets, F. J., Mufson, E. J., Sanberg, P. R., *et al.* (1995). Neuropathological evidence of graft survival and striatal reinnervation after the

transplantation of fetal mesencephalic tissue in a patient with Parkinson's disease. *N Engl J Med* 332, 1118-24.

Kravitz, A. V., Freeze, B. S., Parker, P. R., Kay, K., Thwin, M. T., Deisseroth, K. *et al*. .(2010) Regulation of parkinsonian motor behaviours by optogenetic control of basal ganglia circuitry. *Nature.* 466, 622-6.

Kull, B., Svenningsson, P. & Fredholm, B. B. (2000). Adenosine A(2A) receptors are colocalized with and activate g(olf) in rat striatum. *Mol Pharmacol* 58, 771-7.

Kumar, N., Van Gerpen, J. A., Bower, J. H. & Ahlskog, J. E. (2005). Levodopa-dyskinesia incidence by age of Parkinson's disease onset. *Mov Disord* 20, 342-4.

Kumar, R., Riddle, L., Griffin, S. A., Grundt, P., Newman, A. H. & Luedtke, R. R. (2009). Evaluation of the D3 dopamine receptor selective antagonist PG01037 on L-dopa-dependent abnormal involuntary movements in rats. *Neuropharmacology* 56, 944-55.

Lanciego, J. L. (2012). Basal Ganglia Circuits: What's Now and Next? *Front Neuroanat* 6, 4.

Lanciego, J. L., Gonzalo, N., Castle, M., Sanchez-Escobar, C., Aymerich, M. S. & Obeso, J. A. (2004). Thalamic innervation of striatal and subthalamic neurons projecting to the rat entopeduncular nucleus. *Eur J Neurosci.* 19, 1267-77.

Lanciego, J. L., Luquin, N. & Obeso, J. A. (2012). Functional neuroanatomy of the basal ganglia. *Cold Spring Harb Perspect Med* 2, a009621.

Lavin, A. & Garcia-Munoz, M. (1986). Electrophysiological changes in substantia nigra after dynorphin administration. *Brain Res* 369, 298-302.

Lawhorn, C., Smith, D. M. & Brown, L. L. (2009). Partial ablation of mu-opioid receptor rich striosomes produces deficits on a motor-skill learning task. *Neuroscience.* 163, 109-19.

Lazo, P. S., Dorfman, K., Noguchi, T., Mattei, M. G. & Bravo, R. (1992). Structure and mapping of the fosB gene. FosB downregulates the activity of the fosB promoter. *Nucleic Acids Res.* 20, 343-50.

Le Moine, C., Normand, E. & Bloch, B. (1991). Phenotypical characterization of the rat striatal neurons expressing the D1 dopamine receptor gene. *Proc Natl Acad Sci U S A* 88, 4205-9.

Le Moine, C., Normand, E., Guitteny, A. F., Fouque, B., Teoule, R. & Bloch, B. (1990a). Dopamine receptor gene expression by enkephalin neurons in rat forebrain. *Proc Natl Acad Sci U S A* 87, 230-4.

Le Moine, C., Tison, F. & Bloch, B. (1990b). D2 dopamine receptor gene expression by cholinergic neurons in the rat striatum. *Neurosci Lett.* 117, 248-52.

Lebel, M., Chagniel, L., Bureau, G. & Cyr, M. (2010). Striatal inhibition of PKA prevents levodopa-induced behavioural and molecular changes in the hemiparkinsonian rat. *Neurobiol Dis.* 38, 59-67

Ledo, F., Carrion, A. M., Link, W. A., Mellstrom, B. & Naranjo, J. R. (2000b). DREAM-alphaCREM interaction via leucine-charged domains derepresses downstream regulatory element-dependent transcription. *Mol Cell Biol* 20, 9120-6.

Ledo, F., Kremer, L., Mellstrom, B. & Naranjo, J. R. (2002). Ca2+-dependent block of CREB-CBP transcription by repressor DREAM. *EMBO J.* 21, 4583-92.

Ledo, F., Link, W. A., Carrion, A. M., Echeverria, V., Mellstrom, B. & Naranjo, J. R. (2000a). The DREAM-DRE interaction: key nucleotides and dominant negative mutants. *Biochim Biophys Acta* 1498, 162-8.

Lees, A. J., Hardy, J. & Revesz, T. (2009). Parkinson's disease. *Lancet* 373, 2055-66.

Levis, M. J. & Bourne, H. R. (1992). Activation of the alpha subunit of Gs in intact cells alters its abundance, rate of degradation, and membrane avidity. *J Cell Biol* 119, 1297-307.

Li, J. Y., Englund, E., Holton, J. L., Soulet, D., Hagell, P., Lees, A. J., *et al*. (2008). Lewy bodies in grafted neurons in subjects with Parkinson's disease suggest host-to-graft disease propagation. *Nat Med* 14, 501-3.

Lilliehook, C., Bozdagi, O., Yao, J., Gomez-Ramirez, M., Zaidi, N. F., Wasco, W., *et al*. (2003). Altered Abeta formation and long-term potentiation in a calsenilin knock-out. *J Neurosci* 23, 9097-106.

Lindgren, H. S., Andersson, D. R., Lagerkvist, S., Nissbrandt, H. & Cenci, M. A. (2010). L-DOPA-induced dopamine efflux in the striatum and the substantia nigra in a rat model of Parkinson's disease: temporal and quantitative relationship to the expression of dyskinesia. *J Neurochem* 112, 1465-76.

Link, W. A., Ledo, F., Torres, B., Palczewska, M., Madsen, T. M., Savignac, M., *et al*. (2004). Day-night changes in downstream regulatory element antagonist modulator/potassium channel interacting protein activity contribute to circadian gene expression in pineal gland. *J Neurosci* 24, 5346-55.

Livak, K. J. & Schmittgen, T. D. (2001). Analysis of relative gene expression data using real-time quantitative PCR and the 2(-Delta Delta C(T)) Method. *Methods* 25, 402-8.

Lundblad, M., Picconi, B., Lindgren, H. & Cenci, M. A. (2004). A model of L-DOPA-induced dyskinesia in 6-hydroxydopamine lesioned mice: relation to motor and cellular parameters of nigrostriatal function. *Neurobiol Dis* 16, 110-23.

Ma, Y., Tang, C., Chaly, T., Greene, P., Breeze, R., Fahn, S., *et al*. (2010). Dopamine cell implantation in Parkinson's disease: long-term clinical and (18)F-FDOPA PET outcomes. *J Nucl Med* 51, 7-15.

Malenka, R.C. (2003). Synaptic plasticity and AMPA receptor trafficking. *Ann N Y Acad Sci* 1003, 1-11.

Malinow, R., Mainen, Z. F. & Hayashi, Y. (2000). LTP mechanisms: from silence to four-lane traffic. *Curr Opin Neurobiol.* 10, 352-7.

Mallet, N., Ballion, B., Le Moine, C. & Gonon, F. (2006). Cortical inputs and GABA interneurons imbalance projection neurons in the striatum of parkinsonian rats. *J Neurosci.* 26, 3875-84.

Manning-Bog, A. B., McCormack, A. L., Purisai, M. G., Bolin, L. M. & Di Monte, D. A. (2003). Alpha-synuclein overexpression protects against paraquat-induced neurodegeneration. *J Neurosci* 23, 3095-9.

Marcotte, E. R., Sullivan, R. M. & Mishra, R. K. (1994). Striatal G-proteins: effects of unilateral 6-hydroxydopamine lesions. *Neurosci Lett* 169, 195-8.

Marin, C., Jimenez, A., Tolosa, E., Bonastre, M. & Bove, J. (2004). Bilateral subthalamic nucleus lesion reverses L-dopa-induced motor fluctuations and facilitates dyskinetic movements in hemiparkinsonian rats. *Synapse.* 51, 140-50.

Matamales, M., Bertran-Gonzalez, J., Salomon, L., Degos, B., Deniau, J. M., Valjent, E., *et al.* (2009). Striatal medium-sized spiny neurons: identification by nuclear staining and study of neuronal subpopulations in BAC transgenic mice.4770e ,4 One PLoS

Mayford, M., Bach, M. E., Huang, Y. Y., Wang, L., Hawkins, R. D. & Kandel, E. R. (1996). Control of memory formation through regulated expression of a CaMKII transgene. *Science.* 274, 1678-83.

Mela, F., Millan, M. J., Brocco, M. & Morari, M. (2010). The selective D(3) receptor antagonist, S33084, improves parkinsonian-like motor dysfunction but does not affect L-DOPA-induced dyskinesia in 6-hydroxydopamine hemi-lesioned rats. *Neuropharmacology* 58, 528-36.

Moratalla, R., Quinn, B., DeLanney, L. E., Irwin, I., Langston, J. W. & Graybiel, A. M. (1992). Differential vulnerability of primate caudate-putamen and striosome-matrix dopamine systems to the neurotoxic effects of 1-methyl-4-phenyl-1,2,3,6-tetrahydropyridine. *Proc Natl Acad Sci U S A.* 89, 3859-63.

Moratalla, R., Vallejo, M., Elibol, B. & Graybiel, A. M. (1996a). D1-class dopamine receptors influence cocaine-induced persistent expression of Fos-related proteins in striatum. *Neuroreport* 8, 1-5.

Moratalla, R., Xu, M., Tonegawa, S. & Graybiel, A. M. (1996b). Cellular responses to psychomotor stimulant and neuroleptic drugs are abnormal in mice lacking the D1 dopamine receptor. *Proc Natl Acad Sci U S A* 93, 14928-33.

Moratalla, R., Elibol, B., Vallejo, M., & Graybiel, A. M. (1996c). Network-level changes in expression of inducible Fos-Jun proteins in the striatum during chronic cocaine treatment and withdrawal. *Neuron* 17, 147-56.

Murer, M. G. & Moratalla, R. (2011). Striatal Signaling in L-DOPA-Induced Dyskinesia: Common Mechanisms with Drug Abuse and Long Term Memory Involving D1 Dopamine Receptor Stimulation. *Front Neuroanat* 5, 51.

Nambu, A., Kaneda, K., Tokuno, H. & Takada, M. (2002). Organization of corticostriatal motor inputs in monkey putamen. *J Neurophysiol* 88, 1830-42.

Nambu, A., Tokuno, H. & Takada, M. (2002). Functional significance of the cortico-subthalamo-pallidal 'hyperdirect' pathway. *Neurosci Res* 43, 111-7.

Naranjo, J. R. & Mellstrom, B. (2012). Ca2+-dependent transcriptional control of Ca2+ homeostasis. *J Biol Chem* 287, 31674-80.

Naranjo, J. R., Mellstrom, B., Achaval, M. & Sassone-Corsi, P. (1991). Molecular pathways of pain: Fos/Jun-mediated activation of a noncanonical AP-1 site in the prodynorphin gene. *Neuron* 6, 607 -17.

Nash, J. E., Johnston, T. H., Collingridge, G. L., Garner, C. C. & Brotchie, J. M. (2005). Subcellular redistribution of the synapse-associated proteins PSD-95 and SAP97 in animal models of Parkinson's disease and L-DOPA-induced dyskinesia. *FASEB J* 19, 583-5.

Nunes, I., Tovmasian, L. T., Silva, R. M., Burke, R. E. & Goff, S. P. (2003). Pitx3 is required for development of substantia nigra dopaminergic neurons. *Proc Natl Acad Sci U S A* 100, 4245-50.

Nutt, J. G. (2000). Clinical pharmacology of levodopa-induced dyskinesia. *Ann Neurol* 47, S160-4; discussion S164-6.

Obeso, J. A., Guridi, J., Nambu, A. & Crossman, A. R. (2013). Motor manifestations and basal ganglia output activity: the paradox continues. *Mov Disord.* 28, 416-8.

Obeso, J. A., Rodriguez-Oroz, M. C., Chana, P., Lera, G., Rodriguez, M. & Olanow, C. W. (2000). The evolution and origin of motor complications in Parkinson's disease. *Neurology* 55, S13-20; discussion S21-3.

Oh, J. D., Chartisathian, K., Ahmed, S. M. & Chase, T. N. (2003). Cyclic AMP responsive element binding protein phosphorylation and persistent expression of levodopa-induced response alterations in unilateral nigrostriatal 6-OHDA lesioned rats. *J Neurosci Res* 72, 768-80.

Olanow, C. W. & Brundin, P. (2013). Parkinson's disease and alpha synuclein: is Parkinson's disease a prion-like disorder? *Mov Disord* 28, 31-40.

Osawa, M., Tong, K. I., Lilliehook, C., Wasco, W., Buxbaum, J. D., Cheng, H. Y., *et al*. (2001). Calcium-regulated DNA binding and oligomerization of the neuronal calcium-sensing protein, calsenilin/DREAM/KChIP3. *J Biol Chem* 276, 41005-13.

Papa, S. M., Boldry, R. C., Engber, T. M., Kask, A. M. & Chase, T. N. (1995). Reversal of levodopa-induced motor fluctuations in experimental parkinsonism by NMDA receptor blockade. *Brain Res* 701, 13-8.

Papa, S. M., Engber, T. M., Kask, A. M. & Chase, T. N. (1994). Motor fluctuations in levodopa treated parkinsonian rats: relation to lesion extent and treatment duration. *Brain Res* 662, 69-74.

Pavon, N., Martin, A. B., Mendialdua, A. & Moratalla, R. (2006). ERK phosphorylation and FosB expression are associated with L-DOPA-induced dyskinesia in hemiparkinsonian mice. *Biol Psychiatry* 59, 64-74.

Paxinos, G. & Franklin, K. B.J. (2004). The mouse brain in Stereotaxic Coordinates, Second Edition. *Elsevier Science U S A.*

Pearce, R. K., Jackson, M., Smith, L., Jenner, P. & Marsden, C. D. (1995). Chronic L-DOPA administration induces dyskinesias in the 1-methyl-4- phenyl-1,2,3,6-tetrahydropyridine-treated common marmoset (Callithrix Jacchus). *Mov Disord* 10, 731-40.

Penit-Soria, J., Durand, C., Besson, M. J. & Herve, D. (1997). Levels of stimulatory G protein are increased in the rat striatum after neonatal lesion of dopamine neurons. *Neuroreport* 8, 829-33.

Penney, J. B., Jr. & Young, A. B. (1986). Striatal inhomogeneities and basal ganglia function. *Mov Disord*. 1, 3-15.

Perier, C., Marin, C., Jimenez, A., Bonastre, M., Tolosa, E. & Hirsch, E. C. (2003). Effect of subthalamic nucleus or entopeduncular nucleus lesion on levodopa-induced neurochemical changes within the basal ganglia and on levodopa-induced motor alterations in 6-hydroxydopamine-lesioned rats. *J Neurochem* 86, 1328-37.

Piccini, P., Brooks, D. J., Bjorklund, A., Gunn, R. N., Grasby, P. M., Rimoldi, O., *et al*. (1999). Dopamine release from nigral transplants visualized in vivo in a Parkinson's patient. *Nat Neurosci* 2, 1137-40.

Piccini, P., Lindvall, O., Bjorklund, A., Brundin, P., Hagell, P., Ceravolo, R., *et al*. (2000). Delayed recovery of movement-related cortical function in Parkinson's disease after striatal dopaminergic grafts. *Ann Neurol* 48, 689-95.

Piccini, P., Weeks, R. A. & Brooks, D. J. (1997). Alterations in opioid receptor binding in Parkinson's disease patients with levodopa-induced dyskinesias. *Ann Neurol.* 42, 720-6.

Picconi, B., Centonze, D., Hakansson, K., Bernardi, G., Greengard, P., Fisone, G., *et al.* (2003). Loss of bidirectional striatal synaptic plasticity in L-DOPA-induced dyskinesia. *Nat Neurosci.* 6, 501-6.

Pinna, A., Corsi, C., Carta, A. R., Valentini, V., Pedata, F. & Morelli, M. (2002). Modification of adenosine extracellular levels and adenosine A(2A) receptor mRNA by dopamine denervation. *Eur J Pharmacol* 446, 75-82.

Pons, R., Syrengelas, D., Youroukos, S., Orfanou, I., Dinopoulos, A., Cormand, B., *et al*. (2013). Levodopa-induced dyskinesias in tyrosine hydroxylase deficiency. *Mov Disord* 28, 1058-63.

Porras, G., Berthet, A., Dehay, B., Li, Q., Ladepeche, L., Normand, E., *et al*. (2012). PSD-95 expression controls L-DOPA dyskinesia through dopamine D1 receptor trafficking. *J Clin Invest* 122, 3977-89.

Porras, G., De Deurwaerdere, P., Li, Q., Marti, M., Morgenstern, R., Sohr, R., *et al*. (2014). L-dopa-induced dyskinesia: beyond an excessive dopamine tone in the striatum. *Sci Rep* 4, 3730.

Premont, J., Perez, M., Blanc, G., Tassin, J. P., Thierry, A. M., Herve, D. *et al*. (1979). Adenosine-sensitive adenylate cyclase in rat brain homogenates: kinetic characteristics, specificity, topographical, subcellular and cellular distribution. *Mol Pharmacol.* 16, 790-804.

Prensa, L., Gimenez-Amaya, J. M. & Parent, A. (1999). Chemical heterogeneity of the striosomal compartment in the human striatum. *J Comp Neurol* 413, 603-18.

Puschmann, A. (2013). Monogenic Parkinson's disease and parkinsonism: clinical phenotypes and frequencies of known mutations. *Parkinsonism Relat Disord* 19, 407-15.

Rangel-Barajas, C., Silva, I., Lopez-Santiago, L. M., Aceves, J., Erlij, D. & Floran, B. (2011). L-DOPA-induced dyskinesia in hemiparkinsonian rats is associated with up-regulation of adenylyl cyclase type V/VI and increased GABA release in the substantia nigra reticulata. *Neurobiol Dis* 41, 51-61.

Rascol, O., Brooks, D. J., Korczyn, A. D., De Deyn, P. P., Clarke, C. E., Lang, A. E., *et al*. (2006). Development of dyskinesias in a 5-year trial of ropinirole and L-dopa. *Mov Disord* 21, 1844-50.

Rascol, O., Nutt, J. G., Blin, O., Goetz, C. G., Trugman, J. M., Soubrouillard, C., *et al*. (2001). Induction by dopamine D1 receptor agonist ABT-431 of dyskinesia similar to levodopa in patients with Parkinson disease. *Arch Neurol* 58, 249-54.

Recasens, A., Dehay, B., Bove, J., Carballo-Carbajal, I., Dovero, S., Perez-Villalba, A., *et al*. (2014). Lewy body extracts from Parkinson disease brains trigger alpha-synuclein pathology and neurodegeneration in mice and monkeys. *Ann Neurol.* 75, 351-62.

Rico, A. J., Barroso-Chinea, P., Conte-Perales, L., Roda, E., Gomez-Bautista, V., Gendive, M., *et al.* (2010). A direct projection from the subthalamic nucleus to the ventral thalamus in monkeys. *Neurobiol Dis.* 39, 381-92.

Rivas, M., Mellstrom, B., Torres, B., Cali, G., Ferrara, A. M., Terracciano, D., *et al.* (2009). The DREAM protein is associated with thyroid enlargement and nodular development. *Mol Endocrinol.* 23, 862-70.

Rivas, M., Villar, D., Gonzalez, P., Dopazo, X. M., Mellstrom, B. & Naranjo, J. R. (2011). Building the DREAM interactome. *Sci China Life Sci* 54, 786-92.

Rivera, A., Alberti, I., Martin, A. B., Narvaez, J. A., de la Calle, A. & Moratalla, R. (2002a). Molecular phenotype of rat striatal neurons expressing the dopamine D5 receptor subtype. *Eur J Neurosci.* 16, 2049-58.

Rivera, A., Cuellar, B., Giron, F. J., Grandy, D. K., de la Calle, A. & Moratalla, R. (2002b). Dopamine D4 receptors are heterogeneously distributed in the striosomes/matrix compartments of the striatum. *J Neurochem* 80, 219-29.

Rodnitzky, R. L. & Narayanan, N. S. (2014). Amantadine's role in the treatment of levodopa-induced dyskinesia. *Neurology.* 82, 288-9.

Rodriguez-Oroz, M. C., Jahanshahi, M., Krack, P., Litvan, I., Macias, R., Bezard, E., *et al.* (2009). Initial clinical manifestations of Parkinson's disease: features and pathophysiological mechanisms. *Lancet Neurol.* 8, 1128-39.

Saka, E., Goodrich, C., Harlan, P., Madras, B. K. & Graybiel, A. M. (2004). Repetitive behaviors in monkeys are linked to specific striatal activation patterns. *J Neurosci* 24, 7557-65.

Sakagami, H., Sawamura, Y. & Kondo, H. (1995). Synchronous patchy pattern of gene expression for adenylyl cyclase and phosphodiesterase but discrete expression for G-protein in developing rat striatum. *Brain Res Mol Brain Res* 33, 185-91.

Sako, W., Morigaki, R., Nagahiro, S., Kaji, R. & Goto, S. (2010). Olfactory type G-protein alpha subunit in striosome-matrix dopamine systems in adult mice. *Neuroscience* 170, 497-502.

Samadi, P., Bedard, P. J. & Rouillard, C. (2006). Opioids and motor complications in Parkinson's disease. *Trends Pharmacol Sci* 27, 512-7.

Sandyk, R. & Snider, S. R. (1986). Naloxone treatment of L-dopa-induced dyskinesias in Parkinson's disease. *Am J Psychiatry* 143, 118.

Santini, E., Feyder, M., Gangarossa, G., Bateup, H. S., Greengard, P. & Fisone, G. (2012). Dopamine- and cAMP-regulated phosphoprotein of 32-kDa (DARPP-32)-dependent activation of extracellular signal-regulated kinase (ERK) and mammalian target of rapamycin complex 1 (mTORC1) signaling in experimental parkinsonism. *J Biol Chem* 287, 27806-12.

Santini, E., Sgambato-Faure, V., Li, Q., Savasta, M., Dovero, S., Fisone, G. *et al*. (2010). Distinct changes in cAMP and extracellular signal-regulated protein kinase signalling in L-DOPA-induced dyskinesia. *PLoS One* 5, e12322.

Santini, E., Valjent, E. & Fisone, G. (2008). Parkinson's disease: levodopa-induced dyskinesia and signal transduction. *FEBS J.* 275, 1392-9.

Santini, E., Valjent, E., Usiello, A., Carta, M., Borgkvist, A., Girault, J. A., *et al.* (2007). Critical involvement of cAMP/DARPP-32 and extracellular signal-regulated protein kinase signaling in L -DOPA-induced dyskinesia. *J Neurosci.* 27, 6995-7005.

Sanz, C., Mellstrom, B., Link, W. A., Naranjo, J. R. & Fernandez-Luna, J. L. (2001). Interleukin 3-dependent activation of DREAM is involved in transcriptional silencing of the apoptotic Hrk gene in hematopoietic progenitor cells. *EMBO J.* 20, 2286-92.

Sato, F., Lavallee, P., Levesque, M. & Parent, A. (2000). Single-axon tracing study of neurons of the external segment of the globus pallidus in primate. *J Comp Neurol.* 417, 17-31.

Savignac, M., Pintado, B., Gutierrez-Adan, A., Palczewska, M., Mellstrom, B. & Naranjo, J. R. (2005). Transcriptional repressor DREAM regulates T-lymphocyte proliferation and cytokine gene expression. *EMBO J* 24, 3555-64.

Schapira, A. H. (2008). Mitochondria in the aetiology and pathogenesis of Parkinson's disease. *Lancet Neurol* 7, 97-109.

Schapira, A. H., Emre, M., Jenner, P. & Poewe, W. (2009). Levodopa in the treatment of Parkinson's disease. *Eur J Neurol* 16, 982-9.

Schlachetzki, J. C., Marxreiter, F., Regensburger, M., Kulinich, A., Winner, B. & Winkler, J. (2014). Increased tyrosine hydroxylase expression accompanied by glial changes within the non-lesioned hemisphere in the 6-hydroxydopamine model of Parkinson's disease. *Restor Neurol Neurosci*.

Schuster, S., Doudnikoff, E., Rylander, D., Berthet, A., Aubert, I., Ittrich, C., *et al*. (2009). Antagonizing L-type Ca2+ channel reduces development of abnormal involuntary movement in the rat model of L-3,4-dihydroxyphenylalanine-induced dyskinesia. *Biol Psychiatry* 65, 518-26.

Schuster, S., Nadjar, A., Guo, J. T., Li, Q., Ittrich, C., Hengerer, B. *et al*. (2008). The 3-hydroxy-3-methylglutaryl-CoA reductase inhibitor lovastatin reduces severity of L-DOPA-induced abnormal involuntary movements in experimental Parkinson's disease. *J Neurosci. 28, 4311-6.*

Shepherd, J. D. & Huganir, R. L. (2007). The cell biology of synaptic plasticity: AMPA receptor trafficking. *Annu Rev Cell Dev Biol* 23, 613-43.

Silverdale, M. A., Kobylecki, C., Hallett, P. J., Li, Q., Dunah, A. W., Ravenscroft, P., *et al*. (2010). Synaptic recruitment of AMPA glutamate receptor subunits in levodopa-induced dyskinesia in the MPTP-lesioned nonhuman primate. *Synapse* 64, 177-80.

Singleton, A. B., Farrer, M. J. & Bonifati, V. (2013). The genetics of Parkinson's disease: progress and therapeutic implications. *Mov Disord* 28, 14-23.

Smidt, M. P., Smits, S. M., Bouwmeester, H., Hamers, F. P., van der Linden, A. J., Hellemons, A. J., *et al.* (2004). Early developmental failure of substantia nigra dopamine neurons in mice lacking the homeodomain gene Pitx3. *Development.* 131, 1145-55.

Smith, G. A., Heuer, A., Dunnett, S. B. & Lane, E. L. (2012). Unilateral nigrostriatal 6-hydroxydopamine lesions in mice II: predicting l-DOPA-induced dyskinesia. *Behav Brain Res* 226, 281-92.

Soloaga, A., Thomson, S., Wiggin, G. R., Rampersaud, N., Dyson, M. H., Hazzalin, C. A., *et al*. (2003). MSK2 and MSK1 mediate the mitogen- and stress-induced phosphorylation of histone H3 and HMG-14. *EMBO J.* 22, 2788-97.

Spreafico, F., Barski, J. J., Farina, C. & Meyer, M. (2001). Mouse DREAM/calsenilin/KChIP3: gene structure, coding potential, and expression. *Mol Cell Neurosci* 17, 1-16.

Steece-Collier, K., Rademacher, D. J. & Soderstrom, K. (2012). Anatomy of Graft-induced Dyskinesias: Circuit Remodeling in the Parkinsonian Striatum. *Basal Ganglia* 2, 15-30.

Stocchi, F., Jenner, P. & Obeso, J. A. (2010). When do levodopa motor fluctuations first appear in Parkinson's disease? *Eur Neurol* 63, 257-66.

Stoessl, A. J., Polanski, E. & Frydryszak, H. (1993). The opiate antagonist naloxone suppresses a rodent model of tardive dyskinesia. *Mov Disord* 8, 445-52.

Suarez, L. M., Solis, O., Carames, J. M., Taravini, I. R., Solis, J. M., Murer, M. G. *et al*. (2014). L-DOPA Treatment Selectively Restores Spine Density in Dopamine Receptor D2-Expressing Projection Neurons in Dyskinetic Mice. *Biol Psychiatry* 75, 711-22.

Surmeier, D. J., Bargas, J., Hemmings, H. C., Jr., Nairn, A. C. & Greengard, P. (1995). Modulation of calcium currents by a D1 dopaminergic protein kinase/phosphatase cascade in rat neostriatal neurons. *Neuron* 14, 385-97.

Surmeier, D. J., Eberwine, J., Wilson, C. J., Cao, Y., Stefani, A. & Kitai, S. T. (1992). Dopamine receptor subtypes colocalize in rat striatonigral neurons. *Proc Natl Acad Sci U S A* 89, 10178-82.

Tajima, K. & Fukuda, T. (2013). Region-specific diversity of striosomes in the mouse striatum revealed by the differential immunoreactivities for mu-opioid receptor, substance P, and enkephalin. *Neuroscience* 241, 215-28.

Takimoto, K., Yang, E. K. & Conforti, L. (2002). Palmitoylation of KChIP splicing variants is required for efficient cell surface expression of Kv4.3 channels. *J Biol Chem.* 277, 26904-11.

Tamim, M. K., Samadi, P., Morissette, M., Gregoire, L., Ouattara, B., Levesque, D., *et al.* (2010). Effect of non-dopaminergic drug treatment on Levodopa induced dyskinesias in MPTP monkeys: common implication of striatal neuropeptides. *Neuropharmacology.* 58, 286-96.

Tanaka, M., Kim, Y. M., Lee, G., Junn, E., Iwatsubo, T. & Mouradian, M. M. (2004). Aggresomes formed by alpha-synuclein and synphilin-1 are cytoprotective. *J Biol Chem* 279, 4625-31.

Tanimura, Y., King, M. A., Williams, D. K. & Lewis, M. H. (2011). Development of repetitive behavior in a mouse model: roles of indirect and striosomal basal ganglia pathways. *Int J Dev Neurosci* 29, 461-7.

Taylor, J. L., Bishop, C. & Walker, P. D. (2005). Dopamine D1 and D2 receptor contributions to L-DOPA-induced dyskinesia in the dopamine-depleted rat. *Pharmacol Biochem Behav* 81, 887-93.

Tekumalla, P. K., Calon, F., Rahman, Z., Birdi, S., Rajput, A. H., Hornykiewicz, O., *et al.* (2001). Elevated levels of DeltaFosB and RGS9 in striatum in Parkinson's disease. *Biol Psychiatry* 50, 813-6.

Thomsen, M. B., Wang, C., Ozgen, N., Wang, H. G., Rosen, M. R. & Pitt, G. S. (2009). Accessory subunit KChIP2 modulates the cardiac L-type calcium current. *Circ Res.* 104, 1382-9.

Tomiyama, M., Kimura, T., Maeda, T., Tanaka, H., Kannari, K. & Baba, M. (2004). Upregulation of striatal adenosine A2A receptor mRNA in 6-hydroxydopamine-lesioned rats intermittently treated with L-DOPA. *Synapse* 52, 218-22.

Tong, J., Fitzmaurice, P. S., Ang, L. C., Furukawa, Y., Guttman, M. & Kish, S. J. (2004). Brain dopamine-stimulated adenylyl cyclase activity in Parkinson's disease, multiple system atrophy, and progressive supranuclear palsy. *Ann Neurol* 55, 125-9.

Tong, J., Wong, H., Guttman, M., Ang, L. C., Forno, L. S., Shimadzu, M., *et al.* (2010). Brain alpha-synuclein accumulation in multiple system atrophy, Parkinson's disease and progressive supranuclear palsy: a comparative investigation. *Brain* 133, 172-88.

Ungerstedt, U. (1968). 6-Hydroxy-dopamine induced degeneration of central monoamine neurons. *Eur J Pharmacol* 5, 107-10.

Usiello, A., Baik, J. H., Rouge-Pont, F., Picetti, R., Dierich, A., LeMeur, M., *et al.* (2000). Distinct functions of the two isoforms of dopamine D2 receptors. *Nature* 408, 199-203.

Valjent, E., Bertran-Gonzalez, J., Herve, D., Fisone, G. & Girault, J. A. (2009). Looking BAC at striatal signaling: cell-specific analysis in new transgenic mice. *Trends Neurosci* 32, 538-47.

van den Munckhof, P., Gilbert, F., Chamberland, M., Levesque, D. & Drouin, J. (2006). Striatal neuroadaptation and rescue of locomotor deficit by L-dopa in aphakia mice, a model of Parkinson's disease. *J Neurochem* 96, 160-70.

Watabe-Uchida, M., Zhu, L., Ogawa, S. K., Vamanrao, A. & Uchida, N. (2012). Whole-brain mapping of direct inputs to midbrain dopamine neurons. *Neuron.* 74, 858-73.

Westin, J. E., Vercammen, L., Strome, E. M., Konradi, C. & Cenci, M. A. (2007). Spatiotemporal pattern of striatal ERK1/2 phosphorylation in a rat model of L-DOPA-induced dyskinesia and the role of dopamine D1 receptors. *Biol Psychiatry* 62, 800-10.

White, N. M. & Hiroi, N. (1998). Preferential localization of self-stimulation sites in striosomes/patches in the rat striatum. *Proc Natl Acad Sci U S A* 95, 6486-91.

Winkler, C., Kirik, D., Bjorklund, A. & Cenci, M. A. (2002). L-DOPA-induced dyskinesia in the intrastriatal 6-hydroxydopamine model of parkinson's disease: relation to motor and cellular parameters of nigrostriatal function. *Neurobiol Dis* 10, 165-86.

Wu, L. J., Mellstrom, B., Wang, H., Ren, M., Domingo, S., Kim, S. S., *et al*. (2010). DREAM (downstream regulatory element antagonist modulator) contributes to synaptic depression and contextual fear memory. *Mol Brain* 3, 3.

Xiong, H., Kovacs, I. & Zhang, Z. (2004). Differential distribution of KChIPs mRNAs in adult mouse brain. *Brain Res Mol Brain Res* 128, 103-11.

Xu, M., Koeltzow, T. E., Santiago, G. T., Moratalla, R., Cooper, D. C., Hu, X. T., *et al*. (1997). Dopamine D3 receptor mutant mice exhibit increased behavioral sensitivity to concurrent stimulation of D1 and D2 receptors. *Neuron* 19, 837-48.

Xu, M., Moratalla, R., Gold, L. H., Hiroi, N., Koob, G. F., Graybiel, A. M. *et al*. (1994). Dopamine D1 receptor mutant mice are deficient in striatal expression of dynorphin and in dopamine-mediated behavioral responses. *Cell* 79, 729-42.

Yajima, Y., Akita, Y., Saito, T. & Kawashima, S. (1998). VIP induces the translocation and degradation of the alpha subunit of Gs protein in rat pituitary GH4C1 cells. *J Biochem* 123, 1024-30.

Zahniser, N. R., Simosky, J. K., Mayfield, R. D., Negri, C. A., Hanania, T., Larson, G. A., *et al*. (2000). Functional uncoupling of adenosine A(2A) receptors and reduced responseto caffeine in mice lacking dopamine D2 receptors. *J Neurosci* 20, 5949-57.

Zhang, D., Zhang, L., Lou, D. W., Nakabeppu, Y., Zhang, J. & Xu, M. (2002). The dopamine D1 receptor is a critical mediator for cocaine-induced gene expression. *J Neurochem* 82, 1453-64.

Zhang, Y., Meredith, G. E., Mendoza-Elias, N., Rademacher, D. J., Tseng, K. Y. & Steece-Collier, K. (2013). Aberrant restoration of spines and their synapses in L-DOPA-induced dyskinesia: involvement of corticostriatal but not thalamostriatal synapses. *J Neurosci.* 33, 11655-67.

Zhang, Y., Su, P., Liang, P., Liu, T., Liu, X., Liu, X. Y., *et al.* (2010). The DREAM protein negatively regulates the NMDA receptor through interaction with the NR1 subunit. *J Neurosci.* 30, 7575-86.

Zhuang, X., Belluscio, L. & Hen, R. (2000). G(olf)alpha mediates dopamine D1 receptor signaling. *J Neurosci* 20, RC91.

Appendix

1. Genetic inactivation of dopamine D1 but not D2 receptors inhibits L-DOPA-induced dyskinesia and histone activation.

Darmopil S., Martín A.b., Ruiz-DeDiego, I., Ares-Santos S, Moratalla R

2009. *Biol Psychiatry.* 66, 603-13391-403

Genetic Inactivation of Dopamine D1 but Not D2 Receptors Inhibits L-DOPA–Induced Dyskinesia and Histone Activation

Sanja Darmopil, Ana B. Martín, Irene Ruiz De Diego, Sara Ares, and Rosario Moratalla

Background: Pharmacologic studies have implicated dopamine D1-like receptors in the development of dopamine precursor molecule 3,4-dihydroxyphenyl-L-alanine (L-DOPA)-induced dyskinesias and associated molecular changes in hemiparkinsonian mice. However, pharmacologic agents for D1 or D2 receptors also recognize other receptor family members. Genetic inactivation of the dopamine D1 or D2 receptor was used to define the involvement of these receptor subtypes.

Methods: During a 3-week period of daily L-DOPA treatment (25 mg/kg), mice were examined for development of contralateral turning behavior and dyskinesias. L-DOPA-induced changes in expression of signaling molecules and other proteins in the lesioned striatum were examined immunohistochemically.

Results: Chronic L-DOPA treatment gradually induced rotational behavior and dyskinesia in wildtype hemiparkinsonian mice. Dyskinetic symptoms were associated with increased FosB and dynorphin expression, phosphorylation of extracellular signal-regulated kinase, and phosphoacetylation of histone 3 (H3) in the lesioned striatum. These molecular changes were restricted to striatal areas with complete dopaminergic denervation and occurred only in dynorphin-containing neurons of the direct pathway. D1 receptor inactivation abolished L-DOPA-induced dyskinesias and associated molecular changes. Inactivation of the D2 receptor had no significant effect on the behavioral or molecular response to chronic L-DOPA.

Conclusions: Our results demonstrate that the dopamine D1 receptor is critical for the development of L-DOPA-induced dyskinesias in mice and in the underlying molecular changes in the denervated striatum and that the D2 receptor has little or no involvement. In addition, we demonstrate that H3 phosphoacetylation is blocked by D1 receptor inactivation, suggesting that inhibitors of H3 acetylation and/or phosphorylation may be useful in preventing or reversing dyskinesia.

Key Words: Dopaminergic denervation, dynorphin, ERK1/2, FosB, Parkinson's disease, phosphoacetylated histone 3

Parkinson disease (PD) is caused by degeneration of midbrain dopaminergic neurons that project to the striatum. Despite extensive investigation and new therapeutic approaches, the dopamine precursor molecule 3,4-dihydroxyphenyl-L-alanine (L-DOPA) remains the most effective and most commonly used noninvasive treatment for PD. However, chronic treatment and disease progression lead to changes in the brain's response to L-DOPA, resulting in a lower therapeutic window and the appearance of abnormal involuntary movements. These movements, known as dyskinesias, interfere significantly with normal motor activity and are associated with changes in striatal gene expression.

Our hypothesis is that these changes are the result of intermittent stimulation of supersensitive dopamine receptors in denervated striatal neurons (1). These receptors have increased coupling to $G\alpha_{olf}$ (2), resulting in greater stimulation of adenylyl cyclase, which activates the extracellular signal-regulated kinase (ERK) pathway (3) and triggers posttranslational modification of histones (4), leading to gene transcription (5). All dopamine receptor (R) subtypes (D1-D5) are present in the striatum, although D1R and D2R are the most abundant. These two dopamine receptors exhibit opposite functions, and their expression is segregated: D1R and D2R are expressed in neurons of direct and indirect striatal output pathways, respectively. Some molecular changes correlated with dyskinesias such as increased FosB and dynorphin expression are confined to D1R-containing neurons, whereas p-ERK and Nurr1 expression have been described in both D1R- and D2R-containing neurons (6,7). Although dopamine receptors are clearly involved in dyskinesias, the contribution of each dopamine receptor subtype has not been demonstrated definitively, and the signaling pathways that trigger long-term changes that maintain dyskinesias are not fully defined.

Pharmacologic studies implicate both the D1/D5 and D2/D3 receptor families in the development of dyskinesias. In patients, chronic treatment with a nonselective dopamine agonist with a short plasma half-life is more likely to induce dyskinesia than treatment with D2R agonists with long plasma half-lives (8). In rodents, dyskinesias can be induced by D1-type (D1/D5) or D2-type (D2/D3) agonists (9–12) with D1/D5 agonists having the most powerful dyskinetogenic effect (7,12,13). Consistent with this, D1/D5 antagonists are more effective inhibitors of L-DOPA-induced dyskinesia than D2 antagonists (7,12–14).

Because D1 receptors greatly outnumber D5 receptors in the striatum, it is tempting to assume that the striatal actions of mixed D1/D5 ligands are due to the D1 receptor. However, there are several examples in which the less abundant dopamine receptor is the major player for specific functions. In the hippocampus, D5R are much more abundant than D1R, but the D5 receptors do not play a role in spatial learning or hippocampal long-term potentiation, whereas D1 receptors are critical in these processes (15). In addition, within the striatum itself, where D1 is predominant, D1 and D5 receptors are equally required for striatal

From the Cajal Institute, Consejo Superior de Investigaciones Científicas and Centro de Investigación Biomédica en Red para Enfermedades Neurodegenerativas, Instituto de Salud Carlos III, Madrid, Spain.
Address correspondence to Rosario Moratalla, Ph.D., Cajal Institute, Avenida Dr. Arce 37, 28002 Madrid, Spain. E-mail: moratalla@cajal.csic.es.
Received Feb 12, 2009; revised Apr 7, 2009; accepted Apr 17, 2009.

0006-3223/09/$36.00
doi:10.1016/j.biopsych.2009.04.025

BIOL PSYCHIATRY 2009;66:603–613

synaptic plasticity and play different roles in corticostriatal long-term synaptic transmission (16). Thus, it is essential to test the hypothesis that D1 and not D5 receptors are responsible for the development of abnormal movements and molecular changes following L-DOPA. Currently, available pharmacologic tools do not distinguish between different subtypes within the same family (e.g., between D1 and D5 or between D2 and D3) (17,18). Using our mouse model of dyskinesias (3) and knockout technology, we investigated the specific roles of the D1R and D2R in the development of dyskinesia and associated molecular changes after chronic L-DOPA treatment.

Methods and Materials

Animals

This study was carried out in mice lacking D1R (15,16,19,20) or D2R (21–23) generated by homologous recombination as described previously. Wildtype (WT) and homozygote $D1^{-/-}$ and $D2^{-/-}$ (knockout [KO]) mice used in this study were derived from mating heterozygous mice. Genotype was determined by polymerase chain reaction analysis. The maintenance of animals followed guidelines from European Union Council Directive (86/609/European Economic Community) and experimental protocols were approved by the Consejo Superior de Investigaciones Científicas Ethics Committee.

Procedure for intrastriatal 6-hydroxydopamine (6-OHDA) administration was described previously (3,24). Mice recovered for 4 weeks after the lesion and then began L-DOPA methyl ester (Sigma-Aldrich, Madrid, Spain) treatment. During the 3 week treatment, 6-OHDA or sham-operated animals received a daily injection of 10 mg/kg benserazide hydrochloride (Sigma-Aldrich), a peripheral blocker of L-DOPA decarboxylase, followed 20 min later by an intraperitoneal injection of 25 mg/kg of L-DOPA. Control animals were injected with an equivalent amount of saline. Rotational behavior and dyskinesias were studied in the same group of animals, on alternate days, twice a week for each behavior as described previously (3).

Immunohistochemistry

Following behavioral analysis, animals were anesthetized and perfused with 4% paraformaldehyde in phosphate buffer (pH 7.4) 1 hour or 20 min (animals used for p-ERK immunohistochemistry) after the last L-DOPA/saline injection. Immunostaining was carried out in free-floating coronal brain sections (40 μm thick) using a standard avidin-biotin immunocytochemical protocol (25,26) with the following rabbit antisera: tyrosine hydroxylase (TH; 1:1000; Chemicon, Temecula, California), FosB (1:10,000, Santa Cruz Biotechnology, Santa Cruz, California), dynorphin-B (dyn-B; 1:10,000, Serotec, Oxford, United Kingdom), met-enkephalin (met-Enk; 1:1000, Incstar, Stillwater, Minnesota), phosphop44/42 mitogen-activated protein (MAP) kinase (Thr202/Tyr204; p-ERK1/2; 1:250; Cell Signaling Technology, Beverly, Massachusetts), and antiphospho (Ser10)-acetyl (Lys14)-Hystone 3 (p-AcH3; 1:500; Upstate, Cell Signaling Solutions, Lake Placid, New York) and mouse monoclonal met-Enk antisera (1:10; 27). Double-labeling immunohistochemistry protocols are described in Supplement 1.

Quantification of TH, FosB, dyn B, p-ERK, and p-AcH3 immunoreactivity was carried out using an image analysis system (AIS, Imaging Research, Linton, United Kingdom) as in Granado *et al.* (28). For both lesioned and unlesioned striatal sides, immunostaining intensity and number of immunolabeled nuclei/cells were determined in 4–6 animals per group using five serial rostrocaudal sections per animal and three counting frames (dorsal, dorsolateral, and lateral) per section (.091 mm^2 each frame). Images were digitized with Leica microscope under 40× lens. Before counting, images were thresholded at a standardized gray-scale level, empirically determined by two observers to allow detection of stained nuclei/cells from low to high intensity, with suppression of lightly stained nuclei (15). The data are presented as number of stained nuclei per mm^2 (mean ± standard error) in the lesioned and unlesioned striatum. Immunostaining intensities in the lesioned side are presented as fold increase over the value from the unlesioned striatum.

Statistical Analysis

Behavior was analyzed using repeated measures three-way analysis of variance (ANOVA; contralateral turns) or two-way ANOVA (dyskinesia scores) using time, lesion/treatment (sham/L-DOPA, lesion/saline, lesion/L-DOPA) and genotype (WT, KO) or time and genotype as the within and between-subject variables, respectively, followed by planned comparisons (a priori analysis). Quantifications of immunolabeling were analyzed by two-way ANOVA with genotype and lesion as between-subject variables followed by Scheffe post hoc test. Immunostaining intensities were compared by Student's *t* test. Data are expressed as mean ± standard error of mean. Statistical significance level was set at $p < .05$.

Results

Dopamine D1, but Not D2, Receptors Are Required for Rotational Sensitization Induced by L-DOPA in Hemiparkinsonian Mice

To establish the role of the D1 and D2 dopamine receptor subtypes in the development of behavioral sensitization and dyskinesias, we used genetically engineered mice lacking either the dopamine D1 or D2 receptor. Contralateral rotations were evaluated as a measure of behavioral sensitization to L-DOPA (25 mg/kg/day) for 3 weeks (3). Twice a week, we measured the total number of contralateral turns for 120 min. We also counted the contralateral turns during the first 20 min after L-DOPA administration to assess changes in time to onset of the response (Figure 1). As observed previously (3), in hemiparkinsonian WT littermates of both knockouts ($D1R^{WT}$ and $D2R^{WT}$), L-DOPA induced a gradual increase in contralateral turns in both the 20- and 120 min windows (Figure 1). However, in $D1R^{-/-}$ animals, contralateral rotations were completely abolished, for both time intervals (Figure 1A and 1B). In contrast, there was no significant difference between the rotational behavior of $D2R^{-/-}$ mice and $D2^{WT}$ mice at any point during chronic L-DOPA treatment (Figure 1C and 1D). Rotational behavior of the $D2^{WT}$ and $D1^{WT}$ animals was similar (Figure 1A and 1C).

Dopamine D1, but Not D2, Receptors Are Required for the Development of Dyskinesia Following L-DOPA Treatment in Hemiparkinsonian Mice

To measure L-DOPA-induced dyskinesias in hemiparkinsonian mice, we assessed orofacial, limb, and locomotive dyskinesia and axial dystonia. Dyskinetic symptoms were monitored twice a week over the 3-week course of the treatment as previously described (3). In WT animals, the time course and intensity of the L-DOPA response was similar to that found in an earlier study (3). Dyskinesias are already apparent at 2 days of treatment, with dyskinetic symptoms at maximal intensity 30 min and 60 min after L-DOPA, decreasing gradually to baseline values

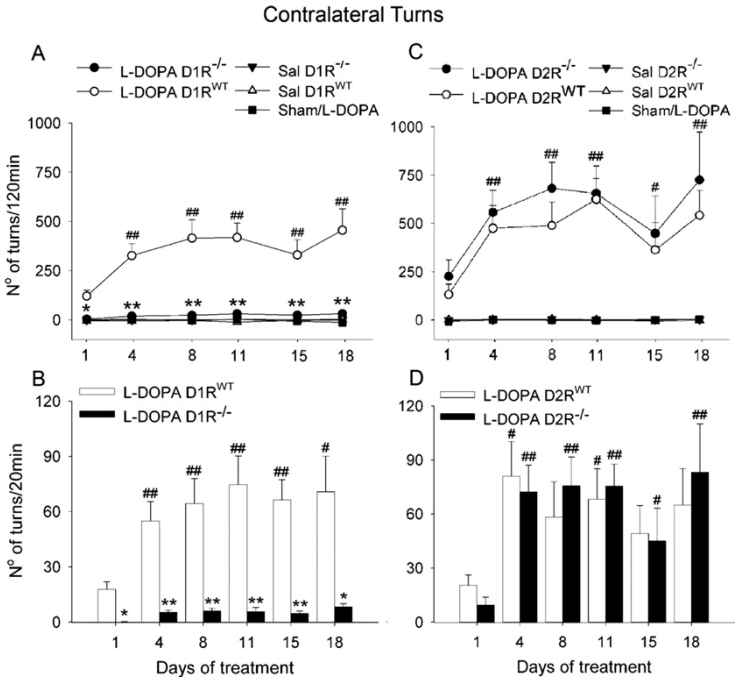

Figure 1. Genetic inactivation of dopamine D1 receptors blocked L-DOPA-induced dyskinesias in hemiparkinsonian mice. Time course for dopamine precursor molecule 3,4-dihydroxyphenyl-L-alanine (L-DOPA)-induced contralateral turning in hemiparkinsonian $D1R^{-/-}$ **(A)** and $D2R^{-/-}$ **(C)** mice and their wildtype (WT) littermates. Data points indicate the total number of contralateral turns (mean ± SEM) in 120 min following L-DOPA (25 mg/kg) administration. **(A)** Inactivation of D1R completely abolished turning behavior. Three-way analysis of variance (ANOVA) with repeated measures showed significant differences for genotype [$F(1,33) = 9.5; p = 4 \times 10^{-3}$], treatment [$F(2,33) = 15.8; p = 1.5 \times 10^{-5}$], genotype × treatment [$F(2,33) = 11.8; p = 1.4 \times 10^{-4}$] and treatment × time [$F(10,165) = 3; p = 1.8 \times 10^{-3}$]. **(C)** Inactivation of D2R has no effect on turning behavior. Statistical analysis showed significant differences for treatment [$F(2,36) = 21.7; p = 6.6 \times 10^{-7}$], time [$F(5,180) = 3.8; p = 2.5 \times 10^{-3}$], and treatment × time [$F(10,180) = 4.1; p = 4.7 \times 10^{-4}$]. All lesioned WT and $D2R^{-/-}$ mice treated with L-DOPA exhibit significantly more contralateral turns than control animals (sham/L-DOPA and 6-OHDA/saline) at all time points. **(B and D)** Histograms show the number of contralateral turns in the initial 20 min following L-DOPA administration. **(B)** Inactivation of D1R abolished behavioral sensitization. Two-way ANOVA with repeated measures showed significant differences for genotype [$F(1,15) = 14.1; p = 4 \times 10^{-3}$] and time [$F(5,75) = 2.7; p = 2.8 \times 10^{-2}$]. **(D)** Inactivation of D2R had no effect on behavioral sensitization. Statistical analysis showed significant differences for time [$F(5,80) = 7.8; p = 4.8 \times 10^{-6}$]. $^{*}p < .01$; $^{**}p < .0001$ versus wildtype $^{\#}p < .05$; $^{\#\#}p < .001$ versus first day of treatment after two or three-way ANOVA with repeated measures and planned comparisons, $n = 5$–10 per group. In Histogram B, differences versus first day of treatment are shown together for $D2R^{-/-}$ and $D2R^{WT}$ animals.

by 2 hours (data not shown). Because the dyskinesia scores at 30 and 60 min after L-DOPA administration were equivalent, we present only the 30 min scores (Figure 2; see also Figure 1 and 2A in Supplement 1). In contrast, $D1R^{-/-}$ animals showed a near-complete absence of orofacial and limb dyskinesias and very low-grade axial dystonia and locomotive dyskinesias (Figure 2). $D1R^{-/-}$ animals exhibit significantly less of all four dyskinetic symptoms at all time points, with the exception of orofacial dyskinesia on day 19 (Figure 2). In contrast, the L-DOPA-induced dyskinetic behaviors in $D2R^{-/-}$ and $D2R^{WT}$ animals were not significantly different from each other (Figure 1 in Supplement 1). The absence of dyskinetic symptoms observed in $D1R^{-/-}$ was also clearly evident in the posture of the animals, which was close to normal, compared with that of WT or $D2R^{-/-}$ animals (Figure 2 in Supplement 1), which showed great lateral deviation, twisted posture, and limb dyskinesia.

Dopamine D1, but Not D2, Receptors Are Required for the L-DOPA-Induced FosB and Dynorphin Expression

Increased FosB and dynorphin expression in the dorsolateral lesioned striatum correlates with the appearance of dyskinesia (3,4,29). We evaluated the effect of knocking out D1R or D2R on striatal FosB and dynorphin expression after chronic L-DOPA administration in hemiparkinsonian mice. In $D1R^{WT}$ and $D2R^{WT}$ animals, L-DOPA induced marked expression of FosB and dynorphin in the dorsolateral part of the lesioned striatum but not the unlesioned side. The anatomic distribution of FosB and dynorphin expression strictly overlaid striatal areas with complete denervation. The neurons enduring these molecular changes were completely denervated. An identical distribution of FosB and dynorphin expression was observed in hemiparkinsonian $D2R^{-/-}$ mice (Figure 3). In sharp contrast, there was no increase in FosB or dynorphin expression in $D1R^{-/-}$ mice, despite complete striatal denervation (Figures 3 and 4A).

We counted FosB- and dynorphin-positive neurons per mm^2 in the dorsolateral striatum. In $D1R^{WT}$, $D2R^{WT}$, and $D2R^{-/-}$ animals, L-DOPA induced approximately a 30-fold increase in FosB and a 10-fold increase in dynorphin-positive neurons in lesioned compared to the unlesioned striatum. Dynorphin staining intensity was also greater in the cytoplasm and neuropil of striatal areas with complete denervation: optical density measurements in L-DOPA-treated WT mice revealed a 160% increase in intensity compared to the comparable region on the unle-

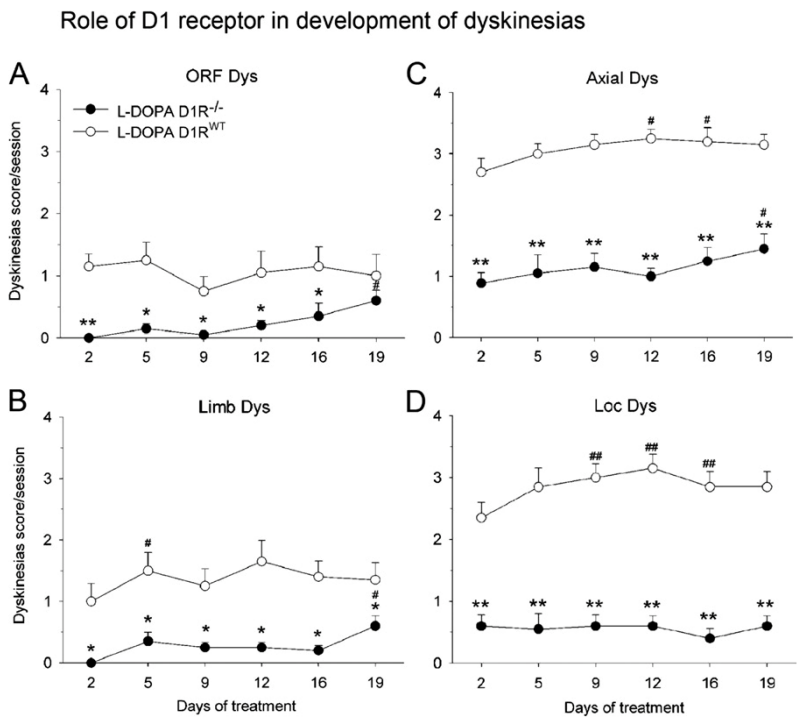

Figure 2. Genetic inactivation of dopamine D1 receptors blocked dopamine precursor molecule 3,4-dihydroxyphenyl-L-alanine (L-DOPA)-induced dyskinesias in hemiparkinsonian mice. Time course of appearance of dyskinetic symptoms: orofacial dyskinesias (ORF dys) **(A)**, limb dyskinesias (limb dys) **(B)**, axial dystonia (axial dys) **(C)**, and locomotor dyskinesias (loc dys) **(D)**. Movements were evaluated 30 min after L-DOPA (25 mg/kg) administration in $D1R^{WT}$ and $D1R^{-/-}$ hemiparkinsonian mice. Two-way ANOVA with repeated measures showed significant differences for genotype in all four types of dyskinetic symptoms: ORF dys [$F(1,18) = 10.8, p = 4.1 \times 10^{-3}$], loc dys [$F(1,18) = 95.3, p = 1.3 \times 10^{-8}$], limb dys [$F(1,18) = 21.5, p = 4 \times 10^{-4}$], axial dys [$F(1,18) = 104, p = 6.6 \times 10^{-9}$] and a significant effect on time for limb dys [$F(5,90) = 2.5, p = 3.6\ 10^{-2}$] and axial dys [$F(5,90) = 2.4, p = 4.5\ 10^{-2}$]. Data points represent the mean ± SEM. $^{*}p < .05$; $^{**}p < .0001$ versus $D1R^{WT}$; $^{\#}p < .05$, $^{\#\#}p < .005$ versus first day of treatment after two-way ANOVA with repeated measures and planned comparisons, $n = 10$ per group.

sioned side (Figure 4E). These L-DOPA-induced increases in FosB and dynorphin expression disappear in $D1R^{-/-}$ animals (Figure 4B, 4D, and 4E), although a few FosB-positive cells were observed in $D1R^{-/-}$ mice. We also quantified the area of FosB-immunoreactive (-ir) nuclei. L-DOPA treatment induced a twofold increase in the area of FosB-ir nuclei in the lesioned striatum of WT and $D2R^{-/-}$ mice, but no change in the area of FosB-ir nuclei in $D1R^{-/-}$ (Figure 4C).

Dopamine D1 but not D2 Receptors Blocked L-DOPA-Induced Phosphorylation of ERK and Phosphoacetylation of Histone Three in the Lesioned Striatum

We have shown previously that chronic L-DOPA-treatment in hemiparkinsonian animals greatly increased phosphorylation of ERK1/2 on Thr202 and Tyr204 (p-ERK) in the lesioned striatum (3). More recently, others have shown that this increase is directly correlated with the severity of dyskinetic symptoms (4,7). We examined p-ERK in the knockout animals and found that L-DOPA did not induce p-ERK in $D1R^{-/-}$ animals (Figure 5A), but in $D2R^{-/-}$ animals, p-ERK expression was similar to that in WT littermates (Figure 5A). These results are consistent with our behavior results implicating D1R, but not D2R, in the appearance of dyskinetic symptoms. Phosphorylation of ERK1/2 results in the sequential phosphorylation of MSK-1 and phospho acetylation of histone 3 (p-AcH3) (5,14,30). Chronic L-DOPA treatment increased phosphorylation of H3 on Ser10 and acetylation on Lys14 in the lesioned striatum with an identical expression-pattern to that described for FosB and dynorphin. As seen for induction of FosB and dynorphin, inactivation of D1R completely blocked L-DOPA-induced p-AcH3 in the depleted striatum, whereas inactivation of D2R had no significant effect (Figure 5A).

We counted p-ERK1/2- and p-AcH3-positive cells in both sides of the striatum in WT animals and found that L-DOPA produces a 15-fold increase in the number of p-ERK-ir cells and a 300-fold increase in p-AcH3-ir nuclei on the lesioned side compared with the unlesioned side (Figure 5B and 5D). p-ERK was also induced in the neuropil (Figure 5A and 5C), as reflected by an increase in optical density similar to the increase in the number of p-ERK-positive cells.

Phenotype of the Striatal Neurons Underlying the Molecular Changes Associated with Dyskinesia

To determine whether these molecular changes all occur in the same population of striatal neurons, we carried out double immunostaining assays. FosB and p-AcH3 were both coexpressed with dynorphin but not with enkephalin (markers of direct and indirect pathway neurons respectively). Similarly, the few scattered FosB nuclei observed in $D1R^{-/-}$ mice were in enkephalin-negative neurons (data not shown). These results were obtained using both classical DAB/DAB-nickel (Figures 6A, 6A′, 6B, 6B′ and 6C) and double immunofluorescence methods (Figure 6C′). Furthermore, FosB expression and p-AcH3 appeared only in those direct pathway neurons with increased dynorphin expression consequent to L-DOPA treatment (Figure 6A and A′, 6B and 6B′), suggesting that these changes were coordinated.

The Extent of the Dopaminergic Lesion Correlates with Dyskinesia Score, Contralateral Rotational Behavior and Induction of Molecular Changes

To confirm that the extent of the dopaminergic lesion did not differ between the various groups of animals studied here, we assessed the percentage of striatum with complete loss of TH-ir fibers for each group of animals. We found no significant differences between groups (44 ± 3% for $D1R^{WT}$; 52 ± 7% $D1R^{-/-}$; 41 ± 7% for $D2R^{WT}$; 31 ± 4% $D2R^{-/-}$; Figure 7A). In addition, we found that the percentage of striatal area with

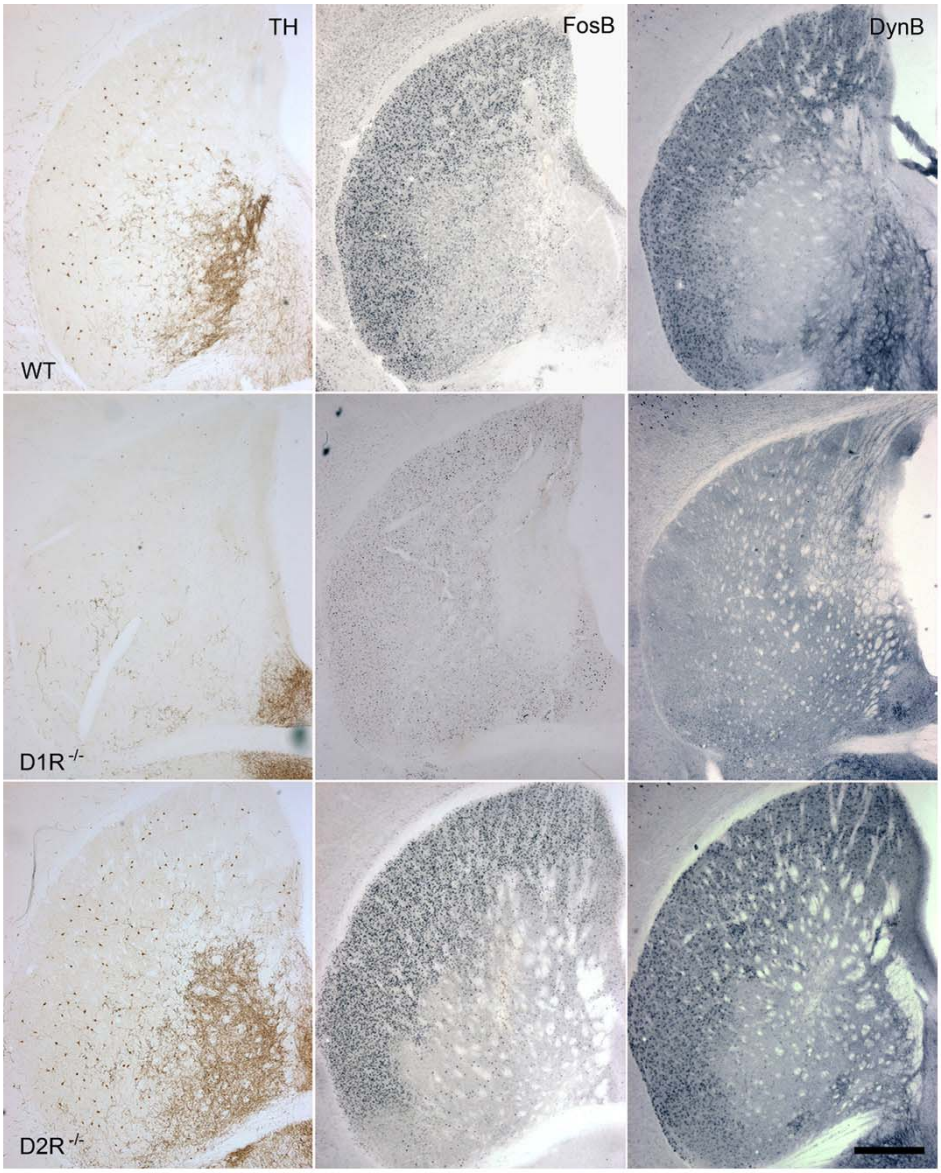

Figure 3. Genetic inactivation of dopamine D1 but not D2 receptors inhibits FosB and dynorphin (dyn) expression induced by chronic dopamine precursor molecule 3,4-dihydroxyphenyl-L-alanine (L-DOPA) treatment in the lesioned striatum. Photomicrographs of adjacent coronal striatal sections from wildtype (WT) (top), D1R$^{-/-}$ (middle) and D2R$^{-/-}$ (bottom) mice sacrificed 1 hour after the last L-DOPA injection and immunostained for tyrosine hydroxylase (TH), FosB, and dyn. Chronic L-DOPA treatment induced marked FosB and dyn expression in the striatal areas that are devoid of TH-immunoreactive fibers in WT and D2R$^{-/-}$ hemiparkinsonian mice. Note that in the striatum of D1R$^{-/-}$ hemiparkinsonian animals, L-DOPA does not induce FosB or dyn B expression. Scale bar = 500 μm.

complete dopaminergic lesion strongly correlated with the total dyskinesia score (Figure 7B, r = .91, $p > .001$) and with the total number of contralateral turns in 120 min (Figure 7C, r = .71, $p > .01$) on the last day of evaluation. Interestingly, all the molecular changes we observed in dyskinetic animals-increased FosB, dynorphin, p-ERK, p-AcH3-presented the same anatomic pattern of expression (Figure 7D and 7E) and were exclusively restricted to neurons and striatal areas with complete denervation (Figure 7). To strengthen this evidence, double immunostaining for TH and FosB revealed that the distribution of remaining TH fibers in the lesioned striatum is directly opposite to the distribution of L-DOPA-induced FosB expression (Figure 7F). Together, these findings indicate that complete denervation in these regions is required to trigger the molecular changes underlying dyskinesias.

Discussion

The findings we describe here strongly support a compulsory role for the D1R subtype in the development of dyskinesia and

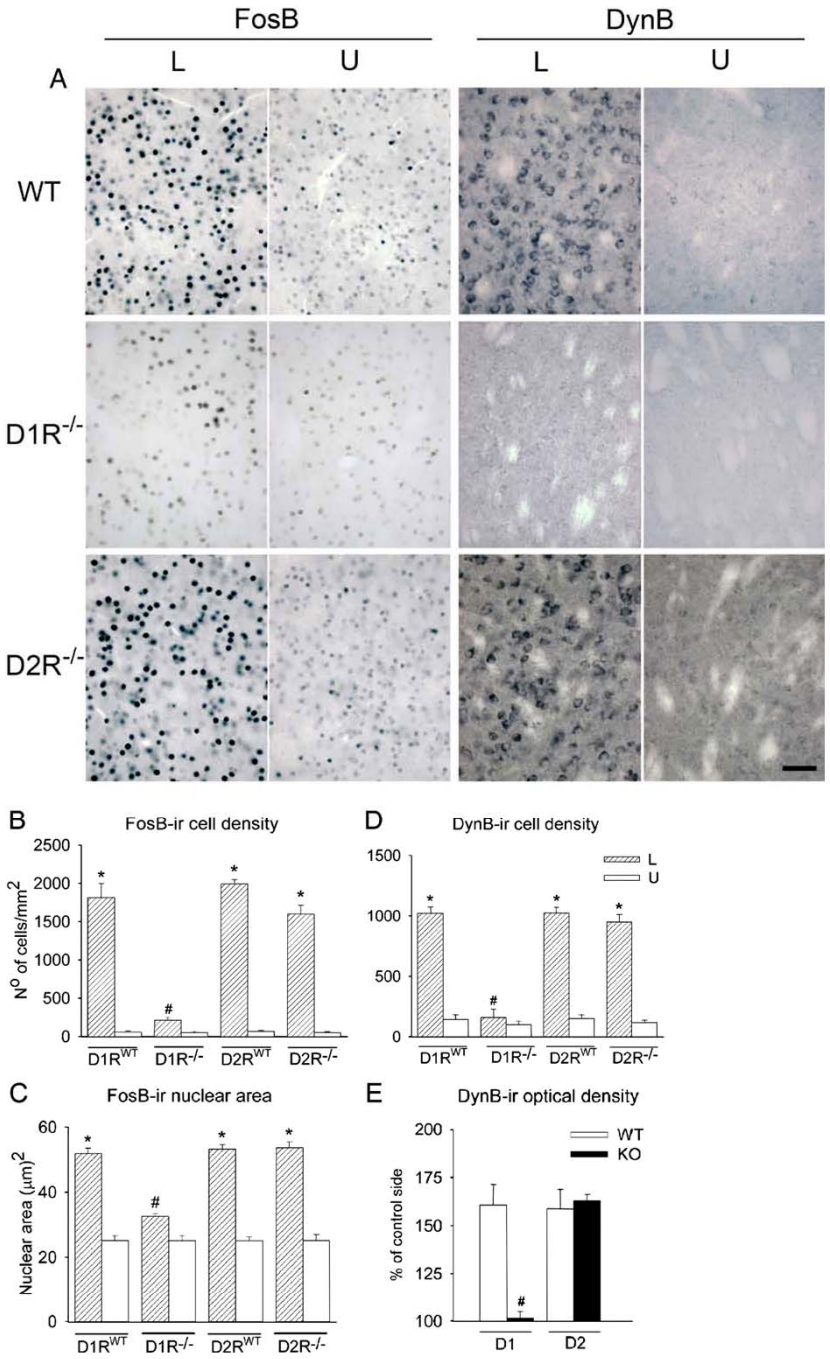

Figure 4. Role of dopamine D1 and D2 receptors in FosB and dyn expression in the striatum of hemiparkinsonian wildtype (WT), D1R$^{-/-}$, and D2R$^{-/-}$ mice following chronic dopamine precursor molecule 3,4-dihydroxyphenyl-L-alanine (L-DOPA) treatment. High power photomicrographs of coronal sections from the lesioned (L) and unlesioned (U) striatum of L-DOPA-treated WT, D1R$^{-/-}$ and D2R$^{-/-}$ mice sacrificed 1 hour after the last L-DOPA injection and stained for FosB or dyn **(A)**. Scale bar = 50 μm. Histograms represent quantification of **(B)** FosB- and **(D)** dynorphin-B (dyn-B)-positive cells (mean ± SEM) and nuclear area stained for FosB **(C)** in the lesioned and unlesioned striatum of hemiparkinsonian WT, D1R$^{-/-}$ and D2R$^{-/-}$ mice. Inactivation of D1R but not D2R abolished FosB and dyn expression induced by L-DOPA treatment. Two-way analysis of variance (ANOVA) showed significant differences between genotypes for D1R$^{-/-}$ mice for FosB- immunoreactive (ir) cell density [$F(1,52) = 101$], nuclear area [$F(1,56) = 72.2$], and dyn cell density [$F(1,32) = 171$] and between lesioned and unlesioned striatum for FosB-ir cell density: D1R^{WT} [$F(1,52) = 241$], D2R^{WT} [$F(1,52) = 253$], D2R$^{-/-}$ mice [$F(1,52) = 164$]; nuclear area: D1R^{WT} [$F(1,56) = 119$], D2R^{WT} [$F(1,56) = 123$], D2R$^{-/-}$ mice [$F(1,56) = 70.3$]; and dyn cell density: D1R^{WT} [$F(1,32) = 178$], D2R^{WT} [$F(1,32) = 177$], D2R$^{-/-}$ mice [$F(1,32) = 160$]. $^{*}p < 10^{-7}$ versus unlesioned side, $^{\#}p < 10^{-7}$ versus D1R^{WT} after two-way ANOVA followed by Scheffe post hoc test. **(E)** Optical density of dyn-B immunoreactivity in lesioned striatum expressed as a percentage of dyn-B-ir on the unlesioned side. $^{\#}p < .01$ versus D1R^{WT}, Student's *t* test.

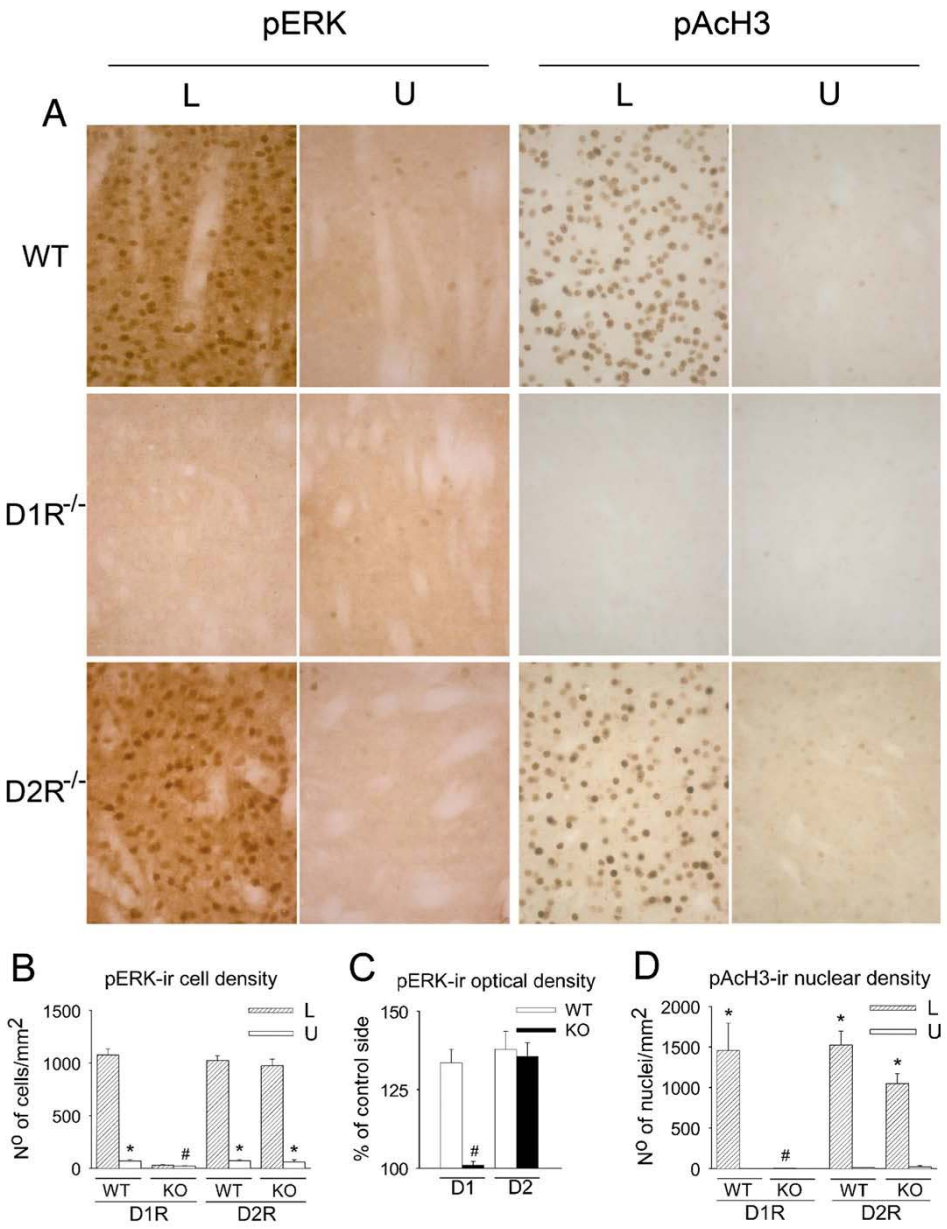

Figure 5. Genetic inactivation of dopamine D1 but not D2 receptors inhibits the phosphorylation of both extracellular signal-regulated kinase (ERK)1/2 and (Ser10)-acetyl (Lys14)-Hystone 3 (AcH3) induced by chronic dopamine precursor molecule 3,4-dihydroxyphenyl-L-alanine (L-DOPA) in the lesioned striatum. High-power photomicrographs of coronal sections from the lesioned (L) and unlesioned (U) striatum of L-DOPA-treated wildtype (WT), $D1R^{-/-}$, and $D2R^{-/-}$ hemiparkinsonian mice, sacrificed 1 hour after the last L-DOPA injection. Sections were immunostained for p-ERK1/2 or for p-AcH3 **(A)**. Scale bar = 50 μm. Histograms show the quantification of p-ERK1/2-positive cells **(B)**, phosphohistone AcH3-positive nuclei in the striatum **(D)** in WT, $D1R^{-/-}$, and $D2R^{-/-}$ hemiparkinsonian mice treated chronically with L-DOPA. Two-way analysis of variance (ANOVA) showed significant differences between genotypes for $D1R^{-/-}$ mice for p-ERK1/2-immunoreactive (ir) cell density [$F(1,32) = 174$] and p-AcH3-ir cell density [$F(1,24) = 81.4$] and between lesioned and unlesioned striatum for p-ERK1/2-ir cell density: $D1R^{WT}$ [$F(1,32) = 179$], $D2R^{WT}$ [$F(1,32) = 176$], $D2R^{-/-}$ mice [$F(1,32) = 161$]; and p-AcH3-ir density: $D1R^{WT}$ [$F(1,24) = 81.7$], $D2R^{WT}$ [$F(1,24) = 88.6$], $D2R^{-/-}$ mice [$F(1,24) = 40.9$]. Data represent mean ± SEM, $^{*}p < .001$ versus unlesioned side, $^{\#}p < 10^{-5}$ versus $D1R^{WT}$ after two-way ANOVA and followed by Scheffe posthoc test. **(C)** Optical density of p-ERK1/2-ir expressed as percent of staining in unlesioned striatum. $^{\#}p < .01$, versus $D1R^{WT}$, Student's *t* test.

rotational response following L-DOPA administration as well as in the molecular changes associated with these behaviors. In contrast, the D2R appears to have little effect on any of these. We demonstrate that these L-DOPA-induced molecular changes, including the phosphoacetylation of H3, occur in the direct pathway neurons within the fully denervated region of the striatum. Finally, we demonstrate a strong correlation between the extent of fully dopamine-denervated areas in the striatum and severity of dyskinesias.

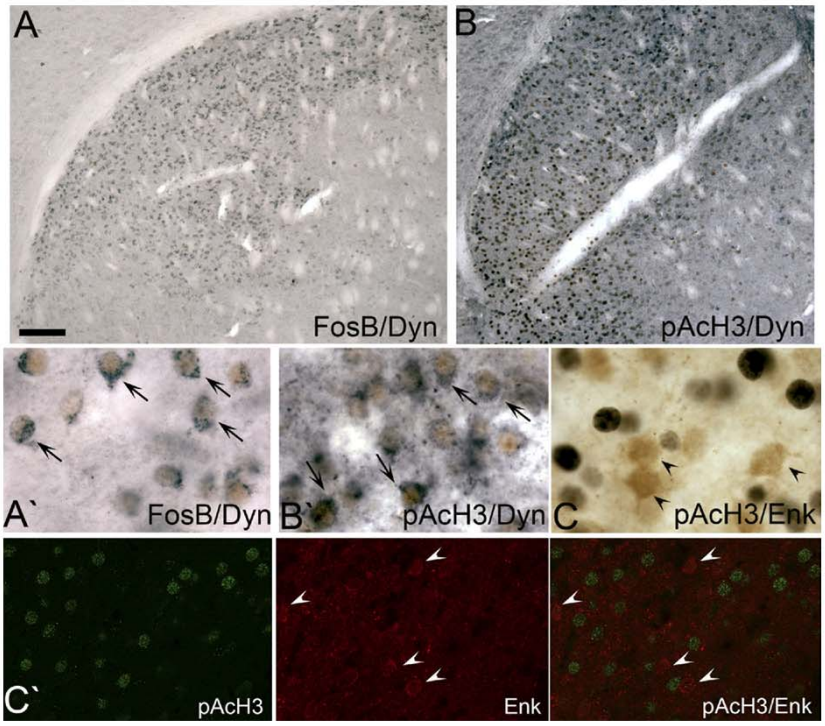

Figure 6. Phenotype of the striatal neurons underlying molecular changes associated with dyskinesia. High-magnification photographs showing colocalization of molecular changes in the same striatal denervated area **(A, B)** and in the same neurons **(A′, B′)** (arrows). Double immunostaining for **(B)** dynorphin-B (dyn-B; gray) and FosB (brown) **(A, A′)** and for dyn-B (gray) and p-AcH3 (brown) **(B, B′)**. **(C and C′)** p-AcH3 expression (gray) was not present in enkephalin (Enk)-immunoreactive (ir) neurons (brown, arrowheads) revealed by DAB/Ni double immunostaining **(C)** or by fluorescent double immunostaining with p-AcH3-ir (green) and Enk-ir (arrowheads) shown in red **(C′)**. Scale = 140 μm **(A, B)**, 20 μm **(A′, B′, C)**, and 34 μm **(C′)**.

D1, but Not D2, Receptors Are Required for L-DOPA-Induced Rotational Response and Dyskinesia in Hemiparkinsonian Animals

Contralateral rotation response, a commonly used measure of behavioral sensitization to L-DOPA, is triggered by denervation-induced supersensitivity of dopamine receptors in the dopamine-depleted striatum. This molecular mechanism is associated with the appearance of L-DOPA-induced dyskinesias as well (31). This striking reduction in contralateral turns and dyskinesias in $D1R^{-/-}$ agrees with previous studies using D1/D5 agents. Pharmacologic studies in hemiparkinsonian rats supported a major role for the D1-type receptors in the development of contralateral turning (6,12); and dyskinesias (6,7,9,10,12,13) during L-DOPA treatment. Studies in humans and other primates concur that D1-type receptors are important for dyskinesias (32–35). However, these pharmacologic agents do not distinguish between D1 and D5 effects (18,36), thus our results are the first to specifically establish the critical role of D1R in the development of rotational response and dyskinesia.

In contrast, our data clearly indicate little role for the D2R in either rotational response or development of dyskinesia. This result contradicts previous data obtained using pharmacologic blockade (12) or stimulation (9) of D2 receptors, which suggested that dopamine D2R play a role in the development of rotational response. This discrepancy is likely because the D2 agents used in these previous studies are not specific: they act on other D2-like dopamine receptors (17,37–39). Although stimulation of D2-like receptors, especially D3R, can induce rotational behavior (12), our data indicate that this contribution is minor or dependent on D1R stimulation because no rotation develops in the absence of the D1R observed in our study or with D1/D5R blockage (40). Similarly, previous studies have reported that agonists acting preferentially at D2R vary in their ability to induce dyskinesia in rats (9–12,41). In humans and primates, dyskinetic responses were observed after prolonged treatment with D2 or D2/D3 agonists (35,42), whereas D2R-preferred antagonists, administered in combination with L-DOPA, reduced dyskinesia scores by approximately 50% (12,13). Again, the discrepancy between these previous findings and the results we report here is likely due to the lack of specificity of the D2 agents used, which also bind D3 and D4 receptors (17,37–39). Our data clearly show that D2R are not required for dyskinesias in hemiparkinsonian mice.

Despite the increased motor behavior displayed by $D1R^{-/-}$ in baseline conditions (15,16), in lesioned mice L-DOPA treatment does not induce dyskinetic movements. Thus, their hypermobility does not overcome blockade of dyskinesia. Similarly, the inability to move observed in $D2R^{-/-}$ mice (43) does not block the appearance of L-DOPA-induced dyskinetic movements in these mice. Therefore, differences in basal locomotor activity do not interfere with the appearance of dyskinesia. These results indicate that although normal locomotor activity and dyskinetic movements may involve the basal ganglia motor circuit, after denervation, different molecular mechanisms and anatomic substrates may be important.

D1, but Not D2, Receptor Is Required for Induction of Molecular Markers of Dyskinesia

Increased FosB expression after L-DOPA is causally linked with dyskinesia in rats (44) and mice (3,29). L-DOPA also induces expression of the opioid neuropeptide dynorphin in WT hemiparkinsonian mice as happens in PD patients (45) and in 1-methyl-4-phenyl-1,2,3,6-tetrahydropyridine–treated monkeys (46). Dynorphin expression occurs downstream of L-DOPA-induced Fos activation in neurons of striatonigral pathway in rodents (3,7,44), altering the dynamic of this pathway, after repetitive stimulation of D1 receptors and thus underlying behavioral sensitization (19,47). Phosphorylation of ERK1/2 occurs upstream of FosB and dynorphin expression and seems to be

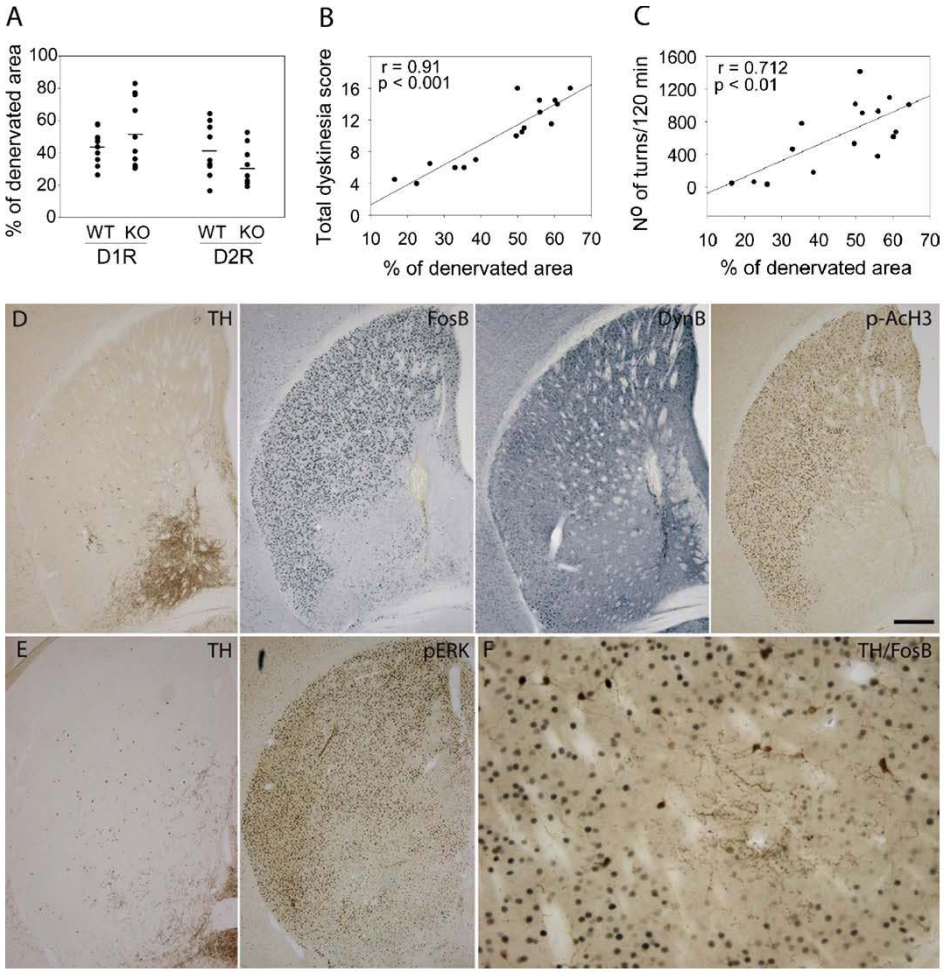

Figure 7. The extent of the striatal lesion correlates with development of dyskinesia and contralateral rotational response in wildtype (WT) animals. **(A)** Extent of striatal lesion in animals of each genotype as assessed by the percentage of total striatal area on the lesioned side that is completely denervated ($n = 10$ for each genotype). Any striatal area with optical density of tyrosine hydroxylase (TH)-immunoreactive (ir) fibers less than 5% was considered completely denervated. **(B and C)** Simple linear regression analysis illustrating the correlation between the percentage of total striatum that is completely denervated and the total dyskinesia score **(B)** or the number of turns in 120 min **(C)**. Behaviors were analyzed following the final dopamine precursor molecule 3,4-dihydroxyphenyl-L-alanine (L-DOPA) administration on Day 19 in WT animals. **(B)** $n = 16$; $r = .91$, $p < .001$; **(C)** $r = .71$, $p < .01$. **(D–F)** Histological pattern of L-DOPA-induced molecular changes in the lesioned striatum of WT animals. **(D)** Consecutive coronal sections through the lesioned striatum of mice sacrificed 1 hour after the last L-DOPA administration were immunostained for TH, FosB, dynorphin-B (dyn-B), antiphospho (Ser10)-acetyl (Lys14)-hystone 3 (p-AcH3). Scale = 400 μm. **(E)** Consecutive coronal sections through the lesioned striatum of mice sacrificed 20 min after the last L-DOPA injection were immunostained for TH and p- extracellular signal-regulated kinase 1/2 (p-ERK). Scale = 400 μm. **(F)** High-magnification photograph showing double immunostaining for TH (gray) and FosB (brown) showing an inhibition of FosB expression by remaining TH fibers. Scale = 120 μm.

limited to the same direct pathway neurons that overexpress FosB and dynorphin. p-ERK can trigger histone-phosphoacetylation and thus can have a cumulative effect on chromatin modification. In addition, FosB may interact with chromatin remodeling factors, providing a molecular basis for long-term alterations in gene expression (48,49). The increase in p-AcH3 we observed after L-DOPA treatment is consistent with one previous study (14) but conflicts with another (30) that found no change in p-H3 and decrease in Ac-H3 in MPTP-lesioned and L-DOPA-treated mice. These discrepancies may be due to differences in the mouse model used or differences in dose and duration of L-DOPA treatment, which would suggest that the threshold for histone modification by L-DOPA is more sensitive than some other molecular markers.

We now provide evidence that selective inactivation of D1R abolishes expression of all markers related to chronic L-DOPA treatment (FosB, dynorphin, p-ERK) including p-AcH3 in the lesioned striatum, whereas inactivation of D2R does not affect expression of these markers, in strict correspondence with our behavioral observations. Therefore, D1R activation is crucial for the stimulation of the MAPK- and cyclic adenosine monophosphate/PKA-dependent gene-expression pathways. These results are consistent with studies in rats in which administration of D1/D5 antagonists abolished L-DOPA induced FosB and p-ERK1/2 expression (7). The only alternative explanation of our results is that inactivation of D1R induced a dynorphin cell loss in the striatum of $D1R^{-/-}$ mice. Thus, our data add specificity to the pharmacologic data, indicating that the D1R, is required for

L-DOPA induced increases in FosB and dynorphin expression and p-ERK1/2 and extends these results to p-AcH3 in the lesioned striatum, strengthening the association between these molecular changes and the development of behavioral sensitization and dyskinesias.

The Severity of L-DOPA-Induced Dyskinesia Is Correlated with the Extent of Dopaminergic Depletion in the Lesioned Striatum

We found a strong correlation between the total dyskinesia score and the percentage of striatal area with complete dopamine depletion. The rotational response was also correlated with the extent of completely lesioned area but to a lesser extent. Although others (50) found that the magnitude of TH loss in the striatum is only a weak predictor of dyskinesias we consider that this disagreement with our data arises from the different approaches to determine the magnitude of TH-loss in the striatum. Whereas the previous study measured the average TH density in the whole striatum, our data are more specific and evaluate only the percentage of striatal area with complete denervation, verifying a high correlation between denervation and the intensity of dyskinesia. Our data agree with results showing that in denervated areas L-DOPA is converted to dopamine and released by striatal serotoninergic fibers (51), inducing dyskinesias (52,53) and FosB expression (51).

Moreover, our current and previous data (3) show that L-DOPA-induced increases in FosB, dynorphin, p-ERK, and p-AcH3 are all restricted to striatal areas completely free of TH fibers. A similar pattern of expression was observed for increased neurotensin and D3R mRNA in L-DOPA-treated rats (6). These results suggest that denervated striatal neurons hyperrespond to L-DOPA with a set of molecular changes in signaling and gene expression (54,55).

Phenotype of the Striatal Neurons Underlying the Molecular Changes Associated with Dyskinesia

Our data demonstrate that L-DOPA-induced p-AcH3 and FosB are localized in direct pathway neurons expressing D1R and only in those that are completely denervated and also overexpress dynorphin. These results are in line with the opposing functional roles of the two striatal output pathways. Whereas L-DOPA, which promotes movements, activates direct pathway neurons, D2R antagonists induce FosB in the indirect pathway neurons that mediate motor inhibition (56). In line with these results, the few FosB nuclei observed in $D1R^{-/-}$ were in enkephalin-negative neurons, indicating that these cells are direct pathway neurons or NOS interneurons (3).

Previous studies of L-DOPA-induced signaling in lesioned striatum were contradictory: Westin *et al.* (7) found p-ERK in both direct and indirect pathway neurons, whereas a more recent study found p-ERK expression only in direct pathway neurons (14). Our results confirm that p-ERK occurs exclusively in direct and significantly extend these findings by identifying that p-ERK and p-AcH3 occur only in those direct pathway neurons that are completely denervated and overexpress dynorphin. These results strongly suggest that any increase in p-ERK in indirect pathway neurons is not sustained for long enough to produce downstream changes. In addition, we demonstrate that inactivation of D1R completely blocks all the described molecular changes in these neurons, despite the presence of D5R (26) in these neurons.

Postranslational histone modification, including phosphorylation and acetylation, appears to modulate both the accessibility of chromatin for RNA transcription and how well chromatin serves as a template for transcription (49). Thus, H3 phosphoacetylation in dopamine-denervated cells may be a critical step in altering the response of these cells to L-DOPA and could provide the molecular basis for sustained chromatin modification and gene expression.

In conclusion, our data demonstrate that D1R are instrumental in the development of L-DOPA-induced dyskinesia in mice, without significant participation of D2R. Activation of D1R leads to expression of immediate early genes and downstream proteins in direct pathway neurons within the fully denervated region of the lesioned striatum. The p-AcH3 and the presumed modification of chromatin structure in these cells may be critical, opening the way for new gene expression in response to L-DOPA. Our data support this possibility and suggest that specific agents that inhibit histone modifications could help prevent or reverse the side effects of L-DOPA treatment in PD.

This research was supported by grants from the Spanish Ministerio de Sanidad y Consumo (Grant No. FIS PI07-1073), Plan Nacional Sobre Drogas, and Centro de Investigación Biomédica en Red para Enfermedades Neurodegenerativas. We thank Emilia Rubio and Ana Hernandez for their excellent technical assistance and Carmen Hernández for her help with video material.

The authors report no biomedical financial interests or potential conflicts of interest.

Supplementary material cited in this article is available online.

1. Chase TN, Oh JD, Blanchet PJ (1998): Neostriatal mechanisms in Parkinson's disease. *Neurology* 51:S30–S35.
2. Corvol JC, Muriel MP, Valjent E, Feger J, Hanoun N, Girault JA, *et al.* (2004): Persistent increase in olfactory type G-protein alpha subunit levels may underlie D1 receptor functional hypersensitivity in Parkinson's disease. *J Neurosci* 24:7007–7014.
3. Pavon N, Martin AB, Mendialdua A, Moratalla R (2006): ERK phosphorylation and FosB expression are associated with L-DOPA-induced dyskinesia in hemiparkinsonian mice. *Biol Psychiatry* 59:64–74.
4. Santini E, Valjent E, Usiello A, Carta M, Borgkvist A, Girault JA, *et al.* (2007): Critical involvement of cAMP/DARPP-32 and extracellular signal-regulated protein kinase signaling in L-DOPA-induced dyskinesia. *J Neurosci* 27:6995–7005.
5. Santini E, Valjent E, Fisone G (2008): Parkinson's disease: Levodopa-induced dyskinesia and signal transduction. *FEBS J* 275:1392–1399.
6. St-Hilaire M, Landry E, Levesque D, Rouillard C (2005): Denervation and repeated L-DOPA induce complex regulatory changes in neurochemical phenotypes of striatal neurons: Implication of a dopamine D1-dependent mechanism. *Neurobiol Dis* 20:450–460.
7. Westin JE, Vercammen L, Strome EM, Konradi C, Cenci MA (2007): Spatiotemporal pattern of striatal ERK1/2 phosphorylation in a rat model of L-DOPA-induced dyskinesia and the role of dopamine D1 receptors. *Biol Psychiatry* 62:800–810.
8. Nutt JG (2000): Clinical pharmacology of levodopa-induced dyskinesia. *Ann Neurol* 47:S160–S164.
9. Carta AR, Lucia F, Annalisa P, Silvia P, Nicola S, Nicoletta S, *et al.* (2008): Behavioral and biochemical correlates of the dyskinetic potential of dopaminergic agonists in the 6-OHDA lesioned rat. *Synapse* 62:524–533.
10. Delfino MA, Stefano AV, Ferrario JE, Taravini IR, Murer MG, Gershanik OS (2004): Behavioral sensitization to different dopamine agonists in a parkinsonian rodent model of drug-induced dyskinesias. *Behav Brain Res* 152:297–306.
11. Ding Y, Restrepo J, Won L, Hwang DY, Kim KS, Kang UJ (2007): Chronic 3,4-dihydroxyphenylalanine treatment induces dyskinesia in aphakia mice, a novel genetic model of Parkinson's disease. *Neurobiol Dis* 27:11–23.
12. Monville C, Torres EM, Dunnett SB (2005): Validation of the L-DOPA-induced dyskinesia in the 6-OHDA model and evaluation of the effects of selective dopamine receptor agonists and antagonists. *Brain Res Bull* 68:16–23.
13. Taylor JL, Bishop C, Walker PD (2005): Dopamine D1 and D2 receptor contributions to L-DOPA-induced dyskinesia in the dopamine-depleted rat. *Pharmacol Biochem Behav* 81:887–893.

14. Santini E, Alcacer C, Cacciatore S, Heiman M, Herve D, Greengard P, *et al.* (2009): L-DOPA activates ERK signaling and phosphorylates histone H3 in the striatonigral medium spiny neurons of hemiparkinsonian mice. *J Neurochem* 108:621–633.
15. Granado N, Ortiz O, Suarez LM, Martin ED, Cena V, Solis JM, *et al.* (2008): D1 but not D5 dopamine receptors are critical for LTP, spatial learning, and LTP-induced arc and zif268 expression in the hippocampus. *Cereb Cortex* 18:1–12.
16. Centonze D, Grande C, Saulle E, Martin AB, Gubellini P, Pavon N, *et al.* (2003): Distinct roles of D1 and D5 dopamine receptors in motor activity and striatal synaptic plasticity. *J Neurosci* 23:8506–8512.
17. Kvernmo T, Hartter S, Burger E (2006): A review of the receptor-binding and pharmacokinetic properties of dopamine agonists. *Clin Ther* 28: 1065–1078.
18. Tiberi M, Caron MG (1994): High agonist-independent activity is a distinguishing feature of the dopamine D1B receptor subtype. *J Biol Chem* 269:27925–27931.
19. Moratalla R, Xu M, Tonegawa S, Graybiel AM (1996): Cellular responses to psychomotor stimulant and neuroleptic drugs are abnormal in mice lacking the D1 dopamine receptor. *Proc Natl Acad Sci U S A* 93:14928–14933.
20. Xu M, Moratalla R, Gold LH, Hiroi N, Koob GF, Graybiel AM, *et al.* (1994): Dopamine D1 receptor mutant mice are deficient in striatal expression of dynorphin and in dopamine-mediated behavioral responses. *Cell* 79:729–742.
21. Kelly MA, Rubinstein M, ASA, SL, Zhang G, Saez C, *et al.* (1997): Pituitary lactotroph hyperplasia and chronic hyperprolactinemia in dopamine D2 receptor-deficient mice. *Neuron* 19:103–113.
22. Kelly MA, Low MJ, Rubinstein M, Phillips TJ (2008): Role of dopamine D1-like receptors in methamphetamine locomotor responses of D2 receptor knockout mice. *Genes Brain Behav* 7:568–577.
23. Murer MG, Dziewczapolski G, Salin P, Vila M, Tseng KY, Ruberg M, *et al.* (2000): The indirect basal ganglia pathway in dopamine D(2) receptor-deficient mice. *Neuroscience* 99:643–650.
24. Darmopil S, Muneton-Gomez VC, de Ceballos ML, Bernson M, Moratalla R (2008): Tyrosine hydroxylase cells appearing in the mouse striatum after dopamine denervation are likely to be projection neurones regulated by L-DOPA. *Eur J Neurosci* 27:580–592.
25. Grande C, Zhu H, Martin AB, Lee M, Ortiz O, Hiroi N, *et al.* (2004): Chronic treatment with atypical neuroleptics induces striosomal FosB/DeltaFosB expression in rats. *Biol Psychiatry* 55:457–463.
26. Rivera A, Alberti I, Martin AB, Narvaez JA, de la CA, Moratalla R (2002): Molecular phenotype of rat striatal neurons expressing the dopamine D5 receptor subtype. *Eur J Neurosci* 16:2049–2058.
27. Martinez-Murillo R, Blasco I, Alvarez FJ, Villalba R, Solano ML, Montero-Caballero MI, *et al.* (1988): Distribution of enkephalin-immunoreactive nerve fibres and terminals in the region of the nucleus basalis magnocellularis of the rat: A light and electron microscopic study. *J Neurocytol* 17:361–376.
28. Granado N, Escobedo I, O'Shea E, Colado I, Moratalla R (2008): Early loss of dopaminergic terminals in striosomes after MDMA administration to mice. *Synapse* 62:80–84.
29. Lundblad M, Picconi B, Lindgren H, Cenci MA (2004): A model of L-DOPA-induced dyskinesia in 6-hydroxydopamine lesioned mice: Relation to motor and cellular parameters of nigrostriatal function. *Neurobiol Dis* 16:110–123.
30. Nicholas AP, Lubin FD, Hallett PJ, Vattem P, Ravenscroft P, Bezard E, *et al.* (2008): Striatal histone modifications in models of levodopa-induced dyskinesia. *J Neurochem* 106:486–494.
31. van Kampen JM, Stoessl AJ (2003): Effects of oligonucleotide antisense to dopamine D3 receptor mRNA in a rodent model of behavioural sensitization to levodopa. *Neuroscience* 116:307–314.
32. Blanchet PJ, Gomez-Mancilla B, Bedard PJ (1995): DOPA-induced "peak dose" dyskinesia: Clues implicating D2 receptor-mediated mechanisms using dopaminergic agonists in MPTP monkeys. *J Neural Transm Supplementum* 45:103–112.
33. Calon F, Morissette M, Goulet M, Grondin R, Blanchet PJ, Bedard PJ, *et al.* (1999): Chronic D1 and D2 dopaminomimetic treatment of MPTP-denervated monkeys: Effects on basal ganglia GABA(A)/benzodiazepine receptor complex and GABA content. *Neurochem Int* 35:81–91.
34. Goulet M, Grondin R, Blanchet PJ, Bedard PJ, Di PT (1996): Dyskinesias and tolerance induced by chronic treatment with a D1 agonist administered in pulsatile or continuous mode do not correlate with changes of putaminal D1 receptors in drug-naive MPTP monkeys. *Brain Res* 719: 129–137.
35. Rascol O, Nutt JG, Blin O, Goetz CG, Trugman JM, Soubrouillard C, *et al.* (2001): Induction by dopamine D1 receptor agonist ABT-431 of dyskinesia similar to levodopa in patients with Parkinson's disease. *Arch Neurol* 58:249–254.
36. Sunahara RK, Guan HC, O'Dowd BF, Seeman P, Laurier LG, *et al.* (1991): Cloning of the gene for a human dopamine D5 receptor with higher affinity for dopamine than D1. *Nature* 350:614–619.
37. Martelle JL, Nader MA (2008): A review of the discovery, pharmacological characterization, and behavioral effects of the dopamine D2-like receptor antagonist eticlopride. *CNS Neurosci Ther* 14:248–262.
38. Millan MJ, Seguin L, Gobert A, Cussac D, Brocco M (2004): The role of dopamine D3 compared with D2 receptors in the control of locomotor activity: A combined behavioural and neurochemical analysis with novel, selective antagonists in rats. *Psychopharmacology* 174:341–357.
39. Newman-Tancredi A, Cussac D, Audinot V, Nicolas JP, De CF, Boutin JA, *et al.* (2002): Differential actions of antiparkinson agents at multiple classes of monoaminergic receptor. II. Agonist and antagonist properties at subtypes of dopamine D(2)-like receptor and alpha(1)/alpha(2)-adrenoceptor. *J Pharmacol Exp Ther* 303:805–814.
40. Bordet R, Ridray S, Carboni S, Diaz J, Sokoloff P, Schwartz JC (1997): Induction of dopamine D3 receptor expression as a mechanism of behavioral sensitization to levodopa. *Proc Natl Acad Sci U S A* 94:3363–3367.
41. Lundblad M, Usiello A, Carta M, Hakansson K, Fisone G, Cenci MA (2005): Pharmacological validation of a mouse model of L-DOPA-induced dyskinesia. *Exp Neurol* 194:66–75.
42. Pearce RK, Banerji T, Jenner P, Marsden CD (1998): De novo administration of ropinirole and bromocriptine induces less dyskinesia than L-DOPA in the MPTP-treated marmoset. *Mov Disord* 13:234–241.
43. Kelly MA, Rubinstein M, Phillips TJ, Lessov CN, Burkhart-Kasch S, Zhang G, *et al.* (1998): Locomotor activity in D2 dopamine receptor-deficient mice is determined by gene dosage, genetic background, and developmental adaptations. *J Neurosci* 18:3470–3479.
44. Andersson M, Hilbertson A, Cenci MA (1999): Striatal fosB expression is causally linked with L-DOPA-induced abnormal involuntary movements and the associated upregulation of striatal prodynorphin mRNA in a rat model of Parkinson's disease. *Neurobiol Dis* 6:461–474.
45. Piccini P, Weeks RA, Brooks DJ (1997): Alterations in opioid receptor binding in Parkinson's disease patients with levodopa-induced dyskinesias. *Ann Neurol* 42:720–726.
46. Brotchie JM, Henry B, Hille CJ, Crossman AR (1998): Opioid peptide precursor expression in animal models of dystonia secondary to dopamine-replacement therapy in Parkinson's disease. *Adv Neurol* 78:41–52.
47. Steiner H, Gerfen CR (1998): Role of dynorphin and enkephalin in the regulation of striatal output pathways and behavior. *Exp Brain Res* 123:60–76.
48. Shen HY, Kalda A, Yu L, Ferrara J, Zhu J, Chen JF (2008): Additive effects of histone deacetylase inhibitors and amphetamine on histone H4 acetylation, cAMP responsive element binding protein phosphorylation and DeltaFosB expression in the striatum and locomotor sensitization in mice. *Neuroscience* 157:644–655.
49. Tsankova N, Renthal W, Kumar A, Nestler EJ (2007): Epigenetic regulation in psychiatric disorders. *Nat Rev Neurosci* 8:355–367.
50. Putterman DB, Munhall AC, Kozell LB, Belknap JK, Johnson SW (2007): Evaluation of levodopa dose and magnitude of dopamine depletion as risk factors for levodopa-induced dyskinesia in a rat model of Parkinson's disease. *J Pharmacol Exp Ther* 323:277–284.
51. Carlsson T, Carta M, Munoz A, Mattsson B, Winkler C, Kirik D, *et al.* (2008): Impact of grafted serotonin and dopamine neurons on development of L-DOPA-induced dyskinesias in parkinsonian rats is determined by the extent of dopamine neuron degeneration. *Brain* 132:319–335.
52. Carta M, Carlsson T, Kirik D, Bjorklund A (2007): Dopamine released from 5-HT terminals is the cause of L-DOPA-induced dyskinesia in parkinsonian rats. *Brain* 130:1819–1833.
53. Carta M, Carlsson T, Munoz A, Kirik D, Bjorklund A (2008): Serotonin-dopamine interaction in the induction and maintenance of L-DOPA-induced dyskinesias. *Prog Brain Res* 172:465–478.
54. Jenner P (2008): Molecular mechanisms of L-DOPA-induced dyskinesia. *Nat Rev Neurosci* 9:665–677.
55. Nadjar A, Gerfen CR, Bezard E (2009): Priming for L-DOPA-induced dyskinesia in Parkinson's disease: A feature inherent to the treatment or the disease? *Prog Neurobiol* 87:1–9.
56. Hiroi N, Graybiel AM (1996): Atypical and typical neuroleptic treatments induce distinct programs of transcription factor expression in the striatum. *J Comp Neurol* 374:70–83.

2. Activation of DREAM (downstream regulatory element antagonist modulator), a calcium-binding protein, reduces L-DOPA-induced dyskinesia in mice

Ruiz-DeDiego, I., Mellström, B., Vallejo, M., Naranjo, J. R., Moratalla R

2014. *Biol Psychiatry.* Doi: 10.1016/j.biopsych.2014.03.023

PRIORITY COMMUNICATION

Activation of DREAM (Downstream Regulatory Element Antagonistic Modulator), a Calcium-Binding Protein, Reduces L-DOPA-Induced Dyskinesias in Mice

Irene Ruiz-DeDiego, Britt Mellstrom, Mario Vallejo, Jose R. Naranjo, and Rosario Moratalla

Background: Previous studies have implicated the cyclic adenosine monophosphate/protein kinase A pathway as well as FosB and dynorphin-B expression mediated by dopamine D_1 receptor stimulation in the development of 3,4-dihydroxyphenyl-L-alanine (L-DOPA)–induced dyskinesia. The magnitude of these molecular changes correlates with the intensity of dyskinesias. The calcium-binding protein downstream regulatory element antagonistic modulator (DREAM) binds to regulatory element sites called DRE in the DNA and represses transcription of target genes such as *c-fos*, fos-related antigen-2 (*fra-2*), and prodynorphin. This repression is released by calcium and protein kinase A activation. Dominant-active DREAM transgenic mice (daDREAM) and DREAM knockout mice ($DREAM^{-/-}$) were used to define the involvement of DREAM in dyskinesias.

Methods: Dyskinesias were evaluated twice a week in mice with 6-hydroxydopamine lesions during long-term L-DOPA (25 mg/kg) treatment. The impact of DREAM on L-DOPA efficacy was evaluated using the rotarod and the cylinder test after the establishment of dyskinesia and the molecular changes by immunohistochemistry and Western blot.

Results: In daDREAM mice, L-DOPA-induced dyskinesia was decreased throughout the entire treatment. In correlation with these behavioral results, daDREAM mice showed a decrease in FosB, phosphoacetylated histone H3, dynorphin-B, and phosphorylated glutamate receptor subunit, type 1 expression. Conversely, genetic inactivation of DREAM potentiated the intensity of dyskinesia, and $DREAM^{-/-}$ mice exhibited an increase in expression of molecular markers associated with dyskinesias. The DREAM modifications did not affect the kinetic profile or antiparkinsonian efficacy of L-DOPA therapy.

Conclusions: The protein DREAM decreases development of L-DOPA-induced dyskinesia in mice and reduces L-DOPA-induced expression of FosB, phosphoacetylated histone H3, and dynorphin-B in the striatum. These data suggest that therapeutic approaches that activate DREAM may be useful to alleviate L-DOPA-induced dyskinesia without interfering with the therapeutic motor effects of L-DOPA.

Key Words: Abnormal involuntary movements, dopaminergic denervation, dynorphin-B, FosB, Parkinson's disease, phospho-GluR1

Despite extensive research focused on discovering therapeutic alternatives, the dopamine precursor molecule 3, 4-dihydroxyphenyl-L-alanine (L-DOPA), remains the most effective and widely used noninvasive therapy for Parkinson's disease. Chronic administration of L-DOPA and disease progression cause the appearance of abnormal involuntary movements known as dyskinesias in most patients. L-DOPA-induced dyskinesia (LID) is causally linked with hyperstimulation of dopamine D_1 receptors (D1Rs) located on direct pathway medium spiny neurons of the severely denervated striatum (1–3). In the dopamine-depleted striatum, L-DOPA activates a cyclic adenosine monophosphate (cAMP)–dependent signaling cascade via protein kinase A (PKA) activation (4,5), resulting in abnormally increased phosphorylation of cAMP-regulated phosphoprotein of 32 kDa (DARPP-32) and activation of the Ras/extracellular signal-regulated kinase signaling pathway in the same neurons (1,6–9). These events induce transcriptional changes resulting in increased expression of FosB, phospho-(Ser10)-acetyl-(Lys14)-histone-3 (P-AcH3), and dynorphin-B (10,11).

In addition, the increased activation of the cAMP/PKA/DARPP-32 pathway observed in dyskinesia induces persistent phosphorylation of the alpha-amino-3-hydroxy-5-methyl-4-isoxazole propionic acid (AMPA) glutamate receptor subunit, type 1 (GluR1) at Ser845 (6,7) via protein phosphatase-1 inhibition, enhancing excitatory glutamatergic transmission in D1R-containing neurons and increasing *N*-methyl-D-aspartate receptor (NMDAR) activation (12–15). Enhanced synaptic transmission in LID has been associated with altered redistribution and trafficking of D1Rs (16) along with a massive accumulation of postsynaptic density protein 95 (PSD-95) in the synaptic membrane (17). It has been shown that PSD-95 modulates LID in rats and monkeys by its direct interaction with D1Rs (18). In addition, D1R-mediated activation of adenylyl cyclase/PKA triggers calcium entry through voltage-dependent calcium channels (19), and treatment with the L-type calcium channel antagonist isradipine diminishes dyskinesias (20), further supporting the idea that calcium entry into direct pathway striatal neurons after D1R stimulation contributes to LID.

Despite the progress made in recent years, the intracellular signaling mechanism downstream of D1R-PKA–dependent activation is not fully established. The downstream regulatory element antagonist modulator (DREAM), also known as calsenilin and KChIP3, is a calcium-binding protein that mediates calcium-dependent and cAMP-dependent transcriptional responses (21,22). In striatal neurons, moderate levels of DREAM are present

From the Cajal Institute (IRDD, RM); Centro Nacional de Biotecnología (BM, JRN); Instituto de Investigaciones Biomédicas Alberto Sols (MV) all part of Consejo Superior de Investigaciones Científicas (CSIC); CIBERNED (IRDD, BM, JRN, RM); and CIBERDEM (MV), Instituto de Salud Carlos III (ISCIII), Madrid, Spain.

Address correspondence to Rosario Moratalla, Ph.D., Cajal Institute (Consejo Superior de Investigaciones Científicas), Avda. Dr. Arce 37, Madrid 28002, Spain; E-mail: moratalla@cajal.csic.es.

Received Oct 4, 2013; revised Mar 5, 2014; accepted Mar 20, 2014.

0006-3223/$36.00
http://dx.doi.org/10.1016/j.biopsych.2014.03.023

in the neuropil and cell soma (23–25). In basal conditions, DREAM binds to a regulatory element called DRE, located downstream from the transcription initiation site, repressing the transcription of target genes, including prodynorphin, *c-fos*, and Fos-related antigen-2 (*fra-2*) (26,27). Repression mediated by DREAM is reversed by calcium and by its PKA-dependent interaction with phospho-CREM, the cAMP-response element modulator (26,28–30). Outside the nucleus, DREAM directly interacts with several proteins (31), including NR1 subunit (32) and PSD-95 (33), inhibiting NMDAR function and its surface expression.

Based on these observations and on our previous data demonstrating a close association between LID and overexpression of FosB and dynorphin-B (1,10), we propose that DREAM, located downstream of D1R-dependent cAMP/PKA activation, plays an important role in the cascade of molecular events leading to LID. If this hypothesis is true, DREAM could provide a site for intervention to improve the efficacy of L-DOPA treatment, while preventing the upregulation of target genes associated with dyskinesia. To investigate this possible role of DREAM in LID, we used DREAM knockout and dominant active DREAM transgenic mice in a mouse model of dyskinesias.

Methods and Materials

Animals

This study was carried out in transgenic mice 3–6 months old expressing a dominant active mutant DREAM (daDREAM) (34,35) or in DREAM-deficient mice (22,36). Both genetically modified animals and wild-type (WT) controls were maintained in a C57BL/6 background. In the daDREAM mice, expression of the transgene, a bicistronic construct including the daDREAM mutant, an internal ribosome entry site sequence, and the *lacZ* reporter, was driven by the calcium/calmodulin-dependent protein kinase type II alpha promoter (37). The transgenic line (JN26) used in this study has a telencephalic-specific expression with high levels of transgene expression in the striatum (Figure S1 in Supplement 1). Homozygous daDREAM and DREAM knockout ($DREAM^{-/-}$) mice were derived from mating the corresponding heterozygous mice. Genotyping was performed by polymerase chain reaction (PCR) as described previously (35,36). Bacterial artificial chromosome–transgenic D1R-tomato mice (38) were used to study DREAM striatal localization. All animal procedures followed guidelines from the European Union Council Directive (86/609/European Economic Community), and experimental protocols were approved by the Consejo Superior de Investigaciones Científicas Ethics Committee.

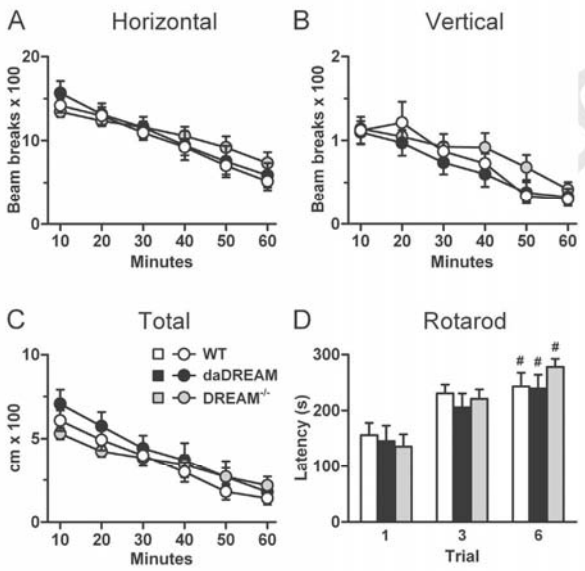

Figure 1. Genetic modification of DREAM protein levels does not alter basal locomotor activity. **(A)** Horizontal and **(B)** vertical locomotor activity (beam breaks) and **(C)** total distance traveled (cm) during 60 min were measured in a multicage activity meter system. **(D)** Latency (sec) to fall in the rotarod test at constant acceleration. daDREAM transgenic and $DREAM^{-/-}$ mice behave similarly to WT mice and show similar improvement in motor coordination. The data expressed as mean ± SEM were analyzed by two-way analysis of variance with repeated measures followed by Newman-Keuls test. Significant differences for trial were found [$F_{2,64} = 22.38$, $p < .001$]. $^{\#}p < .01$ vs. trial 1. $n = 10$–12. DREAM, downstream regulatory element antagonist modulator; $DREAM^{-/-}$, DREAM knockout; daDREAM, dominant-active DREAM; WT, wild-type.

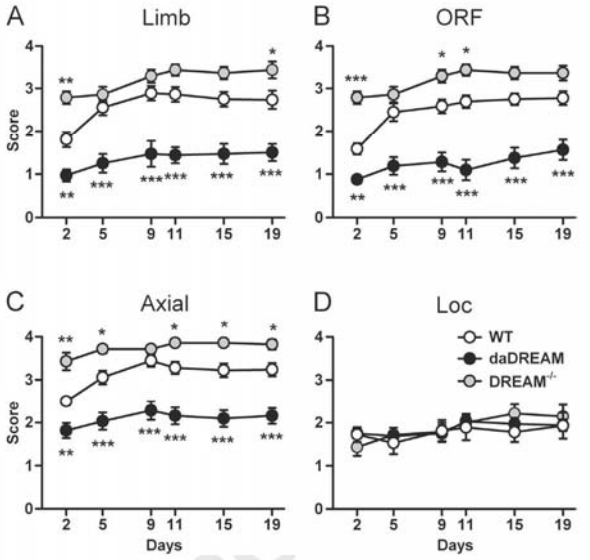

Figure 2. DREAM overexpression daDREAM mice decreases L-DOPA–induced dyskinesia in hemiparkinsonian mice, whereas genetic inactivation of DREAM ($DREAM^{-/-}$) potentiates L-DOPA-induced dyskinesia. Time course of appearance of dyskinetic symptoms is shown: Limb, ORF, Axial, and Loc. Movements were evaluated 40 min after L-DOPA (25 mg/kg) administration at the indicated days. daDREAM mice showed a lower dyskinetic score for limb and orofacial dyskinesia and for axial dystonia compared with WT mice, whereas inactivation of DREAM in $DREAM^{-/-}$ mice significantly increased these dyskinetic symptoms. No statistically significant differences were found for locomotive dyskinesia. Data are expressed as mean ± SEM. Two-way analysis of variance with repeated measures followed by Newman-Keuls test showed significant differences for genotype [$F_{2,190} = 25.52$, $p < .001$ for Limb; $F_{2,190} = 34.47$, $p < .001$ for ORF; $F_{2,190} = 28.43$, $p < .001$ for Axial] and for time [$F_{5,190} = 14.00$, $p < .001$ for Limb; $F_{5,190} = 14.23$, $p < .001$ for ORF; $F_{5,190} = 8.92$, $p < .001$ for Axial]. $^{*}p < .05$, $^{**}p < .01$, $^{***}p < .001$ vs. WT mice. $n = 8$–15. Axial, axial dystonia; DREAM, downstream regulatory element antagonist modulator; $DREAM^{-/-}$, DREAM knockout; daDREAM, dominant-active DREAM; Limb, limb dyskinesia; Loc, locomotive dyskinesia; ORF, orofacial dyskinesia; WT, wild-type.

6-Hydroxydopamine Lesion and L-DOPA Treatment

Animals received unilateral stereotaxic injections (2 × 2 μL) of 6-hydroxydopamine (6-OHDA) hydrobromide (20 mmol/L, containing .02% ascorbic acid; Sigma-Aldrich, St. Louis, Missouri) as

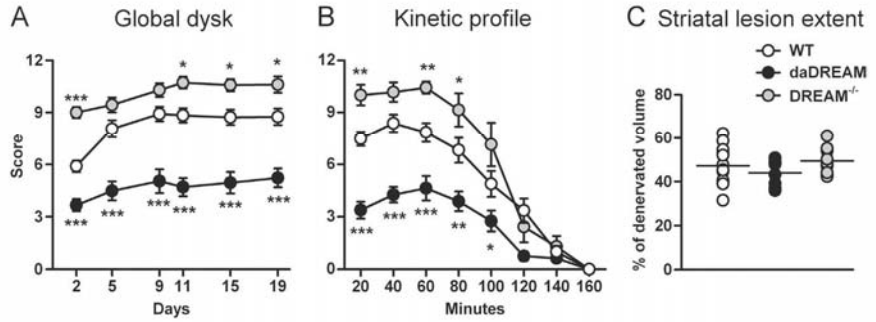

Figure 3. DREAM content modulates the Global dysk score. **(A)** Time course of Global dysk score in daDREAM transgenic and in DREAM$^{-/-}$ mice compared with their WT littermates, evaluated 40 min after L-DOPA (25 mg/kg) administration at the indicated days. Overexpression of DREAM decreased L-DOPA-induced dyskinesia score for the entire treatment period, whereas inactivation of DREAM increased L-DOPA-induced dyskinesia score. Two-way ANOVA with repeated measures followed by Newman-Keuls test showed significant differences for genotype [$F_{2,190} = 34.01$, $p < .001$], time [$F_{5,190} = 19.34$, $p < .001$], and genotype × time [$F_{10,190} = 2.12$, $p < .05$]. **(B)** Kinetic profile of dyskinetic symptoms evaluated once every 20 min during 160 min on day 20 of L-DOPA treatment. Overexpression of DREAM reduced L-DOPA-induced dyskinesia score during the entire half-life of L-DOPA, whereas genetic inactivation of DREAM increased dyskinesia. Two-way ANOVA with repeated measures followed by Newman-Keuls test showed significant differences for genotype [$F_{2,196} = 13.51$, $p < .001$], time [$F_{7,196} = 99.56$, $p < .001$], and genotype × time [$F_{14,196} = 5.44$, $p < .001$]. **(C)** Scatter diagram of the extent of striatal lesions assessed by percentage of striatal volume completely denervated. No statistically significant differences were found among genotypes by one-way ANOVA. Global L-DOPA-induced dyskinesia scores expressed as mean ± SEM. *$p < .05$, **$p < .01$, ***$p < .001$ vs. WT mice. $n = 8$–15. ANOVA, analysis of variance; DREAM, downstream regulatory element antagonist modulator; DREAM$^{-/-}$, DREAM knockout; daDREAM, dominant-active DREAM; Global dysk, global dyskinetic; WT, wild-type.

described previously (39). After 3 weeks of recovery, mice received a daily intraperitoneal injection of 25 mg/kg of L-DOPA methyl ester (Sigma-Aldrich) 20 min after benserazide hydrochloride (10 mg/kg; Sigma-Aldrich) for a 3-week period.

Behavioral Analysis

Locomotor Activity and Motor Coordination. Horizontal and vertical activity and total distance traveled were recorded in mice as described previously (40). Motor coordination was measured in the Rota-Rod (Ugo Basile, Varese, Italy) following an accelerating protocol, with increasing speed from 4–40 rpm over a 5-min period as described (41). Mice were tested in six consecutive trials 20 min apart. Measurements were done before injection of 6-OHDA (naïve); 3 weeks after lesion (parkinsonian); and during L-DOPA treatment (dyskinetic) on day 9, 24 hours after the last L-DOPA injection to avoid exhaustion and the peak dyskinesia.

Dyskinetic Score. Dyskinesias induced by L-DOPA were evaluated twice a week for 3 weeks, 40 minutes after L-DOPA injection, using a 0–4 severity scale as described previously (1,38). The time course of L-DOPA response for each genotype was evaluated on day 20, for 1 min every 20 min during 160 min after L-DOPA injection.

Cylinder Test. The cylinder test was performed according to Espadas *et al.* (42) before the 6-OHDA lesion; 3 weeks after lesion; and on day 17 the chronic L-DOPA treatment, 140 min after L-DOPA injection to avoid dyskinetic symptoms. Spontaneous ipsilateral and contralateral forelimb touches to the cylinder were counted for 3 min to assess forelimb asymmetry.

Immunohistochemistry and Image Analysis

Mice were killed 1 hour after the last L-DOPA injection, and immunohistochemistry studies were performed as described previously (43,44) using the following antibodies: tyrosine hydroxylase (TH) (1:1000; Millipore, Temecula, California), FosB (1:7500; Santa Cruz Biotechnology, Santa Cruz, California), dynorphin-B 1-29 (leumorphin) (1:10;000; Serotec, Oxford, United Kingdom), P-AcH3 (1:1500; Upstate Cell Signaling Solutions, Lake Placid, New York), DREAM (FL-214) (1:250; Santa Cruz Biotechnology), and Hoechst (1 μg/mL; Sigma-Aldrich).

The extent of dopaminergic lesions was quantified using Neurolucida software (MBF Bioscience, Williston, Vermont), depicting the border of striatal areas with complete loss of TH-immunoreactive fibers with a 4× lens using seven to nine serial rostrocaudal sections per animal. Quantification of FosB, P-AcH3, and dynorphin-B immunoreactivity was carried out as described previously (10,45).

Reverse Transcription Quantitative PCR (RT-qPCR)

Total RNA from isolated striata was extracted using the Illustra RNAspin kit (GE Healthcare Europe, Barcelona, Spain). Quantitative PCR for DREAM and TH was performed with TaqMan Assay on Demand primers and the TaqMan Universal PCR Master Mix, No AmpErase UNG (Applied Biosystems, Madrid, Spain). The PCR reactions were performed in triplicate in a 7900HT Fast Real-Time PCR System (Applied Biosystems). Expression of target genes was normalized using the 18S expression and calculated using the delta-delta Ct method (46).

Western Blot

Animals were sacrificed by decapitation 30 min after the last L-DOPA injection, and striatal tissue was dissected and homogenized. Western blot analysis was performed with primary antibodies against phospho-Ser845-GluR1 (1:7500; Millipore), TH (1:4000; Millipore), and β-actin (1:50,000; Sigma-Aldrich) as a loading control. Blots were developed by chemiluminescence (ECL Plus; GE Healthcare, Little Chalfont, United Kingdom) and quantified by densitometry.

Statistical Analysis

Behavioral data and quantifications of immunolabeling were analyzed by two-way analysis of variance followed by Newman-Keuls post hoc test. The extent of the dopaminergic lesion and DREAM messenger RNA (mRNA) expression were analyzed by one-way analysis of variance. Differences were considered statistically significant at $p < .05$.

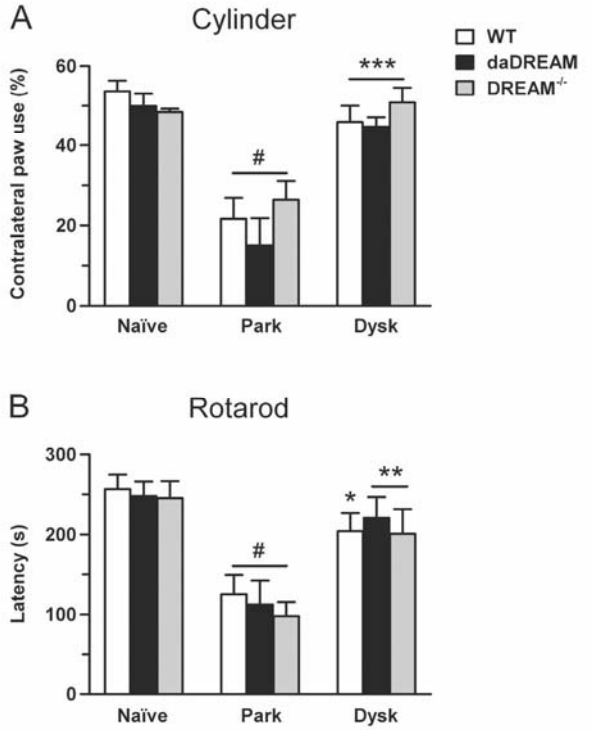

Figure 4. Genetic manipulation of DREAM does not modify the therapeutic effect of L-DOPA. **(A)** Forelimb use asymmetry was assessed with the cylinder test and **(B)** motor coordination was assessed with the rotarod before lesion (naïve), 3 weeks after 6-hydroxydopamine lesion and during chronic L-DOPA treatment on day 17, 140 min after administration of L-DOPA **(A)**, or on day 9, 24 hours after administration of L-DOPA **(B)**. Data from the cylinder test are expressed as percentage of wall contacts performed with the contralateral limb and in sec for the rotarod. Mean ± SEM values were analyzed by two-way analysis of variance followed by Newman-Keuls test showing significant differences for treatment: **(A)** [$F_{2,61} = 48.23$, $p < .001$] and **(B)** [$F_{2,83} = 27.70$, $p < .001$]. $^{\#}p < .001$ versus naïve; $^{*}p < .05$, $^{**}p < .01$, $^{***}p < .001$ versus Park group. No statistically significant differences among genotypes were found in any of the three conditions tested—naïve, Park, or Dysk. $n = 6$–9. daDREAM, dominant-active DREAM transgenic; DREAM$^{-/-}$, DREAM knockout; Dysk, dyskinetic; Park, parkinsonian; WT, wild-type.

Results

Basal Locomotor Activity and Motor Coordination Are Normal in DREAM Mutant Mice

Although no morphologic differences were evident between genotypes, we carried out spontaneous locomotor activity and rotarod tests before the 6-OHDA lesion to rule out any motor impairment in the mutant mice that could interfere with L-DOPA behavioral studies. In the absence of any external challenge, daDREAM, DREAM$^{-/-}$, and WT mice showed similar horizontal and vertical activity, as indicated by the number of beam breaks measured in a multicage activity meter system (Figure 1A,B). Ambulatory activity measured as total distance traveled was also similar among the three genotypes (Figure 1C). Over time, as the mice habituated to the environment, the number of beam breaks and the distance traveled diminished, with a similar profile in all three genotypes. No statistically significant differences between genotypes were found in the rotarod test (Figure 1D). All animals achieved a significant increase ($p < .001$) in the latency to fall from the rotating rod at the sixth and last trial compared with the first trial, showing a similar capacity of motor learning in the rotarod. Taken together, these results indicated that alterations in DREAM expression do not modify spontaneous locomotor activity or motor coordination.

DREAM Modulates L-DOPA-Induced Dyskinesias

To examine the role of DREAM in dyskinesias in hemiparkinsonian/6-OHDA-lesioned mice, we assessed axial dystonia and forelimb, orofacial, and locomotive dyskinesia in daDREAM, DREAM$^{-/-}$, and corresponding WT littermates 40 min after L-DOPA administration. The L-DOPA injections were given daily, and assessments were done twice a week, as described previously (1,10).

In WT mice, LID symptoms were already apparent at the beginning of the treatment and progressively increased to reach a plateau in the second week of L-DOPA administration (Figure 2). The daDREAM mice showed a significant reduction in dyskinetic movements, in particular for limb ($p < .001$) and orofacial ($p < .001$) symptoms, as well as for axial dystonia ($p < 0.001$) compared with WT littermates. Meanwhile, the DREAM$^{-/-}$ mice showed a significant enhancement in limb ($p < .05$) and orofacial ($p < .01$) dyskinesia as well as axial dystonia ($p < .05$). These changes were apparent from the first day of L-DOPA administration and lasted over the entire 3-week treatment. No difference in locomotive dyskinesia was observed among genotypes, indicating that DREAM modification does not compromise the motor stimulant effect of L-DOPA.

We calculated the global dyskinetic score of daDREAM and DREAM$^{-/-}$ mice and evaluated the time course of L-DOPA response in both genotypes. Although dyskinesia was observed in both daDREAM and WT mice, the total score achieved by daDREAM mice was significantly lower ($p < .001$) compared with WT mice for all time points evaluated (Figure 3A). On the other hand, the total dyskinetic score was higher in DREAM$^{-/-}$ mice compared with WT littermates. The difference was statistically significant ($p < .05$), although it was smaller than the difference observed between the daDREAM and the WT mice.

To look for differences in the kinetic profile of L-DOPA responses among genotypes, we determined the duration of the dyskinetic response and the peak severity of the symptoms by evaluating the time course of L-DOPA response in daDREAM and DREAM$^{-/-}$ mice on day 20 of L-DOPA administration (Figure 3B). Dyskinetic symptoms were scored for 1 min every 20 min during the 160 min following L-DOPA administration. Dyskinesia was evident at 20 min, peaked between 40 and 60 min, and declined significantly at 100 min after L-DOPA before disappearing at 140 min for both genotypes. Although the time course of L-DOPA response was similar in both groups of mice, daDREAM mice exhibited significantly lower dyskinesia compared with WT mice throughout the entire duration of the L-DOPA response. Finally, there were no statistically significant differences between DREAM$^{-/-}$ and WT mice in the duration of the L-DOPA response. As in daDREAM mice, the response was evident 20 min after L-DOPA and disappeared after 140 min. However, a difference was again observed in the intensity of the dyskinetic symptoms, which were stronger in DREAM$^{-/-}$ mice until 120 min, when the dyskinetic scores were similar for the duration of the effect. These time course results show that changes in DREAM do not alter the kinetic profile of L-DOPA as demonstrated by the duration of the L-DOPA response.

To exclude that the extent of the dopaminergic lesion in the three genotypes was different, which could influence the results,

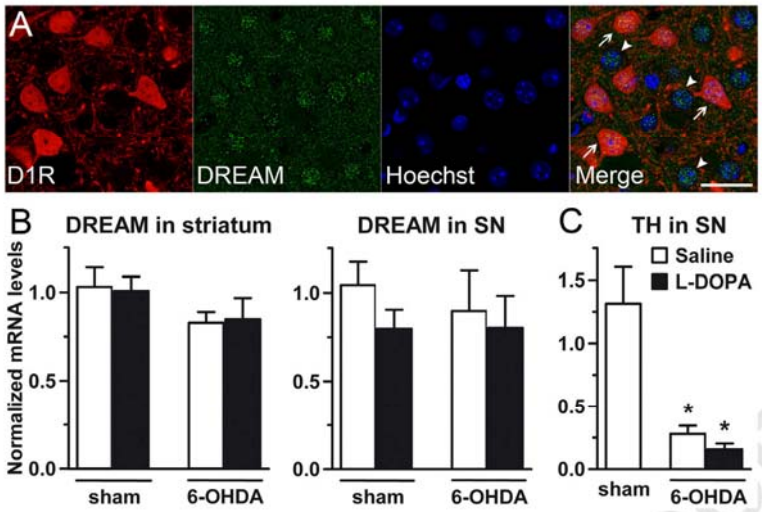

Figure 5. DREAM expression in striatum and SN. **(A)** Representative high-resolution striatal confocal images of naïve bacterial artificial chromosome–transgenic dopamine D1R–tomato mice illustrating DREAM (green) expression in D1R-positive (red) and in D1R-negative medium spiny neurons. Hoechst (blue) stain identifies the nuclei. Arrows indicate examples of dual DREAM-positive and D1R-positive neurons; arrowheads point to DREAM-positive and D1R-negative neurons. Scale bar = 25 μm. Histograms show **(B)** DREAM and **(C)** TH mRNA levels analyzed by reverse transcription quantitative polymerase chain reaction and normalized to 18S mRNA in wild-type mice. Treatment with 6-OHDA and L-DOPA does not modify DREAM transcripts in striatum or SN. **(C)** The TH levels in SN were quantified to confirm the efficacy of 6-OHDA lesion. Data (mean ± SEM) are expressed as normalized values and analyzed by one-way analysis of variance followed by Newman-Keuls test [$F_{2,17} = 10.54$, $p < .001$]. *$p < .01$ vs. WT naïve mice. $n = 5$–7. $D1R$, D_1 receptor; DREAM, downstream regulatory element antagonist modulator; $DREAM^{-/-}$, DREAM knockout; daDREAM, dominant-active DREAM; mRNA, messenger RNA; 6-OHDA, 6-hydroxydopamine; SN, substantia nigra; TH, tyrosine hydroxylase.

we assessed the percentage of striatal volume with a complete loss of TH-immunoreactive fibers for each group of animals (Figure 3C). We found no statistically significant difference between groups (daDREAM, 44.2% ± 2%; $DREAM^{-/-}$, 48.7% ± 2%; and WT, 46.2% ± 2%).

Antiparkinsonian Effect of L-DOPA Is Maintained in DREAM Mutant Mice

To rule out that the different dyskinetic score induced by L-DOPA in DREAM mutant mice is not due to an altered motor response to L-DOPA in these mice, we carried out the cylinder and rotarod tests to measure the antiparkinsonian effect of L-DOPA (42,47). In the cylinder test, naïve mice used both forelimbs similarly, whereas lesioned mice showed a significant ($p < .001$) asymmetry in forelimb use (Figure 4A). As expected, L-DOPA significantly ($p < .001$) recovered the contralateral paw use. Importantly, no significant differences were observed among the three genotypes, indicating that the genetic manipulation of DREAM does not affect the motor impairment induced by the lesion or the therapeutic effect of L-DOPA. Similar results were observed with the rotarod, which evaluates motor coordination (Figure 4B), strengthening the data from the cylinder test and further confirming that modifications in DREAM do not alter the antiparkinsonian efficacy of L-DOPA.

DREAM Is Expressed in Direct and Indirect Striatal Projection Neurons

Previous studies demonstrated that DREAM is expressed in the striatum and substantia nigra (23–25). Using naïve bacterial artificial chromosome–transgenic D1R-tomato mice to differentiate direct from indirect pathway neurons, we observed moderate DREAM signal in both D1R-positive (red fluorescence) and D1R-negative (no fluorescence) medium spiny neurons (Figure 5A). This immunolabeling was preferentially nuclear but was also evident in the cytoplasm and in the neuropil. Quantification experiments of DREAM carried out by RT-qPCR demonstrated that L-DOPA treatment to sham or lesioned animals did not modify DREAM mRNA expression in the striatum or in the substantia nigra (Figure 5B). RT-qPCR was also used to measure TH mRNA in the same animals to confirm the efficacy of 6-OHDA lesion (Figure 5C).

DREAM Regulates Key Molecular Determinants of LID

Several studies have correlated the increased levels of FosB, P-AcH3, and dynorphin-B in the dorsolateral lesioned striatum with the appearance of LID (1,11,48). We evaluated the effect of the genetic modification of DREAM on the striatal levels of these markers after chronic L-DOPA administration in hemiparkinsonian mice. The number of FosB-positive neurons was threefold lower in the lesioned striatum of daDREAM transgenic mice ($p < .001$) and just slightly increased in $DREAM^{-/-}$ mice ($p < .01$) compared with WT mice (Figure 6A,B). The presence of histone H3 phosphorylated on Ser10 and acetylated on Lys14 was significantly modified in the striatum ipsilateral to the lesion with a 2.5-fold decrease in the number of P-AcH3-positive nuclei in daDREAM mice ($p < .001$) and a 1.5-fold increase in $DREAM^{-/-}$ mice compared with WT mice ($p < .001$) (Figure 6C,D). Finally, scanning of the dynorphin-B-positive area, including cytoplasm and neuropil, revealed a 39% reduction ($p < .01$) and a 65% increase ($p < .001$) relative to the total area scanned in daDREAM and $DREAM^{-/-}$ mice, respectively (Figure 6E,F). No statistically significant differences were found in any of these molecular markers in the unlesioned striatum of daDREAM, $DREAM^{-/-}$, and WT mice, which served as a negative control for these experiments. As an additional control for the specificity of these changes, we verified that L-DOPA-induced changes were

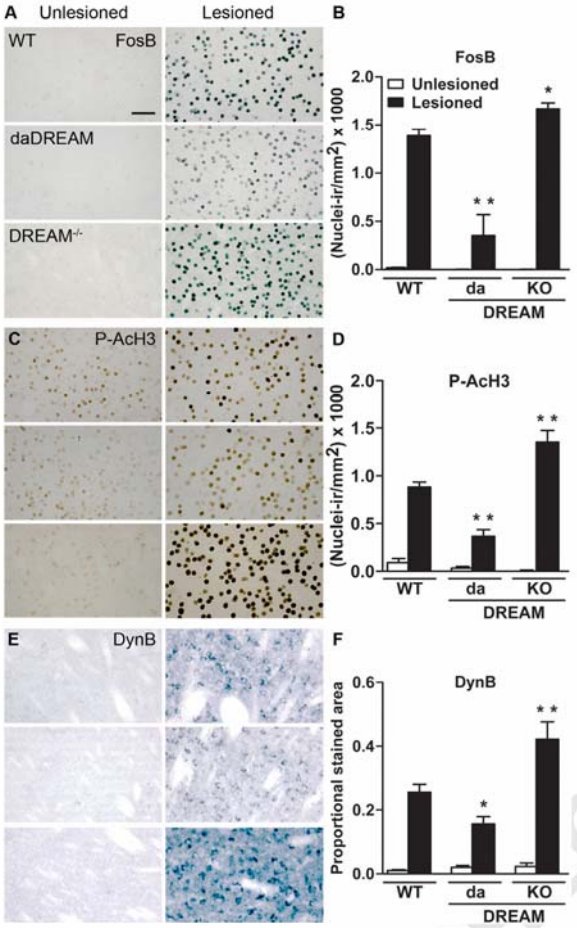

Figure 6. DREAM overexpression reduces, whereas its inactivation potentiates, FosB, P-AcH3, and DynB protein expression induced by L-DOPA. **(A, C, E)** High-power photomicrographs of unlesioned and lesioned striatum of WT, daDREAM and DREAM$^{-/-}$ mice sacrificed 1 hour after the last L-DOPA injection, immunostained for FosB, P-AcH3, and DynB. Scale bar = 50 μm. **(B, D, F)** Histograms represent the quantification of FosB and P-AcH3 immunoreactive positive nuclei and DynB immunoreactive area in the unlesioned and lesioned striatum of hemiparkinsonian WT, daDREAM, and DREAM$^{-/-}$ mice. Note the higher expression in DREAM$^{-/-}$ mice compared with WT mice and the decreased expression in daDREAM mice. Data (mean ± SEM) representing positive nuclei **(B, D)** and proportional stained area **(F)** were analyzed by two-way analysis of variance followed by Newman-Keuls test. Significant differences were found for genotype × treatment [$F_{2,47}$ = 30.55, $p < .001$ for FosB; $F_{2,41} = 21.67$, $p < .001$ for P-AcH3; $F_{2,24} = 12.13$, $p < .001$ for DynB]. *$p < .01$, **$p < .001$ vs. lesioned WT mice. DREAM, downstream regulatory element antagonist modulator; DREAM$^{-/-}$, DREAM knockout; daDREAM, dominant-active DREAM; DynB, dynorphin B; WT, wild-type.

strictly restricted to the completely denervated striatal area (Figure S2 in Supplement 1), as we have shown before (2,10,38). These results indicate that genetic manipulation of DREAM does not modify the expression pattern of the molecular markers of dyskinesia in mice. These findings correlate well with our behavioral results and implicate DREAM in the regulation of FosB, P-AcH3, and dynorphin-B levels.

LID-Associated Phosphorylation of GluR1 Is Attenuated in daDREAM Mice

It is well documented that in the striatum of 6-OHDA-lesioned mice (6) and 1-methyl-4-phenyl-1,2,3,6-tetrahydropyridine lesion monkeys (49), chronic L-DOPA administration results in PKA-dependent hyperphosphorylation of the GluR1 subunit of the glutamate AMPA receptor at serine 845. We examined whether the genetic modification of DREAM modifies the phosphorylation state of GluR1 (P-GluR1) induced by L-DOPA. Analysis of striatal extracts showed that L-DOPA treatment induces an increase in P-GluR1 levels in WT lesioned mice, as expected. This increase was evident also in DREAM$^{-/-}$ mice. In contrast, overexpression of DREAM in daDREAM mice inhibited the hyperphosphorylation of GluR1 induced by L-DOPA (Figure 7A). In parallel, measurement of levels of TH protein confirmed a similar efficacy of the 6-OHDA lesion in all samples (Figure 7B).

Discussion

These studies provide evidence that the DREAM protein plays a modulatory role in LID in mice and in the underlying molecular changes within the denervated striatum. Overexpression of a dominant active version of DREAM in transgenic mice dramatically reduced LID, whereas genetic inactivation of DREAM increased dyskinetic symptoms. In strict correspondence with the behavioral observations, molecular markers of dyskinesia induced by chronic L-DOPA treatment, including FosB, dynorphin-B, P-AcH3, and P-GluR1, were decreased in daDREAM mice but increased in DREAM$^{-/-}$ mice. Importantly, modifications in DREAM did not alter the kinetic profile or the antiparkinsonian efficacy of L-DOPA, suggesting that modulation of DREAM function could serve as an intervention target in therapies designed to alleviate LID without interfering with the beneficial effects of L-DOPA treatment.

In agreement with previous observations in naïve DREAM$^{-/-}$ (36,50) and daDREAM (51) adult mutant mice, spontaneous locomotor activity and motor coordination were indistinguishable from WT littermates, suggesting that the differences observed in LID are not due to any motor impairment but rather to the modifications related to DREAM levels. Moreover, dyskinetic differences among genotypes after L-DOPA treatment are not due to alterations of the kinetic profile of L-DOPA by DREAM because all animals showed a similar duration of the L-DOPA response. Mutant mice show similar motor performance skills in the cylinder and rotarod tests, demonstrating that the antiparkinsonian effect of L-DOPA is preserved in mutant animals despite DREAM modifications.

The DREAM protein is a multifunctional calcium-binding protein (52) that acts as a transcriptional repressor to regulate activity-dependent gene expression through direct interaction with regulatory sites in the DNA (26). Our data show that DREAM is present in the nucleus of striatal projection neurons. In these neurons, increased expression of FosB and dynorphin-B after L-DOPA treatment correlates with dyskinesias in patients with Parkinson's disease (53,54), in 1-methyl-4-phenyl-1,2,3,6-tetrahydropyridine–treated monkeys (55,56), and in 6-OHDA-treated rats (48) and mice (1,10,38). Transcriptional repression of FosB and prodynorphin genes in daDREAM mice could be directly related to the observed reduction in development of LID.

Correlating with the behavioral response to L-DOPA, our results show that overexpression of daDREAM diminishes FosB and dynorphin-B expression induced by L-DOPA in denervated striatal neurons, whereas genetic inactivation of DREAM induces

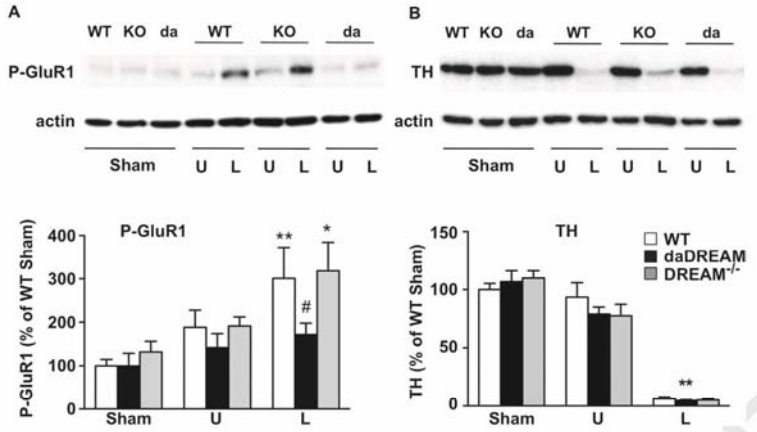

Figure 7. DREAM overexpression inhibits L-DOPA–induced phosphorylation of glutamate receptor subunit, type 1 (P-GluR1) at Ser845. Upper panels show representative autoradiograms of Western blots of striatal extracts from sham-operated and hemiparkinsonian, unlesioned (U) and lesioned (L) striatum of wild-type (WT), dominant-active DREAM transgenic (da), and DREAM knockout (KO) mice chronically treated with 25 mg/kg L-DOPA, incubated with antibodies against P-GluR1 **(A)** and tyrosine hydroxylase (TH) **(B)**. Lower panels show the quantification of Western blots in triplicates. **(A)** Chronic L-DOPA treatment increases P-GluR1 at Ser 845 in DREAM$^{-/-}$ and WT mice, whereas DREAM overexpression blocks L-DOPA-induced GluR1-phosphorylation. **(B)** The TH levels were quantified to confirm the efficacy of 6-hydroxydopamine lesion, and no statistically significant differences were found among genotypes. Relative intensities versus loading control actin (normalized to WT Sham) were analyzed by two-way analysis of variance followed by Newman-Keuls test. Significant differences for genotype [$F_{2,55} = 3.23$, $p < .05$] and for treatment [$F_{2,55} = 12.77$, $p < .001$] were found. $^{\#}p < .05$ versus WT lesioned + L-DOPA; $^{*}p < .01$, $^{**}p < .001$ vs. WT sham-operated mice. daDREAM, dominant-active DREAM transgenic; DREAM$^{-/-}$, DREAM knockout.

the opposite effect. The small increase of FosB and dynorphin-B expression observed in the striatum of DREAM-deficient mice after L-DOPA is in agreement with similar increases observed previously in the spinal cord of DREAM$^{-/-}$ mice (36). By binding to DRE sites located in the 5′-untranslated sequence downstream from the TATA box, DREAM represses the transcription of the immediate early genes *fra-2* and *c-fos* as well as prodynorphin (26,27). Although not previously studied, our data indicate that DREAM may also repress FosB, consistent with the presence of two DRE sites in this gene (57). Dynorphin-B expression is also regulated by D1R activation (58) and by binding of Fos/Jun heterodimers to an AP-1 site in the prodynorphin gene (59). Overexpression of FosB after L-DOPA treatment induces a concomitant increase of dynorphin-B expression in the 6-OHDA lesioned striatum (48). Our data support the notion that DREAM exerts a synergistic double effect: directly, blocking prodynorphin transcription by anchoring to its DRE site, and indirectly, diminishing FosB expression and resulting in dynorphin-B downregulation via AP-1.

The nontranscriptional effects of DREAM have been shown to regulate cell function and synaptic activity, mostly through various specific protein-protein interactions (31). The list of target proteins includes cationic channels (60), membrane receptors (32,61), and membrane docking proteins (33). Because a wide variety of mechanisms underlie synaptic changes associated with LID, including abnormal dendritic spine increases in denervated dopamine D_2 receptor–containing striatal neurons (38) involved in corticostriatal synapses (62), several additional mechanisms could be related to DREAM-mediated changes in LID based on its presence in the cell body as discussed below.

In addition to D1R stimulation, NMDAR activation plays an important role in dyskinesia; treatment with NMDAR antagonists such as MK-801 or amantadine completely abolishes LID (63,64). The DREAM protein has been shown to diminish NMDAR activation (32,33). In cultured neurons, DREAM knockdown with small interfering RNAs significantly enhanced NMDAR-mediated currents, whereas overexpression of DREAM reduced NMDAR activation and its presence in the plasma membrane, indicating that DREAM modulates NMDAR function. Taken together, these data correlate well with our dyskinetic behavioral results. Inactivation of DREAM, which potentiates NMDAR-mediated currents, potentiates dyskinesia, whereas overexpression of DREAM, which inhibits NMDAR function, decreases dyskinesia. It is possible that the inhibitory role of DREAM in LID reported here could be partially related to the negative regulation exerted by DREAM on NMDAR by directly interacting with the NR1 subunit and preventing full activation of the NMDAR complex as shown in cultured hippocampal neurons (32). On the other hand, the documented capacity of DREAM to bind PSD-95 (33), impairing the recruitment of PSD-95 by D1Rs (18), could contribute to the observed reduction of LID. Disruption of the NMDAR-PSD-95 complex increases LID (14), probably by making PSD-95 available for interaction with D1Rs in the synaptic membrane. Displacement of the normal PSD-95 interactome from D1Rs owing to increased DREAM levels could explain the decrease in dyskinesia in daDREAM mice.

Acetylated histone H3 is associated with active chromatin and gene transcription (65), and this effect is synergistically potentiated by phosphorylation (66). Because phosphoacetylation of histone H3 correlates with the intensity of dyskinesias (6,10,11,67), the presence of increased phosphoacetylated histone H3 in DREAM-deficient animals is consistent with increased dynorphin-B and FosB expression and with increased LID. On the contrary, in the presence of the daDREAM repressor, we observed decreased P-AcH3, dynorphin-B, FosB, and LID, as expected. In line with these observations, DREAM has been shown to inhibit transcription by blocking the CREB-CBP histone acetylase complex (29). On the other hand, histone H3 phosphorylation depends on the stimulation of the D1R pathway (10). Although it is possible that this phosphorylation occurs through the D1R/cAMP/PKA/DARPP-32 signaling pathway, it could also be mediated by the reported NMDAR-DREAM interaction through the NR1 receptor subunit (32).

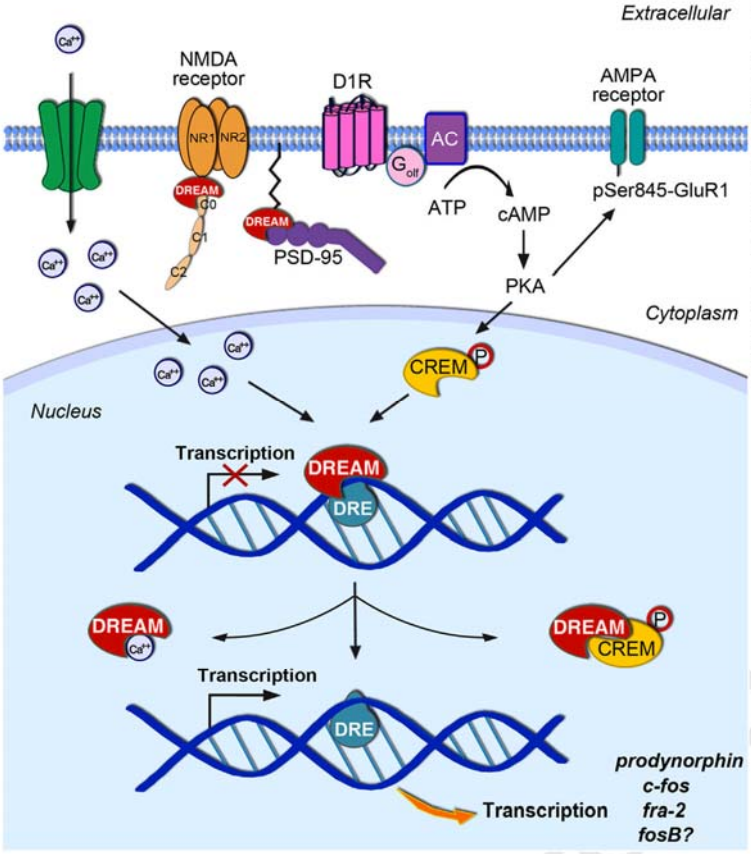

Figure 8. Schematic diagram illustrating the regulatory role of DREAM in the transcriptional and nontranscriptional mechanisms involved in L-DOPA–induced dyskinesia. In the nucleus, DREAM regulates dynorphin-B and possibly FosB expression (and subsequent L-DOPA–induced dyskinesia) by anchoring to DRE sites located downstream from the transcription initiation site of the DNA. This repression is released under conditions of calcium-dependent and protein kinase A (PKA)–dependent interaction with phospho-CREM. In addition, outside the nucleus, DREAM could directly interact with NR1 subunit, inhibiting activation of *N*-methyl-D-aspartate (NMDA) receptors, and with postsynaptic density protein 95 (PSD-95), impairing its recruitment by dopamine D_1 receptors (D1Rs) and decreasing the cAMP/PKA signaling pathway. AMPA, alpha-amino-3-hydroxy-5-methyl-4-isoxazole propionic acid; ATP, adenosine triphosphate; GluR1, glutamate receptor subunit, type 1.

Although a direct DREAM and AMPA receptor interaction has not been described, it is possible that an indirect interaction occurs because overexpression of DREAM significantly blocked L-DOPA-induced phosphorylation of the PKA substrate AMPA receptor subunit GluR1 at Ser845. The phosphorylation of GluR1 after L-DOPA administration is correlated with more recent work from our laboratory (38) showing dendritic spine regrowth in denervated striatal areas. Spine regrowth leads to a recruitment of AMPA receptors to the postsynaptic density (68–70) in an activity-dependent manner (i.e., L-DOPA activation) because in basal conditions this recruitment is inactive. This finding is in line with our Western blot experiments, which revealed similar levels of GluR1 phosphorylation in basal conditions in all mutant mice, consistent with previous work (33).

Finally, DREAM overexpression could control LID development through the regulation of voltage-dependent calcium channels. It has been shown that blockade of L-type calcium channels using the antagonist isradipine decreases dyskinetic symptoms (20), whereas overexpression of DREAM reduces the expression of the *Cav1.2* gene encoding the L-type calcium channel (52) and decreases calcium permeability by direct protein-protein interaction with the L-type and the T-type channel complexes (31,71,72).

In conclusion, this study demonstrates the inhibitory role of DREAM in LID as evidenced by reduction of dyskinetic symptoms in daDREAM mice and a potentiation in DREAM$^{-/-}$ mice. In addition, we demonstrate that this action occurs at least in part by transcriptional repression of target genes, although nontranscriptional mechanisms could also be involved. Dynorphin-B and possibly FosB expression are regulated by DREAM, which represses their transcription by anchoring to DRE sites in the DNA and reducing LID. In addition, outside the nucleus, DREAM could directly interact with the NR1 subunit and PSD-95, regulating activation of NMDAR and D1Rs (Figure 8). The findings we describe in this article validate DREAM as a novel therapeutic target against LID, and we propose that specific modulators of DREAM could be useful in alleviating L-DOPA-induced dyskinesias without interfering with the antiparkinsonian effect of L-DOPA. However, other, as yet uncharacterized transcriptional and nontranscriptional targets of DREAM could also be important, directly or indirectly, in the regulation of LID. Future genome-wide analysis during LID establishment in daDREAM and DREAM$^{-/-}$ mice might expand understanding of the role of DREAM in LID.

This work was supported by grants from the Spanish Ministerios de Economía y Competitividad and Sanidad Política Social e Igualdad, Instituto de Salud Carlos III Grant No. BFU2010-20664, Plan Nacional Sobre Drogas No. 2012/071, Centro de Investigación Biomédica en Red de Enfermedades Neurodegenerativas Ref. No. CB06/05/0055, and Comunidad de Madrid Ref. No. S2011/BMD-2336 to RM; Instituto de Salud Carlos III/CIBERNED, Madrid Community/ Neurodegmodels, and Grant No. SAF2010-21784 from Spanish Ministerios de Economía y Competitividad to JRN; and Spanish

Ministerio de Ciencia e Innovación Grant No. BFU2008-01283, Spanish Ministerios de Economía y Competitividad Grant No. BFU2011-24245, and Centro de Investigación Biomédica en Red de Diabetes y Enfermedades Metabólicas Asociadas (Instituto de Salud Carlos III) to MV. We thank Ms. Emilia Rubio, Mr. Marco de Mesa, and Ms. Paz Gonzalez for their excellent technical assistance.

The authors report no biomedical financial interests or potential conflicts of interest.

Supplementary material cited in this article is available online at http://dx.doi.org/10.1016/j.biopsych.2014.03.023.

1. Pavón N, Martín AB, Mendialdua A, Moratalla R (2006): ERK phosphorylation and FosB expression are associated with L-DOPA-induced dyskinesia in hemiparkinsonian mice. *Biol Psychiatry* 59:64–74.
2. Murer MG, Moratalla R (2011): Striatal signaling in L-DOPA-induced dyskinesia: Common mechanisms with drug abuse and long term memory involving D1 dopamine receptor stimulation. *Front Neuroanat* 5:51.
3. Delfino M, Kalisch R, Czisch M, Larramendy C, Ricatti J, Taravini IR, *et al.* (2007): Mapping the effects of three dopamine agonists with different dyskinetogenic potential and receptor selectivity using pharmacological functional magnetic resonance imaging. *Neuropsychopharmacology* 32:1911–1921.
4. Lebel M, Chagniel L, Bureau G, Cyr M (2010): Striatal inhibition of PKA prevents levodopa-induced behavioural and molecular changes in the hemiparkinsonian rat. *Neurobiol Dis* 38:59–67.
5. Fisone G, Bezard E (2011): Molecular mechanisms of L-DOPA-induced dyskinesia. *Int Rev Neurobiol* 98:95–122.
6. Santini E, Valjent E, Usiello A, Carta M, Borgkvist A, Girault JA, *et al.* (2007): Critical involvement of cAMP/DARPP-32 and extracellular signal-regulated protein kinase signaling in L-DOPA-induced dyskinesia. *J Neurosci* 27:6995–7005.
7. Santini E, Feyder M, Gangarossa G, Bateup HS, Greengard P, Fisone G (2012): Dopamine- and cAMP-regulated phosphoprotein of 32-kDa (DARPP-32)-dependent activation of extracellular signal-regulated kinase (ERK) and mammalian target of rapamycin complex 1 (mTORC1) signaling in experimental parkinsonism. *J Biol Chem* 287: 27806–27812.
8. Schuster S, Nadjar A, Guo JT, Li Q, Ittrich C, Hengerer B, *et al.* (2008): The 3-hydroxy-3-methylglutaryl-CoA reductase inhibitor lovastatin reduces severity of L-DOPA-induced abnormal involuntary movements in experimental Parkinson's disease. *J Neurosci* 28:4311–4316.
9. Fasano S, Bezard E, D'Antoni A, Francardo V, Indrigo M, Qin L, *et al.* (2010): Inhibition of Ras-guanine nucleotide-releasing factor 1 (Ras-GRF1) signaling in the striatum reverts motor symptoms associated with L-dopa-induced dyskinesia. *Proc Natl Acad Sci U S A* 107: 21824–21829.
10. Darmopil S, Martín AB, De Diego IR, Ares S, Moratalla R (2009): Genetic inactivation of dopamine D1 but not D2 receptors inhibits L-DOPA-induced dyskinesia and histone activation. *Biol Psychiatry* 66: 603–613.
11. Santini E, Alcacer C, Cacciatore S, Heiman M, Hervé D, Greengard P, *et al.* (2009): L-DOPA activates ERK signaling and phosphorylates histone H3 in the striatonigral medium spiny neurons of hemiparkinsonian mice. *J Neurochem* 108:621–633.
12. Chase TN, Oh JD, Konitsiotis S (2000): Antiparkinsonian and antidyskinetic activity of drugs targeting central glutamatergic mechanisms. *J Neurol* 247(suppl 2):II36–II42.
13. Hallett PJ, Dunah AW, Ravenscroft P, Zhou S, Bezard E, Crossman AR, *et al.* (2005): Alterations of striatal NMDA receptor subunits associated with the development of dyskinesia in the MPTP-lesioned primate model of Parkinson's disease. *Neuropharmacology* 48:503–516.
14. Gardoni F, Picconi B, Ghiglieri V, Polli F, Bagetta V, Bernardi G, *et al.* (2006): A critical interaction between NR2B and MAGUK in L-DOPA induced dyskinesia. *J Neurosci* 26:2914–2922.
15. Silverdale MA, Kobylecki C, Hallett PJ, Li Q, Dunah AW, Ravenscroft P, *et al.* (2010): Synaptic recruitment of AMPA glutamate receptor subunits in levodopa-induced dyskinesia in the MPTP-lesioned nonhuman primate. *Synapse* 64:177–180.
16. Berthet A, Porras G, Doudnikoff E, Stark H, Cador M, Bezard E, *et al.* (2009): Pharmacological analysis demonstrates dramatic alteration of D1 dopamine receptor neuronal distribution in the rat analog of L-DOPA-induced dyskinesia. *J Neurosci* 29:4829–4835.
17. Nash JE, Johnston TH, Collingridge GL, Garner CC, Brotchie JM (2005): Subcellular redistribution of the synapse-associated proteins PSD-95 and SAP97 in animal models of Parkinson's disease and L-DOPA-induced dyskinesia. *FASEB J* 19:583–585.
18. Porras G, Berthet A, Dehay B, Li Q, Ladepeche L, Normand E, *et al.* (2012): PSD-95 expression controls L-DOPA dyskinesia through dopamine D1 receptor trafficking. *J Clin Invest* 122:3977–3989.
19. Surmeier DJ, Bargas J, Hemmings HC Jr, Nairn AC, Greengard P (1995): Modulation of calcium currents by a D1 dopaminergic protein kinase/phosphatase cascade in rat neostriatal neurons. *Neuron* 14:385–397.
20. Schuster S, Doudnikoff E, Rylander D, Berthet A, Aubert I, Ittrich C, *et al.* (2009): Antagonizing L-type Ca2+ channel reduces development of abnormal involuntary movement in the rat model of L-3, 4-dihydroxyphenylalanine-induced dyskinesia. *Biol Psychiatry* 65: 518–526.
21. Ledo F, Link WA, Carrión AM, Echeverria V, Mellström B, Naranjo JR (2000): The DREAM-DRE interaction: key nucleotides and dominant negative mutants. *Biochim Biophys Acta* 1498:162–168.
22. Cebolla B, Fernández-Pérez A, Perea G, Araque A, Vallejo M (2008): DREAM mediates cAMP-dependent, Ca2+-induced stimulation of GFAP gene expression and regulates cortical astrogliogenesis. *J Neurosci* 28:6703–6713.
23. Spreafico F, Barski JJ, Farina C, Meyer M (2001): Mouse DREAM/calsenilin/KChIP3: Gene structure, coding potential, and expression. *Mol Cell Neurosci* 17:1–16.
24. Xiong H, Kovacs I, Zhang Z (2004): Differential distribution of KChIPs mRNAs in adult mouse brain. *Brain Res Mol Brain Res* 128: 103–111.
25. Duncan CE, Schofield PR, Weickert CS (2009): K(v) channel interacting protein 3 expression and regulation by haloperidol in midbrain dopaminergic neurons. *Brain Res* 1304:1–13.
26. Carrión AM, Link WA, Ledo F, Mellström B, Naranjo JR (1999): DREAM is a Ca2+-regulated transcriptional repressor. *Nature* 398:80–84.
27. Link WA, Ledo F, Torres B, Palczewska M, Madsen TM, Savignac M, *et al.* (2004): Day-night changes in downstream regulatory element antagonist modulator/potassium channel interacting protein activity contribute to circadian gene expression in pineal gland. *J Neurosci* 24: 5346–5355.
28. Ledo F, Carrión AM, Link WA, Mellström B, Naranjo JR (2000): DREAM-alphaCREM interaction via leucine-charged domains derepresses downstream regulatory element-dependent transcription. *Mol Cell Biol* 20:9120–9126.
29. Ledo F, Kremer L, Mellström B, Naranjo JR (2002): Ca2+-dependent block of CREB-CBP transcription by repressor DREAM. *EMBO J* 21: 4583–4592.
30. Osawa M, Tong KI, Lilliehook C, Wasco W, Buxbaum JD, Cheng HY, *et al.* (2001): Calcium-regulated DNA binding and oligomerization of the neuronal calcium-sensing protein, calsenilin/DREAM/KChIP3. *J Biol Chem* 276:41005–41013.
31. Rivas M, Villar D, González P, Dopazo XM, Mellstrom B, Naranjo JR (2011): Building the DREAM interactome. *Sci China Life Sci* 54:786–792.
32. Zhang Y, Su P, Liang P, Liu T, Liu X, Liu XY, *et al.* (2010): The DREAM protein negatively regulates the NMDA receptor through interaction with the NR1 subunit. *J Neurosci* 30:7575–7586.
33. Wu LJ, Mellström B, Wang H, Ren M, Domingo S, Kim SS, *et al.* (2010): DREAM (downstream regulatory element antagonist modulator) contributes to synaptic depression and contextual fear memory. *Mol Brain* 3:3.
34. Gomez-Villafuertes R, Torres B, Barrio J, Savignac M, Gabellini N, Rizzato F, *et al.* (2005): Downstream regulatory element antagonist modulator regulates Ca2+ homeostasis and viability in cerebellar neurons. *J Neurosci* 25:10822–10830.
35. Savignac M, Pintado B, Gutierrez-Adan A, Palczewska M, Mellström B, Naranjo JR (2005): Transcriptional repressor DREAM regulates T-lymphocyte proliferation and cytokine gene expression. *EMBO J* 24: 3555–3564.

36. Cheng HY, Pitcher GM, Laviolette SR, Whishaw IQ, Tong KI, Kockeritz LK, *et al.* (2002): DREAM is a critical transcriptional repressor for pain modulation. *Cell* 108:31–43.
37. Mayford M, Bach ME, Huang YY, Wang L, Hawkins RD, Kandel ER (1996): Control of memory formation through regulated expression of a CaMKII transgene. *Science* 274:1678–1683.
38. Suárez LM, Solís O, Caramés JM, Taravini IR, Solís JM, Murer MG, *et al.* (2013): L-DOPA treatment selectively restores spine density in dopamine receptor D2-expressing projection neurons in dyskinetic mice [published online ahead of print Jun 12]. *Biol Psychiatry*.
39. Darmopil S, Muñetón-Gómez VC, de Ceballos ML, Bernson M, Moratalla R (2008): Tyrosine hydroxylase cells appearing in the mouse striatum after dopamine denervation are likely to be projection neurones regulated by L-DOPA. *Eur J Neurosci* 27:580–592.
40. Granado N, Ortiz O, Suárez LM, Martín ED, Ceña V, Solís JM, *et al.* (2008): D1 but not D5 dopamine receptors are critical for LTP, spatial learning, and LTP-induced arc and zif3268 expression in the hippocampus. *Cereb Cortex* 18:1–12.
41. González-Aparicio R, Moratalla R (2014): Oleoylethanolamide reduces L-DOPA-induced dyskinesia via TRPV1 receptor in a mouse model of Parkinson's disease. *Neurobiol Dis* 62:416–425.
42. Espadas I, Darmopil S, Vergaño-Vera E, Ortiz O, Oliva I, Vicario-Abejón C, *et al.* (2012): L-DOPA-induced increase in TH-immunoreactive striatal neurons in parkinsonian mice: Insights into regulation and function. *Neurobiol Dis* 48:271–281.
43. Ares-Santos S, Granado N, Oliva I, O'Shea E, Martin ED, Colado MI (2012): Dopamine D(1) receptor deletion strongly reduces neurotoxic effects of methamphetamine. *Neurobiol Dis* 45:810–820.
44. Ares-Santos S, Granado N, Espadas I, Martinez-Murillo R, Moratalla R (2014): Methamphetamine causes degeneration of dopamine cell bodies and terminals of the nigrostriatal pathway evidenced by silver staining. *Neuropsychopharmacology* 39:1066–1080.
45. Granado N, Escobedo I, O'Shea E, Colado I, Moratalla R (2008): Early loss of dopaminergic terminals in striosomes after MDMA administration to mice. *Synapse* 62:80–84.
46. Livak K, Schmittgen TD (2001): Analysis of relative gene expression data using real-time quantitative PCR and the $2^{-\Delta\Delta C}$T method. *Methods* 25:402–408.
47. Francardo V, Recchia A, Popovic N, Andersson D, Nissbrandt H, Cenci MA (2011): Impact of the lesion procedure on the profiles of motor impairment and molecular responsiveness to L-DOPA in the 6-hydroxydopamine mouse model of Parkinson's disease. *Neurobiol Dis* 42:327–340.
48. Andersson M, Hilbertson A, Cenci MA (1999): Striatal fosB expression is causally linked with l-DOPA-induced abnormal involuntary movements and the associated upregulation of striatal prodynorphin mRNA in a rat model of Parkinson's disease. *Neurobiol Dis* 6:461–474.
49. Santini E, Sgambato-Faure V, Li Q, Savasta M, Dovero S, Fisone G, *et al.* (2010): Distinct changes in cAMP and extracellular signal-regulated protein kinase signalling in L-DOPA-induced dyskinesia. *PLoS One* 5:e12322.
50. Alexander JC, McDermott CM, Tunur T, Rands V, Stelly C, Karhson D, *et al.* (2009): The role of calsenilin/DREAM/KChIP3 in contextual fear conditioning. *Learn Mem* 16:167–177.
51. Dierssen M, Fedrizzi L, Gomez-Villafuertes R, de Lagran MM, Gutierrez-Adan A, Sahún I, *et al.* (2012): Reduced Mid1 expression and delayed neuromotor development in daDREAM transgenic mice. *Front Mol Neurosci* 5:58.
52. Naranjo JR, Mellström B (2012): Ca2+-dependent transcriptional control of Ca2+ homeostasis. *J Biol Chem* 287:31674–31680.
53. Piccini P, Weeks RA, Brooks DJ (1997): Alterations in opioid receptor binding in Parkinson's disease patients with levodopa-induced dyskinesias. *Ann Neurol* 42:720–726.
54. Tekumalla PK, Calon F, Rahman Z, Birdi S, Rajput AH, Hornykiewicz O, *et al.* (2001): Elevated levels of DeltaFosB and RGS9 in striatum in Parkinson's disease. *Biol Psychiatry* 50:813–816.
55. Berton O, Guigoni C, Li Q, Bioulac BH, Aubert I, Gross CE, *et al.* (2009): Striatal overexpression of DeltaJunD resets L-DOPA-induced dyskinesia in a primate model of Parkinson disease. *Biol Psychiatry* 66: 554–561.
56. Tamim MK, Samadi P, Morissette M, Grégoire L, Ouattara B, Lévesque D, *et al.* (2010): Effect of non-dopaminergic drug treatment on levodopa induced dyskinesias in MPTP monkeys: Common implication of striatal neuropeptides. *Neuropharmacology* 58:286–296.
57. Lazo PS, Dorfman K, Noguchi T, Mattéi MG, Bravo R (1992): Structure and mapping of the fosB gene. FosB downregulates the activity of the fosB promoter. *Nucleic Acids Res* 20:343–350.
58. Moratalla R, Xu M, Tonegawa S, Graybiel AM (1996): Cellular responses to psychomotor stimulant and neuroleptic drugs are abnormal in mice lacking the D1 dopamine receptor. *Proc Natl Acad Sci U S A* 93: 14928–14933.
59. Naranjo JR, Mellström B, Achaval M, Sassone-Corsi P (1991): Molecular pathways of pain: Fos/Jun-mediated activation of a noncanonical AP-1 site in the prodynorphin gene. *Neuron* 6:607–617.
60. An WF, Bowlby MR, Betty M, Cao J, Ling HP, Mendoza G, *et al.* (2000): Modulation of A-type potassium channels by a family of calcium sensors. *Nature* 403:553–556.
61. Rivas M, Mellström B, Torres B, Cali G, Ferrara AM, Terracciano D, *et al.* (2009): The DREAM Protein is associated to thyroid enlargement and nodular development. *Mol Endocrinol* 23:862–870.
62. Zhang Y, Meredith GE, Mendoza-Elias N, Rademacher DJ, Tseng KY, Steece-Collier K (2013): Aberrant restoration of spines and their synapses in L-DOPA-induced dyskinesia: Involvement of corticostriatal but not thalamostriatal synapses. *J Neurosci* 33: 11655–11667.
63. Papa SM, Boldry RC, Engber TM, Kask AM, Chase TN (1995): Reversal of levodopa-induced motor fluctuations in experimental parkinsonism by NMDA receptor blockade. *Brain Res* 701:13–18.
64. Blanchet PJ, Metman LV, Chase TN (2003): Renaissance of amantadine in the treatment of Parkinson's disease. *Adv Neurol* 91:251–257.
65. Harrison IF, Dexter DT (2013): Epigenetic targeting of histone deacetylase: Therapeutic potential in Parkinson's disease? *Pharmacol Ther* 140:34–52.
66. Cheung P, Tanner KG, Cheung WL, Sassone-Corsi P, Denu JM, Allis CD (2000): Synergistic coupling of histone H3 phosphorylation and acetylation in response to epidermal growth factor stimulation. *Mol Cell* 5:905–915.
67. Alcacer C, Santini E, Valjent E, Gaven F, Girault JA, Hervé D (2012): Gα(olf) mutation allows parsing the role of cAMP-dependent and extracellular signal-regulated kinase-dependent signaling in L-3,4-dihydroxyphenylalanine-induced dyskinesia. *J Neurosci* 32: 5900–5910.
68. Malinow R, Mainen ZF, Hayashi Y (2000): LTP mechanisms: From silence to four-lane traffic. *Curr Opin Neurobiol* 10:352–357.
69. Malenka RC (2003): Synaptic plasticity and AMPA receptor trafficking. *Ann N Y Acad Sci* 1003:1–11.
70. Shepherd JD, Huganir RL (2007): The cell biology of synaptic plasticity: AMPA receptor trafficking. *Annu Rev Cell Dev Biol* 23:613–643.
71. Thomsen MB, Wang C, Ozgen N, Wang HG, Rosen MR, Pitt GS (2009): Accessory subunit KChIP2 modulates the cardiac L-type calcium current. *Circ Res* 104:1382–1389.
72. Anderson D, Mehaffey WH, Iftinca M, Rehak R, Engbers JD, Hameed S, *et al.* (2010): Regulation of neuronal activity by Cav3-Kv4 channel signaling complexes. *Nat Neurosci* 13:333–337.